Australian Government
Department of Agriculture, Water and the Environment
Bureau of Meteorology
Geoscience Australia

BIOREGIONAL ASSESSMENTS

CSIRO

Shale, tight and deep coal gas prospectivity of the Cooper Basin

Technical appendix for the Geological and Bioregional Assessment: Stage 2

2020

A scientific collaboration between the Department of Agriculture, Water and the Environment, Bureau of Meteorology, CSIRO and Geoscience Australia

The Geological and Bioregional Assessment Program

The Geological and Bioregional Assessment Program will provide independent scientific advice on the potential impacts from development of selected unconventional hydrocarbon plays on water and the environment. The geological and environmental data and tools produced by the Program will assist governments, industry, landowners and the community to help inform decision making and enhance the coordinated management of potential impacts.

The Program is funded by the Australian Government Department of the Environment and Energy. The Department of the Environment and Energy, Bureau of Meteorology, CSIRO and Geoscience Australia are collaborating to undertake geological and bioregional assessments. For more information, visit http://www.bioregionalassessments.gov.au.

Department of the Environment and Energy

The Department designs and implements Australian Government policy and programs to protect and conserve the environment, water and heritage, promote climate action, and provide adequate, reliable and affordable energy. For more information visit http://www.environment.gov.au.

Bureau of Meteorology

The Bureau of Meteorology is Australia's national weather, climate and water agency. Under the *Water Act 2007*, the Bureau is responsible for compiling and disseminating Australia's water information. The Bureau is committed to increasing access to water information to support informed decision making about the management of water resources. For more information, visit http://www.bom.gov.au/water/.

CSIRO

Australia is founding its future on science and innovation. Its national science agency, CSIRO, is a powerhouse of ideas, technologies and skills for building prosperity, growth, health and sustainability. It serves governments, industries, business and communities across the nation. For more information, visit http://www.csiro.au.

Geoscience Australia

Geoscience Australia is Australia's national geoscience agency and exists to apply geoscience to Australia's most important challenges. Geoscience Australia provides geoscientific advice and information to the Australian Government to support current priorities. These include contributing to responsible resource development; cleaner and low emission energy technologies; community safety; and improving marine planning and protection. The outcome of Geoscience Australia's work is an enhanced potential for the Australian community to obtain economic, social and environmental benefits through the application of first-class research and information. For more information, visit http://www.ga.gov.au.

ISBN-PDF 978-1-921069-20-8

Citation

Lech ME, Wang L, Hall LS, Bailey A, Palu T, Owens R, Skeers N, Woods M, Dehelean A, Orr M, Cathro D and Evenden C (2020) Shale, tight and deep coal gas prospectivity of the Cooper Basin. Technical appendix for the Geological and Bioregional Assessment Program: Stage 2. Department of the Environment and Energy, Bureau of Meteorology, CSIRO and Geoscience Australia, Australia.

Authorship is listed in relative order of contribution.

On 1 February 2020 the Department of the Environment and Energy and the Department of Agriculture merged to form the Department of Agriculture, Water and the Environment. Work for this document was carried out under the then Department of the Environment and Energy. Therefore, references to both departments are retained in this report.

Cover photograph

Cooper Creek in flood, 4 km east of Windorah, March 2018.
Credit: Geological and Bioregional Assessment Program, Russell Crosbie (CSIRO)
Element: GBA-COO-2-343

v20210629

Executive summary

Assessing the regional prospectivity of tight, shale and deep coal gas resources in the Cooper Basin is an integral component of the Australian Government's Geological and Bioregional Assessment Program, which aims to encourage exploration and understand the potential impacts of resource development on water and the environment.

This appendix presents a review of the regional petroleum prospectivity, exploration history, and the characterisation and analysis of shale, deep coal and tight gas in late Carboniferous–Permian Gidgealpa Group of the Cooper Basin.

The Cooper and Eromanga basins form Australia's most developed onshore oil and gas province. Between 1969 and 2014, the Cooper Basin and overlying Eromanga Basin have produced 6.54 trillion cubic feet (Tcf) of gas and contain 256 gas fields and 166 oil fields currently in production. Although commercial production has been underway for over 50 years, the region continues to yield new discoveries.

Over the last ten years, resource exploration companies have pursed a range of unconventional plays within the Permian sediments of the Cooper Basin. These plays include shale gas associated with the Patchawarra Formation and the Roseneath and Murteree shales; deep coal gas accumulations within the Toolachee, Epsilon and Patchawarra formations; and a basin-centred tight gas within the Permian Gidgealpa Group. Given the basin's existing conventional production, and its processing and pipeline infrastructure, these plays are well placed to be rapidly commercialised, pending further exploration success.

Characterisation of the shale, tight and deep coal gas plays in the Cooper Basin was undertaken to support further work on understanding likely development scenarios. The geological properties evaluated include formation depths and extents, source rock properties (net thickness, organic carbon content, quality and maturity), reservoir characteristics (porosity, permeability, gas saturation and brittleness), regional stress regime and pressure gradient.

The relative prospectivity of each play type was mapped at a regional scale across the basin. Areas of higher prospectivity were identified within most depocentres, including the Nappamerri, Patchawarra, Windorah, Allunga and Wooloo troughs, consistent with recent exploration activity. The mapped depth and extent of these shale, tight and deep coal gas plays inform where the plays are most likely to be present within the basin, which in turn aids assessment of potential connectivity to overlying surface water–groundwater systems and associated assets. More data were available in the southern Cooper Basin and consequently there is higher confidence in the maps in this region.

Prospectivity classes are comparative and so a high prospectivity confidence rating does not equate to a measurable probability of success. The results presented here are based on the geological factors required for a viable petroleum play to be present. However due to the large capital expenditure required to extract unconventional resources, if and how an unconventional play is developed will be dependent on its economic viability, along with other cultural and environmental considerations.

Contents

Figures

Tables

Contributors to the Program

The following individuals have contributed to the Geological and Bioregional Assessment Program.

Role or team	Contributor(s)
Program Director	Department of the Environment and Energy: Anthony Swirepik
Program Implementation Board	Department of the Environment and Energy: Beth Brunoro, Nicholas Post Bureau of Meteorology: Kirsten Garwood, Kate Vinot CSIRO: Jane Coram, Warwick MacDonald Geoscience Australia: Stuart Minchin, Richard Blewett
Basin Leader	CSIRO: Kate Holland, Cameron Huddlestone-Holmes, Paul Wilkes Geoscience Australia: Steven Lewis
Program management	CSIRO: Karen Barry, Emanuelle Frery, Linda Merrin, Ruth Palmer Department of the Environment and Energy: Mitchell Bouma, Rod Dann, Andrew Stacey, David Thomas, Alex Tomlinson
Product integration and stakeholder engagement	CSIRO: Clare Brandon, Justine Lacey, Michelle Rodriquez, Sally Tetreault-Campbell
Analysis and visualisation	CSIRO: Dennis Gonzalez, Steve Marvanek Geoscience Australia: Adrian Dehelean, Chris Evenden, Chris Lawson, Bianca Reese, Nigel Skeers, Murray Woods
Basin geology and prospectivity	Geoscience Australia: Lisa Hall (Discipline Leader), Adam Bailey, George Bernardel, Barry Bradshaw, Donna Cathro, Merrie-Ellen Gunning, Amber Jarrett, Megan Lech, Meredith Orr, Ryan Owens, Tehani Palu, Martin Smith, Liuqu Wang
Chemical assessment	CSIRO: Jason Kirby (Discipline Leader), Simon Apte, Lisa Golding, Rai Kookana, Dirk Mallants, Michael Williams
Data management and transparency	Bureau of Meteorology: Andre Zerger (Discipline Leader), Derek Chen, Trevor Christie-Taylor, Donna Phillips CSIRO: Nicholas Car, Philip Davies, Stacey Northover, Matt Stenson Geoscience Australia: Matti Peljo
Hydrogeology	Geoscience Australia: Tim Ransley (Discipline Leader), Sam Buchanan, Scott Cook, Prachi Dixon-Jain, Bex Dunn, Tim Evans, Éamon Lai, Bruce Radke, Baskaran Sundaram
Impact analysis	CSIRO: David Post (Discipline Leader), Brent Henderson, Dane Kasperczyk, James Kear, Regina Sander
Impacts on protected matters	CSIRO: Anthony O'Grady (Discipline Leader), Alexander Herr, Craig MacFarlane, Justine Murray, Chris Pavey, Stephen Stewart
Spatial analysis	CSIRO: Dennis Gonzalez, Steve Marvanek Geoscience Australia: Adrian Dehelean, Murray Woods, Nigel Skeers
Water quantity	CSIRO: Russell Crosbie (Discipline Leader), Jorge Martinez Praveen Kumar Rachakonda, Matthias Raiber, Yongqiang Zhang, Hongxing Zheng

Acknowledgements

This Cooper Stage 2 technical product was reviewed by several groups:

- Internal Peer Review Group: Geoscience Australia: Robert Langford, Merrie-Ellen Gunning, David Robinson
- Technical Peer Review Group: Andrew Boulton, Peter McCabe, Catherine Moore and Jenny Stauber
- State Government Science Technical Review: This group includes scientists from the Queensland and South Australian governments.

Valuable comments were also provided by Tony Hill (Department for Energy and Mining, South Australia); Justin Gorton and Alison Troup (Geological Survey of Queensland); Chad Wilson, Bronwyn Camac, Emma Hissey (Santos); Martin Berry (Icon Energy); Chuck Boyer, Hamechan Madhoo (Schlumberger); Daniel Jarvie (Worldwide Geochemistry).

Abbreviations and acronyms

Abbreviation/acronym	Definition
AER	Australian Energy Regulator
AERA	Australian Energy Resources Assessment
API	American Petroleum Institute
AR	As-received
ASX	Australian Securities Exchange
BI	Brittleness index
CGR	Condensate-to-gas-ratio
CO_2	Carbon dioxide
CSG	Coal seam gas
DOM	Dispersed organic matter
DSDRE	Department of State Development Resources and Energy
DST	Drill stem test
EC	Electrical conductivity
EIA	United States Energy Information Administration
GIP	Gas-in-place
GMI	Gidgealpa–Merrimelia–Innamincka
GOR	Gas-to-oil ratio
HI	Hydrogen Index
HI_o	Original Hydrogen Index
JNP	Jackson–Naccowlah–Pepita
Ma	Million years before the present
MD	Measured depth along borehole
MDRT	Measured depth along borehole from rotary table
MEM	Mechanical earth model
mMD	Measured depth in metres
MSL	Mean sea level
NGMA	National Geoscience Mapping Accord
NORR	Net organically rich ratio
NRM	Natural resource management
NSW	New South Wales
PDPM	Pressure decay permeability
PEPS–SA	Petroleum Exploration and Production System–South Australia
PHIGF	Gas-filled porosity
PRMS	Petroleum Resources Management System
Qld	Queensland

Abbreviation/acronym	Definition
QPED	Queensland Petroleum Exploration Data
REM	Roseneath Shale, Epsilon Formation, Murteree Shale
RHOB	Bulk density
R_o	Maturity
SA	South Australia
SEM	Scanning electron microscopy
SPE	Society of Petroleum Engineers
TOC	Total organic carbon
TR	Transformation ratio
USGS	United States Geological Survey
WMS	Web map service
wt	Weight
XRD	X-ray Diffraction

Units

Unit	Description
bbl	Barrels
bbl/mmscf	Barrels per million standard cubic feet
g/cc	Grams per cubic centimetre
km	Kilometres
kPa	Kilopascals
MPa	Megapascals
MPa/km	Megapascals per kilometre
m	Metres
mD	Millidarcy
mg HC/g TOC	Milligrams of hydrocarbons per gram of total organic carbon
mg/g	Milligrams per gram
mg/L	Milligrams per litre
mmcfd	Million cubic feet per day
mmscf	Million standard cubic feet
mol%	Molar fraction (as a percentage)
MW	Megawatt
PJ	Petajoules - 1015 joules
psi	Pounds per square inch
psi/ft	Pounds per square inch per foot
scc/g	Standard cubic centimetres per gram
scf	Standard cubic foot
scfd	Standard cubic foot per day
scf/stb	Standard cubic foot per stock tank barrel
stb	Stock tank barrel
Tcf	Trillion - 10^{12} cubic feet
TJ	Terrajoules
%Ro	Vitrinite reflectance (as a percentage)
vol%	Volume (as a percentage)
wt%	Weight (as a percentage)

The Geological and Bioregional Assessment Program

The $35.4 million Geological and Bioregional Assessment (GBA) Program is assessing the potential environmental impacts of shale and tight gas development to inform regulatory frameworks and appropriate management approaches. The geological and environmental knowledge, data and tools produced by the Program will assist governments, industry, landowners and the community by informing decision making and enabling the coordinated management of potential impacts.

In consultation with state and territory governments and industry, three geological basins were selected based on prioritisation and ranking in Stage 1: Cooper Basin, Isa Superbasin and Beetaloo Sub-basin. In Stage 2, geological, hydrological and ecological data were used to define 'GBA regions': the Cooper GBA region in Queensland, SA and NSW; the Isa GBA region in Queensland; and the Beetaloo GBA region in NT. In early 2018, deep coal gas was added to the assessment for the Cooper GBA region, as this play is actively being explored by industry.

The GBA Program will assess the potential impacts of selected shale and tight gas development on water and the environment and provide independent scientific advice to governments, landowners, the community, business and investors to inform decision making. Geoscience Australia and CSIRO are conducting the assessments. The Program is managed by the Department of the Environment and Energy and supported by the Bureau of Meteorology.

The GBA Program aims to:

- inform government and industry and encourage exploration to bring new gas supplies to the East Coast Gas Market within five to ten years
- increase understanding of the potential impacts on water and the environment posed by development of shale, tight and deep coal gas resources
- increase the efficiency of assessment and ongoing regulation, particularly through improved reporting and data provision/management approaches
- improve community understanding of the industry.

The GBA Program commenced in July 2017 and comprises three stages:

- **Stage 1 Rapid regional basin prioritisation** identified and prioritised geological basins with the greatest potential to deliver shale and/or tight gas to the East Coast Gas Market within the next five to ten years.
- **Stage 2 Geological and environmental baseline assessments** is compiling and analysing available data for the three selected regions to form a baseline and identify gaps to guide collection of additional baseline data where needed. This analysis includes a geological basin assessment to define structural and stratigraphic characteristics and an environmental data synthesis.
- **Stage 3 Impact analysis and management** will analyse the potential impacts to water resources and matters of environmental significance to inform and support Commonwealth and State management and compliance activities.

The PDF of this report and the supporting technical appendices are available at https://www.bioregionalassessments.gov.au/geological-and-bioregional-assessment-program.

About this report

Presented in this technical appendix is a description of the regional prospectivity of shale, tight and deep coal gas resources of the Cooper GBA region. It provides information about the regional petroleum prospectivity, exploration history, and the characterisation and analysis of shale, tight and deep coal gas in the Cooper GBA region. The structure and focus of the synthesis report and technical appendices, prepared for the program reflect the needs of government, industry, landowners and community groups.

Technical appendices

Other technical appendices that support the geological and environmental baseline assessment for the Cooper GBA region are:

- Owens R, Hall L, Smith M, Orr M, Lech M, Evans T, Skeers N, Woods M and Inskeep C (2020) Geology of the Cooper GBA region.
- Evans TJ, Martinez J, Lai ÉCS, Raiber M, Radke BM, Sundaram B, Ransley TR, Dehelean A, Skeers N, Woods M, Evenden C and Dunn B (2020) Hydrogeology of the Cooper GBA region.
- O'Grady AP, Herr A, MacFarlane CM, Merrin LE and Pavey C (2020) Protected matters for the Cooper GBA region.
- Kirby JK, Golding L, Williams M, Apte S, Mallants D and Kookana R (2020) Qualitative (screening) environmental risk assessment of drilling and hydraulic fracturing chemicals for the Cooper GBA region.
- Kear J and Kasperczyk D (2020) Hydraulic fracturing and well integrity review for the GBA regions.

All maps for the Cooper GBA region use the Map Grid of Australia (MGA) projection (zone 54) and the Geocentric Datum of Australia 1994 (GDA 1994).

1 Summary

The Cooper Basin is a Carboniferous to Triassic sedimentary basin (Figure 1 and Figure 2). It covers an area of approximately 130,000 km^2, is up to 2500 m thick and occurs at depths between 1000 and 4500 m below sea level. It is overlain by the Jurassic to Cretaceous Eromanga and Cenozoic Lake Eyre basins.

The Cooper Basin and the overlying Eromanga Basin form Australia's largest onshore conventional hydrocarbon producing province. Between 1969 and 2014, the Cooper and Eromanga basins produced 6.54 Tcf of gas (Geoscience Australia, 2018) and the region continues to yield new discoveries. Resource exploration companies are currently pursuing a range of unconventional gas plays in the Cooper Basin, focused on shale, tight and deep coal gas hosted within the Permian succession.

This appendix presents a review of the regional petroleum prospectivity, exploration history, and the characterisation and analysis of shale, tight and deep coal gas plays hosted in the Cooper Basin. This process aims to address the geological factors likely to assist in identifying the presence of viable petroleum plays, and makes no attempt to factor extraction technology, economic, political, or social factors into the assessment.

The regional geology context of the Cooper GBA region and adjacent areas underpinning this prospectivity review are described in the accompanying geology technical appendix (Owens et al., 2020).

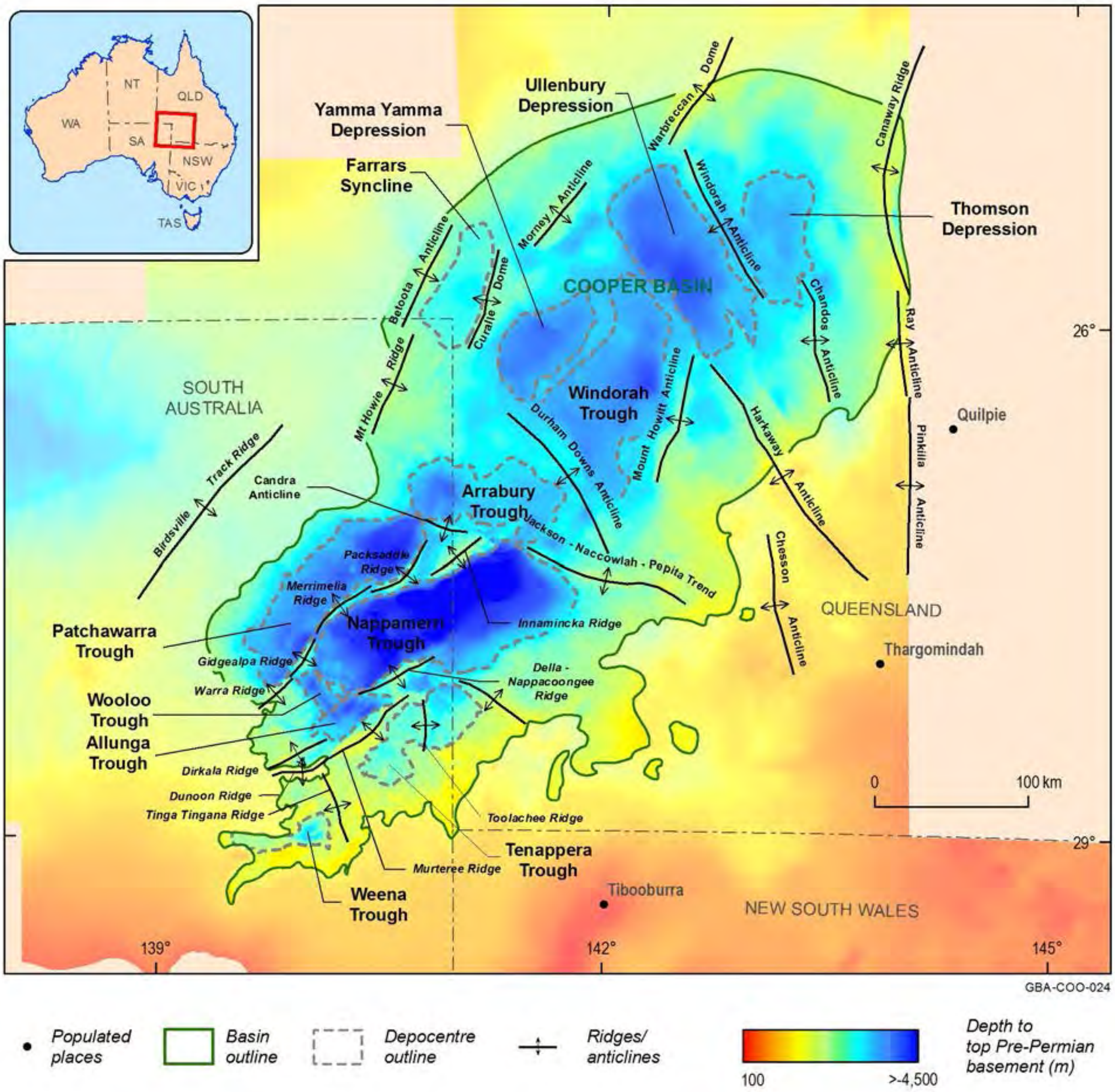

Figure 1 Cooper Basin structural elements overlain on top of the pre-Permian basement horizon

Source: Adapted from Hall et al. (2015a). Structural elements are modified from Draper (2002); Gravestock and Jensen-Schmidt (1998); McKellar (2013); and Ransley et al. (2012)
Data: Cooper Basin outline from Raymond et al. (2018); hill-shade derived from 9-second DEM (Hutchinson et al., 2008); depth to pre-Permian basement from Hall et al. (2016a); structural elements from Hall et al. (2015a), anticlines as regional trends only.
Element: GBA-COO-024

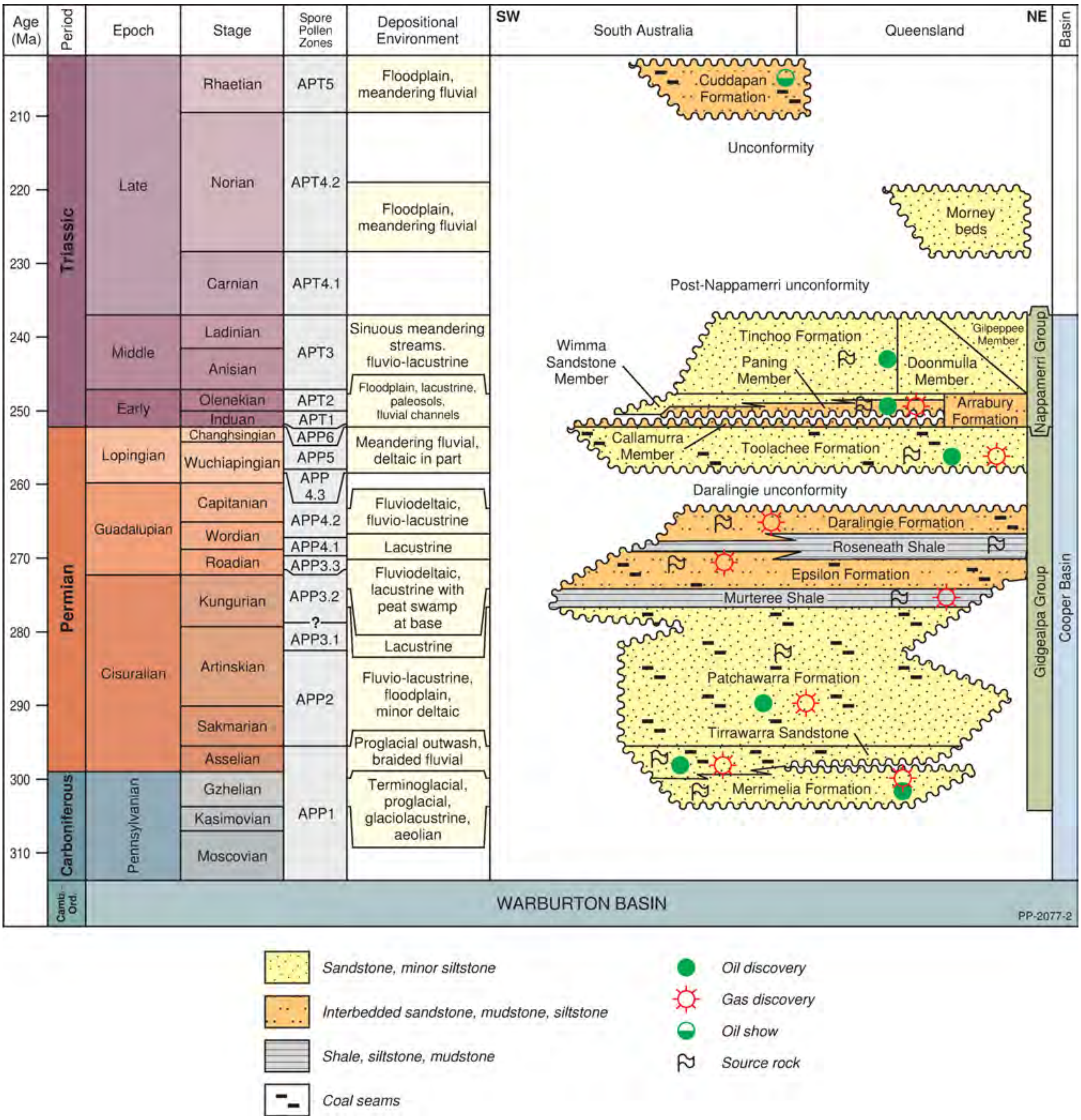

Figure 2 Stratigraphy of the Cooper Basin showing depositional facies, conventional petroleum occurrences and identified source rocks

Source: Hall et al. (2015a); see also the geology technical appendix (Owens et al., 2020)
Element: GBA-COO-2-173

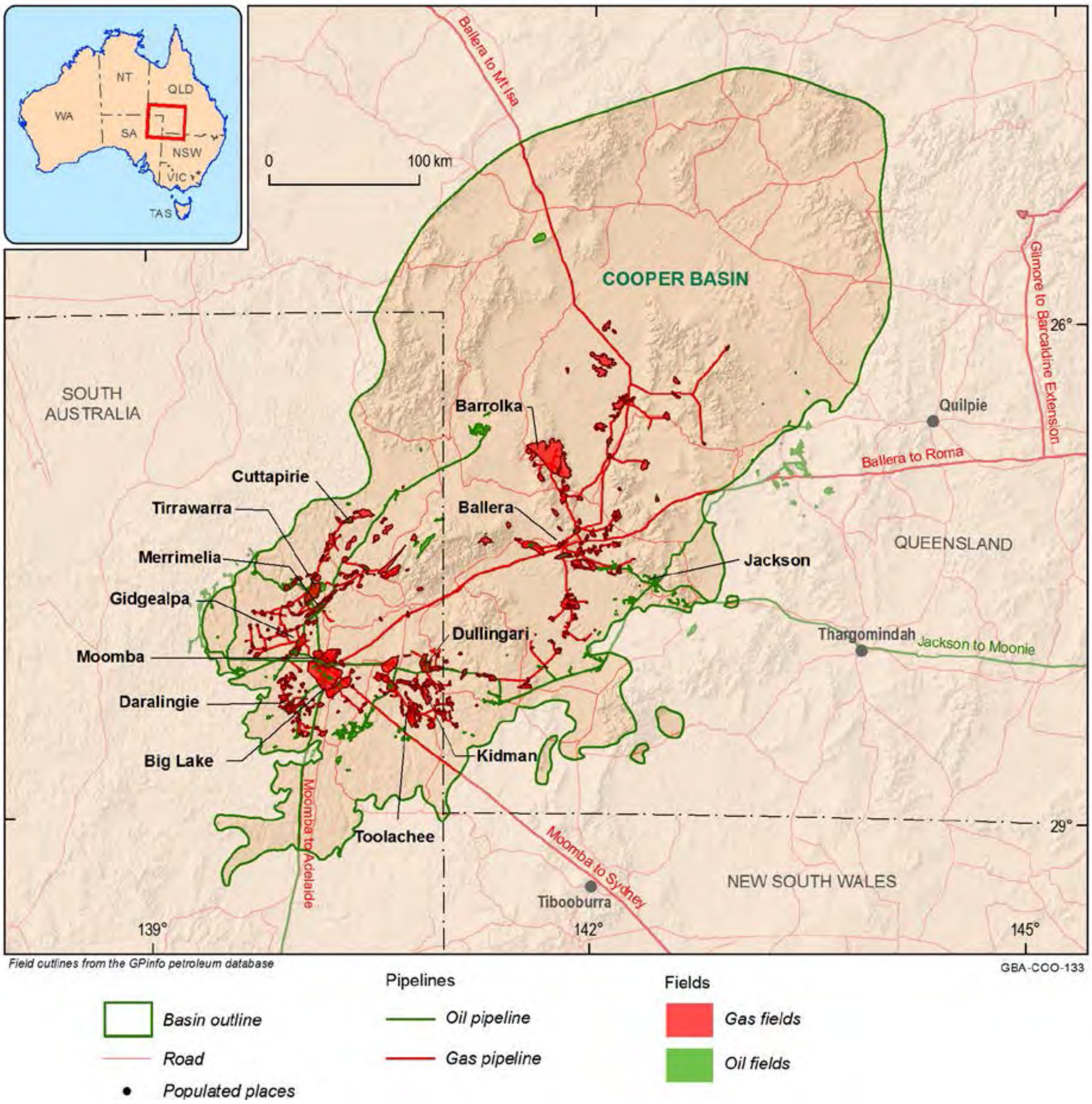

Figure 3 Cooper Basin fields, pipelines and production facilities

Data: Cooper Basin outline from Raymond et al. (2018); Hill-shade derived from 9-second DEM from Hutchinson et al. (2008); Roads from Geoscience Australia (2017); Field outlines and pipeline routes from the GPinfo petroleum database, a Petrosys Pty Ltd product (Petrosys Pty Ltd, 2019)
Element: GBA-COO-133

2 Conventional and unconventional gas

Naturally occurring oil and gas accumulations may be differentiated by the terms 'conventional' and 'unconventional', depending on how the petroleum is trapped in the reservoir rock (Figure 4).

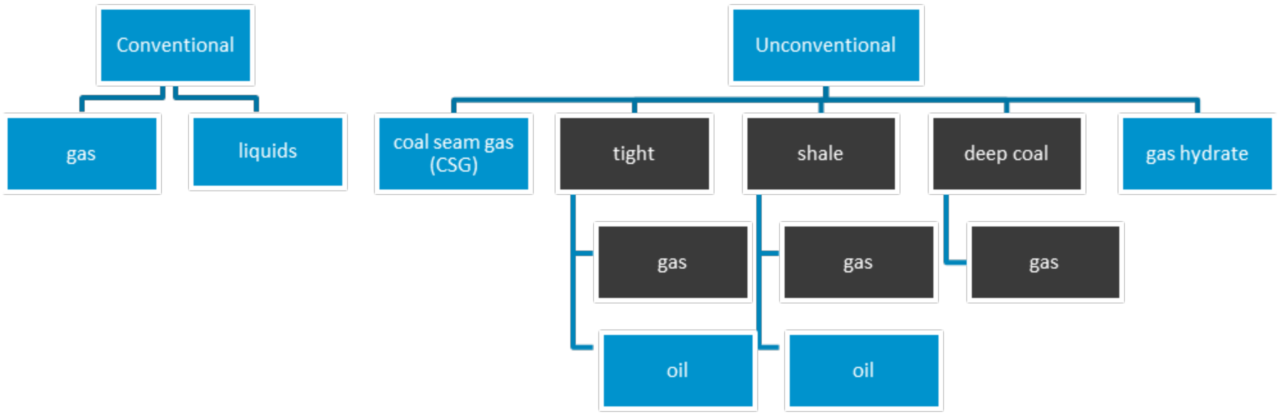

Figure 4 The different types of conventional and unconventional hydrocarbons

Unconventional play types considered for the Cooper GBA region are shown in dark blue. Deep coal gas has been included for Cooper Basin only.
Source: After Cook et al. (2013a)
Element: GBA-COO-2-252

Conventional petroleum accumulations (Figure 4 and Figure 5) are so called because they have the longest association with petroleum exploration and production, and are considered the norm (i.e. conventional) by the industry. These accumulations were the first to be exploited historically as they are relatively easy to find, and have produced the majority of oil and gas worldwide to date. However, they are relatively rare, comprising a small part of the petroleum continuum.

Conventional petroleum accumulations occur as discrete accumulations trapped by a geological structure and/or stratigraphic feature, typically bounded by a down-dip contact with water and capped by impermeable rock (Figure 5). The petroleum was not formed *in situ*; but migrated from the source rocks into a trap containing porous and permeable reservoir rocks.

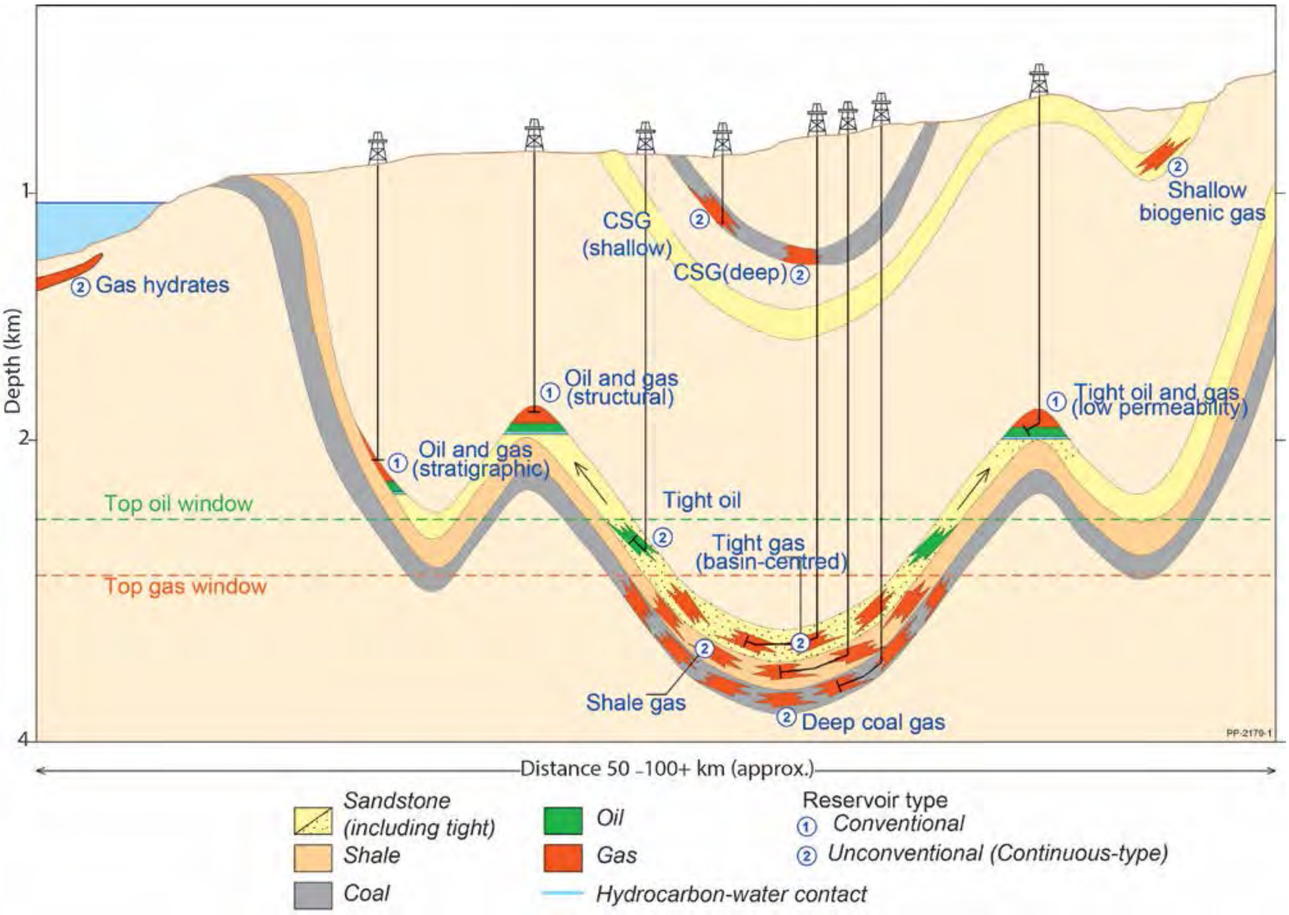

Figure 5 Schematic showing some of the typical types of oil and gas accumulations. These types of conventional and unconventional petroleum accumulations are commonly observed in sedimentary basins, except for gas hydrates, which are located in sediments on the deep continental shelf

The 'oil window' refers to the maturity range in which oil is generated from oil-prone organic matter. Below is the 'gas window', which refers to the maturity range in which gas is generated from organic matter.
Source: Schenk and Pollastro (2002); Cook et al. (2013b); Schmoker et al. (1995)
Element: GBA-COO-2-172

The term 'unconventional' is used to refer to the collection of petroleum accumulations that are characterised by low permeability and require reservoir stimulation to develop. They include shale oil, shale gas, tight gas, basin-centred gas, coal seam gas, deep coal gas and gas (methane) hydrates (Figure 4 and Figure 5). 'Unconventional' and 'conventional' petroleum accumulations can form from the same source rocks (Schmoker, 2002; Schmoker et al., 1995), but due to differences in expulsion, transport, and trap mechanisms, hydrocarbons are extracted using different methods.

The unconventional gas accumulations present in the Cooper Basin include shale gas, tight gas, deep coal gas and coal seam gas (Goldstein et al., 2012; Hall et al., 2019). These are described in more detail below.

2.1 Tight gas

Tight gas is natural gas trapped in siltstone and sandstone reservoirs characterised by low porosity (<8–10%) and permeability (<0.1 mD). Tight gas reservoirs have been exploited for several decades in Australia (Cook et al., 2013b).

Tight gas may occur in discrete reservoirs, where migrated gas accumulates in rocks with low porosity and permeability, in a similar manner to conventional accumulations (e.g. Shanley and Robinson (2004)). Alternatively, tight gas may occur in distributed gas accumulations which have been referred to in the United States as basin-centred tight gas (Law and Curtis, 2002; Schmoker et al., 1995). They are low permeability gas reservoirs which are commonly abnormally overpressured, lack an apparent down dip water contact and are pervasively gas saturated (Fall et al., 2002; Law and Curtis, 2002). The combined effect of high water pressure and capillary pressure resulting from narrow pore throats in the tight reservoirs prevents hydrocarbons from migrating freely and so they remain trapped. These reservoirs can be laterally and vertically extensive, with gas saturation pervasive throughout. The rate of migration of gas into the reservoir exceeds the rate of gas migrating out of the reservoir, often resulting in overpressure. This implies that these reservoirs exist when gas is being actively generated from a nearby source.

Both discrete and distributed basin-centred tight gas accumulations coexist in the Cooper Basin. The pervasive basin-centred gas are present in multiple depocentres across the Cooper Basin, where depths exceed 2800 m (Goldstein et al., 2012; Core Energy Group, 2016; Icon Energy, 2015; Department of Natural Resources, 2018b). The discrete tight gas plays are located within and surrounding conventional fields; for example, the tight gas sands of the Patchawarra Formation in the Moomba and Big Lake fields on the southern end of the Nappamerri Trough. These discrete tight gas plays are produced as part of conventional gas field development so have not been assessed as a separate play type for this study.

2.2 Shale gas

Shale gas is natural gas hosted in sedimentary rocks (commonly shales) with low to moderate porosity (with a pore size of 0.005–0.1 µm; Nelson, 2009) and very low permeability. Shales are a common petroleum source rock and may retain more petroleum than they expel during the thermal maturation process of organic matter. Once the gas has generated, it remains trapped in the shale, where it is either absorbed on to the organic matter in a free state in the pores and fractures of the rock. Shale gas plays usually occur at depths greater than 1000 m to 1500 m below the earth's surface. Shale reservoirs occur with significant (10–100 km) lateral continuity and can be of considerable thickness (>100 m). Where shales act as both the petroleum source and reservoir rock, they are sometimes referred to as 'self-sourcing reservoirs'.

2.3 Deep coal gas

Deep coal gas is natural gas hosted in coals at depths typically greater than 2000 m below the land surface that do not require dewatering as part of gas extraction process. At these greater depths, the lack of well-developed cleats and decrease in fracture permeability mean than hydraulic stimulation is often required to release the gas.

2.4 Coal seam gas

Coal seam gas is natural gas extracted from coal seams found at depths typically less than 1000 m below the land surface and is predominantly (>95%) methane. The gas is transiently held in place either in the fractures or adsorbed onto the coal's surface by the pressure of formation water in the coal. The large surface area to volume ratio of coals makes them very high capacity reservoirs, Coal seam gas plays require dewatering as part of gas extraction process, in contrast to shale, tight and deep coal gas which do not.

Coal seam gas can be either thermogenic or biogenic. Biogenic gas is produced by microorganisms under the surface of the earth, whereas thermogenic natural gas results from chemical reactions that occur as organic material in the rock is heated as it is buried.

Coal seam gas (including deep CSG in the Weena Trough of the Cooper Basin) was considered as part of the Bioregional Assessment Program (Smith et al., 2016) and hence is not included in the Cooper GBA Region Geological and Bioregional Assessment.

3 Petroleum prospectivity of the Cooper Basin

The Cooper and Eromanga basins have produced 6.54 Tcf of gas since 1969 (Geoscience Australia, 2018). They contain 256 gas fields and 166 oil fields currently in production, and they are nationally significant in providing gas to the East Coast Gas Market (Table 1; Figure 6) (Hall et al., 2015a). There is active exploration and development of oil and gas resources in the Cooper and Eromanga basins, with most of the basin covered by exploration permits, retention licences and production licences (Figure 6).

Table 1 Cooper Basin petroleum prospectivity summary

PETROLEUM PROSPECTIVITY - GENERAL	
Petroleum systems	Proven (Gondwanan)
Prospectivity	High
Conventional discoveries	256 gas fields and 166 oil fields currently in production (Cooper Basin and surrounding area)
Hydrocarbon production–total to date	6.54 Tcf cumulative conventional gas production; no coal seam gas (CSG) (includes overlying Eromanga Basin; current to 2014)
2P Reserves	1.54 Tcf conventional; no CSG (includes overlying Eromanga Basin; current to 2014) (Geoscience Australia, 2018)
Remaining resources (reserves + contingent resources)	3.2 Tcf conventional; 0.4 Tcf CSG; see below for shale/tight gas (includes overlying Eromanga Basin; current to 2014) (Geoscience Australia, 2018)
Undiscovered resource estimates	0.9 Tcf conventional; 6.7 Tcf deep CSG (Smith et al., 2016); see below for shale and tight gas (at P50)) (Geoscience Australia, 2018)
PETROLEUM PROSPECTIVITY–SHALE/TIGHT GAS	
Unconventional play types	Tight gas, shale gas, deep coal
No of wells targeting shale/tight gas plays	> 80
Production–shale/tight gas	Minor shale and tight gas production from Moomba 191, 193H and 194 (Santos, 2012, 2013a, b)
2P Reserves–shale/tight gas	None currently reported
Remaining resources (reserves + contingent resources)–shale/tight gas	8.74 Tcf shale gas; 0.84 Tcf tight gas (includes overlying Eromanga Basin) (Geoscience Australia, 2018)
Undiscovered resource estimates–shale/tight/deep coal gas	Combined potentially recoverable shale gas in place (GIP) (5% recovery factor at P50) of 6.9 Tcf in the Roseneath Shale (prospective area wet gas 3834 km^2, dry gas 3403 km^2) and Murteree Shale (prospective area wet gas 3454 km^2, dry gas 3291 km^2) (Geoscience Australia, 2018). Combined potentially recoverable tight GIP (5% recovery factor at P50) of 50.9 Tcf in the Patchawarra Formation (prospective area wet gas 14,426 km^2, dry gas 3417 km^2), Epsilon Formation (prospective area wet gas 5413 km^2, dry gas 3401 km^2), Daralingie Formation (prospective area wet gas 4691 km^2, dry gas 3102 km^2) and Toolachee Formation (prospective area wet gas 15,070 km^2, dry gas 2725 km^2) (Geoscience Australia, 2018). Preliminary deterministic sales of Permian coal GIP of 181.05 Tcf (Core Energy Group, 2016; Goldstein, 2016).
Hydrocarbon shows, tests–shale/tight gas	Production from Moomba 191, 193H and 194 (Santos, 2012, 2013a, b)

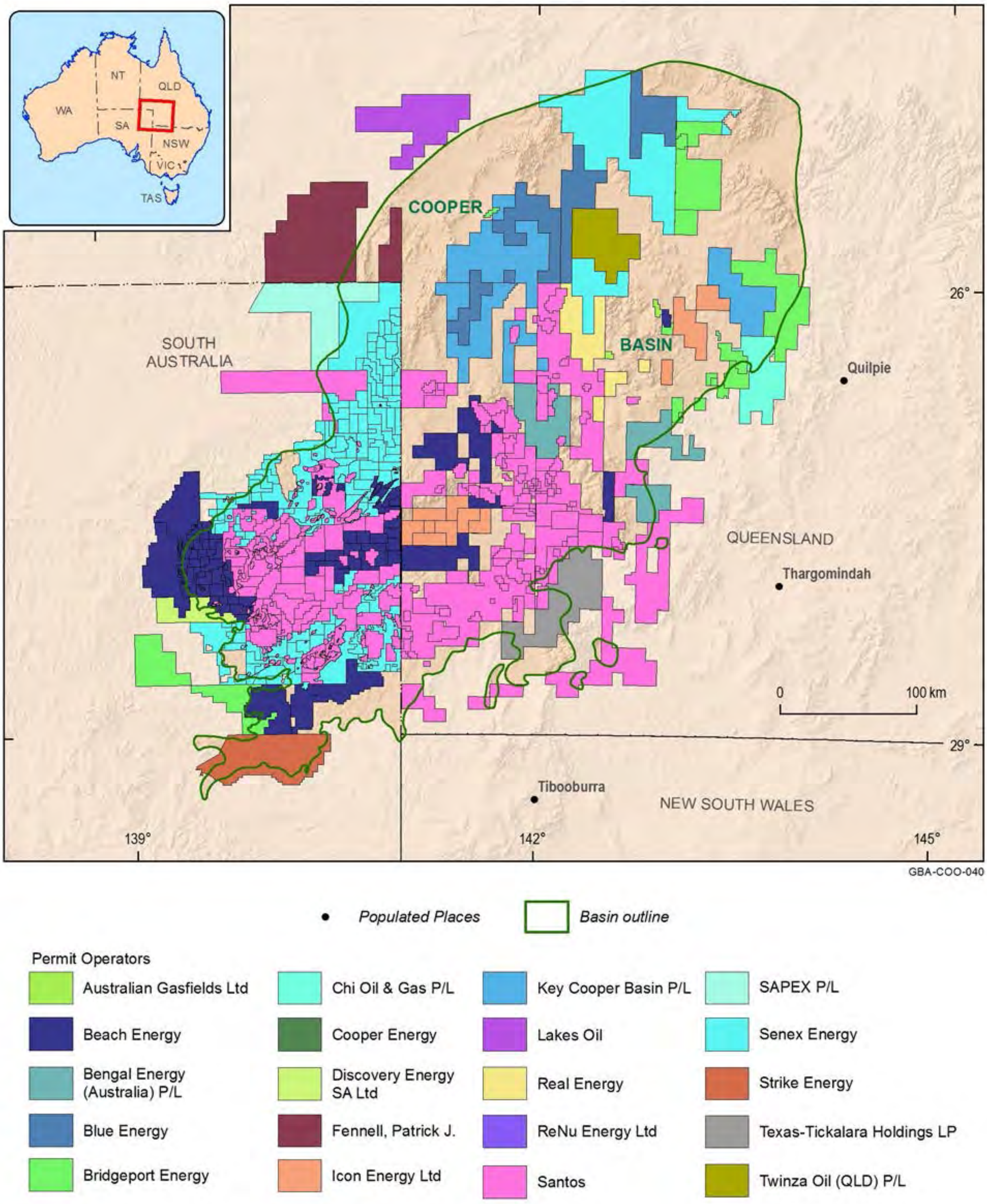

Figure 6 Cooper Basin exploration, retention and production permit operators

Data: Permit operators and outlines are provided from GPinfo petroleum database, a Petrosys Pty Ltd product (Petrosys Pty Ltd, 2019); Cooper Basin outline from Raymond et al. (2018); Hill-shade derived from 9-second DEM from Hutchinson et al. (2008)
Element: GBA-COO-040

3.1 Exploration history

The following history of exploration history in the Cooper Basin is updated from summaries by O'Neil (1998), Hall et al. (2015a), Goldstein et al. (2012) and Greenstreet (2015) (Table 2).

Table 2 Summary of exploration status

EXPLORATION STATUS	
Seismic lines	>81,000 line km of 2D seismic; >10,000 km^2 of 3D seismic
Number of petroleum wells	>3000
Exploration status–conventional	Producing/mature
Exploration status–coal seam gas	Under assessment
Exploration status–shale/tight/deep coal gas	Underexplored

3.1.1 Conventional petroleum exploration

The first Oil Exploration Licence (OEL) was granted in 1945 to A.J. Keast on behalf of Zinc Corp. Ltd. It covered 10,360 km^2 between Lake Frome and the NSW border, in the southern part of the Cooper Basin in South Australia. Exploration in the basin by Santos began in 1954. Their initial wildcat well, Innamincka 1 drilled in 1959, was the first well to drill through the Cooper Basin succession, reaching gently dipping Ordovician beds at a depth of 3852 m. The well penetrated thick Triassic sediments underlain by a thin Permian section. Oil and gas potential was suggested by minor hydrocarbon shows in sediments within the Mesozoic succession. Thirty five cores were taken during the drilling and ten drill stem tests were run, providing evidence of both gas with water and oil-cut mud in the Permian and Mesozoic sections (O'Neil, 1998).

Over the next few years new seismic data were acquired and more wells were drilled that increased the geological understanding of the basin. This work culminated in several wells being drilled along the Gidgealpa–Merrimelia–Innamincka (GMI) Ridge. The well Gidgealpa 1 was drilled in 1963 and penetrated a thick Permian section with several sands with good reservoir properties and gas shows, but well stability issues meant that these could not be tested (O'Neil, 1998). The second well (Gidgealpa 2) was drilled on-structure and drill stem tests in the Permian sands, after the discovery of gas on 31 December 1963, indicated a flow of 56,634 m^3/day (2 mmcfd) and on completion, produced gas and condensate (O'Neil, 1998; Santos, 2018a, 2018d). The discovery of commercial gas at Gidgealpa 2 attracted new players to the basin and an increase in exploration activity.

The discovery of natural gas in the Moomba 1 well by Delhi–Santos in 1966 was followed by further exploration wells, proving the existence of large widespread gas reserves and paving the way for the commercial development of the Cooper Basin (O'Neil, 1998). Initial gas sales to Adelaide began in 1969, followed by Sydney in 1976 and Brisbane 20 years later (Santos, 2018a).

The first Permian oil discovery was announced by Bridge Oil in 1970 when light crude oil flowed from the Tirrawarra Sandstone in their Tirrawarra 1 well, while the first Jurassic-hosted oil was discovered in Strzelecki 3 (1978) in the Hutton Sandstone of the overlying Eromanga Basin (Santos, 2018a).

Between 2009 and 2014, there was a revival in exploration activity in the Cooper Basin driven by high resource prices, and an increased interest in newly identified unconventional hydrocarbon plays in the basin. In 2014, a new record of 119 petroleum wells were drilled in the SA part of the basin, coupled with major 3D seismic acquisition. In 2015, activity levels began to taper during a period of low global oil prices, but infill gas development drilling and oil discovery appraisals still continued (Hall et al., 2015b).

There is currently active exploration and development of conventional oil and gas resources in the Cooper Basin. Key operators include Beach Energy, Icon Energy, Santos and Senex Energy (Figure 6). The flanks of the major depocentres remain the main targets for conventional oil and gas explorers. Here, reservoirs in the Cooper and Eromanga basins are charged from source rocks in the troughs. Major gas fields include Moomba and Big Lake on the South Australian side and Challum in Queensland, whereas the western flank of the basin is a hotspot for oil exploration and production.

3.1.2 Unconventional exploration

There is active exploration targeting a range of unconventional plays within the Cooper Basin (Goldstein et al., 2012; Hillis et al., 2001; Greenstreet, 2015) and, to date, at least 80 wells have been drilled to test primary and secondary targets for shale, tight and deep coal gas plays (Figure 8) (Business Queensland - Queensland Government, 2018; Department for Energy and Mining (SA), 2018a).

In December 2011, Santos drilled Moomba 191, the first dedicated vertical shale gas well, which flowed gas at 2.7 mmcfd from shales in the Roseneath-Epsilon-Murteree (REM) section (Santos, 2012, 2018a). Following completion, this was connected to the Moomba processing facilities in October 2012, bringing the first shale gas production to the East Coast Gas Market (Goldstein et al., 2012; Santos, 2012, 2018a).

Although the presence of a pervasive tight gas accumulation in the Nappamerri Trough (Figure 1) had been suspected for over two decades (e.g. Hillis et al., 2001), in 2011 this was confirmed by the intersection of gas saturated sands outside of structural closure in the Encounter 1 and Holdfast 1 wells (Beach Energy, 2011a, 2011b; Goldstein et al., 2012) (Figure 7). Since this time extensive exploration for tight and shale gas by Beach Energy, Drillsearch (owned by Beach Energy as of 2016), Santos and Senex has resulted in the drilling of over 20 wells in the western Nappamerri Trough in South Australia (e.g. Department for Energy and Mining (SA), 2018a; Beach Energy, 2014). In Queensland a further ten wells have been drilled by Beach Energy and Drillsearch, examining the shale and tight gas resource potential of the Gidgealpa Group in the eastern Nappamerri Trough (Figure 8) (Business Queensland - Queensland Government, 2018; Beach Energy, 2014).

Figure 7 Holdfast 1 wellhead in the Cooper Basin

Source: Department for Energy and Mining, South Australia, October 2012
Credit: Jarrod Spencer
Element: GBA-COO-2-186

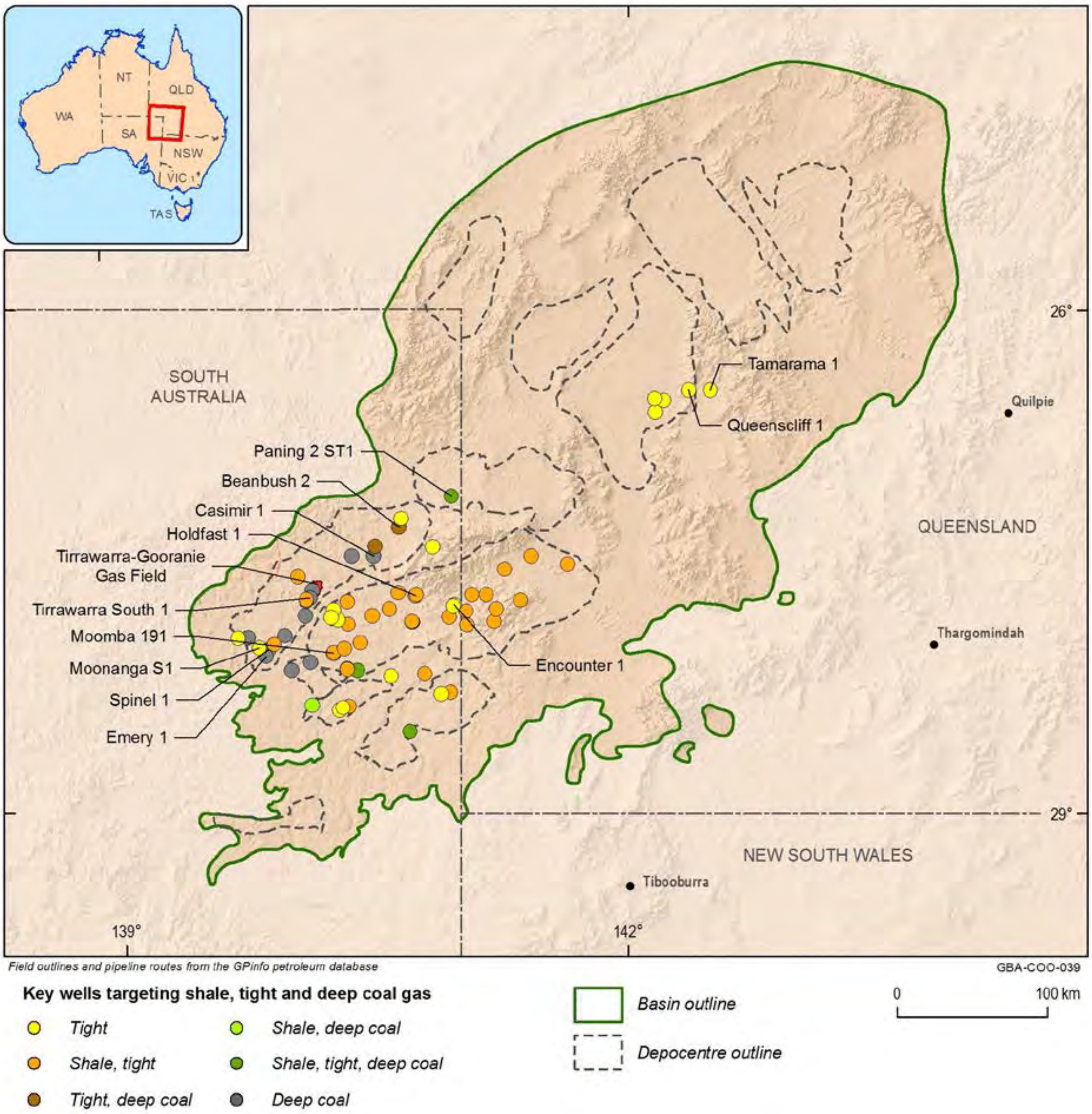

Figure 8 Key wells targeting selected unconventional gas plays in the Cooper Basin

Data: Wells targeting shale, tight and deep coal gas plays are compiled from Department of Natural Resources Mines and Energy (Qld) (2018a); Department for Energy and Mining (SA) (2017, 2018a) and company websites (e.g. Real Energy, 2014, 2018; Beach Energy, 2018; Senex Energy Ltd, 2013; Beach Energy, 2015c); Cooper Basin outline from Raymond et al. (2018)
Element: GBA-COO-039

The productivity of the deep Permian coals was initially proven by Santos at the Moomba 77 well in 2007, which flowed gas to surface at 100,000 scfd from a fracture stimulated deep Patchawarra Formation (Goldstein et al., 2012). The Cooper Basin's first stand-alone deep coal producer, Tirrawarra South 1, in the Patchawarra Trough, flowed wet gas and was successfully brought online in 2015 (Santos, 2015). Additional significant exploration activity for deep coal gas includes the following:

- In the Arrabury Trough, Paning 2 intersected 70 m of Permian coals and 117 m of net gas pay in the Toolachee Formation, which flowed at a maximum rate of 90,000 scfd during a four day production test (Senex Energy Ltd, 2013).

- In the eastern Patchawarra Trough, Beanbush 2, a stand-alone appraisal well, targeted both conventional gas and deep coal gas from seams in the upper and middle Patchawarra Formation, Epsilon and Toolachee formations (Beach Energy, 2015c).
- An eight well exploration program by Santos in the southern Patchawarra Trough also tested the gas potential of both conventional plays and unconventional deep coal zones (including Spinel 1, Emery 1 and Moonanga South 1) (Santos, 2015).
- A six well drilling program conducted around the Tirrawarra and Gooranie fields in the Patchawarra Trough (approximately 50 km north of Moomba) included one deep coal hydraulic stimulation per well (Beach Energy, 2015a).
- Approximately 75 km north of Moomba in the northern Patchawarra Trough, Casimir 1 targeted multiple deep coal seams in the Toolachee and Epsilon formations as a primary objective and deep coal seams in the Patchawarra Formation as a secondary objective. The well intersected 11 Permian coals suitable for hydraulic fracturing with net thickness of 55 m and was cased and suspended for future completion, hydraulic stimulation and flow testing (Beach Energy, 2018).

3.2 *Reserve and resource estimates*

Total reported gas reserves and resources for the Cooper-Eromanga Basin couplet are listed in Table 3 (Geoscience Australia, 2018). Further details of shale, tight and deep coal gas reserves and resources are described below. Note the petroleum industry in Australia uses the Petroleum Resources Management System (PRMS, 2007) for classification of oil and gas resources of companies registered on the Australian Securities Exchange (ASX ,2014; RISC, 2013).

Table 3 Total reported Cooper–Eromanga Basin gas reserves and resources

Gas resource Type	2P Reserves (Tcf)	Remaining resources (reserves + contingent resources) (Tcf)	Prospective Resources (Tcf)
Conventional	1.54	3.2	0.9
Deep CSG	0	0.4	6.5
Shale	0	8.75	138.3
Tight	0	0.84	1019.0
Total	1.54	13.9	1164.7

Deep CSG resources have not been assessed as part of the previous Bioregional Assessment Program (Australian Government, 2018). Deep coal gas resources remain unassessed
Source: AERA, Geoscience Australia (2018)

Although three wells targeting shale and tight gas plays in the Cooper Basin have sustained production (Moomba 191, 193H and 194) (Santos, 2013), no reserves of shale, tight or deep Permian coal gas are currently reported.

Beach Energy, Drillsearch, Santos and Senex have reported contingent resources for shale, tight and deep coal gas plays in the Cooper Basin, current to 2017 (Hall et al., 2018). The most significant 2C Contingent Resources for unconventional gas (3.52 Tcf) are associated with the Cooper Basin Joint Venture (Santos, 2012).

Table 4 Industry reported unconventional gas Contingent Resources (Tcf) for the Cooper Basin

State	Assessment area	Operator	Contingent resources (Tcf)			Play type	Reservoir	Source
			1C	2C	3C			
QLD	ATP 855 (Nappamerri Trough)	Beach	0.34	1.57	5.84	Shale gas, tight gas	Various	Beach Energy (2015b)
QLD	ATP 940 (100%)	Drillsearch/ Beach	0.22	0.77	1.85	Shale gas, tight gas	Various in Charal 1 and Anakin 1	Drillsearch (2015)
SA	PELs 33 to 49 (Nappamerri Trough)	Beach	0.95	1.96	3.9	Shale gas, tight gas	Various	Upstream Petroleum Resources Working Group (2015)
SA	CBJV (PPLs 7, 8, 9, 11, 101, 102, 113)	Santos	1.73	3.52	6.84	Shale gas, tight gas	Various	Santos (2012)
SA	PEL 115, 516	Senex	0.15	0.84	2.37	Tight gas	Tight sands in the Hornet field	Senex Energy Ltd (2013)
SA	PEL 516 (Allunga Trough)	Senex	0.12	0.7	2.05	Shale gas, tight gas	Patchawarra Formation and Murteree Shale in Sasanof 1	Senex Energy Ltd (2013)
SA	Arrabury Trough	Senex	0.91	0.421	1.055	Deep coal gas	Toolachee Formation in Paning 1	Senex Energy Ltd (2013)

Refer to the source references for further details on assessment area, methodology and associated uncertainties
Source: Hall et al. (2018)

In addition, Senex booked 2C resources of 0.421 Tcf for Patchawarra Formation coals around Paning 2 (PEL 90) in the Arrabury Trough (Senex Energy Ltd, 2013).

It should be noted though that in 2016, Beach Energy reduced the contingent resources associated with the Nappamerri Trough Natural Gas Project from their annual reserves statement (Beach Energy, 2016). Beach stated that the results of stage 1 of the exploration program "demonstrated that the high cost of addressing fundamental technical issues means the Nappamerri Trough Natural Gas Project is unlikely to be developed commercially in the medium term".

Geoscience Australia estimates the following undiscovered, potentially recoverable unconventional gas resource for the Cooper Basin:

- Potentially recoverable shale gas (5% at P50) resources of 7 Tcf in the Nappamerri, Patchawarra and Tenappera troughs (Geoscience Australia, 2018).
- Potentially recoverable tight gas resources of 51 Tcf for the Patchawarra, Epsilon, Daralingie and Toolachee formations, including dry, wet and oil associated gas (Geoscience Australia, 2018).

Other published basin scale prospective resource estimates for shale and tight plays in the Cooper Basin are summarised below:

- The US Energy Information Administration (EIA) estimated the technically recoverable shale gas in the Roseneath-Epsilon-Murteree (REM) play in the Cooper Basin. Initial estimate was 85 Tcf (EIA, 2011) which was later revised to 92 Tcf (EIA, 2013).
- AWT Energy Solutions have reported the best estimate on recoverable shale gas resource in the REM is 14 Tcf for wet gas, and 35 Tcf for dry gas (AWT International, 2013).
- The United States Geological Survey published the following F50 (P50) estimate total undiscovered recoverable tight gas resources: 2.215 Tcf in the Patchawarra Trough, 14.547 Tcf in the Nappamerri Trough and 8.975 Tcf in the Queensland troughs (U.S. Geological Survey, 2016).
- Preliminary deterministic sales of Permian coal GIP of 181.05 Tcf (Core Energy Group, 2016; Goldstein, 2016).

It should be noted that there are significant uncertainties associated with prospective resource numbers, which affect how resources are estimated and reported. As a result, the following factors need to be considered when interpreting these data:

- The area covered by each assessment varies. Company numbers are reported for individual permits. In contrast, independent assessments (for example those by federal, state or territory government or independent assessors) have been conducted regionally to capture the entire play area.
- Assessment methodologies differ and the data underpinning them may vary considerably in terms of amount, type and quality (as discussed above).
- Recovery factors are very poorly defined, especially for shale and tight gas plays.

3.3 Gas market access and infrastructure

The Cooper Basin is a major supplier of gas to Australia's East Coast Gas Market, with significant existing pipeline infrastructure connecting the basin to Adelaide, Sydney, Barcaldine, South-east Queensland and Mount Isa (Figure 3; Table 5) (AER, 2017).

Table 5 Summary of market access and infrastructure

INFRASTRUCTURE	
Gas market	Currently supplies to the East Coast Gas Market
Proximity to gas pipelines	Moomba to Adelaide Pipeline - capacity 241 TJ/Day (55 reverse) Moomba to Sydney Pipeline - capacity 439 TJ/Day (382 reverse) Carpentaria Pipeline (Ballera to Mount Isa)–capacity 119 TJ/Day South West QLD Pipeline (Ballera to Wallumbilla)–capacity 404 TJ/Day (340 reverse)
Gas processing facilities	Moomba (SA); Ballera (QLD)
Approx. distance from existing pipelines to area prospective for shale gas, tight gas and/or deep Permian coal gas	<100 km
Road and rail access	Moderately well serviced by road; no rail service
Approximate development timeframe	5–10 years

Source: Hall et al. (2018). Pipeline information from AER (Australian Energy Regulator) (2017). Oil and gas infrastructure from Geoscience Australia (2015b), AER (Australian Energy Regulator) (2017), Santos (2018b) and Santos (2018c). Processing facilities from Geoscience Australia (2015a).

The Cooper Basin is remote with a sparse population. A high proportion of the population is itinerant, working in the oil and gas industry. Other industries include pastoral and tourism. The climate is hot and dry, with infrequent rainfall events sometimes resulting in flooding. Roads into and within the Cooper Basin area are unsealed, with the exception of the Adventure Way. The Adventure Way starts on the Queensland side of the Strzelecki Track near Innamincka, and passes through Ballera and eastwards. Moomba and Ballera are serviced by jet-capable sealed airstrips. Many drilling service providers active in the area are based in Queensland (e.g. Roma, Toowoomba). The Moomba and Ballera water supplies are provided from local bores and purified through a membrane treatment plant (Santos, 2018c, 2018b, 2018d). Electricity is generated at Moomba, on-site via a 20 MW gas-fired power plant, and at Ballera, at a 45 MW gas-fired power plant.

Located approximately 770 km north of Adelaide in South Australia, Moomba is one of two major oil and gas processing and operations supply centres for the Cooper Basin. It is operated by Santos Ltd and owned by Cooper Basin Producers (Figure 3) (Santos, 2018d; Goldstein et al., 2012). The Moomba processing facility produces from 115 gas fields and 28 oil fields through approximately 5600 km of pipelines and flowlines via 24 oil and gas satellite facilities. CO_2 stripping of gas is also performed at the Moomba processing facility. Natural gas liquids, together with stabilised crude oil and condensate, are sent through a 659 km pipeline to Port Bonython near Whyalla. Sales gas is sent from Moomba to Adelaide via a 790 km pipeline, and to Sydney via a 1160 km pipeline (Goldstein et al., 2012; Santos, 2018c). Ethane is sent via a dedicated pipeline to Sydney (Goldstein et al., 2012). The south-west Queensland Pipeline is a 937 km long pipeline from Moomba to

Wallumbilla in south-east Queensland and includes the 180 km Queensland to South Australia/New South Wales Link running from Ballera to Moomba (Goldstein et al., 2012; Santos, 2018c).

Additional processing facilities are located at Ballera in south-west Queensland (Figure 3). The Ballera gas processing facility is owned by Santos Ltd, Delhi Ltd and Origin Ltd, and operated by Santos Ltd (Santos, 2018b). It produces from approximately 45 gas fields (Figure 3) (Santos, 2018b). The Ballera facility also incorporates the Chookoo storage facility that is used for the storage and processing of sales gas at the Chookoo field. Sales gas is sent to Mt Isa via an 800 km pipeline (Santos, 2018b). The remaining gas, natural gas liquids and condensate, are sent to Moomba via the 180 km Ballera-Moomba pipeline (Santos, 2018b). As no crude oil is processed at Ballera, all oil is sent to the Jackson facility 65 km to the south-east (Santos, 2018b).

3.4 Regional petroleum systems

3.4.1 Introduction

Table 6 Summary of regional petroleum systems

Play types - conventional	Conventional oil and gas (sandstone reservoirs with structural traps and pinch out plays on basin margins).
Play types - unconventional	Basin-centred tight gas, low permeability (discrete) tight gas, shale gas, deep coal gas, and coal seam gas.
Reservoirs	Several formations in the Gidgealpa Group and Nappamerri Group (Toolachee, Daralingie, Epsilon and Patchawarra formations and pro-glacial sediments of Tirrawarra Sandstone). Roseneath and Murteree shales are considered unconventional shale gas reservoirs.
Seals	Regional seal is the Nappamerri Group, predominantly sedimentary rocks of the Arrabury Formation with impermeable intraformational seals recognised in all reservoir units except the Tirrawarra Sandstone. Formational seals within Roseneath and Murteree shales of the Gidgealpa Group. Overlying Eromanga Basin sediments also act as a seal across much of the basin.
Source rocks	Source rocks occur throughout the basin; most units that contain coals or coaly shales have some source potential. Richest source rocks are found in the Patchawarra and Toolachee formations.
Hydrocarbon shows	Shows are found within most of the formations and are associated with major reservoir units.

Source: Carr et al. (2016)

Gas is predominantly reservoired in the Cooper Basin, whereas the overlying Eromanga Basin hosts mainly oil. Bradshaw (1993), Bradshaw et al. (1997) and Bradshaw et al. (2012) assigned the oils and gases derived from non-marine Permian source rocks in the Cooper Basin to the Gondwanan Petroleum Supersystem, and the oils derived from Early Cretaceous source rocks in the Eromanga Basin to the Murta Supersystem. However this schema is an oversimplification with many reservoirs having been charged multiple times (Powell et al., 1989; McKirdy et al., 2001; Michaelsen and McKirdy, 2001; Arouri et al., 2004) and the phases of petroleum generation and migration are complex.

3.4.2 Petroleum systems elements

Source rocks

Source rocks are found in all formations of the Permian Gidgealpa Group (Table 6; Figure 2; Figure 9), although source rock quantity and quality varies significantly (Boreham and Hill, 1998; Hall et al., 2016b; Jadoon et al., 2016; Deighton et al., 2003). Coals and coaly shales of the Toolachee, Daralingie, Epsilon and Patchawarra formations, as well as the Roseneath and Murteree shales, all contain good to excellent source rocks (Total Organic Carbon [TOC] >2 wt%), with a range of Type II/III, Type II and Type IV kerogens. There is limited source potential in the latest Carboniferous to early Permian glacial sediments (Tirrawarra Sandstone and possibly the Merrimelia Formation) as well as in the Lower–Middle Triassic Nappamerri Group (Hall et al., 2016b).

Reservoirs and seals

The main commercial reservoirs are in the Patchawarra and Toolachee formations and, to a lesser extent, the Epsilon Formation in south-western Queensland. Commercial reservoirs also exist in the Merrimelia Formation, Tirrawarra Sandstone, Daralingie and Arrabury formations (Gray and Draper, 2002; Gravestock et al., 1998a; Gravestock et al., 1998b). The Roseneath and Murteree shales are shale gas play reservoirs (Goldstein et al., 2012).

The Nappamerri Group is generally regarded as a major basin wide seal to the Gidgealpa Group. The Roseneath Shale is the seal to the Epsilon Formation, and the Murteree Shale provides the seal to the underlying Patchawarra Formation (Figure 9) (Gravestock et al., 1998a; Gray and Draper, 2002). Additional intraformational seals, particularly within the fluvio-deltaic formations, are present throughout the Gidgealpa Group.

Source rock reservoirs

Some of the unconventional plays examined here are source rock reservoirs, where the reservoir rock that would be developed is also the source of hydrocarbons, these include shale gas plays within the Patchawarra Formation, the Murteree and Roseneath shales and deep coal gas plays in the Patchawarra, Epsilon and Toolachee formations.

Gas in shale is stored as adsorbed gas on the organic matter, free gas stored in the pore spaces and dissolved gas in the formation water. Porosity, permeability and fluid saturation are three of the key petrophysical input parameters required for characterising shale plays.

Deep coal plays are similar to shale gas in that porosity, permeability and fluid saturation are key petrophysical input parameters required for characterising them. The coal fabric or planes of weakness inside the coal seams are important for deep coal gas production. Potential coal fabric types include vitrinite cleats, inertinite master joints, other natural fractures, faults, contrasts in lithology and weak bedding planes (Dunlop et al., 2017).

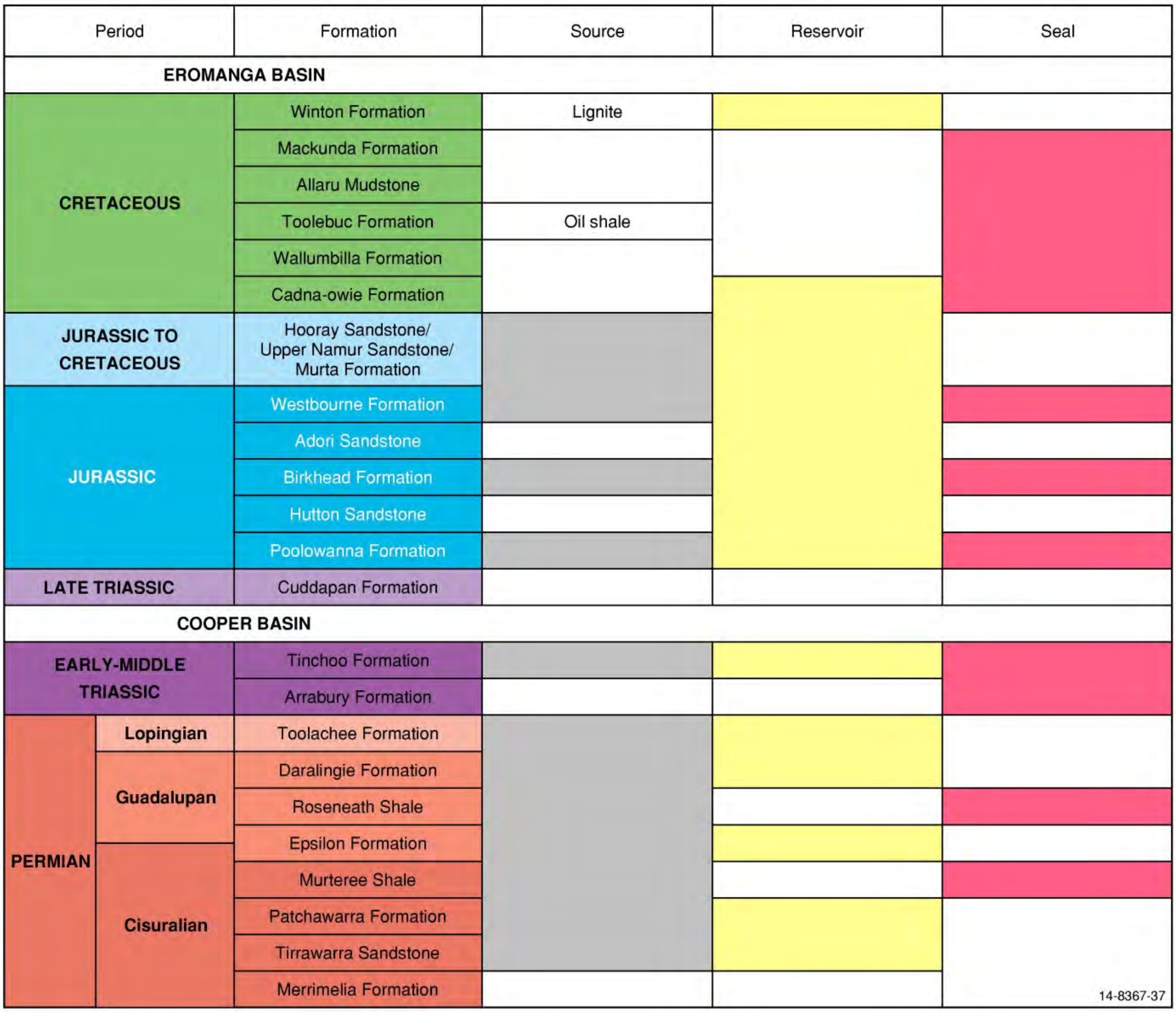

Figure 9 Stratigraphic units and presence of source, conventional reservoir and seal rocks in the Cooper and Eromanga basins

Source: Modified from Deighton et al. (2003)
Element: GBA-COO-2-227

3.4.3 Petroleum geochemistry

Boreham and Summons (1999) used the carbon isotopic compositions of individual n-alkanes to differentiate between different source–reservoir couplets within the Cooper and Eromanga basins. The couplets for most economic accumulations involve either Cooper Basin source and reservoir, or Cooper Basin source and Eromanga Basin reservoir. A subordinate couplet involves Eromanga Basin source and reservoir; however, such oils are predominantly mixed with upwardly migrating oils from the Cooper Basin. There may also be a minor input from pre-Permian sources to reservoirs within both the Cooper and Eromanga basins. Further studies on determining the source of oil and gas in the Cooper-Eromanga basins is provided by Alexander et al. (1998b); Tupper and Burcjhardt (1990); Michaelsen and McKirdy (2001).

The Cooper Basin contains liquid hydrocarbons with a wide range of compositions from light oil condensates to waxy oils, where the majority of the latter have depleted light hydrocarbon content (Elliott, 2015b; Boreham and Summons, 1999; Summons et al., 2002). The oils are characterised by API gravities between 34° and 53°, with the most biodegraded oils typically having the lowest values (Elliott, 2015a) and low sulphur contents (<0.1% S). The liquid hydrocarbons are sourced from terrestrial organic matter contained within Permian coals, shaly coals, coaly shales and fluvial to deltaic shales.

3.4.4 Play types

Conventional exploration in the Cooper Basin has generally focused on stacked gas or oil pools in sandstone reservoir successions within structural traps (anticlinal and faulted trap plays) (Department for Energy and Mining (SA), 2018b). Stratigraphic pinch-out plays, where the reservoir rock tapers out against an impermeable sealing rock, have also been tested along the basin margins, with several commercial successes recorded. Locally, Permian oil has migrated into the underlying Warburton Basin reservoirs on the basin margin and gas has migrated into fractured Ordovician reservoirs fringing the Allunga Trough forming a potential exploration play in the southern part of the basin (Department for Energy and Mining (SA), 2018b). Other stratigraphic plays also remain of significant exploration interest (Radke, 2009; Department for Energy and Mining (SA), 2018b). Hydrocarbon-filled structures may have developed as early as the Permian and have complex reactivation histories (Kulikowski and Amrouch, 2018; Kulikowski et al., 2017).

Resource companies are also pursuing a range of unconventional plays within the basin (Hillis et al., 2001; Goldstein et al., 2012; Greenstreet, 2015; Hall et al., 2015b; Menpes et al., 2013; Menpes and Hill, 2012). The principal shale gas play is the Roseneath-Epsilon-Murteree (REM) play comprising Permian Murteree and Roseneath shales separated by tight sands of the Epsilon Formation (Menpes and Hill, 2012; Goldstein et al., 2012; Greenstreet, 2015; Department for Energy and Mining (SA), 2018c). These formations are generally restricted in extent to the southern part of the basin (Hall et al., 2015b; Hall et al., 2015a). The South Australian Government has defined the Cooper Basin shale gas play fairways based on the following criteria: Murteree Shale exceeds 20 m thickness, total Patchawarra TOC >2% and the base of the Murteree Shale structure surface is greater 2900 m (Department for Energy and Mining (SA), 2018c). Beach Energy has publicly discussed the mineral composition of the shales (characterising them as being high in silica and illite, with moderate siderite, and lacking swelling clays such as smectite) which collectively are conducive to brittleness and ideal for hydraulic stimulation (Trembath et al., 2012). Well data suggests lower porosity than producing shale gas plays in the United States and highlights the requirement for thicker and overpressured shale sections to commercialise the resource (Department for Energy and Mining (SA), 2018c).

Tight gas plays are present in multiple depocentres across the Cooper Basin (Figure 8) (Menpes and Hill, 2012; Goldstein et al., 2012; Greenstreet, 2015; Department for Energy and Mining (SA), 2018c). The most extensive tight gas play lies within the Nappamerri Trough, where the Permian succession reaches over 1.3 km thick and comprises very thermally mature, gas-prone source rocks with interbedded sandstones (Department for Energy and Mining (SA), 2018c). Thick siltstones of the Nappamerri Group act as a regional top seal for the pervasive gas accumulations, and the Roseneath and Murteree shales also assist with gas containment. Generation and expulsion of hydrocarbons from the Cooper Basin source rocks occurred in the mid-Cretaceous

(Hall et al., 2016b). Overpressure has been retained in the Nappamerri Trough (Hillis et al., 2001; Goldstein et al., 2012).

Gas saturated deep coal plays in the Permian Toolachee, Epsilon and Patchawarra formations (which do not require dewatering as part of the gas extraction process) are an additional exploration target in multiple depocentres (Menpes and Hill, 2012; Goldstein et al., 2012; Greenstreet, 2015; Department for Energy and Mining (SA), 2018c), including the Patchawarra, Nappamerri and Arrabury Troughs (Senex Energy Ltd, 2013; Beach Energy, 2018, 2015a, 2015c).

Exploration for coal seam gas (which does require dewatering as part of the gas extraction process) is primarily restricted to the Weena Trough in South Australia (Figure 1), where very large thicknesses of coal are found in the Patchawarra Formation. Thermal maturities are low (<0.75 %Ro) at the base of the Patchawarra Formation (Department for Energy and Mining (SA), 2018c). Coal seam gas plays are not in the scope of the Geological and Bioregional Assessment Program.

4 Shale gas, tight gas and deep coal gas play characterisation

4.1 *Characteristics by formation*

The amount of gas (and oil) present within a play, as well as the proportion of hydrocarbons that can be produced, depends on the geological characteristics of both the source and reservoir rock.

The geological properties of the formations required for each play to be successful were identified and characterised, to underpin further work on understanding likely development scenarios. The physical properties evaluated, which vary by play type, include formation depths and extents, source rock properties (net thickness, TOC, quality and maturity), reservoir characteristics (porosity, permeability, gas saturation and brittleness), regional stress regime and overpressure. The information presented herein builds on a regional geological analysis and conceptualisation of the Cooper GBA region presented in the Geology technical appendix (Owens et al., 2020).

4.1.1 Tirrawarra Sandstone

Key features of the Tirrawarra Sandstone are summarised below in Table 7 and discussed in more detail in the following text.

Table 7 Key features of the Tirrawarra Sandstone

Unconventional Play type	Tight gas
Age	latest Carboniferous to early Permian (upper Gzhelian to Asselian)
Extent	29,900 km^2
Top depth (m)	795–4460 m
Gross formation thickness	0–75 m
Lithology	Sandstone, conglomerates, minor shale interbeds and rare coal
Depositional environment	Fluvio-glacial
Kerogen type	Type III; coal, Dispersed Organic Matter (DOM)
TOC	0–71 wt%
Mean original HI	192 ± 133 mg HC/g TOC
Thermal maturity	Immature (Weena Trough)–over mature (Nappamerri Trough)
Average permeability	1.59 mD
Average effective porosity	0.075 (fraction) in tight pay intervals
Average effective water saturation	0.465 (fraction) in tight pay intervals
Pressure regime	Overpressured
Exploration status	Active exploration target

4.1.1.1 Age and stratigraphic relationships

The Tirrawarra Sandstone is part of the Gidgealpa Group. The Tirrawarra Sandstone interfingers with the underlying Merrimelia and overlying Patchawarra formations (Alexander et al., 1998a). Recent recalibration of the spore-pollen zones (Nicoll et al., 2015) and updates to the 2012 Global Timescale (Gradstein et al., 2012), indicate a late Carboniferous to early Permian age for the Tirrawarra Sandstone (Figure 2).

4.1.1.2 Extent, depth and gross formation thickness

The isopach of the combined glacial facies (including both the Tirrawarra Sandstone and Merrimelia Formation) shows these sediments cover an area of approximately 29,900 km^2 across the southern part of the Cooper Basin (Figure 10) (Hall et al., 2015a; Owens et al., 2020). It should be noted that uncertainties in this map are largely due to the limited number of wells that fully intersect the glacial section and the lack of clear top pre-Permian basement horizon in many areas. Although no isochore thickness map is available for the Tirrawarra Sandstone alone, well intersections indicate that the Tirrawarra Sandstone is widespread across the extent of the combined glacial facies shown in Figure 10.

The thickest accumulations of glacial sediments are located in the southern part of the basin (Figure 10), in the Patchawarra Trough, northern Nappamerri Trough and Weena Trough, and along the GMI Ridge (Figure 1) (Alexander et al., 1998a; Hall et al., 2015a; Delhi Australian Petroleum Ltd, 1968). The total thickness of the glacial sediments reaches over 600 m. However, well intersections indicate that the Tirrawarra Sandstone remains relatively thin, reaching 75 m thick in South Australia, and thinning to 30 to 40 m in Queensland (Gray and McKellar, 2002). North of the Durham Downs Anticline and Jackson–Naccowlah–Pepita (JNP) Trend, the glacial sediments are limited in thickness (10 to 20 m).

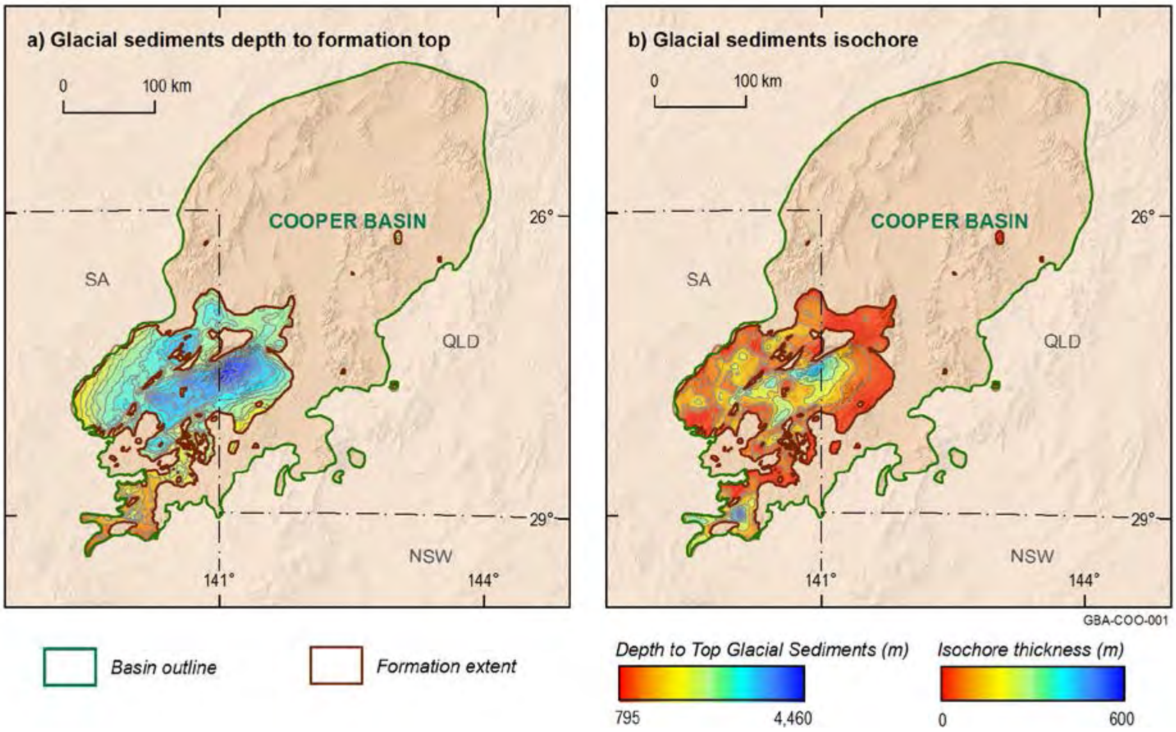

Figure 10 Glacial sediments of Merrimelia Formation and Tirrawarra Sandstone a) top depth, b) total vertical thickness

Source: Hall et al. (2015a)
Data: Hall et al. (2016a); Cooper Basin outline from Raymond et al. (2018)
Element: GBA-COO-001

4.1.1.3 Lithology and palaeoenvironment

The Tirrawarra Sandstone comprises fine to coarse-grained, moderately well sorted sandstone, common conglomerates with minor shale interbeds and rare thin coal seams and stringers (Alexander et al., 1998a; Hall et al., 2015a; McKellar, 2013).The Tirrawarra Sandstone was deposited as reworked unconsolidated glacial sediments by melt-water streams flowing north from retreating glaciers (Alexander et al., 1998a).

The thickest accumulations of glacial sediments follow a deep glacial scour which runs from the southern Patchawarra Trough through the GMI Ridge into the northern Nappamerri Trough and into the Weena Trough (Figure 1; Figure 10) (Alexander et al., 1998a; Hall et al., 2015a; Delhi Australian Petroleum Ltd, 1968). This depositional model results in rapid and dramatic thickness variations, especially in the Weena Trough area. Areas devoid of these units are interpreted as either glacial uplands (e.g. Moomba, Daralingie and Toolachee areas) or uplifted and eroded structures (e.g. GMI Ridge) (Alexander et al., 1998a).

No lithofacies maps are available to further constrain the net thickness and distribution of shale or coal source rock facies.

4.1.1.4 Source rock distribution, geochemistry and maturity

The principal petroleum source rocks of the Tirrawarra Sandstone are shales, with some coaly units.

The total organic content (TOC) distribution for the Tirrawarra Sandstone ranges from 0 to 71 wt% (Figure 11; Hall et al., 2016a). Present day mean hydrogen index (HI) is 132 ± 64 mg HC/g TOC and mean original hydrogen index (HI_o) is estimated at 192 ± 133 mg HC/g TOC (Hall et al., 2016a). The highly variable HI values indicate predominantly gas-prone Type III kerogen of terrigenous origin. Further details on kerogen type are outlined in (Hall et al., 2016b). It is not possible to generate TOC or HI maps for the Tirrawarra Sandstone due to the limited and uneven data distribution. No maturity maps are available for the Tirrawarra Sandstone.

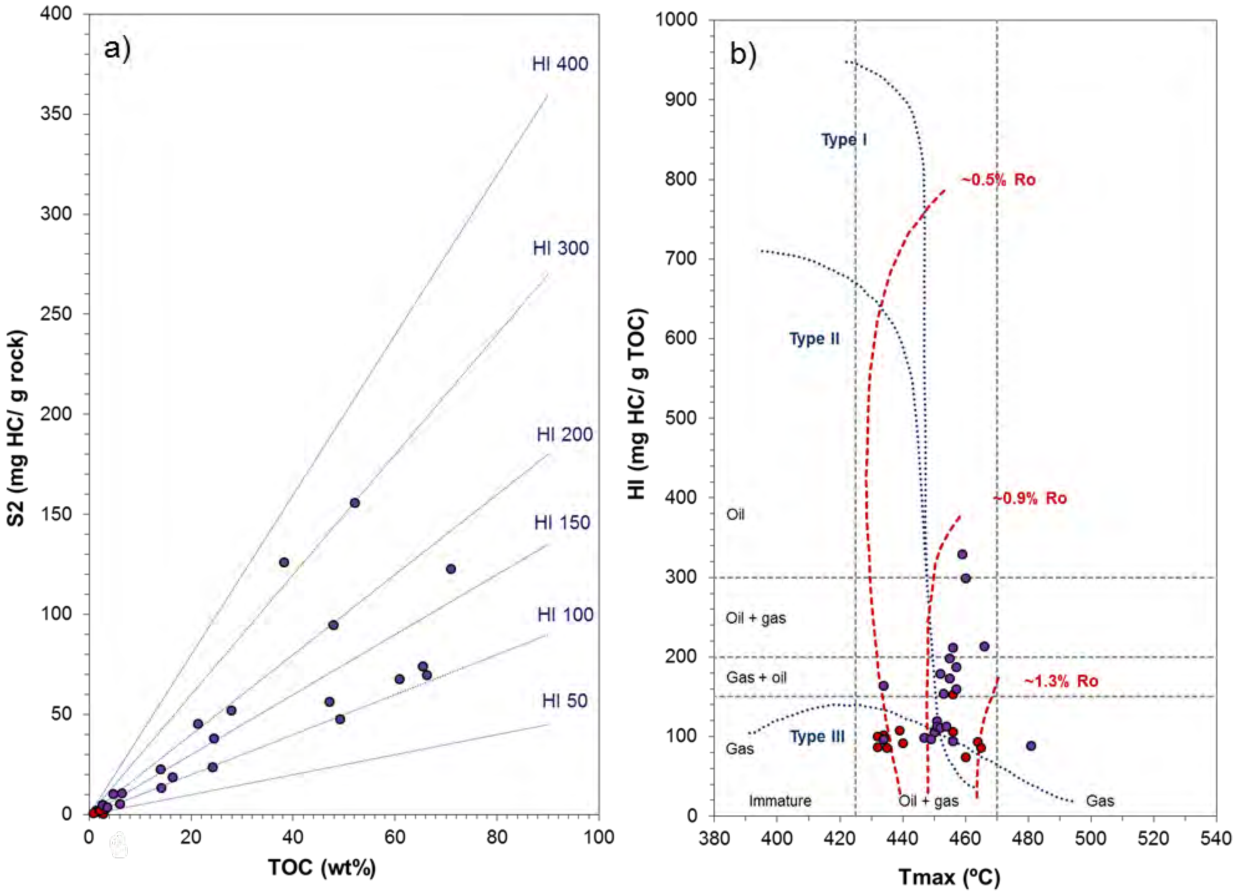

Figure 11 Rock-Eval pyrolysis data plots for the Tirrawarra Sandstone: (a) TOC content vs S2 yield; (b) Tmax vs HI

Purple dots: effective source rocks (TOC > 2 wt%; S1 + S2 > 3 mg HC/g rock); red dots: samples with either no original generation potential or are spent source rocks.
Source: Hall et al. (2016b)
Data: Hall et al. (2016a)
Element: GBA-COO-2-326

4.1.1.5 Tight reservoir characteristics

In the south-eastern Cooper Basin, the Tirrawarra Sandstone is a significant oil reservoir, which also produces free-flow and tight gas (Gravestock et al., 1998a). The Tirrawarra Sandstone is a proven conventional reservoir with uniform reservoir characteristics at a regional scale (Gravestock et al., 1998a), which also has the potential to host significant tight gas reservoirs within its finer grained sandstone and siltstone intervals. The log-derived tight pay thickness (i.e. net productive reservoir thickness), average effective porosity and water saturation statistics for Tirrawarra Sandstone tight reservoirs were calculated from 12 wells (Department for Energy and Mining (SA), 2017, 2018a). The average net pay thickness is 16.96 m, the average effective porosity is 8% and the average water saturation is 48% (Table 8; Figure 12).

Table 8 Tirrawarra Sandstone log-derived tight pay thickness, average effective porosity and water saturation statistics for analysed wells

Well	Net Tight Pay Thickness (m)	Average Effective Porosity (fraction)	Average Water Saturation (fraction)
Minimum	2.13	0.048	0.240
Maximum	55.47	0.107	0.600
Average	16.96	0.076	0.462
Median	9.53	0.080	0.477

The net tight pay interval was defined by the following criteria: volume fraction of shale less than 50%, effective porosity greater than 4% and water saturation less than 70%

Data: Beach Energy wells Boston 1, Boston 2, Streaky 1 and Santos wells Bindah 3, Coonatie 13, Dorodillo 2, Kirralee 2, Langmuir 1, Roswell 1, Tindilpie 11, Tindilpie 12 and Tirrawarra 76 (Department for Energy and Mining (SA), 2017, 2018a)

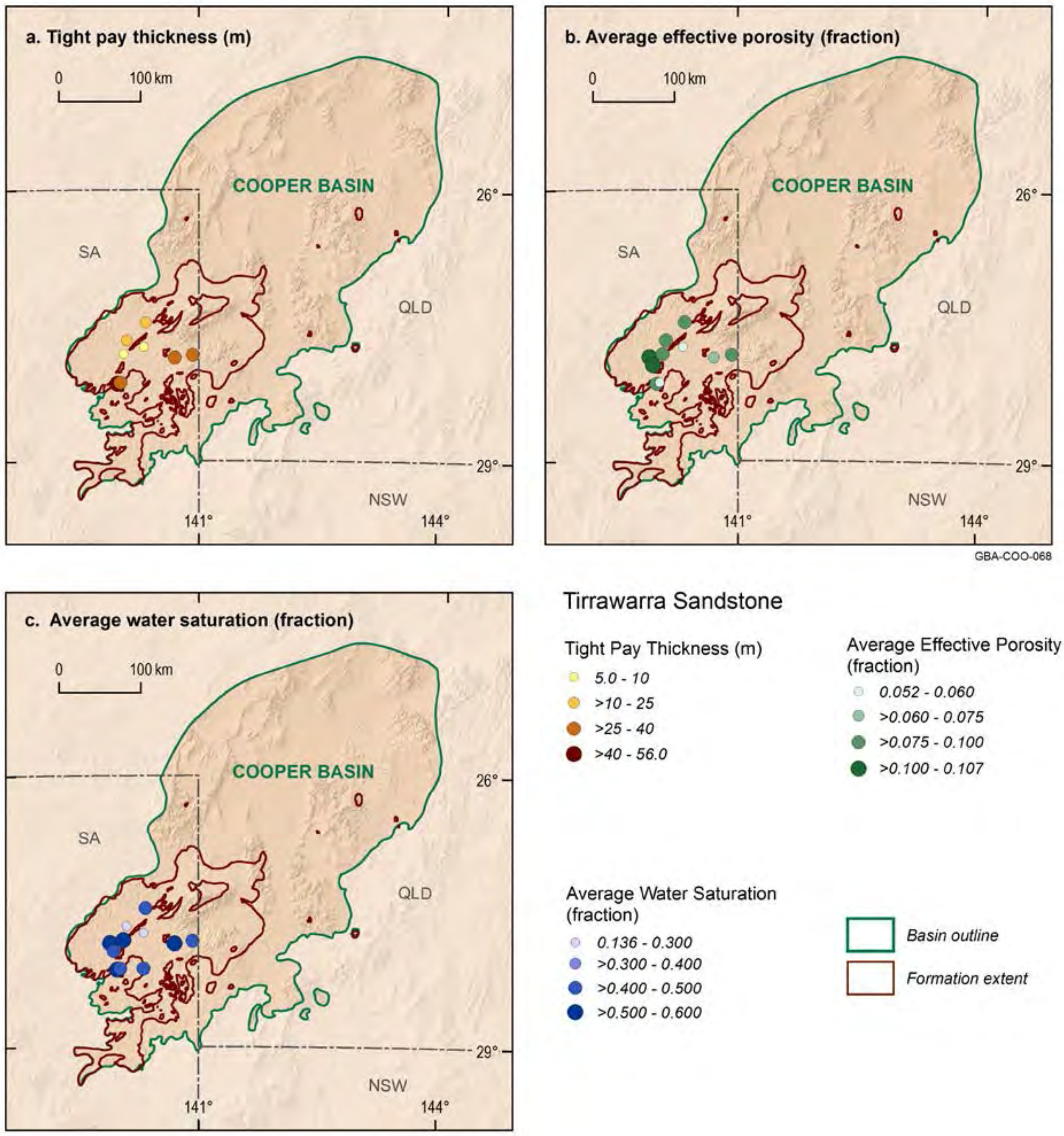

Figure 12 Log-derived (a) tight pay thickness, (b) average effective porosity and (c) average water saturation of the Tirrawarra Sandstone tight reservoirs in the Cooper Basin

Data: Department for Energy and Mining (SA) (2017, 2018a); Cooper Basin outline from Raymond et al. (2018)
Element: GBA-COO-068

4.1.2 Patchawarra Formation

Key features of the Patchawarra Formation are summarised below in Table 9 and discussed in more detail in the following text.

Table 9 Key features of the Patchawarra Formation

Unconventional Play type	Tight, shale and deep coal gas
Age	early Permian (Cisuralian: Sakmarian to early Kungurian)
Extent	69,600 km^2
Top depth (m)	775–3869 m
Gross formation thickness	0–750 m
Lithology	Sandstone, siltstone, shale and coal
Depositional environment	Fluvio-lacustrine, floodplain, minor deltaic
Kerogen type	Type II/III to Type III; coal, DOM
TOC	< 1–88 wt%
Mean original HI	199 ± 82 mg HC/g TOC
Thermal maturity	Immature–over mature
Average permeability	Air permeability of sandstone from 0.106 mD (Gaschnitz 3) to 4.259 mD (Tindilpie 12), 3.08E-05 mD for shales and 1.37E-04 mD for coals
Average effective porosity	0.072 (fraction) in tight pay intervals
Average effective water saturation (sandstone)	0.331 (fraction) in tight pay intervals
Average brittleness index	0.695 (fraction) (Jarvie et al., 2007)
Pressure regime	Overpressured (Nappamerri Trough)
Exploration status	Under assessment/minor production

4.1.2.1 Age and stratigraphic relationships

The Patchawarra Formation is early Permian in age (Figure 2) (Hall et al., 2015a; Owens et al., 2020).

The Patchawarra Formation is part of the Gidgealpa Group. It overlies and interfingers with the glacial sediments of the Tirrawarra Sandstone, or unconformably overlies pre-Permian basement rocks (Figure 2) (Alexander et al., 1998a; McKellar, 2013). Across most of the southern portion of the basin, the Patchawarra Formation is overlain by the Murteree Shale, but towards the edge of the Cooper Basin in South Australia, it is directly overlain by the Toolachee Formation, or by sediments of the Eromanga Basin (Hall et al., 2015a; Owens et al., 2020).

4.1.2.2 Extent, depth and gross formation thickness

The Patchawarra Formation is widespread, covering an area of approximately 69,600 km^2 (Hall et al., 2015a). The northern extent of the Patchawarra Formation is poorly mapped due to sparse well coverage (Hall et al., 2015a).

The Patchawarra Formation is the thickest unit of the Gidgealpa Group (Figure 13), with an average thickness of 130 m and a maximum thickness more than 680 m in the Nappamerri Trough (as intersected in Kirby 1). The unit thins to the north, but still reaches over 300 m thick within the Arrabury Trough. In the southern Windorah Trough and Mt Howitt Anticline regions (Figure 1), well intersections indicate a maximum thickness of around 100 m. Although there is no well control within the Ullenbury Depression, structural geometries suggest that as much as 200 m of Patchawarra Formation may be present within the depocentre (Hall et al., 2015a).

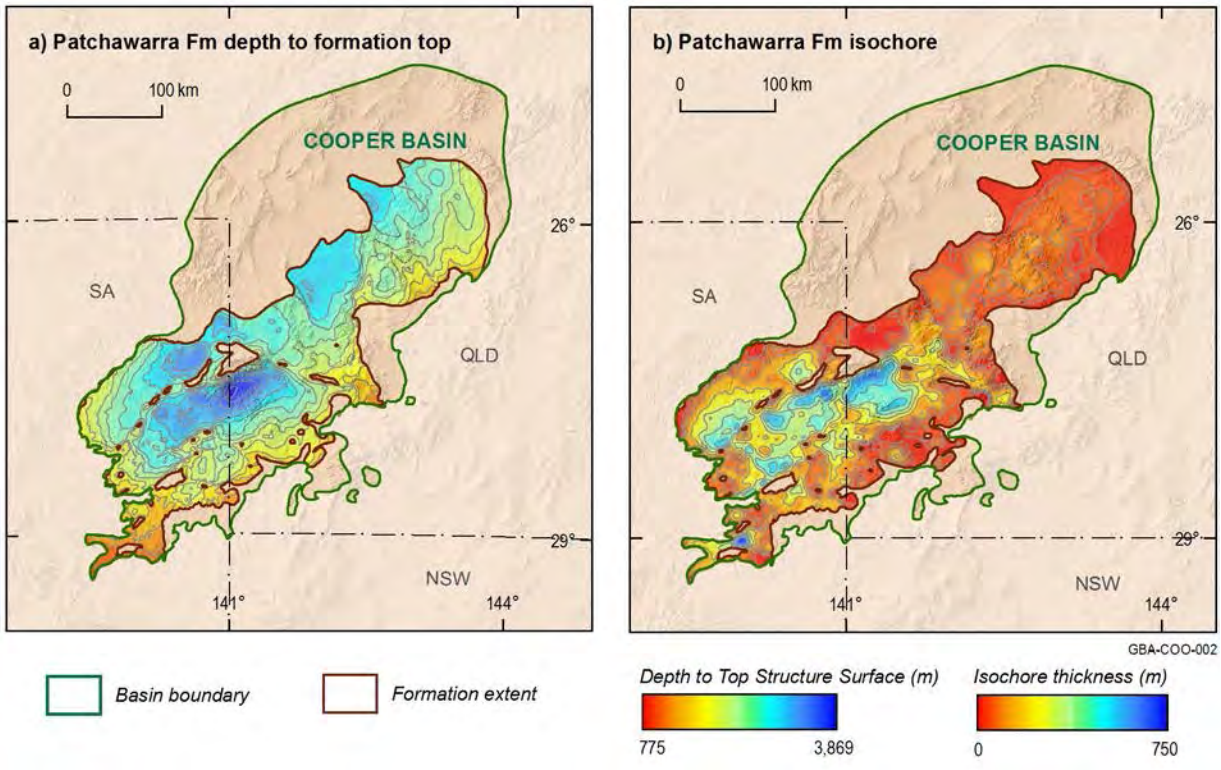

Figure 13 (a) Patchawarra Formation top depth (m) and (b) Patchawarra Formation total vertical thickness (m)

Source: Hall et al. (2015a)
Data: Hall et al. (2016a); Cooper Basin outline from Raymond et al. (2018)
Element: GBA-COO-002

4.1.2.3 Lithology and palaeoenvironment

The Patchawarra Formation consists of interbedded sandstone, siltstone, shale and coal (Figure 14) (Gatehouse, 1972; Kapel, 1966). The Patchawarra Formation is considered to have been deposited by a high sinuosity fluvial system flowing over a floodplain with peat swamps, lakes and gentle uplands (Alexander et al., 1998a; Gray and McKellar, 2002; Hall et al., 2015a; Lang et al., 2002; Strong et al., 2002).

Upward-fining packages from sandstone to carbonaceous siltstone and coal beds are common within the Patchawarra Formation (Alexander et al., 1998a). The lithofacies distribution patterns mapped by Hall et al. (2015a) are consistent with previous depositional models (Alexander et al., 1998a; Gray and McKellar, 2002; Lang et al., 2002; Strong et al., 2002).

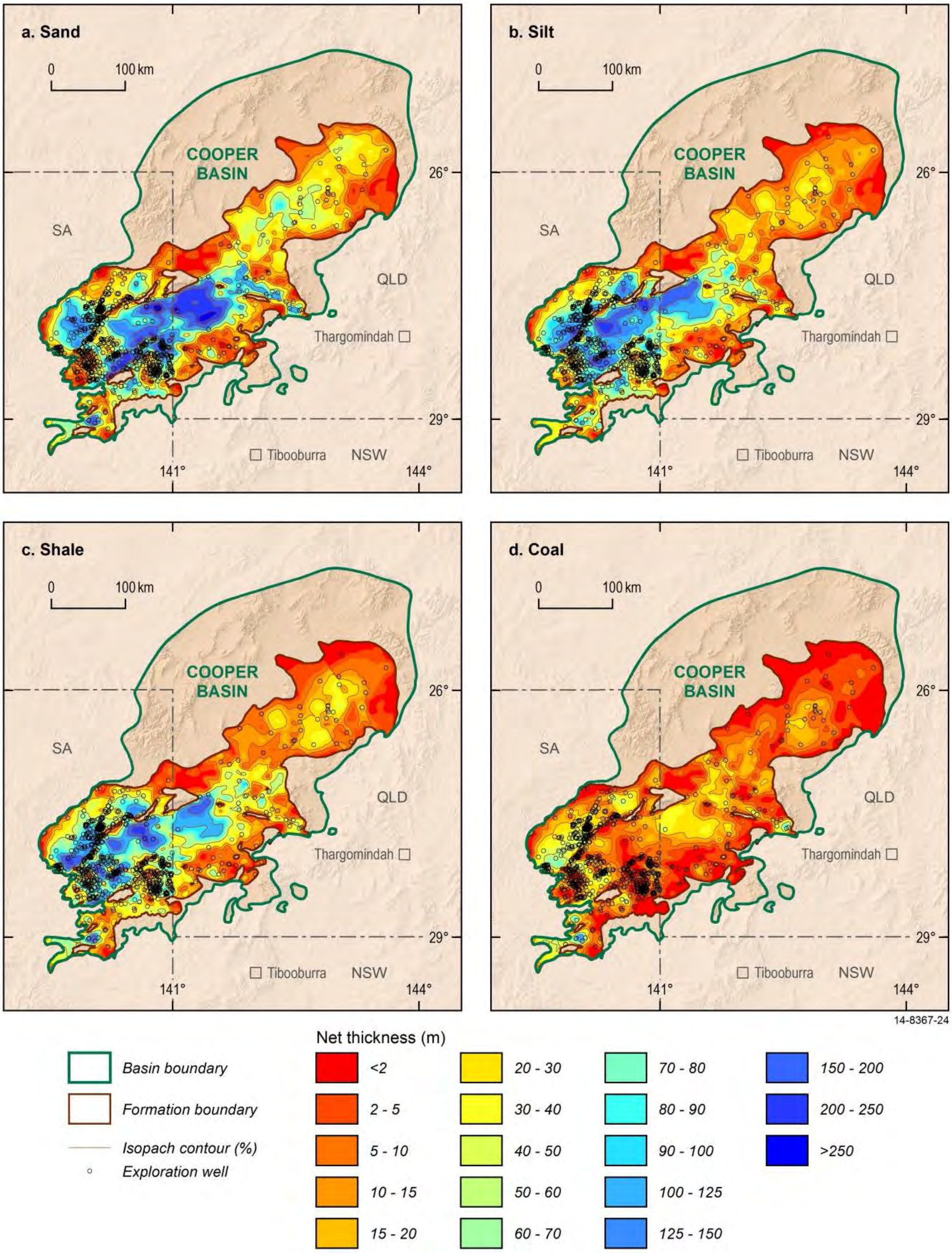

Figure 14 Patchawarra Formation isolith maps by lithology, as total net thickness in metres for (a) sand, (b) silt, (c) shale and (d) coal

Shale incorporates shale, coaly shale and / or shaly coal. These are approximately equivalent to samples with a TOC range of 0.5–50 wt%

Source: Hall et al. (2015a)

Data: Hall et al. (2016a); Cooper Basin outline from Raymond et al. (2018)

Element: GBA-COO-2-308

4.1.2.4 Source rock distribution, geochemistry and maturity

The source rocks of the Patchawarra Formation include shale, coaly shale, shaly coal and coal.

Maps of net coal and shale–shaly coal thickness show an abundance of potential source rock facies within the Patchawarra Formation across the entire formation extent (Figure 14) (Hall et al., 2015a). Net coal thickness (equivalent to clean coals with TOC > 50 wt%) is greatest in the south-western corner of the basin, where it reaches nearly 200 m in Klebb 1 in the Weena Trough (Hall et al., 2015a; Strike Energy, 2015). Net coal thicknesses over 40 m are also observed in the Wooloo and southern Patchawarra troughs (Sun and Camac, 2004; Hall et al., 2015a). In Queensland, north of the JNP Trend, cumulative coal thickness is regionally between 10 and 15 m (Figure 14; Hall et al., 2015a).

The cumulative net thickness of the shale, coaly shale and shaly coal facies (approximately equivalent to samples with a TOC range of 0.5–50 wt%) is greatest in the Nappamerri and southern Patchawarra troughs, where it reaches up to 250 m (Figure 14) (Hall et al., 2015a). Despite a significant reduction in total formation thickness further north, net shale–shaly coal thickness remains greater than 20 m in parts of the Windorah Trough and south of the Ullenbury Depression (Figure 14).

The TOC of Patchawarra Formation ranges from < 1 to 88 wt%, reflecting the broad distribution of lithofacies (Figure 15). The present day TOC map shows good to excellent source rock (TOC > 2 wt%) within the shale, coaly shale and shaly coal facies across the entire formation extent (Figure 16) (Hall et al., 2016b). The TOC content is higher in the Patchawarra Trough and around the basin edges, reflecting the more coal-rich facies present in these regions (Hall et al., 2016b).

The present day mean HI is 149 ± 70 mg HC/g TOC and mean original HI (HI_o) is estimated at 199 ± 82 mg HC/g TOC, indicating a mixture of both oil and gas-prone Type II/III and gas-prone Type III kerogen (Figure 15) (Hall et al., 2016b). The HI_o map (Figure 16) shows broad areas with values between 200 and 300 mg HC/g TOC, and no clear correlation is apparent between original source rock quality and geographic region.

The maturity of the Patchawarra Formation (Figure 17) is highest in the central Nappamerri Trough where it is overmature (maturity, R_o > 3.5%; transformation ratio, TR > 95%) (Hall et al., 2016c). This high maturity reflects both the greater burial depths and proximity to the high heat producing Big Lake Suite granodiorites (Deighton et al., 2003; Deighton and Hill, 1998). In the Patchawarra Trough, maturity ranges from the early oil window (R_o 0.75–0.9%; TR < 50%) in the west to late oil (R_o 1–1.2%; TR > 50–70%) in the east. In the Windorah Trough, the Patchawarra Formation reaches the wet gas window across the Windorah Trough (R_o 1.2–2%; TR > 50–70%; Figure 17) (Hall et al., 2016c). In the Weena Trough, the majority of the Patchawarra Formation remains immature with TRs less than 10%, although a maximum TR of approximately 15% (R_o approximately 0.8%; early oil window) is reached in the central trough.

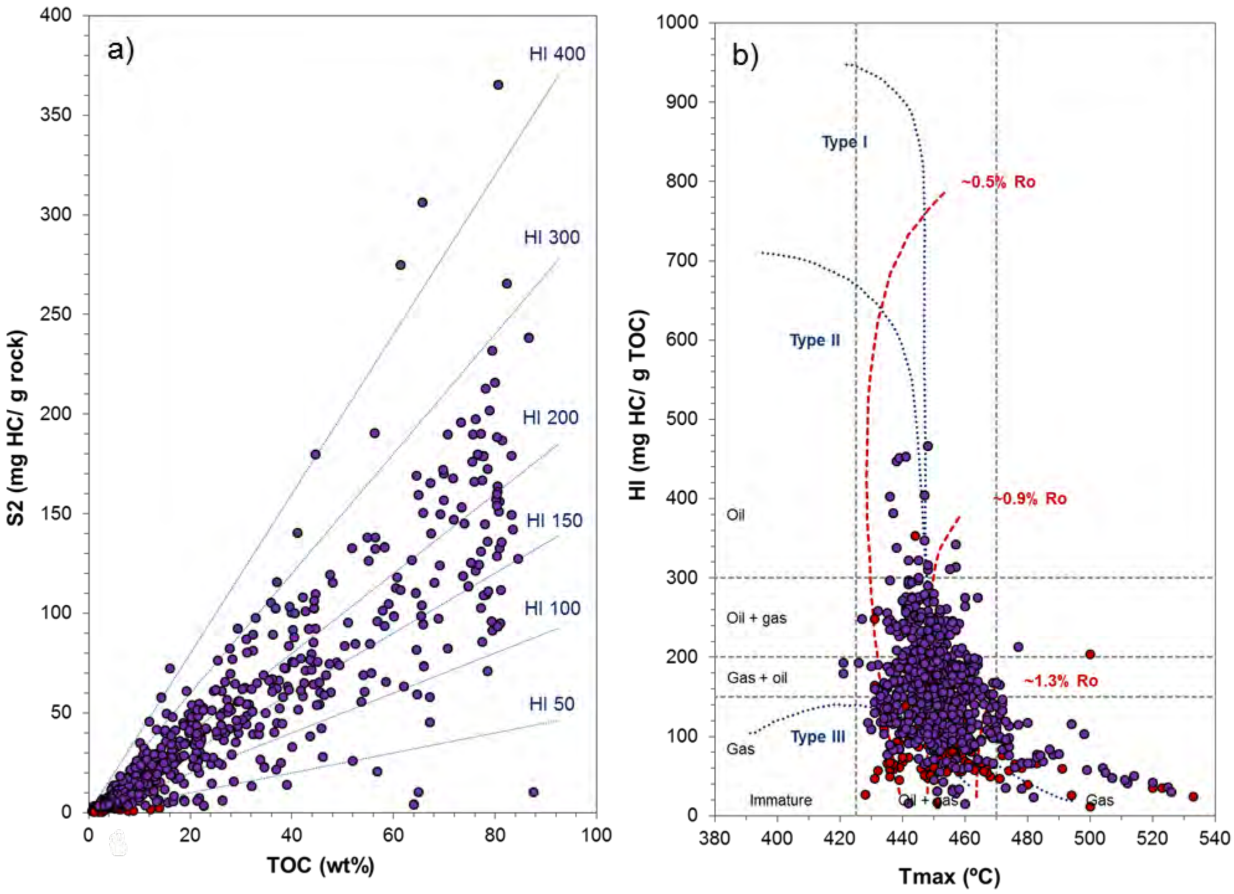

Figure 15 Rock-Eval pyrolysis data plots for the Patchawarra Formation: a) TOC content vs S2 yield; b) Tmax vs HI

Purple dots: Effective source rocks (TOC > 2 wt%; S1 + S2 > 3 mg HC/g rock); red dots: samples with either no original generation potential or are spent source rocks.
Source: Hall et al. (2016b)
Data: Hall et al. (2016a)
Element: GBA-COO-2-298

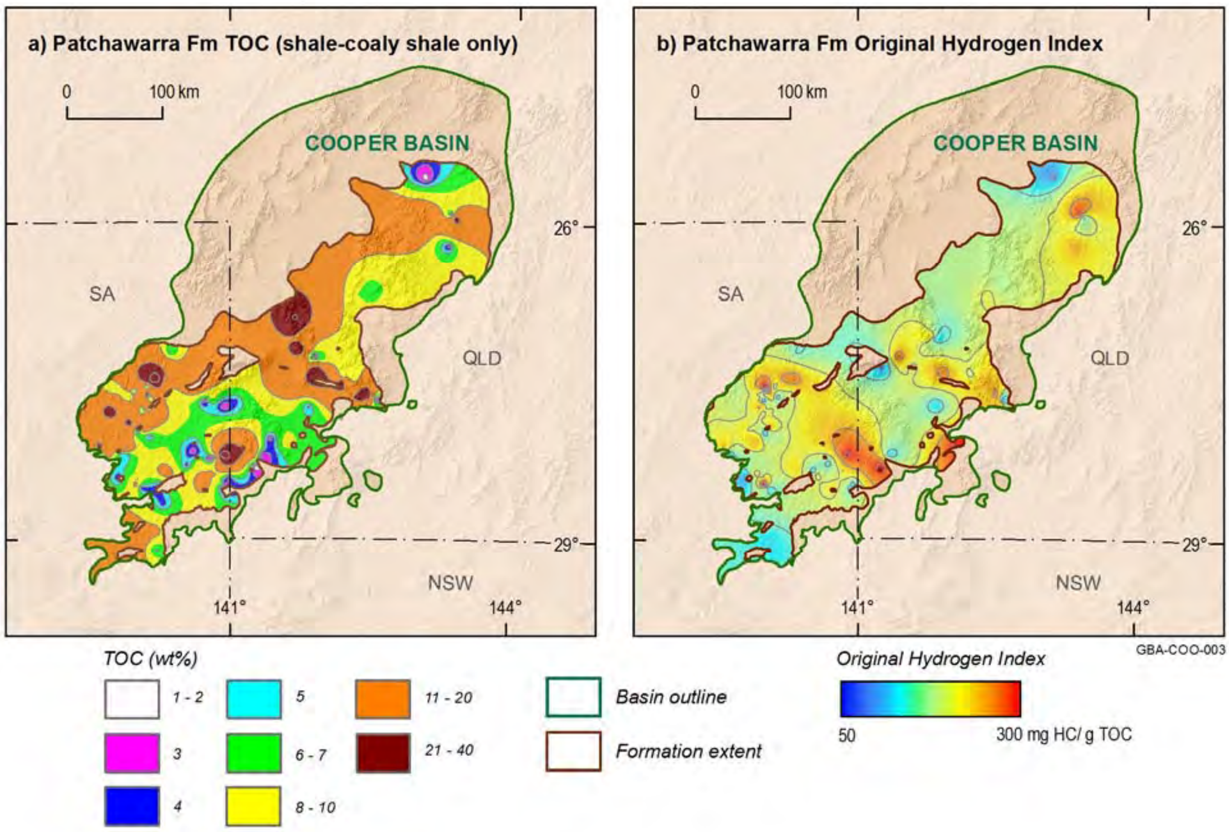

Figure 16 Patchawarra Formation source rock geochemistry maps: (a) Present day average Total Organic Carbon (TOC) (wt%) for shale-coaly shale facies (TOC < 50 wt%) and (b) mean Original Hydrogen Index (HI_o)

Source: Hall et al. (2016b)
Data: Hall et al. (2016a); Cooper Basin outline from Raymond et al. (2018)
Element: GBA-COO-003

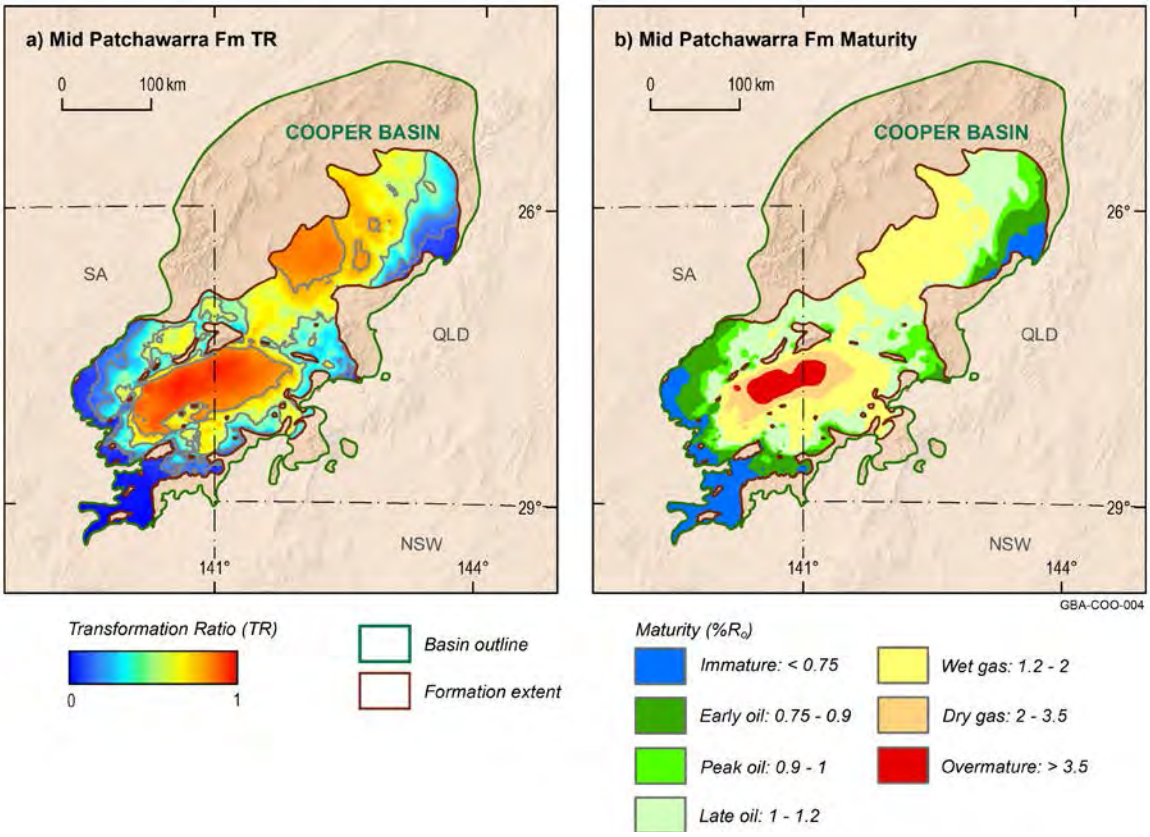

Figure 17 Patchawarra Formation (a) transformation ratio (TR) and (b) maturity (%R_o)

Source: Hall et al. (2016c)
Data: Hall et al. (2016a); Cooper Basin outline from Raymond et al. (2018)
Element: GBA-COO-004

4.1.2.5 Tight reservoir characteristics

While the sandstones within the Patchawarra Formation host the most significant gas-condensate conventional reservoirs in the Cooper Basin (Gravestock et al., 1998a), the formation also hosts potential tight gas reservoirs in both sand and silt-rich units. The net thickness of both sandstone and siltstone intervals of the Patchawarra Formation are greatest in the deepest sections of the basin around the Nappamerri Trough (Figure 1; Figure 14) (Sun and Camac, 2004; Hall et al., 2015a).

Patchawarra Formation tight reservoir net pay thickness, average effective porosity and water saturation were characterised using log data from 29 wells (Department for Energy and Mining (SA), 2017, 2018a; Department of Natural Resources, 2018a). Average tight pay thickness, effective porosity and water saturation are 42.93 m, 7.2% and 33.1% respectively (Table 10; Figure 18).

Table 10 Log-derived tight pay thickness, average effective porosity and water saturation statistics for the Patchawarra Formation tight reservoirs in the Cooper Basin

Well	Tight Pay Thickness (m)	Average Effective Porosity (fraction)	Average Water Saturation (fraction)
Minimum	5.03	0.052	0.136
Maximum	178.23	0.128	0.583
Average	42.93	0.072	0.331
Median	39.29	0.067	0.340

The net tight pay interval was defined by the following criteria: volume fraction of shale less than 50%, effective porosity greater than 4% and water saturation less than 70%, with the exception of two wells (Allunga Trough 1 and Dorodillo 2) which were defined in the well completion reports based on water saturation less than 65%
Data: Beach Energy wells - Boston 1, Boston 2, Dashwood 1, Encounter 1, Halifax 1, Hervey 1, Holdfast 1, Marble 1, Nepean 1, Rapid 1, Streaky 1; Santos wells - Allunga Trough 1, Bindah 3, Bobs Well 2, Coonatie 13, Dorodillo 2, Gaschnitz 1ST1, Kirralee 2, Langmuir 1, Moomba 192, Nephrite South 7, Roswell 1, Tindilpie 11, Tindilpie 12, Tirrawarra 76, Van Der Waals 1, Whanto 4 and Real Energy Queensland wells Queenscliff 1 and Tamarama 1 (Department for Energy and Mining (SA), 2017, 2018a; Department of Natural Resources, 2018a)

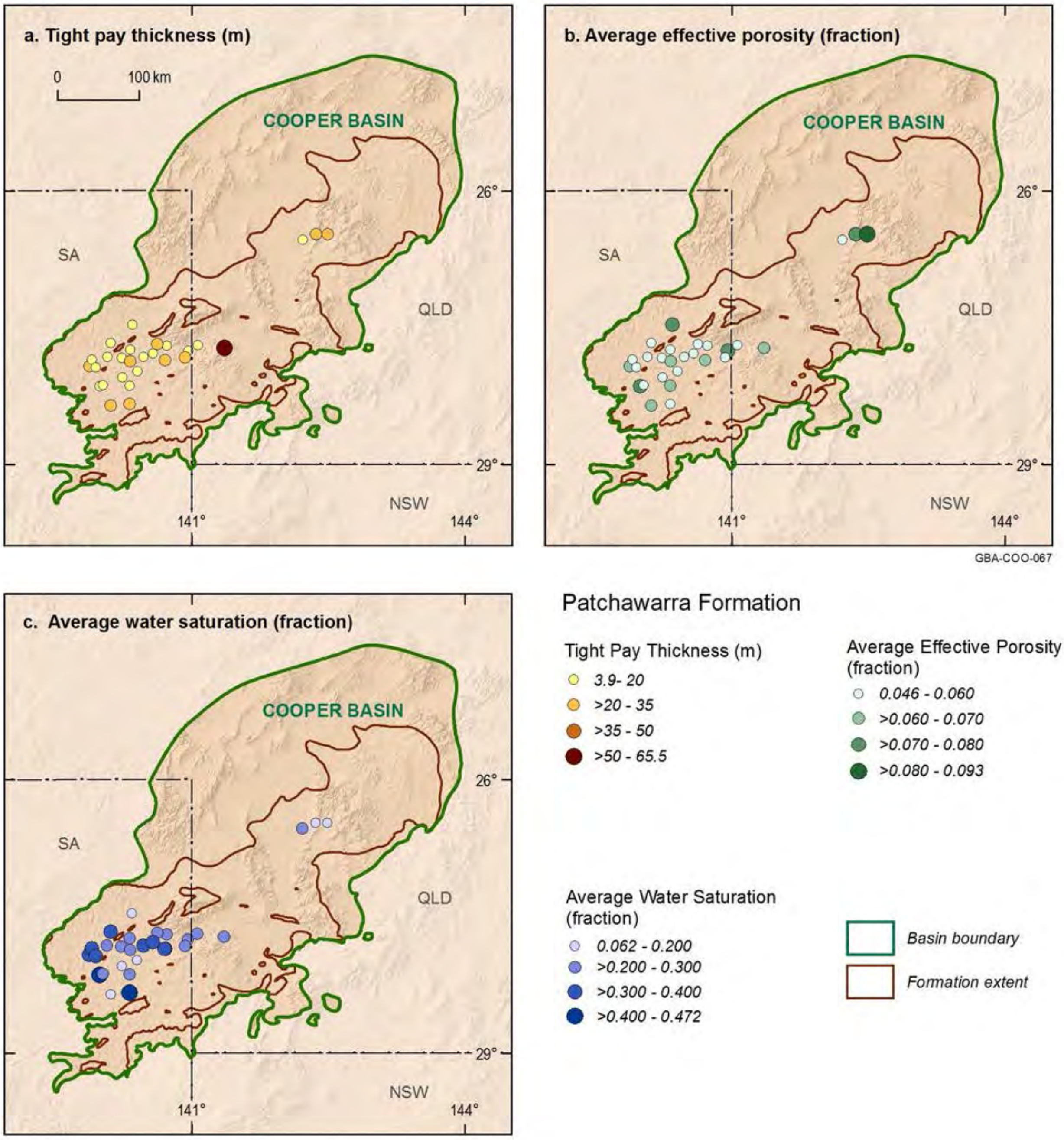

Figure 18 (a) Tight pay thickness, (b) average effective porosity and (c) average water saturation of the Patchawarra Formation tight reservoirs in the Cooper Basin

Data: Department for Energy and Mining (SA) (2017, 2018a); Department of Natural Resources (2018a); Cooper Basin outline from Raymond et al. (2018)
Element: GBA-COO-067

4.1.2.6 Shale and coaly shale reservoir characteristics

Porosity, permeability and fluid saturation are three of the key petrophysical input parameters required for characterising shale plays. Porosity and hydrocarbon saturation are measured in the laboratory using Helium pycnometer and fluid extraction apparatus. Shale permeabilities are measured in a laboratory with a pressure decay technique.

Table 11 shows the laboratory measured shale rock properties (as-received basis) available for the Patchawarra Formation shale rocks from Bobs Well 2 in the Allunga Trough and Tindilpie 11 in the Patchawarra Trough (Department for Energy and Mining (SA), 2018a). The average bulk density is 2.58 g/cc, the average total porosity is 23%, the average water saturation is 56.9% and the average permeability from pressure decay tests is 3.08E-05 mD.

The as-received coaly shale rock properties for Bobs Well 2 include a bulk density of 1.511 g/cc, ash content of 37.6 wt%, grain density of 1.683 g/cc, helium total porosity of 0.052, water saturation of 0.148, gas saturation of 0.825, gas-filled porosity of 0.043 and pressure decay permeability of 3.48E-04 mD (Santos–Delhi–Origin, 2010; Department for Energy and Mining (SA), 2017, 2018a).

Table 11 Average as-received laboratory measured shale rock properties of Patchawarra Formation shale

Well	Top (m)	Bottom (m)	Bulk density (g/cc)	Water saturation (fraction)	Oil saturation (fraction)	Gas saturation (fraction)	Gas-filled Porosity (fraction)	Total porosity (fraction)	Permeability (mD)
Bobs Well 2	2803.4	2803.5	2.41	0.411	0	0.589	0.018	0.030	9.21E-06
	2804.0	2804.1	2.59	0.787	0	0.213	0.004	0.017	9.64E-07
	2804.5	2804.7	2.61	0.605	0	0.395	0.008	0.020	8.18E-06
	2805.2	2805.3	2.61	0.718	0	0.282	0.006	0.022	7.26E-06
	2805.8	2805.9	2.61	0.537	0	0.463	0.011	0.024	4.24E-06
	2806.4	2806.5	2.61	0.803	0	0.197	0.005	0.025	1.54E-06
	2807.0	2807.1	2.60	0.551	0	0.449	0.012	0.027	5.38E-06
	2807.6	2807.7	2.61	0.729	0	0.271	0.006	0.022	4.75E-06
	2808.2	2808.3	2.60	0.894	0	0.106	0.002	0.019	6.87E-07
	2804.7	2804.7	2.61	0.280	0.070	0.650	0.016	0.025	1.21E-04
	2806.5	2806.5	2.61	0.204	0.081	0.715	0.015	0.021	1.18E-04
	2808.2	2808.2	2.56	0.279	0.093	0.628	0.012	0.018	1.08E-04
Tindilpie 11	2907.8	2907.9	2.56	0.596	0.046	0.358	0.010	0.027	1.13E-05
Average			2.58	0.569	0.022	0.409	0.010	0.023	3.08E-05

Data: Bobs Well 2; Tindilpie 11 (Department for Energy and Mining (SA), 2018a)

Gas in shale is stored as adsorbed gas on the organic matter, free gas stored in the pore spaces and dissolved gas in the formation water.

Patchawarra Formation gas desorption test results for Bobs Well 2, Forge 1, Kingston Rule 1 and Tirrawarra 76 (Department for Energy and Mining (SA), 2017, 2018a) show the average total gas contents (as-received basis) are 1.61 scc/g, 0.84 scc/g, 2.01 scc/g and 0.37 scc/g respectively.

The adsorbed gas storage capacity of shales is analysed using isotherm tests, however no such data is available for the Patchawarra Formation.

Table 12 lists the gas desorption test results on the as-received Patchawarra rock samples in Bobs Well 2. The total gas content of the coaly and shales is estimated to average 13.46 scc/g.

Table 12 Gas desorption test results on the as-received Patchawarra Formation coal and shale rock samples in Bobs Well 2

Top depth (m)	Bottom depth (m)	As-received total gas content (scc/g)	Dry, ash free total gas content (scc/g)
2790.4	2791.4	14.55	15.72
2792.3	2793.2	17.12	18.25
2794.1	2795.0	19.6	23.76
2795.9	2796.8	20.15	23.16
2797.8	2798.7	18.21	20.37
2799.6	2800.5	20.63	21.72
2801.4	2802.3	19.47	20.62
2803.2	2804.2	1.63	25.48
2805.1	2806.0	1.64	36.48
2806.9	2807.8	1.55	35.18
	Average	13.46	24.07

Shale with a total gas content of more than 1 scc/g and coal with total gas content of more than 5-10 scc/g are of considered to be of economic significance
Data: Bobs Well 2 (Department for Energy and Mining (SA), 2017, 2018a)

Table 13 compares the statistics of total gas content (as-received) of shale/coaly shale from the Patchawarra Formation with two other formations in the basin.

Table 13 Statistics of the as-received total gas content (scc/g) of shale/coaly shale rocks from relevant formations in the Cooper Basin

Formation	Minimum (scc/g)	Maximum (scc/g)	Average (scc/g)	Median (scc/g)
Roseneath Formation	0.46	4.57	1.36	1.08
Murteree Shale	0.57	4.11	1.60	1.36
Patchawarra Formation	0.27	3.07	1.30	1.40

Data: Bobs Well 2, Encounter 1, Holdfast 1, Kingston Rule 1, Marsden 1, Moomba 175, Moomba 191, Talaq 1, Vintage Crop 1 6 (Department for Energy and Mining (SA), 2017, 2018a)

4.1.2.7 Deep coal reservoir characteristics

The distribution of Patchawarra Formation coal is presented in Figure 13 (Hall et al., 2015a), which shows the bulk of the coal resource is located in the Patchawarra Trough and the south-west and north-east Nappamerri Trough.

Coals in the Weena Trough were assessed in order to better characterise the deep coal gas. It is acknowledged that these are i) shallower targets that are currently the focus of CSG exploration, and ii) localised to the Weena Trough so are unlikely to be representative of the whole basin. However other wells lacked suitable data to undertake a complete assessment and have thus been included. In the Weena Trough area, the average net thickness of the Patchawarra Formation coal seams is 82.3 m in the wells Klebb 1, 2, 3 and 4 (Department for Energy and Mining (SA), 2017, 2018a) (Table 14).

Table 14 Thickness of composite coal seams (m) in the Patchawarra Formation

	Klebb 1	Klebb 2	Klebb 3	Klebb 4	Average
Patchawarra Formation coal seams composite (net) thickness (m)	104.1	83.8	77.4	63.8	82.3

Data: Klebb 1, 2, 3 and 4, (Department for Energy and Mining (SA), 2018a)

The composition of Patchawarra Formation deep coals was assessed in 6 wells in the southern Cooper Basin. The average maceral composition was found to be 62.46 vol% inertinite (Type IV), 32.01 vol% vitrinite (Type III) and minor liptinite (Type II and/or Type I) and mineral components (Table 15, Table 16). According to Dunlop et al. (2017), low vitrinite values, like those seen in the Cooper Basin, create a dull coal which has relatively poor cleat development. The average components of these coal seams based on proximate analysis are presented in Table 17. The average content of volatile matter is 23.97 wt%, indicating the Patchawarra Formation deep coals are mainly the medium-volatile bituminous coals (Mastalerz and Harper, 1998).

Table 15 Average maceral components of the Patchawarra Formation deep coals for 6 wells in the Cooper Basin

Well	Vitrinite (vol%)	Liptinite (vol%)	Inertinite (vol%)	Minerals (vol%)
Davenport 1ST1	23.75	1.30	72.65	2.25
Marsden 1	10.75	1.25	77.40	10.40
Admella 1	26.30	1.50	69.50	2.60
Forge 1	54.70	4.26	39.04	1.98
Kingston Rule 1	55.90	0.00	40.43	3.65
Bobs Well 2	20.66	0.08	75.72	3.56
Average	32.01	1.40	62.46	4.07

Data: Davenport 1ST1, Marsden 1, Admella 1, Forge 1, Kingston Rule 1, Bobs Well 2 (Department for Energy and Mining (SA), 2018a)

Table 16 Statistics of kerogen types of the Patchawarra Formation deep coals from 6 wells

Statistics	Type I %	Type II %	Type III %	Type IV %
Minimum	0.00	0.00	2.10	19.90
Maximum	0.00	6.60	79.60	97.90
Average	0.00	0.30	23.75	75.95
Median	0.00	0.00	13.65	86.35

Data: Davenport 1ST1, Marsden 1, Admella 1, Forge 1, Kingston Rule 1, Bobs Well 2 (Department for Energy and Mining (SA), 2018a)

Table 17 Average components of the Patchawarra Formation coals based on proximate analyses for key wells in the Cooper Basin

Well	Moisture (wt%)	Ash (wt%)	Volatile (wt%)	Fixed carbon (wt%)
Admella 1	2.22	3.76	28.06	65.96
Bobs Well 2	0.77	34.23	12.50	52.50
Davenport 1	3.33	3.66	29.23	63.78
Forge 1	2.38	11.44	36.06	50.12
Kingston Rule 1	0.72	15.28	17.07	66.94
Marsden 1	1.25	25.10	20.90	52.80
Average	1.78	15.58	23.97	58.68

Data: Davenport 1ST1, Marsden 1, Admella 1, Forge 1, Kingston Rule 1, Bobs Well 2 (Department for Energy and Mining (SA), 2018a)

Porosity, permeability and fluid saturation are key petrophysical input parameters required for characterising deep coal plays. The as-received rock property tests for deep coal samples in Bobs Well 2 (28 samples) and Tindilpie 11 (1 sample) (Department for Energy and Mining (SA), 2018a) show an average water saturations of 25.7% (Bobs Well 2) and 32.6% (Tindilpie 11) (Table 18).

Table 18 Statistics of as-received rock properties of the Patchawarra Formation coals in Bobs Well 2 and Tindilpie 11

Well	Statistics	Bulk density (g/cc)	Water saturation (fraction)	Oil saturation (fraction)	Gas saturation (fraction)	Gas-filled Porosity (fraction)	Total porosity (fraction)	Permeability (mD)
Bobs Well 2	Minimum	1.31	0.191	0	0.678	0.035	0.051	1.96E-05
	Maximum	1.54	0.322	0	0.809	0.062	0.078	4.89E-05
	Average	1.36	0.257	0	0.743	0.047	0.063	2.61E-05
	Median	1.34	0.252	0	0.748	0.046	0.060	2.50E-05
Tindilpie 11		1.28	0.326	0.081	0.593	0.037	0.063	1.57E-05

Data: Bobs Well 2 (28 samples) and Tindilpie 11 (1 sample) (Department for Energy and Mining (SA), 2017, 2018a)

Table 19 lists the average total gas content of the Patchawarra Formation deep coal seams in key wells. The average as-received total gas content is 21.06 scc/g.

The adsorbed gas storage capacity of Patchawarra Formation deep coals was analysed using isotherm tests for samples in 7 wells. Results, including measurement gas, ash content, Langmuir parameters and adsorbed gas storage capacity (in situ, scc/g), are summarised in Table 20, Table 21 and Figure 19. In addition to the methane storage capacity analyses, isotherm tests for CO_2 storage capacity were also run on one sample from Bobs Well 2 and two samples from Kingston Rule 1.

Table 19 Average as-received and dry ash free total gas content (scc/g) of the Patchawarra Formation deep coal seams for key wells in the Cooper Basin

Well	As-received total gas content (scc/g)	Dry, ash free total gas content (scc/g)
Admella 1	29.57	31.39
Bobs Well 2	18.53	20.51
Davenport 1	21.82	23.49
Kingston Rule 1	13.33	14.18
Talaq 1	22.04	na
Tindilpie 11	13.5	56.93
Average	21.06	29.30

Data: Admella 1, Bobs Well 2, Davenport 1, Kingston Rule 1, Talaq 1 and Tindeilpie 11 (Department for Energy and Mining (SA), 2017, 2018a)

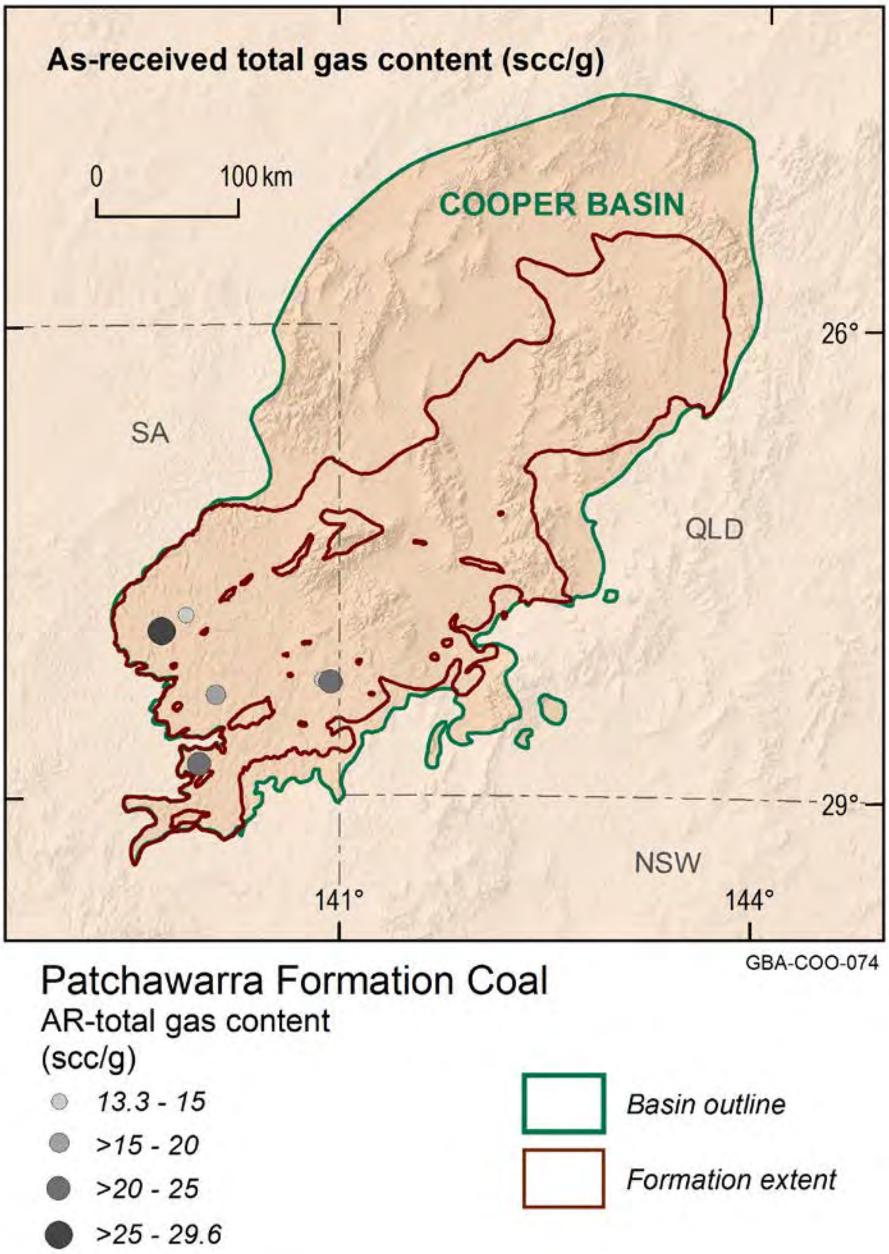

Figure 19 As-received total gas content distribution of the unconventional Patchawarra Formation coals in the Cooper Basin

Data: Department for Energy and Mining (SA) (2017, 2018a); Cooper Basin outline from Raymond et al. (2018)
Element: GBA-COO-074

Based on available data for deep coal, the Patchawarra Formation in situ adsorbed gas storage capacity ranges from 5.93–24.25 scc/g and the in situ Langmuir storage capacity for methane ranges from 7.6–28.83 scc/g (Table 20).

Table 20 Isotherm test parameters under reservoir temperature and adsorbed gas storage capacity (in situ, scc/g) on the Patchawarra Formation deep coal samples for 7 wells in the Cooper Basin

Well	Top depth (m)	Bottom depth (m)	Measurement gas	Ash content (wt frac)	Langmuir storage capacity, in situ (scc/g)	Langmuir pressure (kPa)	Adsorbed gas storage capacity, in situ (scc/g)
Kingston Rule 1	2540.8	2541.1	methane	0.022	17.56	12508.40	11.76
	2627.6	2627.9	methane	0.046	16.53	8366.60	12.54
	2627.6	2627.9	CO_2	0.046	28.33	4417.00	24.25
	2628.7	2629.0	methane	0.036	16.96	8062.50	12.98
	2636.8	2637.1	methane	0.109	16.31	8944.30	12.18
	2636.8	2637.1	CO_2	0.109	21.76	4683.80	18.47
	2648.2	2648.5	methane	0.112	13.39	6171.80	10.86
Davenport 1	1907.1	1907.4	methane	0.039	16.82	13207.36	9.52
	1918.4	1918.7	methane	0.036	16.62	13996.97	9.17
	1995.3	1995.6	methane	0.049	17.88	12905.47	10.22
	2000.3	2000.6	methane	0.022	18.85	12884.78	10.79
Forge 1	1316.2	1317.2	methane	0.021	11.16	10080	6.31
	1313.9	1314.9	methane	0.021	10.98	9890	6.26
	1318.4	1319.4	methane	0.020	11.33	10270	6.35
Admella 1	2612.0	2612.3	methane	0.033	13.11	6124.90	10.63
Marsden 1	2445.0	2457.0	methane	0.531	11.70	11248.60	7.62
	2460.0	2469.0	methane	0.568	9.77	10690.40	6.47
Tindilpie 11	2908.1	2908.4	methane	0.033	14.89	13464.91	10.09
Bobs Well 2	2791.4	2791.9	methane	0.108	12.22	8474.35	9.32
	2793.3	2794.2	methane	0.064	12.85	8184.08	9.88
	2795.1	2796.0	methane	0.037	11.43	7579.41	8.94
	2796.9	2797.8	methane	0.045	12.42	7862.09	9.64
	2798.7	2799.6	methane	0.052	11.22	7035.41	8.92
	2800.5	2801.4	methane	0.036	12.55	7641.46	9.80
	2800.5	2801.4	CO_2	0.036	15.89	3284.66	14.18
	2802.4	2802.9	methane	0.376	7.60	7673.18	5.93

Data: Davenport 1ST1, Forge 1, Marsden 1, Bobs Well 2, Admella 1, Tindilpie 11 and Kingston Rule 1 (Department for Energy and Mining (SA), 2017, 2018a)

The average as-received adsorbed gas storage capacity for Kingstone Rule 1 is 13.22 scc/g (Table 21).

Table 21 Laboratory measured bulk density and as-received multi-component adsorbed gas storage capacity in Kingston Rule 1 (Senex Energy Ltd, 2013; Department for Energy and Mining (SA), 2017, 2018a)

Midpoint depth (m)	Void volume crushed density (g/cc)	As-received multi-component adsorbed gas storage capacity (scc/g)
2540.96	1.289	13.01
2627.78	1.334	13.88
2628.80	1.328	14.16
2636.95	1.403	13.06
2648.32	1.773	12
Average	1.425	13.22

Data: Kingston Rule 1 (Senex Energy Ltd, 2013; Department for Energy and Mining (SA), 2017, 2018a)

The coal fabric or planes of weakness inside the coal seams are important for deep coal gas production. The coal fabric may be at various scales, open, variably cemented by authigenic siderite or kaolinite or closed by high initial reservoir confining stress. They could be reactivated by reservoir stimulation treatments and preferentially dilated by subsequent desorption induced coal matrix shrinkage during gas production. Potential coal fabric types include vitrinite cleats, inertinite master joints, other natural fractures, faults, contrasts in lithology and weak bedding planes (Dunlop et al., 2017).

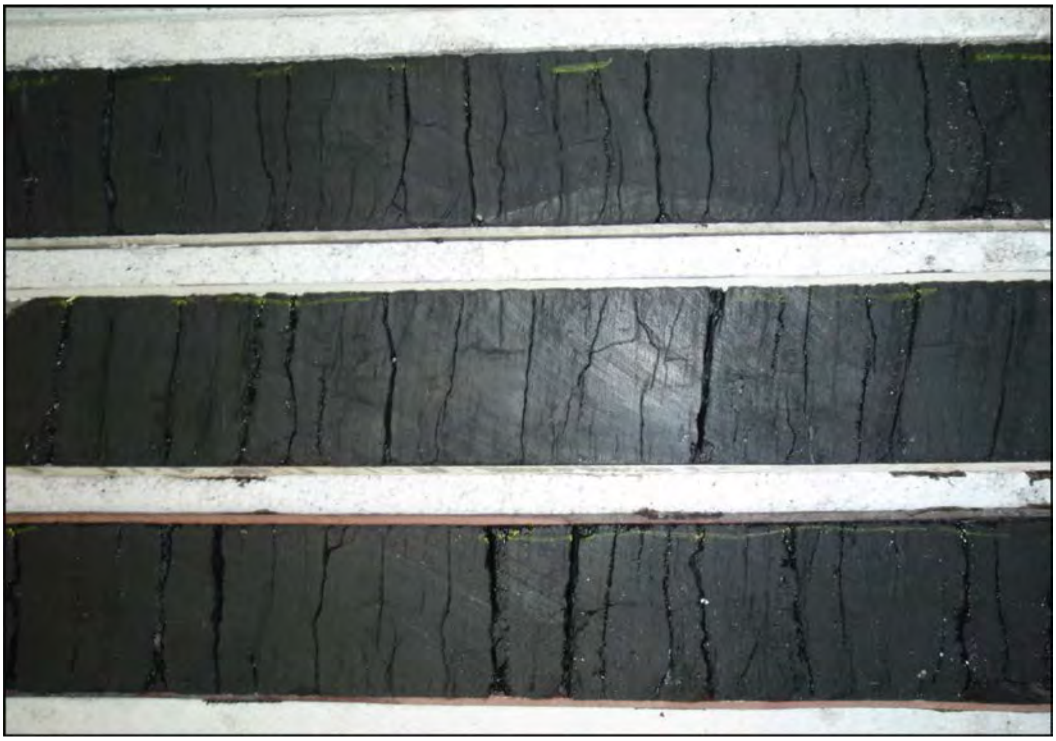

Figure 20 Core photo of Bindah 3 core showing macro-scale appearance that is characteristic of Cooper Basin deep coals

Source: Dunlop et al. (2017); Department for Energy and Mining (SA) (2017). This figure is covered by a Third Party Creative Commons Attribution licence
Element: GBA-COO-2-325

Analysis of full-hole cores acquired to date indicates that deep coal gas reservoirs do not have a significant, pervasively permeable CSG-like cleat system (Figure 20). Generally, vitrinite cleats are mostly associated with isolated, thin vitrinite laminations and lenses, which contribute minimally to the bulk coal volume. Regardless, the thin cleated layers affect the overall coal fabric as they create numerous planes of weakness. These will probably affect the production surface area induced by effective reservoir stimulation (Dunlop et al., 2017).

Compared to the CSG reservoirs, the deep coal gas reservoirs do not have significant mobile formation water or adjacent permeable formation water bearing zone. No reservoir dewatering should be required for gas production from deep coal gas reservoirs.

4.1.2.8 Mineralogy and brittleness

The mineral assemblage and brittleness of the Patchawarra Formation shales and coaly shales were described using X-ray Diffraction (XRD) analyses of 36 shale rock samples from 4 wells (Department for Energy and Mining (SA), 2018a).

The Patchawarra Formation shale rocks mainly consist of quartz, muscovite 2M1 and 1M, siderite, kaolinite/dickite, with minor chlorite, feldspar, anatase and rutile (Table 22). Barite (2.8–13.6 wt%) was also found in Streaky 1 in the Nappamerri Trough. XRD analyses of coaly shale samples in Bob Well 2 show the mineral components include a quartz content of 13.2%, kaolinite content of 15.7%, muscovite 2M1 content of 19.1%, muscovite 1M content of 7.1%, amorphous organic matter content of 44.2%, and minor contents of rutile and anatase (Santos–Delhi–Origin, 2010;

Department for Energy and Mining (SA), 2018a). A ternary plot of the dominant mineral content (wt fraction) of the Patchawarra Formation shales and coaly shales is shown in Figure 21.

Table 22 Main mineral assemblage statistics of the Patchawarra Formation shales analysed by XRD

Statistics	Quartz (wt%)	Clay (wt%)	Siderite (wt%)	Feldspar (wt%)	Anatase (wt%)	Rutile (wt%)
Minimum	35.20	6.00	0.00	0.00	0.10	0.10
Maximum	90.60	56.40	19.00	6.00	0.40	0.70
Average	66.64	26.83	3.50	0.58	0.23	0.40
Median	66.60	19.90	3.00	0.00	0.20	0.40

Data: Bobs Well 2, Kingston Rule 1, Streaky 1 and Tindilpie 11 (Department for Energy and Mining (SA), 2017, 2018a)

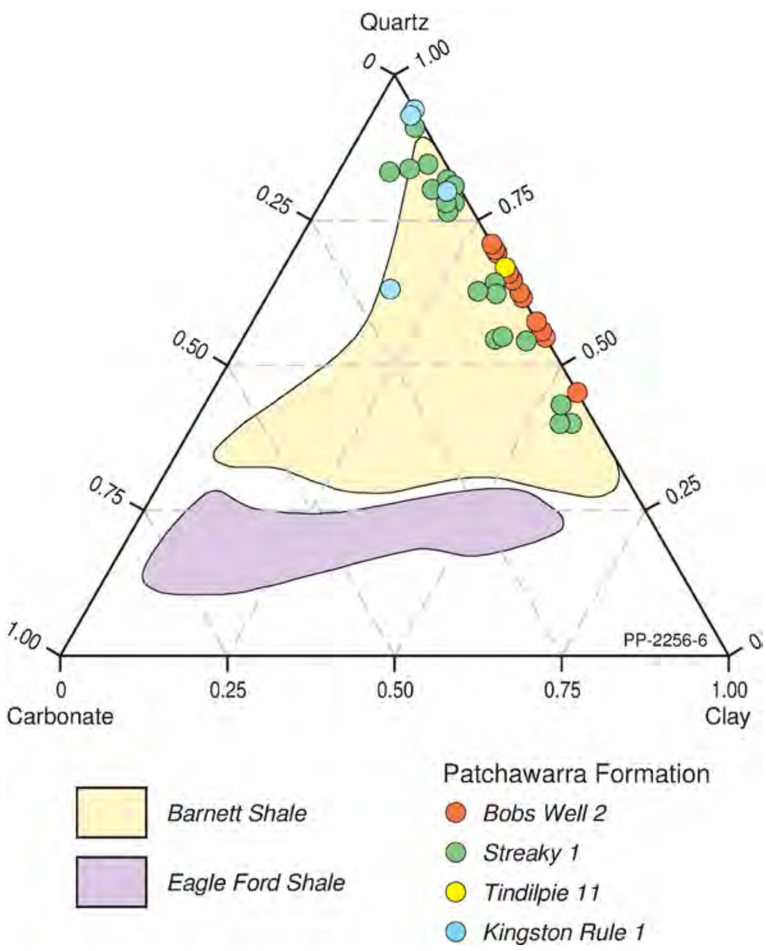

Figure 21 Ternary plot of mineral content (wt fraction) of the Patchawarra Formation shales in the Cooper Basin

For comparison two USA shale plays (the Barnett and Eagle Ford shales) are shown (after Passey et al., 2010).
Data: Bobs Well 2, Kingston Rule 1, and Streaky 1 (Department for Energy and Mining (SA), 2017, 2018a)
Element: PP-2256-6

One common brittleness measure is the ratio of compressive strength to tensile strength (Coates and Parsons, 1966). The higher the magnitude of brittleness, the more brittle the rock. The brittleness index (BI) is used to calculate the brittleness of shale rocks and can be estimated from the normalised Young's modulus and Poisson's ratio (Wang and Gale, 2009; Rickman et al., 2008), or defined by the mineral assemblage (Jarvie et al., 2007; Wang and Gale, 2009). In this study, the brittleness index (BI) is calculated using mineral assemblage (Jarvie et al., 2007), where BI is defined as:

$$\mathrm{BI} = \frac{\mathrm{Q}}{\mathrm{Q+C+Cl}} \quad (1)$$

Where: Q= quartz content (wt%); C= carbonate content (wt%); Cl= clay content (wt%).

In a case study in the Barnett Shale by Perez Altamar and Marfurt (2014), the following brittleness classifications were applied: Brittle: BI > 0.48; Less brittle: BI = 0.32–0.48; Less ductile: BI = 0.16–0.32; and Ductile: BI < 0.16.

Using equation 1, the Patchawarra Formation shales and coaly shales are classified as ‘brittle’ with a BI of 0.695 (Table 23).

Table 23 Average brittleness index of Patchawarra Formation shales estimated using the Jarvie et al. (2007) method for key wells

Well	Average brittleness index
Bobs Well 2	0.611
Kingston Rule 1	0.819
Streaky 1	0.686
Tindilpie 11	0.665
Average	0.695

Data: Bobs Well 2, Kingston Rule 1, Streaky 1 and Tindilpie 11 (Department for Energy and Mining (SA), 2018a)

4.1.2.9 Gas composition

Gas composition analysis on desorbed gas samples from the Patchawarra Formation in 10 wells (Department for Energy and Mining (SA), 2018a) show that on average Patchawarra Formation gas includes 59.31% methane, 8.88% ethane, 2.87% propane and longer chain hydrocarbons, and 28.94% carbon dioxide (Table 24). An average condensate-to-gas ratio (CGR) of 12.54 bbl/mmscf for the Patchawarra Formation was determined from well test data (mainly the DSTs) compiled from publically available well completion reports.

Table 24 Average gas compositions of desorbed gas samples from the Patchawarra Formation in the Cooper Basin

Well	Methane (mol%)	Ethane (mol%)	Propane plus (mol%)	Carbon dioxide (mol%)
Admella 1	49.02	13.92	2.69	34.38
Bobs Well 2	52.80	4.79	0.77	41.68
Davenport 1ST1	60.90	7.15	1.87	30.08
Forge 1	64.31	1.58	0.59	33.52
Kingston Rule 1	68.20	8.73	4.97	18.11
Sasanof 1	41.14	10.94	7.88	40.03
Skipton 1	64.83	11.68	4.78	18.72
Talaq 1	74.33	10.89	1.06	13.72
Tindilpie 11	50.03	16.29	3.96	29.72
Tirrawarra 76	67.58	2.80	0.15	29.46
Average	59.31	8.88	2.87	28.94

Source: Department for Energy and Mining (SA) (2018a)

4.1.3 Murteree Shale

Key features of the Murteree Shale are summarised in Table 25 and discussed in more detail in the following text.

Table 25 Key features of the Murteree Shale

Unconventional Play type	Shale gas
Age	early Permian (Cisuralian: Kungurian stage)
Extent	31,300 km^2
Top depth (m)	1230–3770 m
Gross formation thickness	0–190 m
Lithology	Siltstone and sandstone
Depositional environment	Lacustrine
Kerogen type	Type III; DOM
TOC	0–12.8 wt%
Mean original HI	101 ± 43 mg HC/g TOC
Thermal maturity	Immature–over mature
Average total porosity	0.027 (fraction)
Average total water saturation	0.664 (fraction)
Average permeability	6.69E-03 mD
Average brittleness index	0.374 (fraction)
Pressure regime	Overpressured (Nappamerri Trough)
Exploration status	Under assessment/minor production

4.1.3.1 Age and stratigraphic relationships

The Murteree Shale is early Permian in age (Figure 2) and is associated with palynofloras consistent with spore-pollen zones APP3.2 (Gray and McKellar, 2002; Price, 1997).

The Murteree Shale is part of the Gidgealpa Group. The Murteree Shale conformably overlies and interfingers with the Patchawarra Formation, and is conformably overlain by the Epsilon Formation (Figure 2). Locally, however, the Murteree Shale is unconformably overlain by the late Permian Toolachee Formation due to early to mid-Permian tectonism and erosion that resulted in the Daralingie unconformity (Alexander et al., 1998a; Draper, 2002).

4.1.3.2 Extent, depth and gross formation thickness

The Murteree Shale is widespread within the Cooper Basin, covering an area of approximately 31,300 km^2, and is preserved in the south-western Cooper Basin in the Nappamerri and Tenappera troughs (Figure 22) (Hall et al., 2015a; Owens et al., 2020). It is mostly absent on the JNP Trend and further north (Alexander et al., 1998a; Gray and McKellar, 2002) and appears to pinch out south of the Tinga Tingana Ridge (Figure 1) (Morton, 2016).

The depth to the top of the Murteree Shale ranges from 1230 m along the south-west edge of the formation to a maximum of 3770 m in the Nappamerri Trough (Figure 22) (Hall et al., 2015a).

The Murteree Shale has an average thickness of 33 m, however it reaches a maximum thickness of approximately 190 m in the Nappamerri Trough (Figure 22) (Hall et al., 2015a).

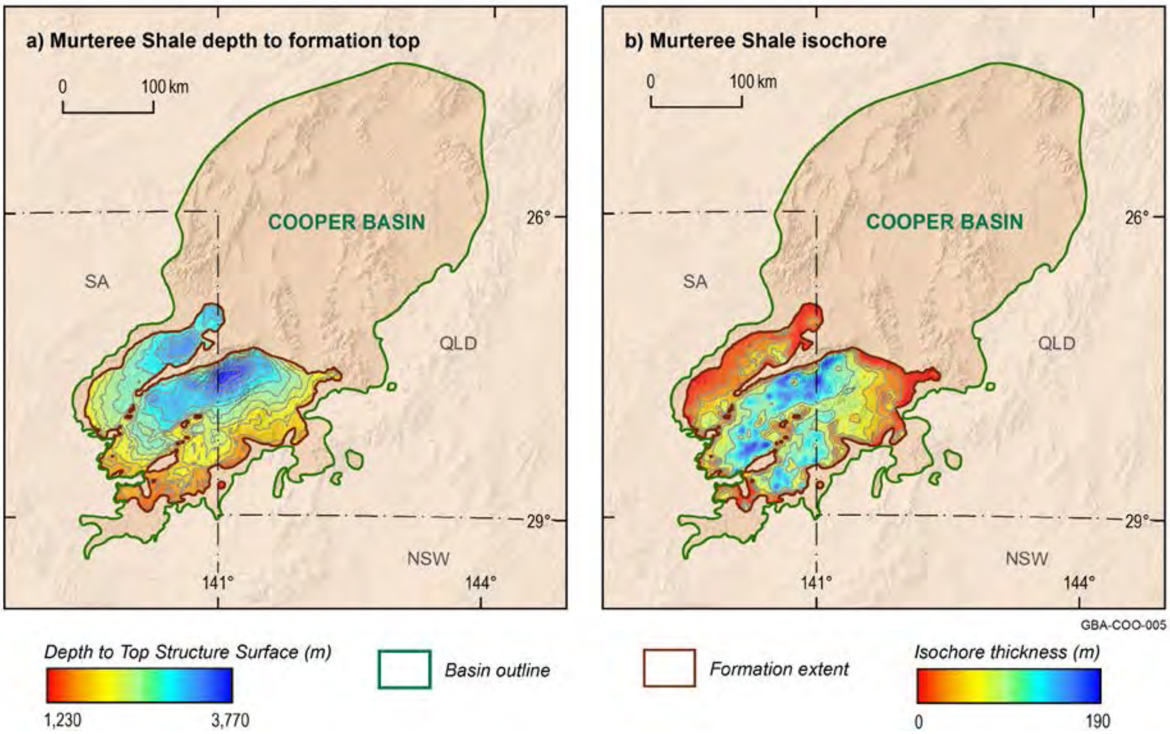

Figure 22 (a) Murteree Shale formation top depth (m) and (b) Murteree Shale total vertical thickness (m)

Source: Hall et al. (2015a)
Data: Hall et al. (2016a); Cooper Basin outline from Raymond et al. (2018)
Element: GBA-COO-005

4.1.3.3 Lithology and palaeoenvironment

The Murteree Shale includes black to dark grey-brown argillaceous siltstone with minor fine-grained sandstone. Carbonaceous material, muscovite and fine-grained pyrite are characteristic of the unit, which becomes sandier in the southern Cooper Basin (Alexander et al., 1998a; Gatehouse, 1972; Gray and McKellar, 2002; McKellar, 2013). Horizontally-laminated siltstone, minor lenticular laminations, rare ripple waves and wavy bedding, and occasional rhythmites and turbidites collectively indicate a deep lake environment with restricted circulation (Alexander et al., 1998a; Gray and McKellar, 2002).

4.1.3.4 Source rock distribution, geochemistry and maturity

The mean TOC content of all samples is 2.7 ± 2.1 wt%, with a range from 0.1 to 12.8% (164 samples) (Hall et al., 2016b). The present day TOC map for the Murteree Shale shows good to excellent source rock potential (TOC > 2 wt%) across the formation, with the highest TOC contents occurring in the Patchawarra Trough and around the basin edges (Figure 23; Figure 24) (Hall et al., 2016b).

Present day source rock quality (mean HI 75 ± 38 mg HC/g TOC) is similar to that of the calculated original source rock quality (mean HI_o 101 ± 43 mg HC/g TOC), which is consistent with the observations from low maturity samples indicating that the organic matter within the shales predominantly comprises dry gas-prone Type III kerogen (Figure 23) (Hall et al., 2016b). This result suggests the low HI values are not a function of high maturity but reflect the quality of the original source rock. Given the current data distribution, there is no evidence for the development of Type I kerogen (HI > 600 mg HC/g TOC), as could have been inferred from the lacustrine depositional environment (Hall et al., 2016b). Instead, the poor liquids potential and a depositional environment conducive to good organic matter preservation indicates a lack of aquatic algal inputs (Hall et al., 2016b).

The net volume of organically rich shales was calculated for the Murteree Shale using the net organically rich ratio (NORR) of shales with TOC > 2 wt% and gross formation thickness. TOC profiles were analysed by comparing the sonic log with the deep resistivity log (Passey et al., 1990; Passey et al., 2010; Cooper et al., 2015) in Encounter 1, Holdfast 1 and Moomba 191. The net organically rich thickness of shale was then calculated as the product of the NORR and gross shale thickness and has an average NORR of 0.6902 (Table 26).

Table 26 Net organically rich ratio (NORR) for the Murteree Shale as calculated from Encounter 1, Holdfast 1 and Moomba 191 in the Nappamerri Trough

Well	Net organically rich ratio (fraction)
Encounter 1	0.6931
Holdfast 1	0.4406
Moomba 191	0.9369
Average	0.6902

The maturity of the Murteree Shale is highest in the central Nappamerri Trough (Figure 25) where it ranges from the wet gas window (Ro 1–1.2%; TR 50–70%) through to overmature (Ro >3.5%; TR >95%; Hall et al., 2016c). This high maturity reflects both the greater burial depths and proximity to the high heat producing Big Lake Suite granodiorites (Deighton et al., 2003; Deighton and Hill, 1998). In the Patchawarra Trough, maturity ranges from the early oil window (R_o 0.75–0.9%; TR < 50%) in the west to late oil (R_o 1–1.2%; TR > 50–70%) in the east.

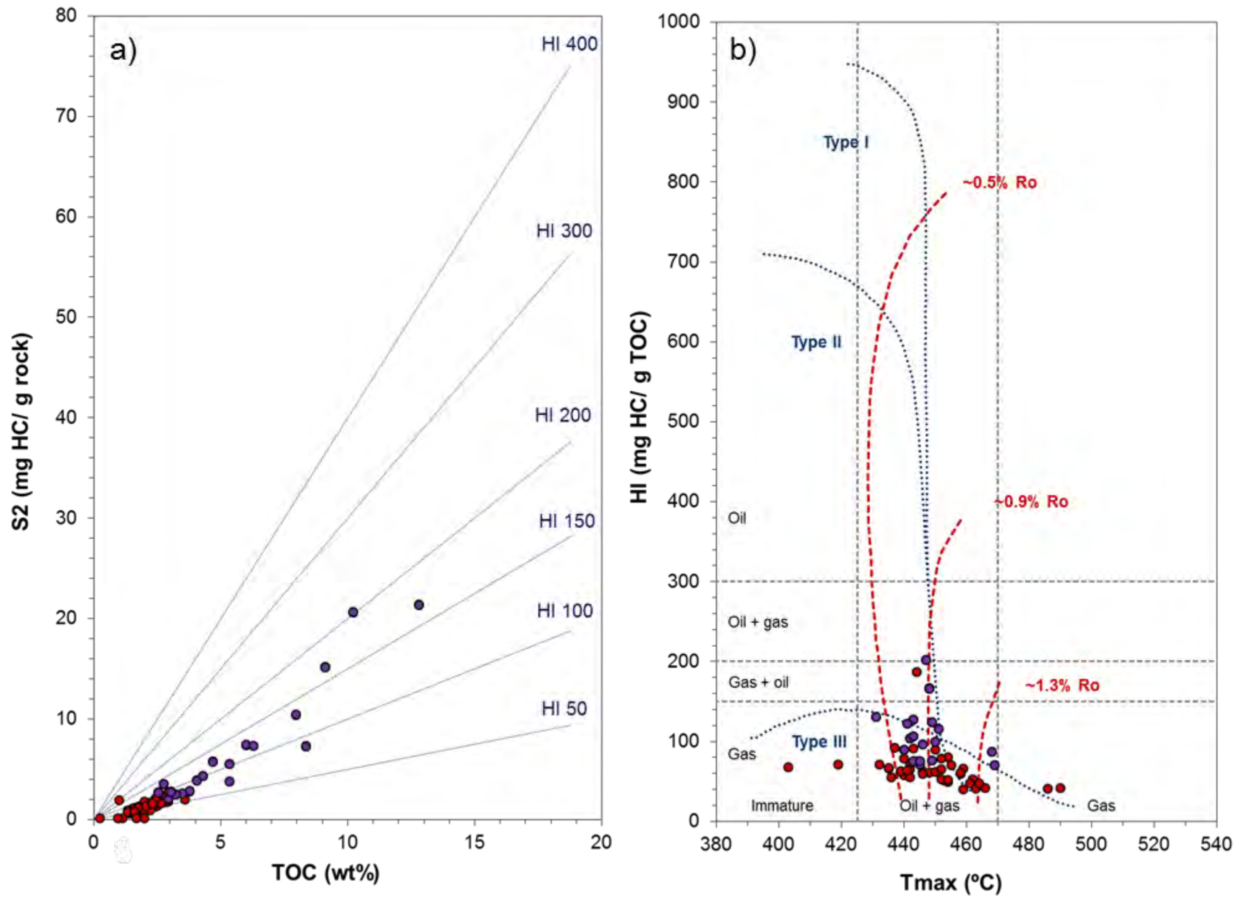

Figure 23 Rock-Eval pyrolysis data plots for the Murteree Shale: (a) TOC content vs S2 yield and (b) T_{max} vs HI

Purple dots: effective source rocks (TOC > 2wt%; S1 + S2 > 3 mg HC/g rock); red dots: samples with either no original generation potential or are spent source rocks.
Source: Hall et al. (2016b)
Data: Hall et al. (2016a)
Element: GBA-COO-2-299

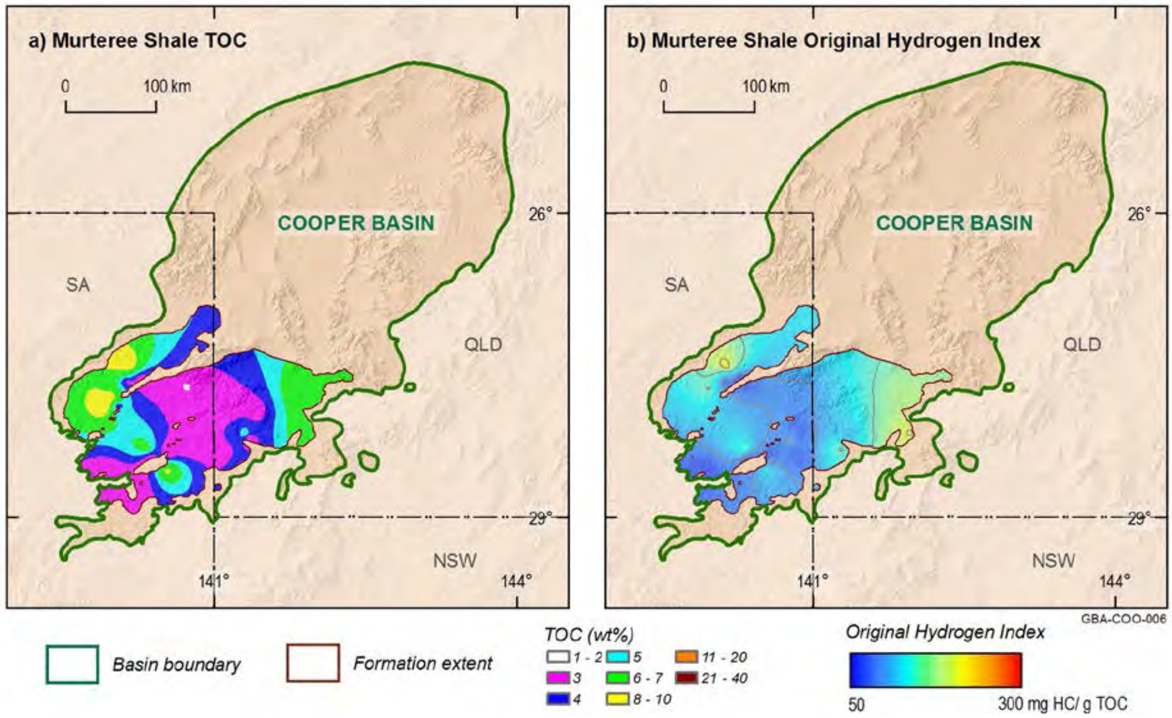

Figure 24 Murteree Shale source rock geochemistry maps: (a) Present day average Total Organic Carbon (TOC) (%) and (b) mean Original Hydrogen Index (HI_o) (mg HC/gTOC)

Source: Hall et al. (2016b)
Data: Hall et al. (2016a); Cooper Basin outline from Raymond et al. (2018)
Element: GBA-COO-006

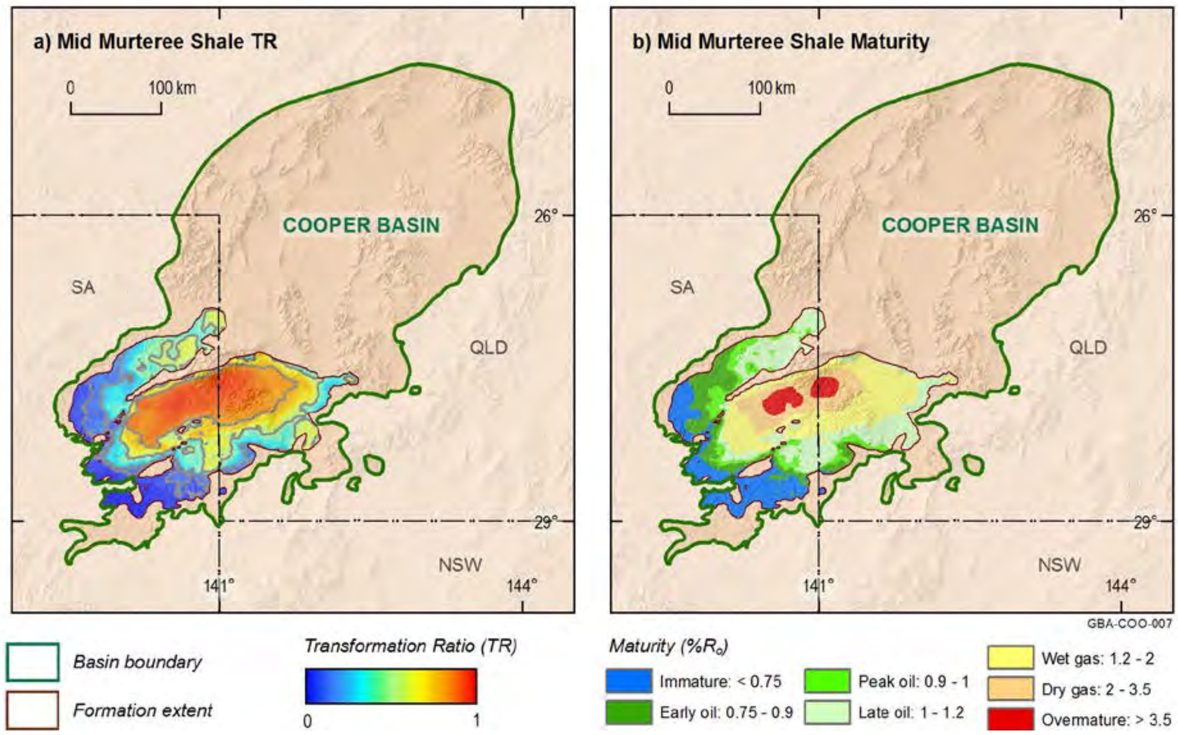

Figure 25 Murteree Shale (a) transformation ratio (TR) and (b) maturity (%R_o)

Source: Hall et al. (2016c)
Data: Hall et al. (2016a); Cooper Basin outline from Raymond et al. (2018)
Element: GBA-COO-007

4.1.3.5 Shale reservoir characteristics

Porosity, permeability and fluid saturation are three of the key petrophysical input parameters required for characterising shale plays. The average shale rock properties of the Murteree Shale are shown in Table 27 and Figure 26 (Department for Energy and Mining (SA), 2018a). Based on laboratory tests (as-received basis) on 68 shale rock samples from 7 wells, the Murteree Shale has an average total porosity of 2.7%, average gas saturation of 30.3% and average permeability of 6.69E-03 mD.

Table 27 Average as-received laboratory measured shale rock properties of Murteree Shale for key wells in the Cooper Basin

Well name	Bulk density (g/cc)	Water saturation (fraction)	Oil saturation (fraction)	Gas saturation (fraction)	Gas-filled Porosity (fraction)	Total porosity (fraction)	Permeability (mD)
Bobs Well 2	2.67	0.535	0.052	0.413	0.011	0.025	1.54E-05
Encounter 1	2.69	0.853	0.000	0.147	0.003	0.019	4.92E-05
Holdfast 1	2.69	0.759	0.000	0.241	0.004	0.016	5.35E-06
Kingston Rule 1	2.66	0.601	0.057	0.342	0.010	0.024	1.18E-02
Marsden 1	2.64	0.705	0.042	0.254	0.012	0.045	1.29E-04
Moomba 191	2.70	0.512	0.075	0.413	0.007	0.017	5.70E-05
Vintage Crop 1	2.64	0.684	0.003	0.313	0.014	0.039	3.47E-02
Average	2.67	0.664	0.033	0.303	0.009	0.027	6.69E-03

Data: Bobs Well 2, Encounter 1, Holdfast 1, Kingston Rule 1, Marsden 1,Moomba 191 and Vintage Crop 1 (Department for Energy and Mining (SA), 2017, 2018a)

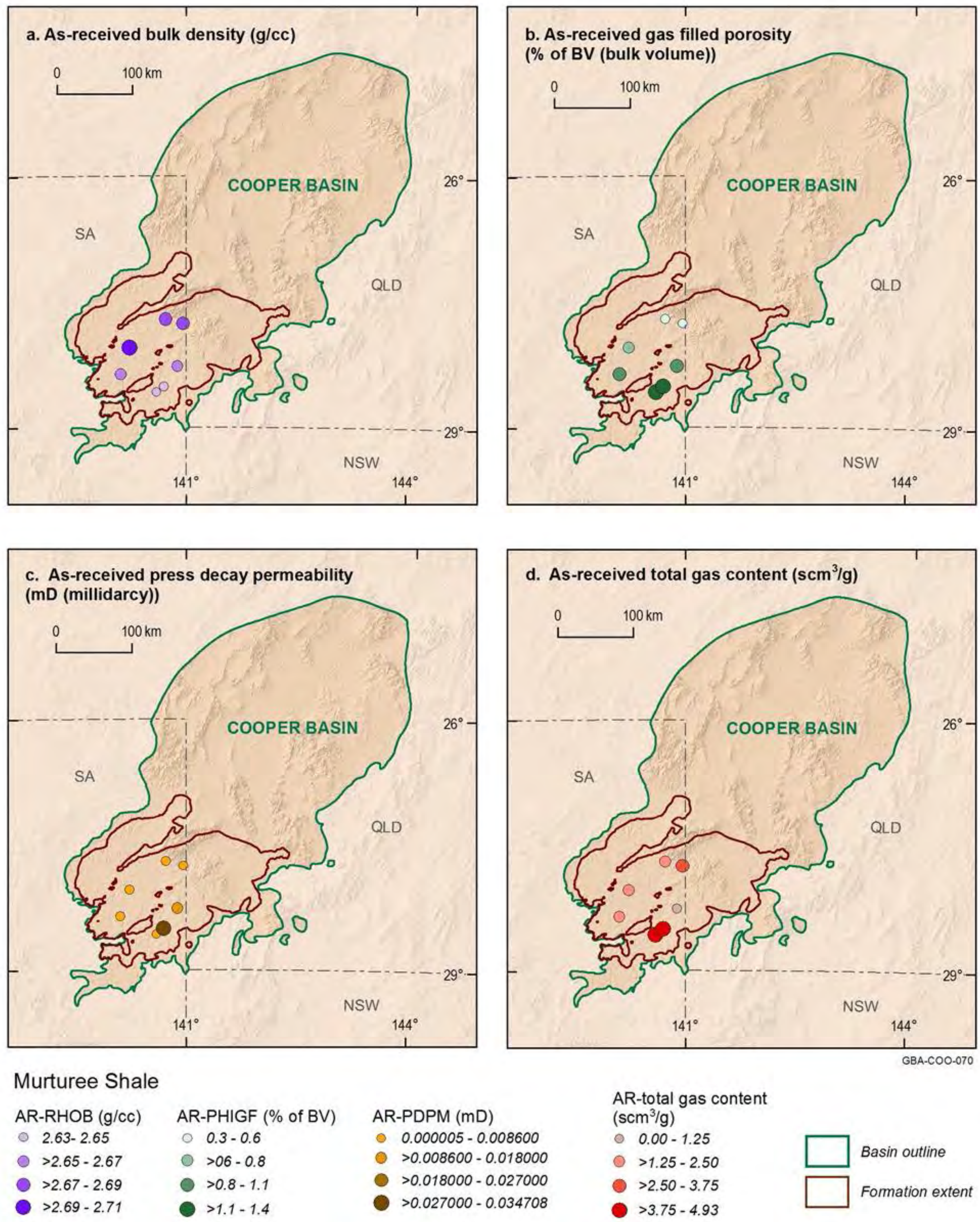

Figure 26 The average as-received (a) bulk density (AR-RHOB), (b) gas-filled porosity, (c) pressure decay permeability (PDPM) and (d) total gas content of the Murteree Shale in the Cooper Basin

Data: Department of Natural Resources (2018a); Department for Energy and Mining (SA) (2017, 2018a); Cooper Basin outline from Raymond et al. (2018)

Element: GBA-COO-070

Gas in shale is stored as adsorbed gas on the organic matter, free gas stored in the pore spaces and dissolved gas in the formation water.

Analysis from 9 wells (Department for Energy and Mining (SA), 2018a) indicates that the Murteree Shale has an average as-received total gas storage capacity of 2.17 scc/g (Table 28).

The adsorbed gas storage capacity of the Murteree Shale was analysed using isotherm tests for shale rock samples from 6 wells. The averaged isotherm test results under the reservoir temperature in the Cooper Basin, including the measurement gas, total organic content (wt fraction), crushed sample density (g/cc), Langmuir storage capacity (in situ, scc/g), Langmuir pressure (kPa) and adsorbed gas storage capacity (in situ, scc/g), are summarised in Table 29.

The average total gas storage capacity (scc/g) and capacities of all three storage mechanisms of the Murteree shales for 3 wells is presented in Table 30. Based on the analysis, the average total gas storage capacity is 1.08 scc/g.

Table 28 Average as-received total gas content (scc/g) of the Murteree Shale shales for key wells in the Cooper Basin

Well	Average as-received total gas content (scc/g)
Encounter 1	2.97
Forge 1	0.69
Holdfast 1	1.81
Kingston Rule 1	1.23
Moomba 191	1.38
Bobs Well 2	1.41
Marsden 1	3.05
Talaq 1	1.32
Vintage Crop 1	4.93
Average	2.17

Data: Encounter 1, Forge 1, Holdfast 1, Kingston Rule 1, Moomba 191, Bobs Well 2, Marsden 1, Talaq 1 and Vintage Crop 1 (Department for Energy and Mining (SA), 2018a).

Table 29 Average isotherm test results on the Murteree Shale shale samples under reservoir temperature in key wells in the Cooper Basin

Well	Measurement Gas	Total Organic Content (wt fraction)	Crushed Density (g/cc)	Langmuir Storage Capacity, in situ (scc/g)	Langmuir Pressure (kPa)	Adsorbed Storage Capacity, in situ (scc/g)
Encounter 1	methane	0.0323	2.569	2.23	10303.85	1.87
Holdfast 1	methane	0.0234	2.750	2.10	24332.71	1.27
Kingston Rule 1	methane	0.0291	2.613	0.49	5202.70	0.40
Kingston Rule 1	CO_2	0.0418	2.537	1.43	3337.75	1.27
Marsden 1	methane	0.0236	2.684	0.39	3347.38	0.34
Moomba 191	methane	0.0230	2.722	0.79	31164.32	0.66
Vintage Crop 1	methane	0.0231	2.747	1.76	23380.35	0.78

Data: Encounter 1, Holdfast 1, Kingston Rule 1, Marsden 1, Moomba 191 and Vintage Crop 1 (Department for Energy and Mining (SA), 2018a)

Table 30 Average total gas storage capacity (scc/g) of the Murteree Shale shales in key wells in the Cooper Basin

Well	Dissolved Gas in Water Storage Capacity (scc/g)	Free Gas Storage Capacity (scc/g)	Adsorbed Gas Storage Capacity (scc/g)	Total Gas Storage Capacity (scc/g)
Moomba 191	0.01	0.31	0.66	0.98
Vintage Crop 1	0.02	0.4	0.8	1.22
Kingston Rule 1	0.01	0.58	0.44	1.03
Average	0.01	0.43	0.63	1.08

Data: Kingston Rule 1, Moomba 191 and Vintage Crop 1 ((Department for Energy and Mining (SA), 2018a))

4.1.3.6 Mineralogy and brittleness

The mineral assemblage and brittleness of the Murteree Shale were described using XRD analyses from 126 shale rock samples from 8 wells (Santos-Beach-Origin, 2012; Department for Energy and Mining (SA), 2018a).

The Murteree Shale comprises quartz, kaolinite, mica/illite, feldspar, chlorite, siderite, rutile and anatase (Table 31). In addition, dolomite and pyrite were also identified by Scanning Electron Microscopy (SEM) imaging of Murteree Shale samples (Jadoon et al., 2016). A ternary plot of the dominant mineral content of the Murteree Shale is shown in Figure 27.

Average brittleness indices (BI) were calculated from mineral composition using the method of Jarvie et al. (2007). Overall, the Murteree Shale is classified as ‘less brittle’, with a total average BI of 0.374 (Table 32).

Table 31 Main mineral assemblage statistics of the Murteree Shale analysed by XRD

Formation	Quartz (wt%)	Clay (wt%)	Siderite (wt%)	Feldspar (wt%)	Anatase (wt%)	Rutile (wt%)
Minimum	13.00	9.20	0.40	0.00	0.10	0.20
Maximum	82.80	64.30	57.00	6.00	2.00	1.00
Average	34.61	52.73	11.06	0.37	0.50	0.67
Median	33.05	54.65	8.75	0.00	0.40	0.60

Data: Bobs Well 2, Encounter 1, Kingston Rule 1, Marsden 1, Holdfast 1, Moomba 191, Streaky 1 and Vintage Crop 1 (Santos-Beach-Origin, 2012; Department for Energy and Mining (SA), 2018a)

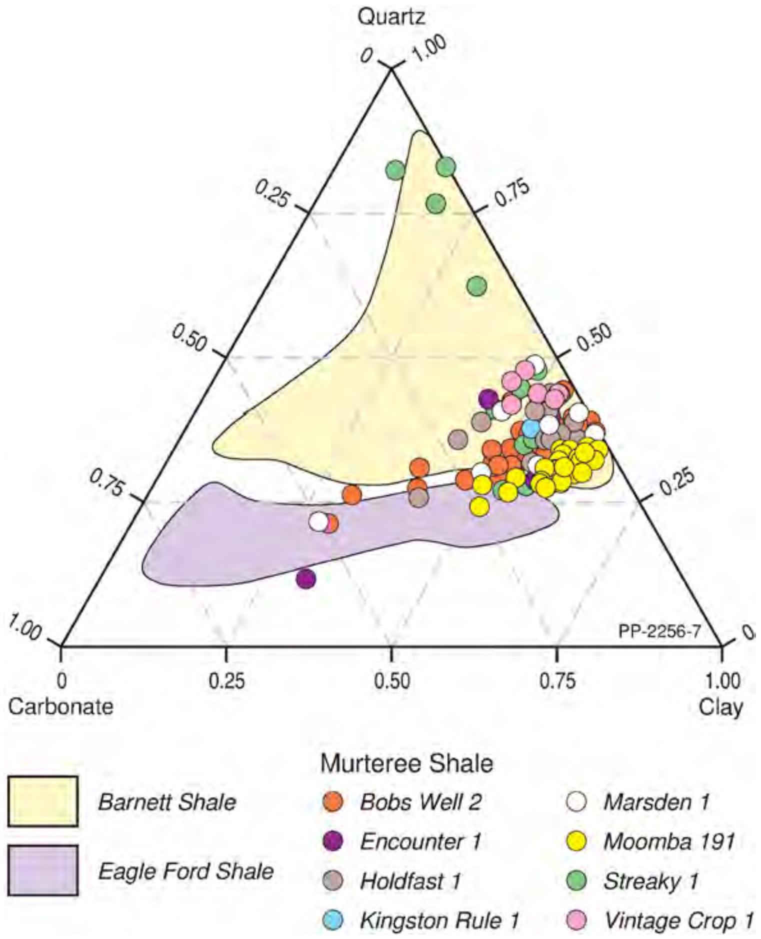

Figure 27 Ternary plot of mineral content (wt% fraction) for shales of the Murteree Shale in the Cooper Basin

For comparison two USA shale plays (the Barnett and Eagle Ford shales) are shown (after Passey et al., 2010).
Data: Bobs Well 2, Encounter 1, Holdfast 1, Kingston Rule 1, Marsden 1, Moomba 191, Streaky 1 and Vintage Crop 1 (Department for Energy and Mining (SA), 2017, 2018a)
Element: PP-2256-7

Table 32 Average brittleness indices for the Murteree Shale estimated from mineral assemblages using the method of Jarvie et al. (2007)

Well	Average brittleness index (BI)
Bobs Well 2	0.346
Encounter1	0.314
Holdfast 1	0.361
Kingston Rule 1	0.368
Marsden 1	0.421
Moomba 191	0.301
Streaky 1	0.459
Vintage Crop 1	0.420
Average	0.374

Data: Bobs Well 2, Encounter 1, Kingston Rule 1, Marsden 1, Holdfast 1, Moomba 191, Streaky 1 and Vintage Crop 1 (Santos-Beach-Origin, 2012; Department for Energy and Mining (SA), 2018a)

4.1.3.7 Gas composition

Gas composition analysis on the desorbed gas samples from the Murteree Shale in 10 wells (Department for Energy and Mining (SA), 2017, 2018a; Department of Natural Resources, 2018a) show that on average Murteree Shale gas includes 60.44% methane, 4.99% ethane, 1.24% propane plus, and 33.32% of carbon dioxide (Table 33; Figure 28). Publically available well test data (mainly DST) in the overlying Epsilon Formation suggests the average condensate-to-gas ratio (CGR) in gas-bearing intervals (23 wells) is approximately 17 bbl/mmscf.

Table 33 Average gas compositions of desorbed gas samples from the Murteree Shale for key wells in the Cooper Basin

Well	Methane (mol%)	Ethane (mol%)	Propane plus (mol%)	Carbon dioxide (mol%)
Bobs Well 2	53.60	5.21	0.78	40.41
Encounter 1	57.54	0.83	0.26	41.37
Holdfast 1	65.27	0.00	0.00	34.73
Kingston Rule 1	72.76	6.12	0.95	20.17
Moomba 191	75.25	0.07	0.01	24.67
Sasanof 1	46.82	5.31	1.12	46.75
Skipton 1	71.18	14.06	3.13	11.62
Talaq 1	53.50	7.81	1.82	36.87
Vintage Crop 1	29.52	4.55	1.51	64.42
Marsden 1	79.00	5.99	2.84	12.17
Average	60.44	4.99	1.24	33.32

Data: Bobs Well 2, Encounter 1, Holdfast 1, Kingston Rule 1, Moomba 191, Sasanof 1, Skipton 1, Talaq 1, Vintage Crop 1 and Marsden 1 (Department for Energy and Mining (SA), 2017, 2018a; Department of Natural Resources, 2018a)

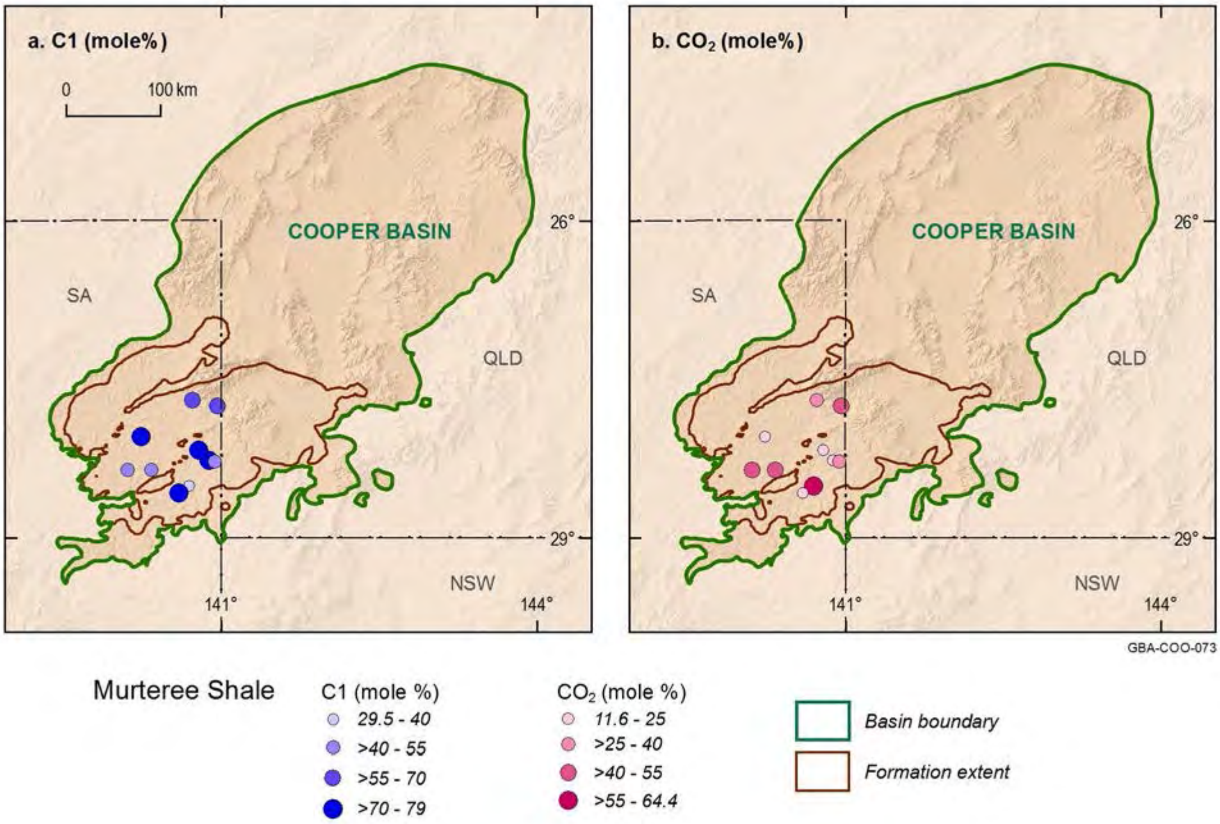

Figure 28 Contents of methane (C1) and carbon dioxide of desorbed gas from the Murteree Shale in the Cooper Basin

Data: Department for Energy and Mining (SA) (2018a); Cooper Basin outline from Raymond et al. (2018)
Element: GBA-COO-073

4.1.4 Epsilon Formation

Key features of the Epsilon Formation are summarised below in Table 34 and discussed in more detail in the following text.

Table 34 Key features of the Epsilon Formation

Unconventional Play type	Tight and deep coal gas
Age	Early/middle Permian (upper Kungurian-Roadian)
Extent	31,400 km^2
Top depth (m)	1225–3625 m
Gross formation thickness	0–220 m
Lithology	Sandstone, siltstone, shale and coal
Depositional environment	Prograding delta, lacustrine
Kerogen type	Type II/III to Type III; coal, DOM
TOC	0–80 wt%
Mean original HI	186 ± 91 mg HC/g TOC
Thermal maturity	Immature–over mature
Average effective porosity	0.067 (fraction) in tight pay intervals
Average effective water saturation	0.33 (fraction) in tight pay intervals
Pressure regime	Overpressured (Nappamerri Trough)
Exploration status	Under assessment/minor production

4.1.4.1 Age and stratigraphic relationships

The Epsilon Formation is assigned a late early Permian to early middle Permian age (Figure 2) based on ages of associated spore-pollen zones (Price, 1997; Gray et al., 2002).

The Epsilon Formation interbeds with and is conformably overlain by the Roseneath Shale, and conformably overlies the Murteree Shale (Figure 2). Where the Roseneath Shale and Daralingie Formation have been eroded, the Epsilon Formation is unconformably overlain by the Toolachee Formation (Alexander et al., 1998a).

4.1.4.2 Extent, depth and gross formation thickness

The Epsilon Formation is widespread across the south-western Cooper Basin, from the Tenappera, Wooloo and Allunga troughs in the south to north of the Patchawarra Trough (Figure 1), covering an area of approximately 31,400 km^2 (Hall et al., 2015a). Its extent north of the JNP Trend is very limited and the formation was eroded from the Dunoon and Murteree ridges, during the middle to late Permian episode of uplift (Alexander et al., 1998a).

The depth to the top of the Epsilon Formation ranges from 1225 m along the south edge of the formation to a maximum of 3625 m in the Nappamerri Trough (Figure 29) (Hall et al., 2015a).

The Epsilon Formation is an average of 50 m thick and reaches thicknesses of 220 m in the Nappamerri Trough (Hall et al., 2015a).

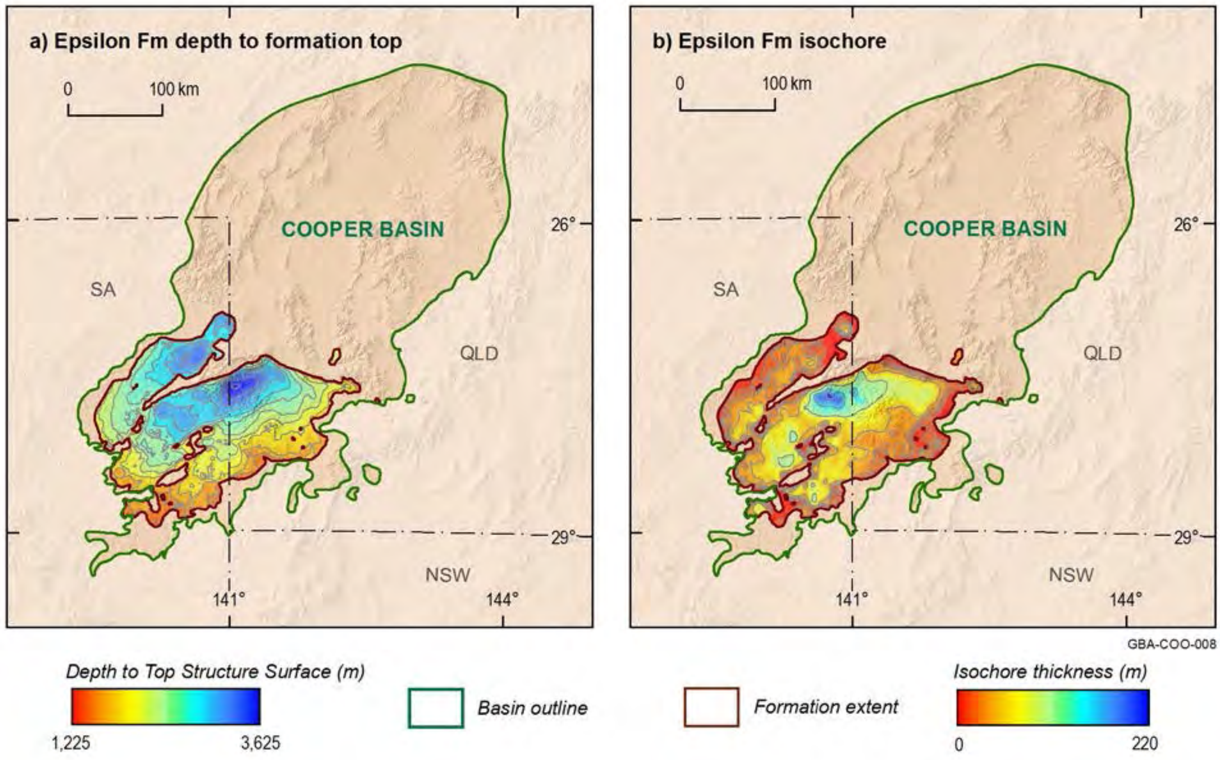

Figure 29 a) Epsilon Formation top depth (m), b) Epsilon Formation total vertical thickness (m)

Source: Hall et al. (2015a)
Data: Hall et al. (2016a); Cooper Basin outline from Raymond et al. (2018)
Element: GBA-COO-008

4.1.4.3 Lithology and palaeoenvironment

The Epsilon Formation comprises fine to medium-grained quartzose sandstone interbedded with dark grey-brown carbonaceous siltstone and shale, and thin to occasionally thick coal seams (Figure 30) (Alexander et al., 1998a; Gatehouse, 1972; Gray and McKellar, 2002; Lang et al., 2002; Lang et al., 2001).

Three major depositional stages have been identified (Lang et al., 2002; Fairburn, 1992): a lower coarsening-upward fine to medium sandy cycle; a coal-dominated middle stage; and an upper progradational succession of shales and sandstones, with occasional coal, up to 45 m thick.

In the early stages of deposition, delta fill and delta slope successions were coeval with beach development, beach barrier and shoreline deposits. Distributary channels developed on a prograding delta and oriented perpendicular to the lake shoreface in the middle stage, and lacustrine or back-barrier lagoonal facies predominated in the late stage of deposition (Fairburn, 1992; Alexander et al., 1998a). The distributary and shoreface sandstone reservoirs are mostly >4 m gross thickness, although locally these reach up to 10–15 m as in the Big Lake, Munkarie and Yapeni fields (Gravestock et al., 1998a).

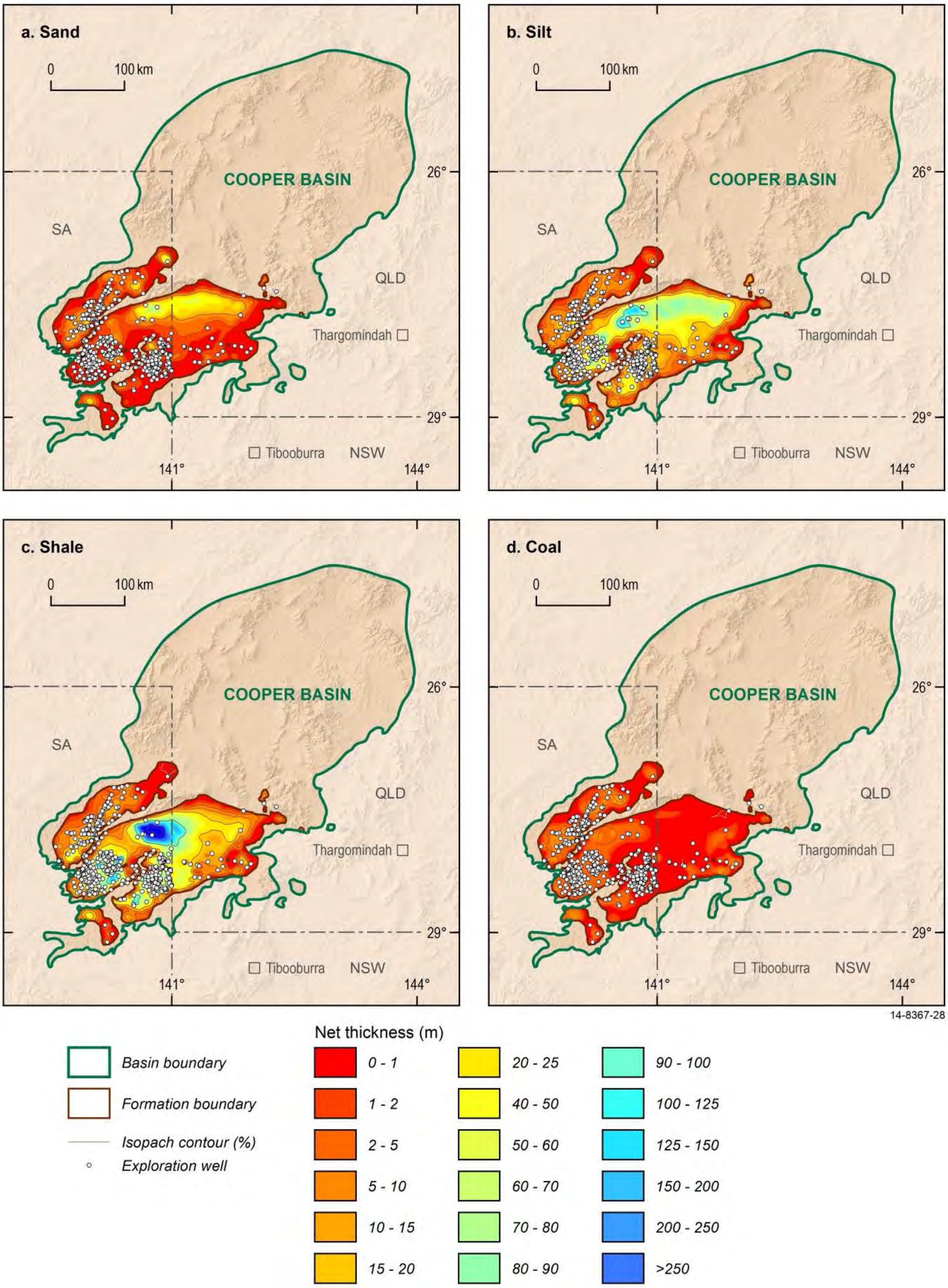

Figure 30 Epsilon Formation isolith maps by lithology, as total net thickness in metres for (a) sand, (b) silt, (c) shale and (d) coal

Shale incorporates shale, coaly shale and / or shaly coal. These are approximately equivalent to samples with a TOC range of 0.5–50 wt%

Source: Hall et al. (2015a)

Data: Hall et al. (2016a); Cooper Basin outline from Raymond et al. (2018)

Element: GBA-COO-2-309

4.1.4.4 Source rock distribution, geochemistry and maturity

The source rocks of the Epsilon Formation include shale, coaly shale, shaly coal and coal.

Although the Epsilon Formation is much thinner and less extensive than the Toolachee and Patchawarra formations, the net coal and shale thickness maps show the presence of potential source rock facies across the entire formation (Figure 30).

The Epsilon Formation cumulative coal thickness (equivalent to clean coals with TOC > 50 wt%) reaches 10–15 m in the Patchawarra and western Nappamerri troughs (Figure 30) (Sun and Camac, 2004; Hall et al., 2015a). The thickest net coal is recorded in Davenport 1 in the Milpera Depression in the south-west of the basin, where it reaches 37 m (Figure 30) (Hall et al., 2015a).

The cumulative net thickness of the shale, coaly shale and shaly coal facies (approximately equivalent to samples with a TOC range of 0.5–50 wt%) is greatest in the deepest sections of the basin around the Nappamerri Trough, where it reaches up to approximately 190 m or more (Figure 30) (Sun and Camac, 2004; Hall et al., 2015a).

The TOC of the Epsilon Formation ranges from <1 to 80 wt% with a mean of 15 wt% (Figure 31) (Hall et al., 2016b). The present day TOC map for the Epsilon Formation shale to shaly coal facies (TOC < 50 wt%) shows good to excellent quantities of TOC in source rock across the entire formation (Figure 31; Figure 32). The TOC content tends to be higher in the Patchawarra Trough and around the basin edges, reflecting the more coal-rich facies in these regions.

The mean of present day HI is 150 ± 84 mg HC/g TOC, ranging from 7–523 mg HC/g TOC, and mean original HI is 186 ± 91 mg HC/g TOC, indicating highly variable source rocks (Figure 31; Figure 32) (Hall et al., 2016b). The coal facies could be a mixture of both oil and gas-prone Type II/III and gas-prone Type III kerogen. The effective source rocks with HI value of more than 300 HC/g TOC suggest the high oil generation potential. The shaly source rocks have a greater component of gas-prone Type III kerogen (Hall et al., 2016b).

The maturity of the Epsilon Formation is highest in the central Nappamerri Trough where it reaches dry gas to overmature (R_o > 3.5%; TR > 95%; Figure 33) (Hall et al., 2016c). In the Patchawarra Trough, maturity ranges from the early oil window (Ro 0.75-0.9%) in the west to late oil (Ro 1–1.2%) in the east.

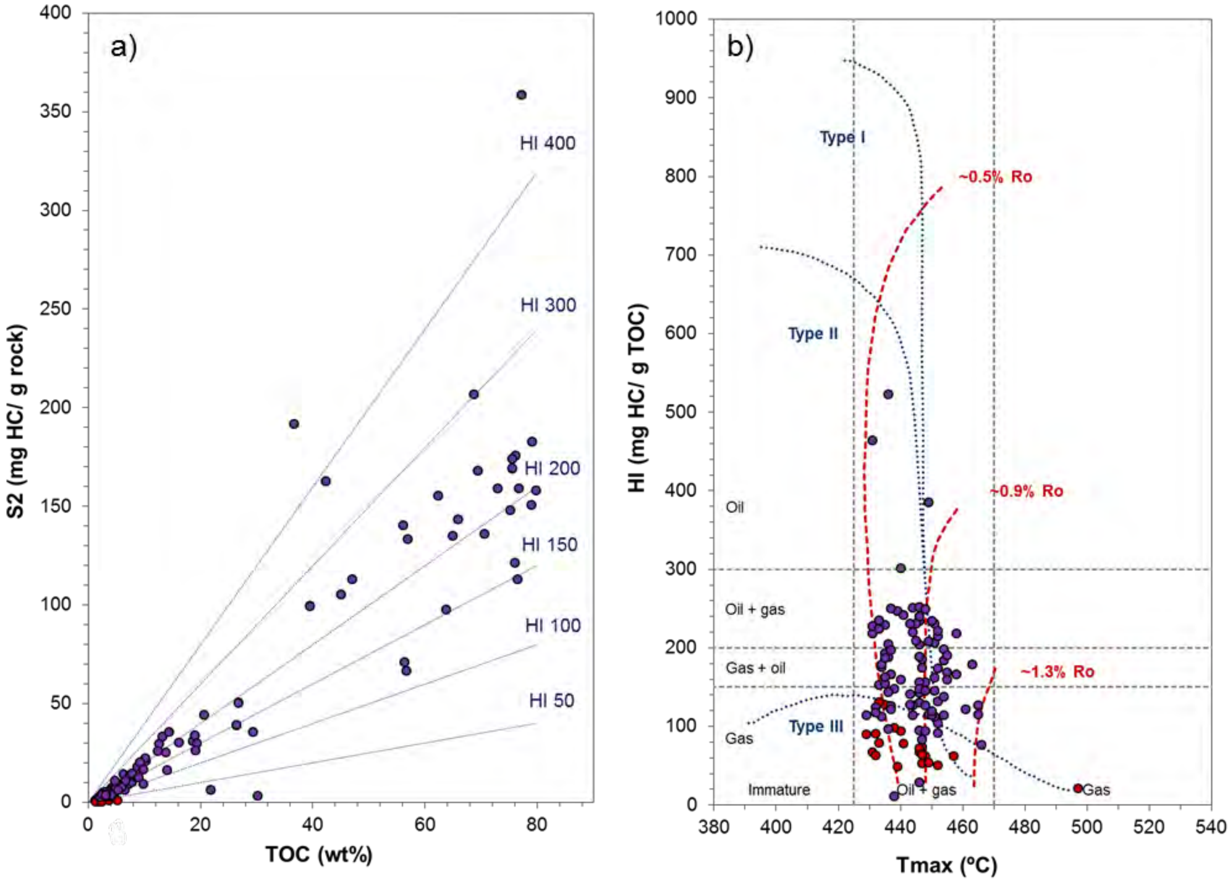

Figure 31 Rock-Eval pyrolysis data plots for the Epsilon Formation: a) TOC content vs S2 yield; b) T_{max} vs HI

Purple dots: effective source rocks (TOC > 2 wt%; S1 + S2 > 3 mg HC/g rock); red dots: samples with either no original generation potential or are spent source rocks.
Source: Hall et al. (2016b)
Data: Hall et al. (2016a)
Element: GBA-COO-2-300

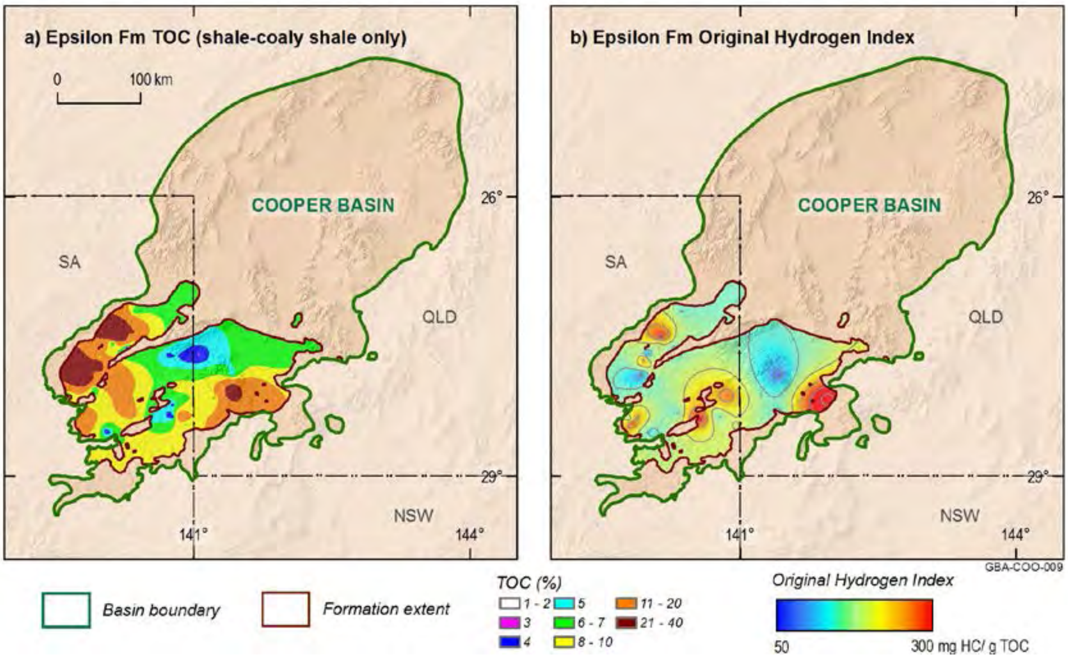

Figure 32 Epsilon Formation source rock geochemistry maps: a) Present day average Total Organic Carbon (TOC) (wt%) for shale-coaly shale facies (TOC < 50 wt%). b) mean Original Hydrogen Index (HI_o) for all source rocks (mg HC/g TOC)

Source: Hall et al. (2016b)
Data: Hall et al. (2016a); Cooper Basin outline from Raymond et al. (2018)
Element: GBA-COO-009

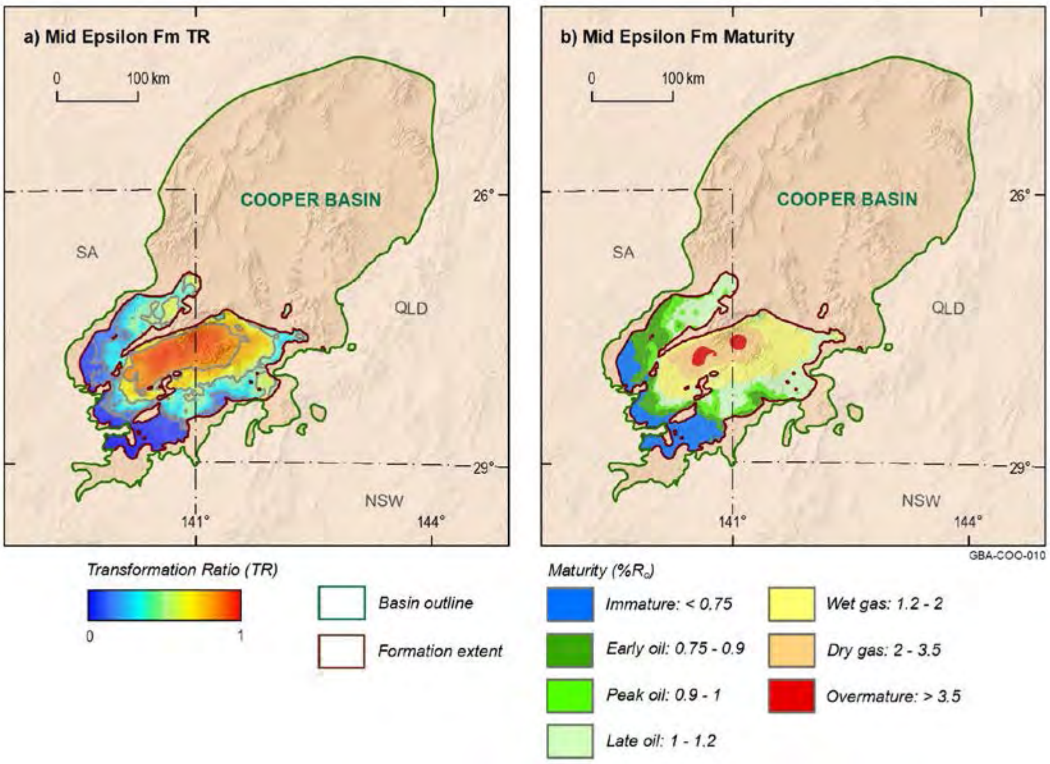

Figure 33 Epsilon Formation a) transformation ratio (TR) and b) maturity (%Ro)

Source: Hall et al. (2016c)
Data: Hall et al. (2016a); Cooper Basin outline from Raymond et al. (2018)
Element: GBA-COO-010

4.1.4.5 Tight reservoir characteristics

There is a wide distribution of good conventional reservoirs in the Epsilon Formation but it is considered less predictable for exploitation in comparison to the Patchawarra and Toolachee formations (Gravestock et al., 1998a). In addition, the Epsilon Formation has the potential to host tight gas plays in both sand and silt-rich units.

Log-derived tight pay thickness, average effective porosity and water saturation of Epsilon Formation tight reservoirs were calculated from 20 wells (Department for Energy and Mining (SA), 2018a). The average net pay thickness is 16.43 m, the average effective porosity is 6.7% and the average water saturation is 33% (Table 35; Figure 34).

Table 35 Log-derived tight pay thickness, average effective porosity and water saturation statistics for the Epsilon Formation tight reservoirs for key wells in the Cooper Basin

Well	Tight Pay Thickness (m)	Average Effective Porosity (fraction)	Average Water Saturation (fraction)
Minimum	3.90	0.046	0.062
Maximum	65.50	0.093	0.472
Average	16.43	0.067	0.330
Median	10.06	0.065	0.320

The net tight pay interval was defined by the following criteria: volume fraction of shale less than 50%, effective porosity greater than 4% and water saturation less than 70%.
Data: Beach Energy wells Boston 1, Boston 2, Dashwood 1, Etty 1, Encounter 1, Halifax 1, Hervey 1, Holdfast 1, Marble 1, Nepean 1, Rapid 1, Streaky 1 and Santos wells Bobs Well 2, Coonatie 13, Gaschnitz 1ST1, Langmuir 1, Moomba 191, Tirrawarra 76, Van Der Waals 1 and Washington 1 (Department for Energy and Mining (SA), 2018a)

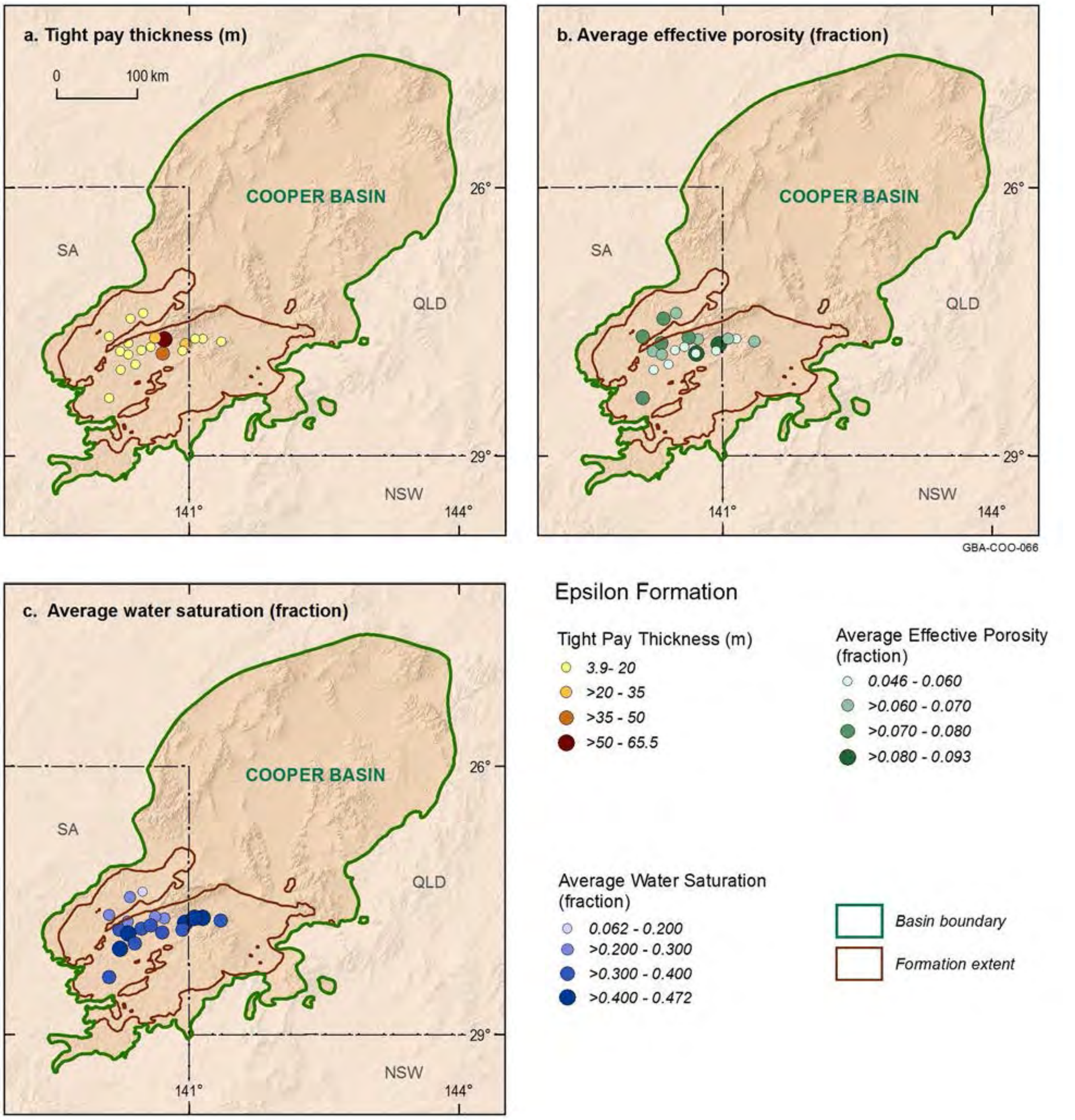

Figure 34 (a) tight pay thickness, (b) average effective porosity and (c) average water saturation of the Epsilon Formation tight reservoirs in the Cooper Basin

Data: Department for Energy and Mining (SA) (2017, 2018a); Department of Natural Resources (2018a); Cooper Basin outline from Raymond et al. (2018)
Element: GBA-COO-066

4.1.4.6 Deep coal reservoir characteristics

The distribution of Epsilon Formation coal is presented in Figure 30 (Hall et al., 2016). In the Weena Trough area, the average net thickness of the Epsilon Formation coal seams is 23.2 m in wells Klebb 1, 2, 3 and 4 (Department for Energy and Mining (SA), 2018a) (Table 36). Compared to the Patchawarra and Toolachee formation coals, the Epsilon Formation coals are thinner and thus considered to be less prospective. Limited data make it difficult to effectively fully characterise the reservoir characteristics of the Epsilon Formation deep coal gas play.

Table 36 Thickness of composite coal seams (m) in the Epsilon Formation

	Klebb 1	Klebb 2	Klebb 3	Klebb 4	Average
Epsilon Formation coal seams composite thickness (m)	27	22.5	21.9	21.4	23.2

Data: wells Klebb 1, 2, 3 and 4, (Department for Energy and Mining (SA), 2018a)

4.1.4.7 Gas composition

The gas composition analysis on the desorbed gas samples from the Epsilon Formation in 6 wells (Department for Energy and Mining (SA), 2017, 2018a) show that on average Epsilon Formation gas includes 57.01% methane, 5.80% ethane, 1.69% propane plus, and 35.49% carbon dioxide (Table 37). An average CGR of 17.11 bbl/mmscf for the Epsilon Formation was determined from well test data (mainly the DSTs) compiled from publically available well completion reports.

Table 37 Average gas compositions of desorbed gas samples from the Daralingie Formation in the Cooper Basin

Well	Methane (mol%)	Ethane (mol%)	Propane plus (mol%)	Carbon dioxide (mol%)
Encounter 1	54.37	2.34	0.32	42.97
Holdfast 1	25.00	0.00	0.00	75.00
Kingston Rule 1	81.44	13.15	5.06	0.35
Moomba 191	69.26	0.18	0.00	30.56
Sasanof 1	48.98	5.84	1.21	43.97
Skipton 1	55.53	11.03	3.40	30.02
Talaq 1	64.53	8.06	1.87	25.54
Average	57.01	5.80	1.69	35.49

Data: Encounter 1, Kingston Rule 1, Moomba 191, Sasanof 1, Skipton 1 and Talaq 1 (Department for Energy and Mining (SA), 2017, 2018a)

4.1.5 Roseneath Shale

Key features of the Roseneath Shale are summarised below Table 38 and discussed in more detail in the following text.

Table 38 Key features of the Roseneath Shale

Unconventional Play type	Shale gas
Age	Middle Permian (upper Roadian-early Wordian)
Extent	21,900 km^2
Top depth (m)	1180–3434 m
Gross formation thickness	0–240 m
Lithology	Siltstone, shale and minor sandstone
Depositional environment	Lacustrine
Kerogen type	Type III; DOM
TOC	0– 22 wt%
Mean original HI	121 ± 38 mg HC/g TOC
Thermal maturity	Immature–over mature
Average permeability	3.30E-03 mD
Average total porosity	0.025 (fraction)
Average total water saturation	0.620 (fraction)
Average brittleness index	0.343 (fraction)
Pressure regime	Overpressured (Nappamerri Trough)
Exploration status	Under assessment/minor production

4.1.5.1 Age and stratigraphic relationships

The Roseneath Shale is assigned a middle Permian age (Figure 2) based on associated palynofloral assemblages (Gray and McKellar, 2002; Price, 1997). Both the lower and upper boundaries are time transgressive.

The Roseneath Shale is part of the Gidgealpa Group. The Roseneath Shale conformably overlies and is interbedded with the Epsilon Formation, and is conformably overlain by and interbedded with the Daralingie Formation (Figure 2) (Alexander et al., 1998a; Owens et al., 2020).

4.1.5.2 Extent, depth and gross formation thickness

The Roseneath Shale occurs mainly in the south-western part of the Cooper Basin where it extends across the Nappamerri, Wooloo, Allunga and Tenappera troughs (Figure 1), and covers an area of approximately 21,900 km^2 (Figure 35) (Hall et al., 2015a). In the Patchawarra Trough, its extent is restricted to the south-western part of the depocentre. The Roseneath Shale is absent from the Dunoon and Murteree ridges and crests of other ridges due to late early-Permian uplift and erosion (Alexander et al., 1998a). South of the Tinga Tingana Ridge, it appears to pinch out (Morton, 2016).

The depth to the top of the Roseneath Shale ranges from 1180 m along the south-west edge of the formation extent to a maximum of 3434 m in the central Nappamerri Trough (Figure 35) (Hall et al., 2015a).

The Roseneath Shale has an average thickness of 57 m. The formation is thickest in the Nappamerri and Tenappera troughs (up to approximately 240 m thick), while it is thinner (< 30 m thick) in the Jackson–Naccowlah East area and the south eastern Patchawarra Trough (Hall et al., 2015a).

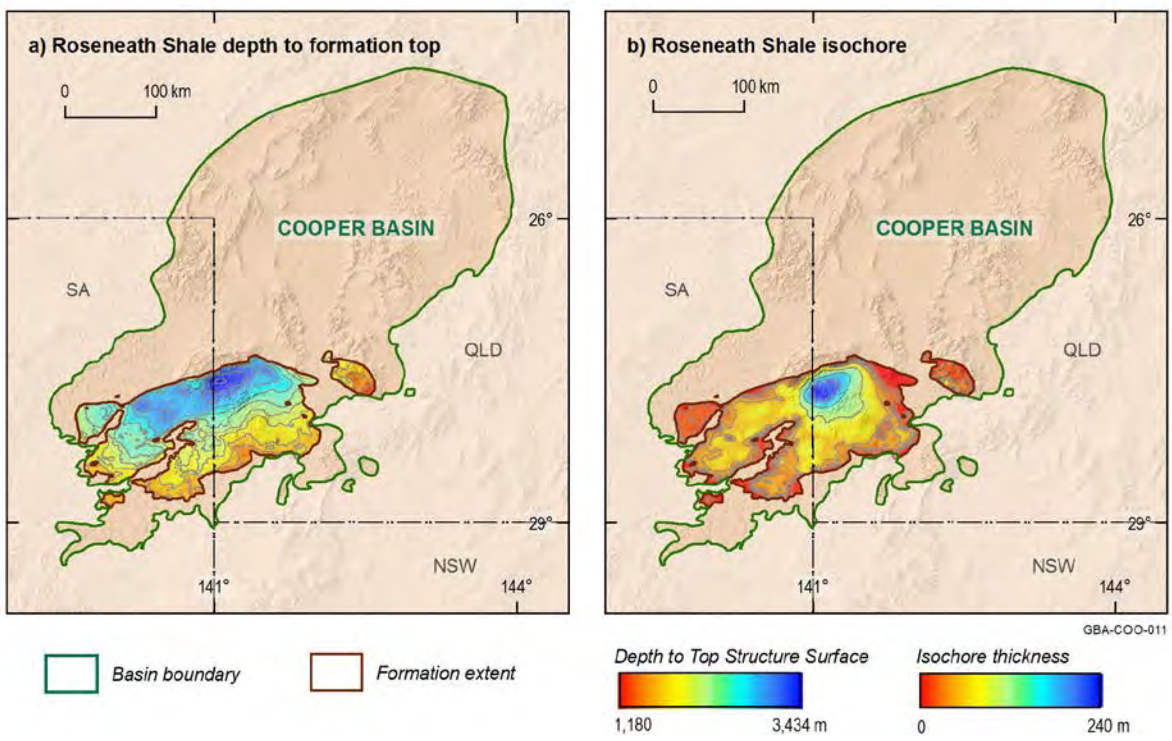

Figure 35 a) Roseneath Shale formation top depth (m); b) Roseneath Shale total vertical thickness (m)

Source: Hall et al. (2015a)
Data: Hall et al. (2016a); Cooper Basin outline from Raymond et al. (2018)
Element: GBA-COO-011

4.1.5.3 Lithology and palaeoenvironment

The Roseneath Shale includes light to dark brown-grey siltstone, mudstone and minor fine-grained sandstone units (Alexander et al., 1998a; Gray and McKellar, 2002; McKellar, 2013). This unit was deposited in a large, relatively deep freshwater lacustrine setting, similar to that of the Murteree Shale (Alexander et al., 1998a).

During deposition of the Epsilon, Roseneath and Daralingie formations, most of the Patchawarra Trough was a stable platform with little or no accommodation space available for sediment accumulation (Boucher, 2001).

The Roseneath Shale siltstones vary from massive to finely laminated, with minor wavy lamination and wave ripples suggesting possible storm reworking. Load marks, flame structures and slump folds indicate mass flows and slope instability. A lacustrine depositional environment similar to that of the Murteree Shale is interpreted (Alexander et al., 1998a).

Large ridges that separate the major troughs in the Cooper Basin typically have no preserved REM play due to a combination of onlap onto palaeo-highs, and erosion during periods of compression and uplift (including early Permian uplift) (Alexander et al., 1998a).

4.1.5.4 Source rock distribution, geochemistry and maturity

The mean TOC content of all samples from the Roseneath Shale is 3.5 ± 3.1 wt%, with a range from 0.1 wt% to 22.4 wt% (133 samples; Figure 36) (Hall et al., 2016b). The present day TOC map shows good to excellent source rock quantities are present across the entire formation, with the highest TOC contents occurring in the Patchawarra Trough and around the basin edges (Figure 37) (Hall et al., 2016b).

Source rock quality (HI 95 ± 32 mg HC/g TOC) is typical of a predominantly dry gas-prone Type III kerogen (Figure 36). The mean calculated HI_o of 121 ± 38 mg HC/g TOC (range 50 to 300 mg HC/g TOC) is consistent with the observed data from low maturity samples and suggests that the low HI values are not a function of high maturity but reflect the quality of the original source rock. Given the current data distribution, there is no evidence for the development of Type I kerogen (HI > 600 mg HC/g TOC), as could have been inferred from the lacustrine depositional environment (Figure 37) (Hall et al., 2016b).

The net volume of organically rich shales was calculated for the Roseneath Shale using the net organically rich ratio (NORR) of shales with TOC > 2 wt% and gross formation thickness. TOC profiles were analysed by comparing the sonic log with the deep resistivity log (Passey et al., 2010; Cooper et al., 2015) in Encounter 1, Holdfast 1 and Moomba 191. The net organically rich thickness of shale was then calculated as the product of the NORR and gross shale thickness (Table 39).

Table 39 Net organically rich ratio (NORR) for the Roseneath Shale as calculated from Encounter 1, Holdfast 1 and Moomba 191 in the Nappamerri Trough

Well	Net organically rich ratio (fraction)
Encounter 1	0.9996
Holdfast 1	0.4461
Moomba 191	0.6727
Average	**0.7061**

The maturity of the Murteree Shale is highest in the central Nappamerri Trough where it ranges from wet gas (R_o 2–2.5%; TR 50–70%) to overmature (R_o > 3.5%; TR > 95%; Figure 38) (Hall et al., 2016c). In the western Patchawarra Trough, maturity ranges from immature to early oil window (R_o 0.75–0.9%).

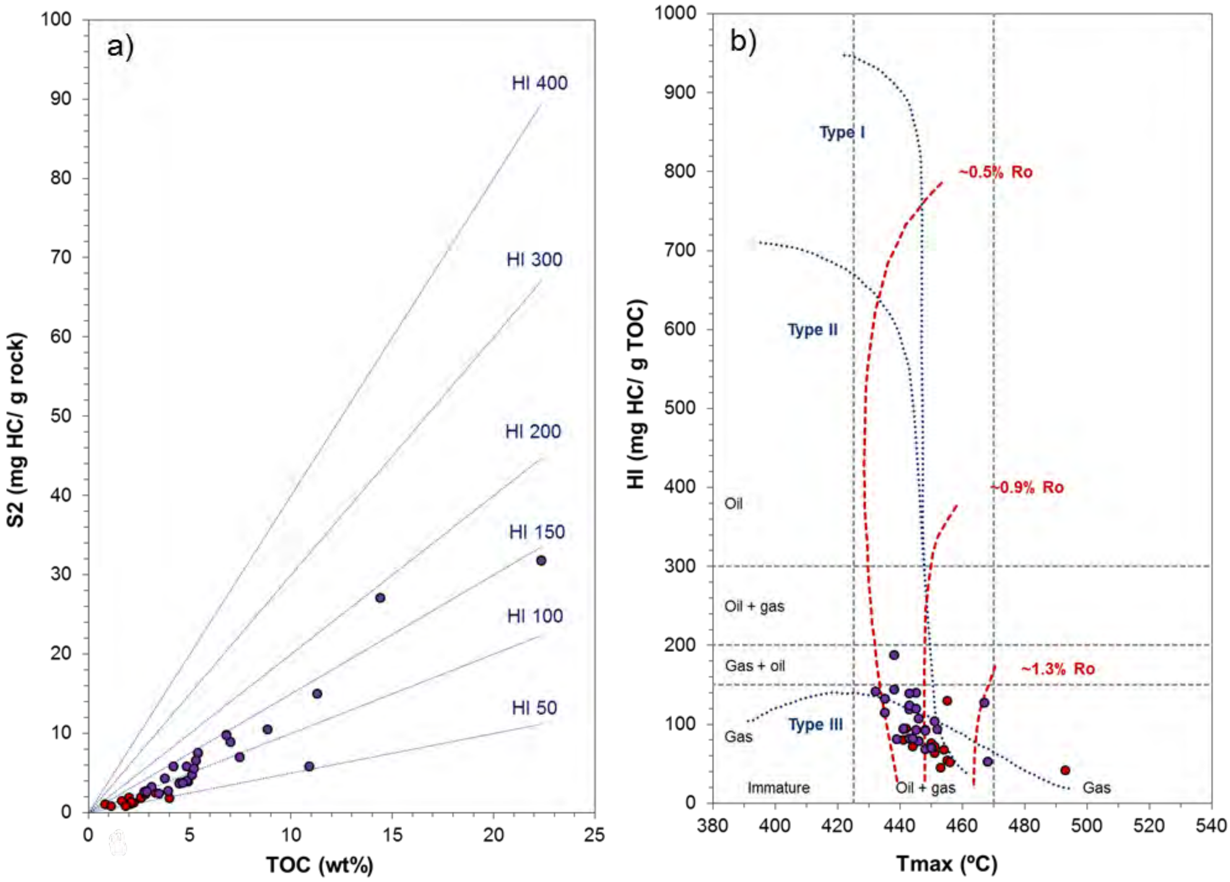

Figure 36 Rock-Eval pyrolysis data plots for the Roseneath Shale: a) TOC content vs S2 yield; b) T_{max} vs HI

Purple dots: effective source rocks (TOC > 2 wt%; S1 + S2 > 3 mg HC/g rock); red dots: samples with either no original generation potential or are spent source rocks

Source: Hall et al. (2016b)

Data: Hall et al. (2016a)

Element: GBA-COO-2-301

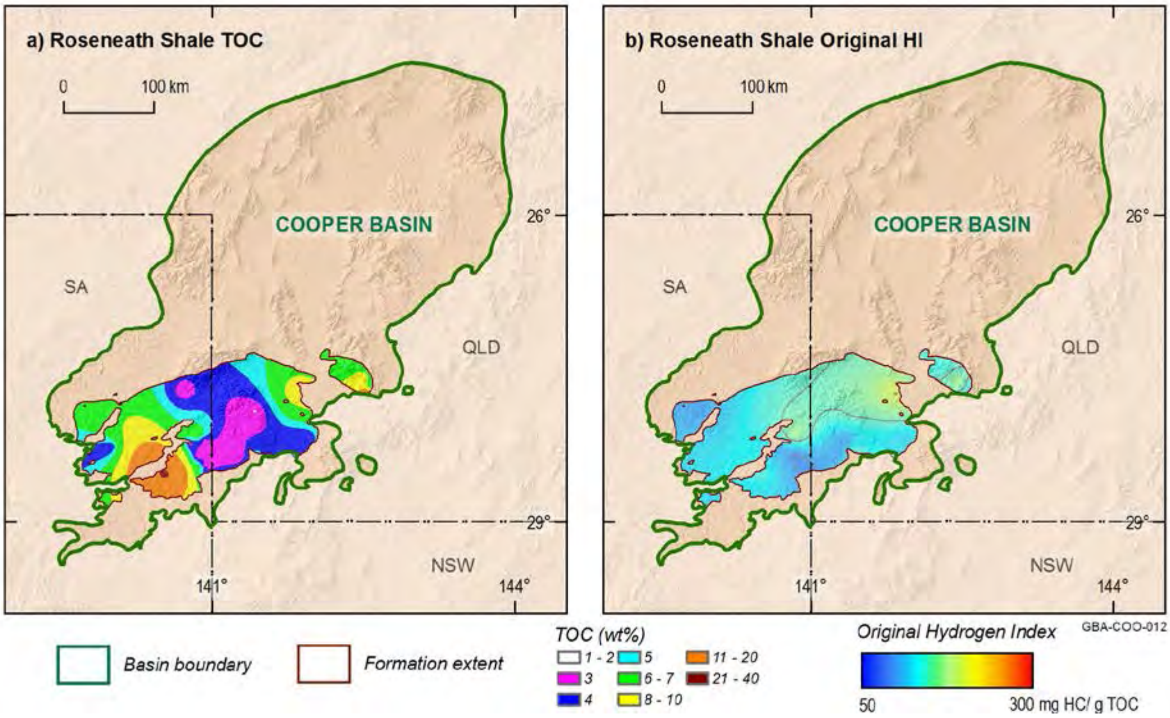

Figure 37 Roseneath Shale source rock geochemistry maps: a) Present day average Total Organic Carbon (TOC) (wt%), b) mean Original Hydrogen Index (HI_o) (mg HC/g TOC)

Source: Hall et al. (2016b)
Data: Hall et al. (2016a); Cooper Basin outline from Raymond et al. (2018)
Element: GBA-COO-012

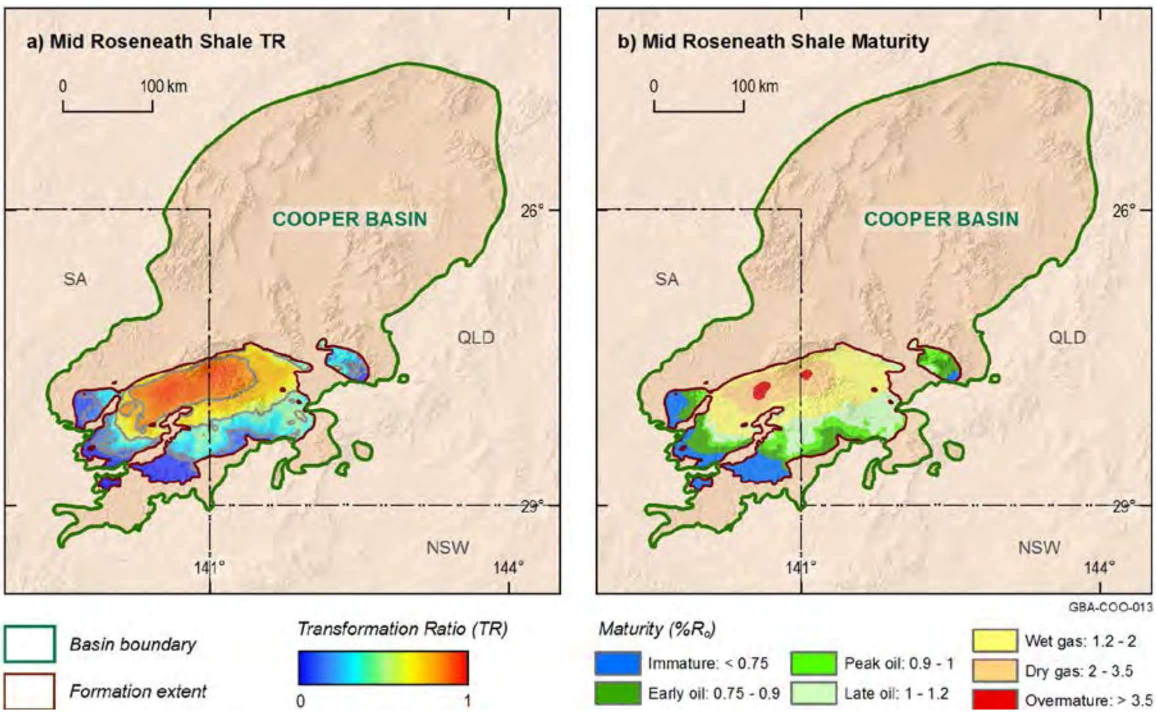

Figure 38 Roseneath Shale a) transformation ratio (TR) and b) maturity (%R_o)

Source: Hall et al. (2016c)
Data: Hall et al. (2016a); Cooper Basin outline from Raymond et al. (2018)
Element: GBA-COO-013

4.1.5.5 Shale reservoir characteristics

Porosity, permeability and fluid saturation are three of the key petrophysical input parameters required for characterising shale plays. The average shale rock properties of the Roseneath Shale are shown in Table 40 and Figure 39 (Department for Energy and Mining (SA), 2017, 2018a). Based on laboratory tests (as-received basis) on 47 Roseneath shale rock samples from 6 wells, the Roseneath Shale has an average total porosity of 2.5%, average water saturation of 62% and average permeability of 3.30E-03 mD (Table 40; Figure 39).

Table 40 Average as-received laboratory measured shale rock properties for the Roseneath Shale for key wells in the Cooper Basin

Well	Bulk density (g/cc)	Water saturation (fraction)	Oil saturation (fraction)	Gas saturation (fraction)	Gas-filled Porosity (fraction)	Total porosity (fraction)	Permeability (mD)
Encounter 1	2.70	0.773	0.000	0.227	0.007	0.032	2.49E-04
Holdfast 1	2.73	0.914	0.000	0.086	0.002	0.014	1.56E-06
Kingston Rule 1	2.59	0.685	0.058	0.256	0.007	0.027	1.01E-02
Moomba 175	2.68	0.000	0.000	0.000	0.020	0.017	8.48E-05
Moomba 191	2.67	0.478	0.073	0.449	0.009	0.021	4.47E-05
Vintage Crop 1	2.68	0.872	0.000	0.128	0.005	0.038	9.30E-03
Average	2.67	0.620	0.022	0.191	0.008	0.025	3.30E-03

Data: Encounter 1, Holdfast 1, Kingston Rule 1, Talaq 1, Moomba 175, Moomba 191 and Vintage Crop 1 (Department for Energy and Mining (SA), 2017, 2018a)

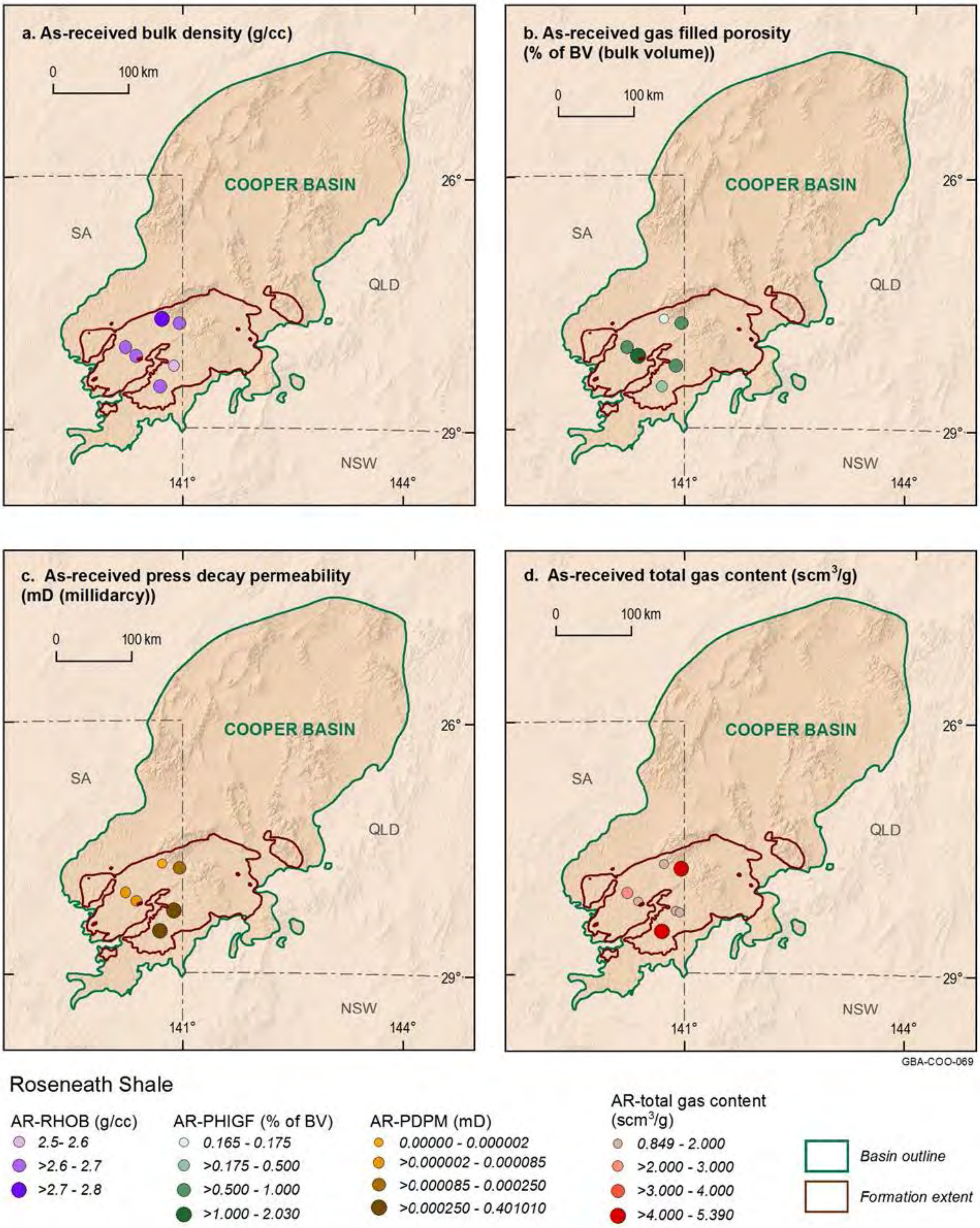

Figure 39 The average as-received (a) bulk density (AR-RHOB), (b) gas-filled porosity (PHIGF), (c) pressure decay permeability (PDPM) and (d) total gas content of the Roseneath Shales in the Cooper Basin

Data: Encounter 1, Holdfast 1, Kingston Rule 1, Talaq 1, Moomba 175 and Moomba 191 (Department for Energy and Mining (SA), 2017, 2018a); Cooper Basin outline from Raymond et al. (2018)
Element: GBA-COO-069

Gas in shale is stored as adsorbed gas on the organic matter, free gas stored in the pore spaces and dissolved gas in the formation water.

Gas desorption test results for shale samples of the Roseneath Shale from 6 wells (Department for Energy and Mining (SA), 2017, 2018a) give an average total gas content (as-received basis) of 1.81 scc/g (Table 41).

The adsorbed gas storage capacity of the Roseneath Shale was analysed using isotherm tests for shale rock samples from 5 wells (Department for Energy and Mining (SA), 2017, 2018a). The averaged isotherm test results under the reservoir temperature in the Cooper Basin, including the measurement gas, total organic content (wt fraction), crushed sample density (g/cc), Langmuir storage capacity (in situ, scc/g), Langmuir pressure (kPa) and adsorbed gas storage capacity (in situ, scc/g), are summarised in Table 29.

Table 43 presents the average total gas storage capacity (scc/g) and capacities of the three storage mechanisms of the Roseneath shales in key wells in the Cooper Basin.

Table 41 Average as-received total gas contents for shales of the Roseneath Shale for key wells in the Cooper Basin

Well	Average as-received total gas content (scc/g)	As-received bulk density (g/cc)
Encounter 1	4.08	2.70
Holdfast 1	0.85	2.73
Kingston Rule 1	1.29	2.59
Moomba 175	1.19	2.68
Moomba 191	2.41	2.67
Talaq 1	1.01	NA[i]
Average	1.81	2.68

Data: Encounter 1, Holdfast 1, Kingston Rule 1, Moomba 175, Moomba 191 and Talaq 1 (Department for Energy and Mining (SA), 2017, 2018a)

Table 42 Average isotherm test results for shales samples from the Roseneath Shale under reservoir temperature in key wells in the Cooper Basin

Well	Measurement Gas	Total Organic Content (wt fraction)	Crushed Density (g/cc)	Langmuir Storage Capacity, in situ (scc/g)	Langmuir Pressure (kPa)	Adsorbed Gas Storage Capacity, in situ (scc/g)
Encounter 1	methane	0.0280	2.881	1.91	10512.26	1.61
Holdfast 1	methane	0.0246	2.792	1.57	23482.28	1.11
Kingston Rule 1	methane	0.0383	2.551	1.19	7114.15	0.91
Kingston Rule 1	CO_2	0.0480	2.514	4.03	6189.50	3.19
Moomba 191	methane	0.0321	2.696	1.06	29854.31	0.83
Vintage Crop 1	methane	0.0216	2.707	1.90	27089.11	0.77

Data: Encounter 1, Holdfast 1, Kingston Rule 1, Moomba 191 and Vintage Crop 1 ((Department for Energy and Mining (SA), 2017, 2018a)

Table 43 Average total gas storage capacity (scc/g) of the Roseneath shales in key wells in the Cooper Basin

Well	Dissolved Gas in Water Storage Capacity (scc/g)	Free Gas Storage Capacity (scc/g)	Adsorbed Gas Storage Capacity (scc/g)	Total Gas Storage Capacity (scc/g)
Moomba 191	0.02	0.41	0.83	1.25
Kingston Rule 1	0.02	0.13	1.09	1.24
Vintage Crop 1	0.02	0.06	0.73	0.81
Average	0.02	0.20	0.88	1.10

Data: Kingston Rule 1, Moomba 191 and Vintage Crop 1 (Department for Energy and Mining (SA), 2017, 2018a)

4.1.5.6 Mineralogy and brittleness

The mineral assemblage and brittleness of the Roseneath Shale were described using XRD analyses of 60 shale rock samples from 6 wells (Santos-Beach-Origin, 2012; Department for Energy and Mining (SA), 2017, 2018a).

On average, the Roseneath Shale is composed mostly of clays (53 wt%) such as kaolinite and mica/illite as well as quartz (21.98 wt%) with minor siderite (9.93 wt%) and other minerals including feldspar, chlorite, rutile and anatase (Table 44). In addition, smectite, dolomite and pyrite were also identified by SEM imaging (Jadoon et al., 2016). A ternary plot of the dominant mineral content of the Roseneath Shale is shown in Figure 27.

Average brittleness indices (BI) were calculated from mineral composition using the method of Jarvie et al. (2007). Overall, the Roseneath Shale is classified as 'less brittle', with a total average BI of 0.343 (Table 45).

Table 44 Main mineral assemblage statistics of the Roseneath Shale analysed by XRD

Formation	Quartz (wt%)	Clay (wt%)	Siderite (wt%)	Feldspar (wt%)	Anatase (wt%)	Rutile (wt%)
Minimum	11.80	0.00	0.00	0.00	0.20	0.20
Maximum	43.00	62.10	6.53	6.00	2.00	1.00
Average	32.98	53.65	9.93	0.72	0.70	0.78
Median	33.00	57.40	6.00	0.00	0.40	0.80

Data: Encounter 1, Holdfast 1, Kingston Rule 1, Moomba 191, Streaky 1 and Vintage Crop 1 (Department for Energy and Mining (SA), 2018a)

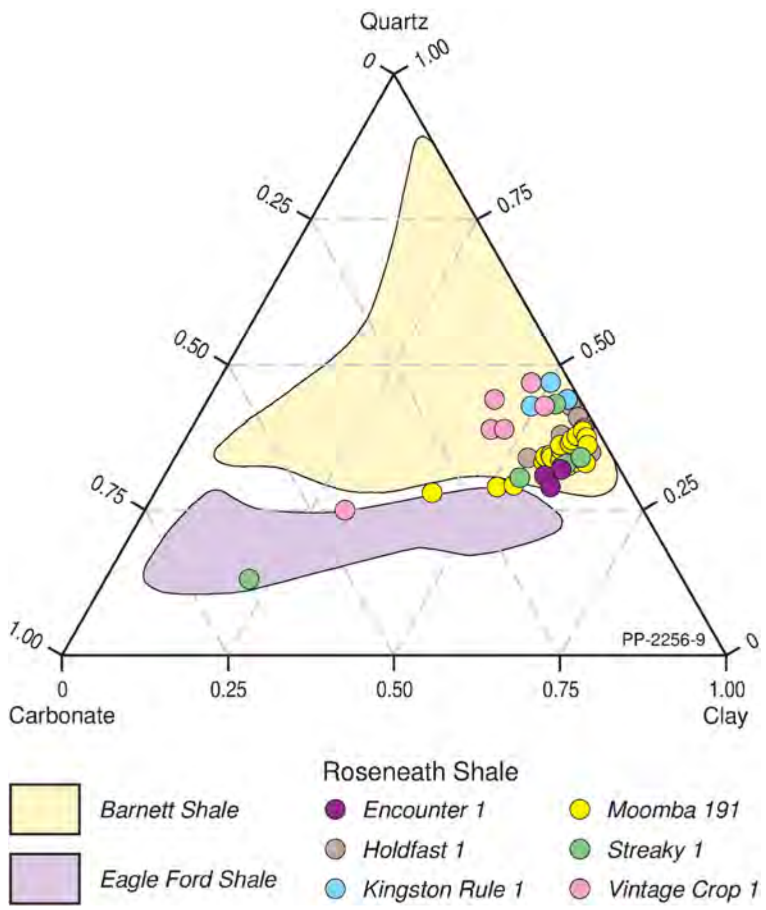

Figure 40 Ternary plot of mineral content (wt fraction) of the Roseneath Shale in the Cooper Basin. USA shale play comparison after Passey et al. (2010)

For comparison two USA shale plays (the Barnett and Eagle Ford shales) are shown (after Passey et al., 2010)

Data: Encounter 1, Holdfast 1, Kingston Rule 1, Moomba 191, Streaky 1 and Vintage Crop 1 (Department for Energy and Mining (SA), 2017, 2018a)

Element: PP-2256-9

Table 45 Average brittleness indices for the Roseneath Shale estimated using the Jarvie et al. (2007) method for key wells

Well	Average brittleness index
Encounter1	0.304
Holdfast 1	0.360
Kingston Rule1	0.393
Moomba 191	0.330
Streaky 1	0.303
Vintage Crop 1	0.371
Average	0.343

Data: Encounter 1, Holdfast 1, Kingston Rule 1, Moomba 191, Streaky 1 and Vintage Crop 1 (Department for Energy and Mining (SA), 2018a)

4.1.5.7 Gas composition

Gas composition analysis on the desorbed gas samples from the Roseneath Shale in 8 wells (Department for Energy and Mining (SA), 2018a) show that on average Roseneath Shale gas includes 58.23% methane, 4.50% ethane, 1.35% propane plus and 35.90% carbon dioxide (Table 46, Figure 41). Publically available well test data (mainly sourced from Drill Seam Tests (DSTs) in the interbedded Epsilon Formation suggests the average condensate-to-gas ratio (CGR) in gas-bearing intervals (23 wells) is approximately 17 bbl/mmscf.

Table 46 Average gas compositions of desorbed gas samples from 8 wells in the Roseneath Shale in the Cooper Basin

Well	Methane (mol%)	Ethane (mol%)	Propane plus (mol%)	Carbon dioxide (mol%)
Encounter 1	66.00	0.74	0.33	32.94
Holdfast 1	54.43	1.87	0.98	42.72
Kingston Rule 1	62.81	9.78	3.42	23.98
Moomba 175	63.57	0.12	0.00	36.31
Moomba 191	77.65	0.37	0.05	21.92
Sasanof 1	49.17	4.99	1.14	44.70
Skipton 1	56.81	10.50	2.66	30.03
Talaq 1	51.60	7.13	1.73	39.55
Vintage Crop 1	42.06	5.04	1.88	50.97
Average	58.23	4.50	1.35	35.90

Data: Encounter 1, Holdfast 1, Kingston Rule 1, Moomba 191, Sasanof 1, Skipton 1, Talaq 1 and Vintage Crop 1 (Department for Energy and Mining (SA), 2018a)

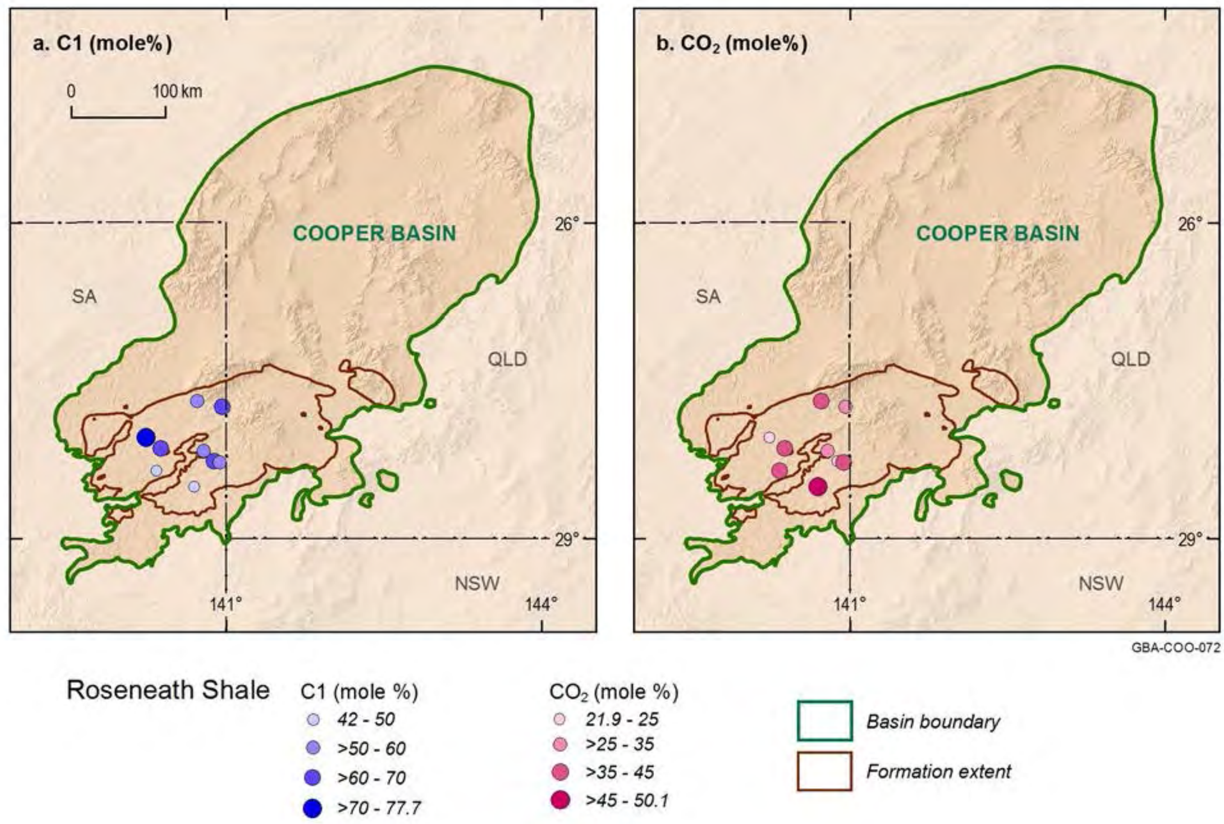

Figure 41 Contents of methane and carbon dioxide of desorbed gas from the Roseneath Shale in the Cooper Basin

Data: Encounter 1, Holdfast 1, Kingston Rule 1, Moomba 191, Sasanof 1, Skipton 1, Talaq 1 and Vintage Crop 1 (Department for Energy and Mining (SA), 2018a); Cooper Basin outline from Raymond et al. (2018)
Element: GBA-COO-072

4.1.6 Daralingie Formation

Key features of the Daralingie Formation are summarised below in Table 47 and discussed in more detail in the following text.

Table 47 Key features of the Daralingie Formation

Unconventional Play type	Tight, shale and deep coal gas
Age	Middle Permian (late Wordian to early-Capitanian)
Extent	19,300 km^2
Top depth (m)	1324–3282 m
Gross formation thickness	0–152 m
Lithology	Sandstone, shale and minor coal
Depositional environment	Fluvio-deltaic
Kerogen type	Type II/III to Type III; coal, DOM
TOC	0–79 wt%
Mean original HI	164 ± 78 mg HC/g TOC
Thermal maturity	Immature–over mature
Average permeability	Insufficient data
Average effective porosity	0.074 (fraction) in tight pay intervals
Average effective water saturation	0.340 (fraction) in tight pay intervals
Pressure regime	Overpressured (Nappamerri Trough)
Exploration status	Under assessment / minor production

4.1.6.1 Age and stratigraphic relationships

The Daralingie Formation is assigned a maximum age of middle Permian (Figure 2) based on updated ages (Nicoll et al., 2015) of associated palynoflora zone APP4.1 (Gray and McKellar, 2002; Price, 1997). The minimum age of the formation is poorly constrained due to an overlying erosional unconformity (Hall et al., 2015a). However, this unconformity is assumed to have initiated in the late middle Permian based on regional tectonic events (Korsch and Totterdell, 2009a, 2009b; Korsch et al., 2009).

The Daralingie Formation is part of the Gidgealpa Group. The Daralingie Formation lies conformably above the Roseneath Shale and disconformably below the Toolachee Formation (Figure 2). Its top was eroded during the Permian uplift in the southern Cooper Basin (Hall et al., 2015a).

4.1.6.2 Extent, depth and gross formation thickness

The Daralingie Formation covers an area of approximately 19,300 km^2 and is restricted to the region south of the GMI Ridge and south-west of the JNP Trend (Figure 1; Figure 42) (Hall et al., 2015a).

The depth to the top of the Daralingie Formation ranges from 1324 m along the south edge of the formation to a maximum of 3282 m in the Nappamerri Trough (Figure 42) (Hall et al., 2015a).

The Daralingie Formation is an average of approximately 50 m thick and reaches thicknesses of about 150 m the Nappamerri Trough (Figure 42) (Hall et al., 2015a).

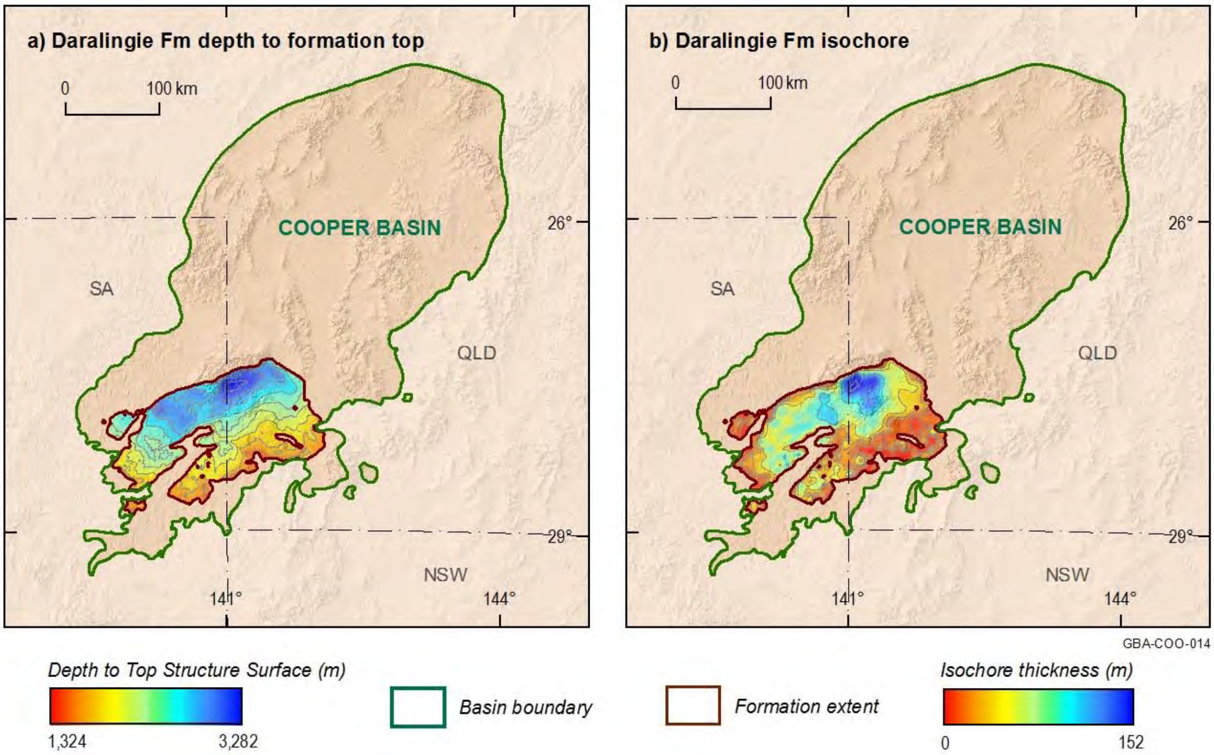

Figure 42 a) Daralingie Formation top depth (m), b) Daralingie Formation total vertical thickness (m)

Source: Hall et al. (2015a)
Data: Hall et al. (2016a); Cooper Basin outline from Raymond et al. (2018)
Element: GBA-COO-014

4.1.6.3 Lithology and palaeoenvironment

The Daralingie Formation is dominated by carbonaceous and micaceous siltstone and mudstone with interbedded, fine- to very fine-grained sandstone and minor coal seams (Alexander et al., 1998a). These rocks form upward-coarsening cycles and were deposited in prograding deltas, and beaches developed as the lake in which the Roseneath Shale was deposited receded (Draper, 2002; Alexander et al., 1998a). Over much of the Cooper Basin, the Daralingie Formation is thin or absent (due to erosional truncation) and is restricted to the southern part of the basin. The amount of uplift and erosion is variable, with up to 100 to 350 m along the ridges and negligible amounts in the troughs (Moussavi-Harami, 1996b; Moussavi-Harami, 1996a).

Fluvial and deltaic environments produced characteristically upward–coarsening cycles of shoaling deltas and beaches on a lake margin during the depositional stage of Daralingie Formation. The Daralingie Formation was deposited by north-easterly prograding delta systems which developed during the recession of “Roseneath Lake” (Alexander et al., 1998a).

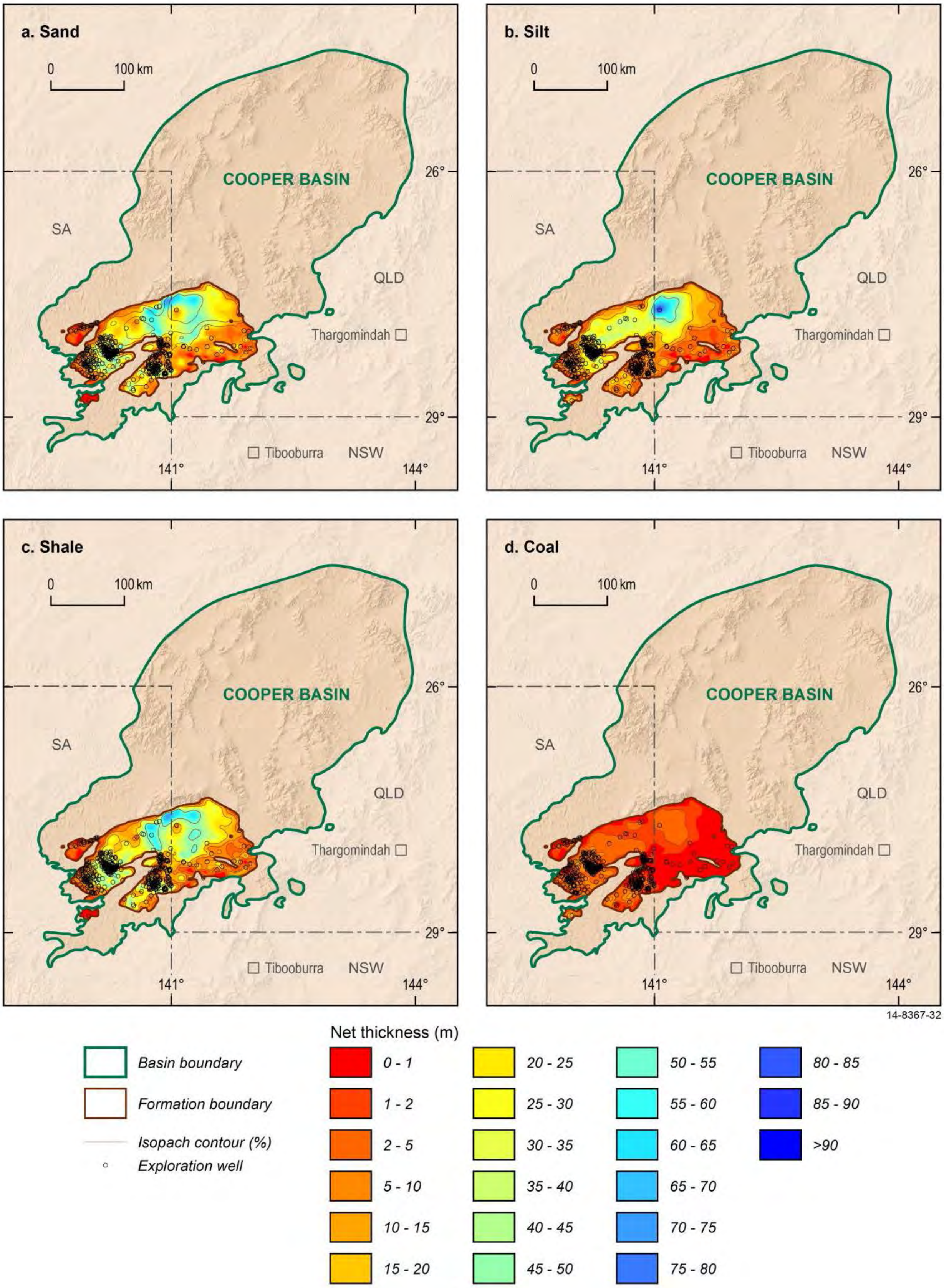

Figure 43 Daralingie Formation isolith maps by lithology, as total net thickness in metres for (a) sand, (b) silt, (c) shale and (d) coal

Shale incorporates shale, coaly shale and / or shaly coal. These are approximately equivalent to samples with a TOC range of 0.5–50 wt%

Source: Hall et al. (2015a); Cooper Basin outline from Raymond et al. (2018)

Element: GBA-COO-2-310

4.1.6.4 Source rock distribution, geochemistry and maturity

The source rocks of the Daralingie Formation include coal, carbonaceous shale and shale.

Although the Daralingie Formation is much thinner and less extensive than the Toolachee and Patchawarra formations, the net coal and shale thickness maps show the potential presence of source rock facies across the entire formation (Hall et al., 2015a).

The Daralingie Formation net cumulative coal thickness (equivalent to clean coals with TOC > 50 wt%) ranges between 1 and 5 m in most regions, but reaches up to 7 to 8 m in the Wooloo and Tenappera troughs (Sun and Camac, 2004; Hall et al., 2015a).

The cumulative net thickness of the shale, coaly shale and shaly coal facies (approximately equivalent to samples with a TOC range of 0.5–50 wt%) is greatest in the deepest sections of the basin in the central Nappamerri Trough, where it reaches up to 65 m in well intersections (Sun and Camac, 2004; Hall et al., 2015a). Shale thicknesses may be greater still in the central part of the eastern Nappamerri Trough but depths here are not currently constrained by open file well data.

The TOC of Daralingie Formation ranges from < 1 wt% to 79 wt% (Figure 44) (Hall et al., 2016b). The present day TOC map for the Daralingie Formation combined shale to shaly coal facies shows good to excellent quantities of source rock (TOC >2 wt%) across the entire formation (Figure 45).

The mean of present day HI is 138 ± 71 mg HC/g TOC, ranging from 25 to 323 mg HC/g TOC, and the original mean HI_o is estimated to be 164 ± 78 mg HC/g TOC. The source quality is consistent with a mixture of both oil and gas-prone Type II to Type III and gas–prone Type III kerogen (Figure 44). The coal-rich source rocks have the mean HI from 184 to 236 mg HC/g TOC, and the shaly source rocks have a mean HI of 114 ± 58 mg HC/g TOC (Hall et al., 2016b).

The maturity of the Daralingie Formation is highest in the central Nappamerri Trough where it mostly lies within the dry gas window (R_o 2-3.5%; Figure 45) (Hall et al., 2016c). Where present in the south-western Patchawarra Trough, it is predominantly immature.

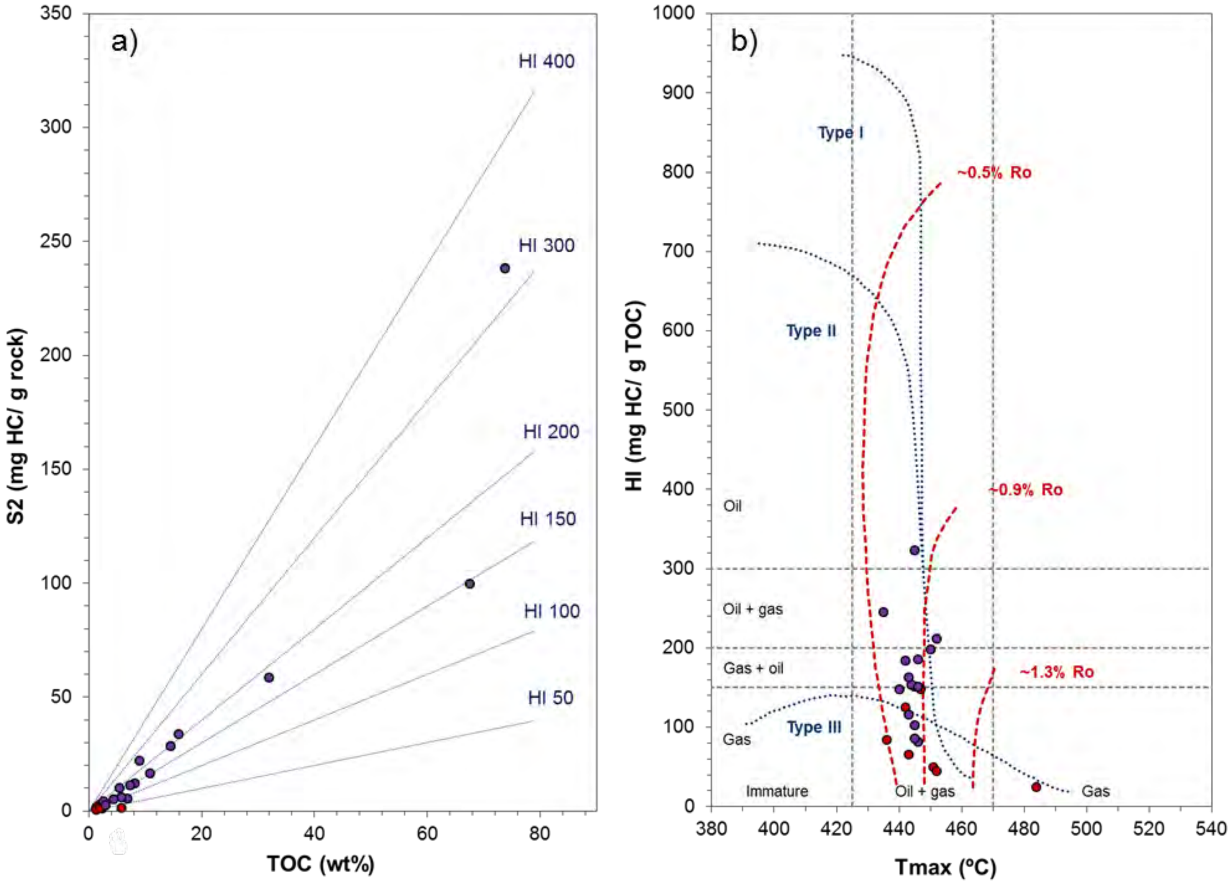

Figure 44 Rock-Eval pyrolysis data plots for the Daralingie Formation: a) TOC content vs S2 yield; b) T_{max} vs HI

Purple dots represent effective source rocks (TOC > 2 wt%; S1 + S2 > 3 mg HC/g rock); red dots: samples with either no original generation potential or are spent source rocks
Source: Hall et al. (2016b)
Data: Hall et al. (2016a)
Element: GBA-COO-2-302

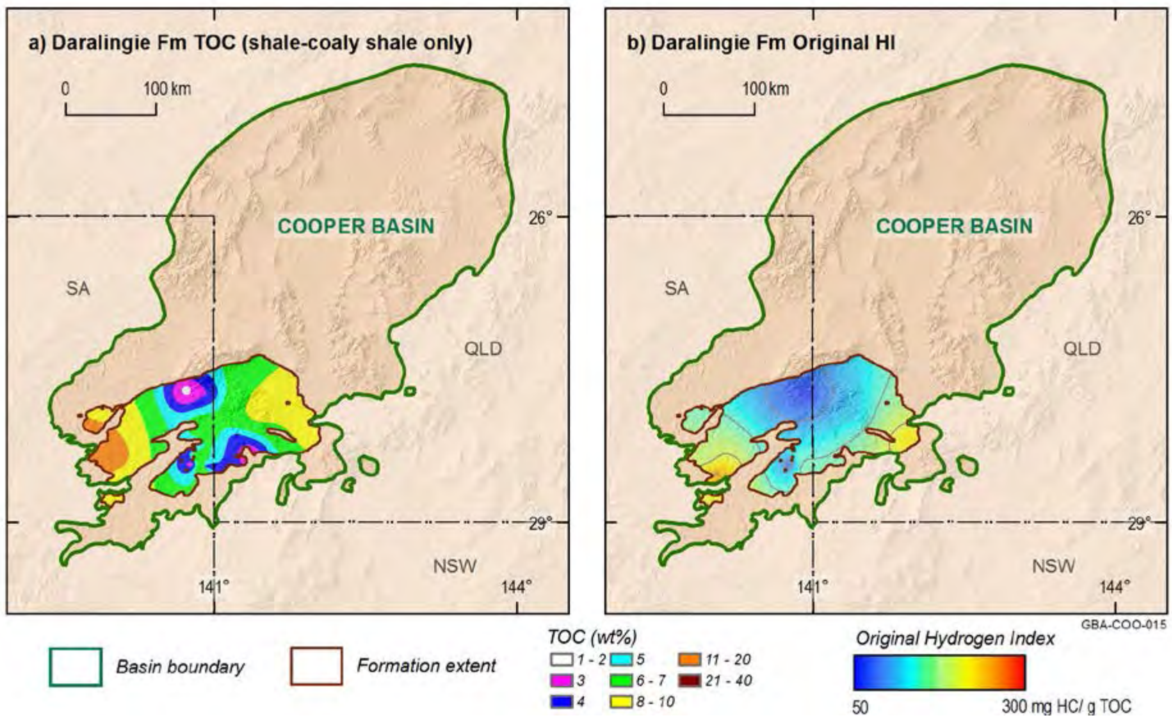

Figure 45 Daralingie Formation source rock geochemistry maps: a) Present day average Total Organic Carbon (TOC) (wt%) for shale-coaly shale facies (TOC < 50 wt%). b) mean Original Hydrogen Index (HI_o) for all source rocks (mg HC/g TOC)

Source: Hall et al. (2016b)
Data: Hall et al. (2016a); Cooper Basin outline from Raymond et al. (2018)
Element: GBA-COO-015

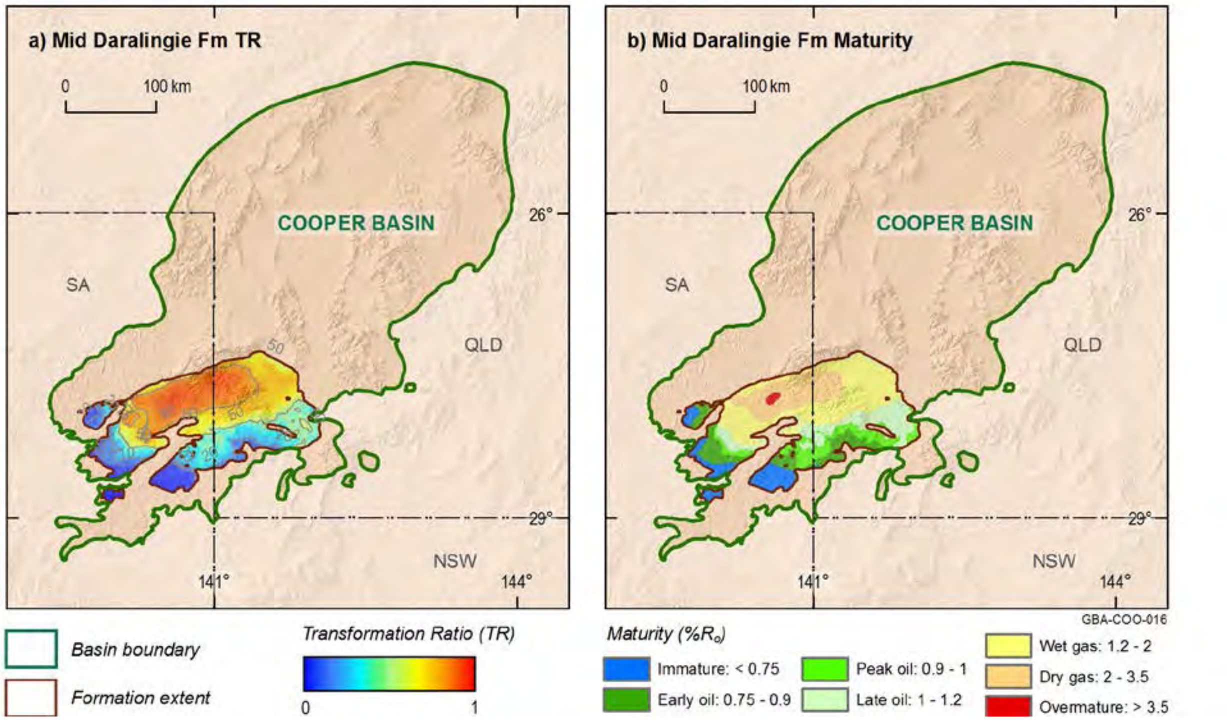

Figure 46 Daralingie Formation a) transformation ratio and b) maturity (Ro%)

Source: Hall et al. (2016c)
Data: Hall et al. (2016a); Cooper Basin outline from Raymond et al. (2018)
Element: GBA-COO-016

4.1.6.5 Tight reservoir characteristics

The Daralingie Formation hosts a range of conventional reservoirs (Gravestock et al., 1998a). In addition, it has the potential to host tight gas plays in finer grained sandstone and siltstone intervals. The net sand thickness of the Daralingie Formation is reaches around 124 m. Net siltstone thickness is greatest in the central Nappamerri Trough, where it reaches a depth of 3282 m (Sun and Camac, 2004; Hall et al., 2015a).

Log-derived tight pay thickness, average effective porosity and water saturation of the Daralingie Formation tight reservoirs were calculated from 15 wells (Department for Energy and Mining (SA), 2017, 2018a). The average net pay thickness is 10.37 m, the average effective porosity is 7.4% and the average water saturation is 34% (Table 48; Figure 47).

Table 48 Log-derived tight pay thickness, average effective porosity and average water saturation statistics for Daralingie Formation tight reservoirs in the Cooper Basin

Well	Tight Pay Thickness (m)	Average Effective Porosity (fraction)	Average Water Saturation (fraction)
Minimum	2.21	0.051	0.201
Maximum	31.09	0.099	0.599
Average	10.37	0.074	0.340
Median	8.50	0.074	0.330

The net tight pay interval was defined by the following criteria: volume fraction of shale less than 50%, effective porosity greater than 4% and water saturation less than 70%.
Data: Beach Energy wells Boston 1, Boston 2, Dashwood 1, Etty 1, Encounter 1, Geoffrey 1, Halifax 1, Hervey 1, Holdfast 1, Nepean 1, Rapid 1, Streaky 1 and Santos wells Moomba 175, Moomba 191 and Moomba 192. (Department for Energy and Mining (SA), 2017, 2018a; Department of Natural Resources, 2018a)

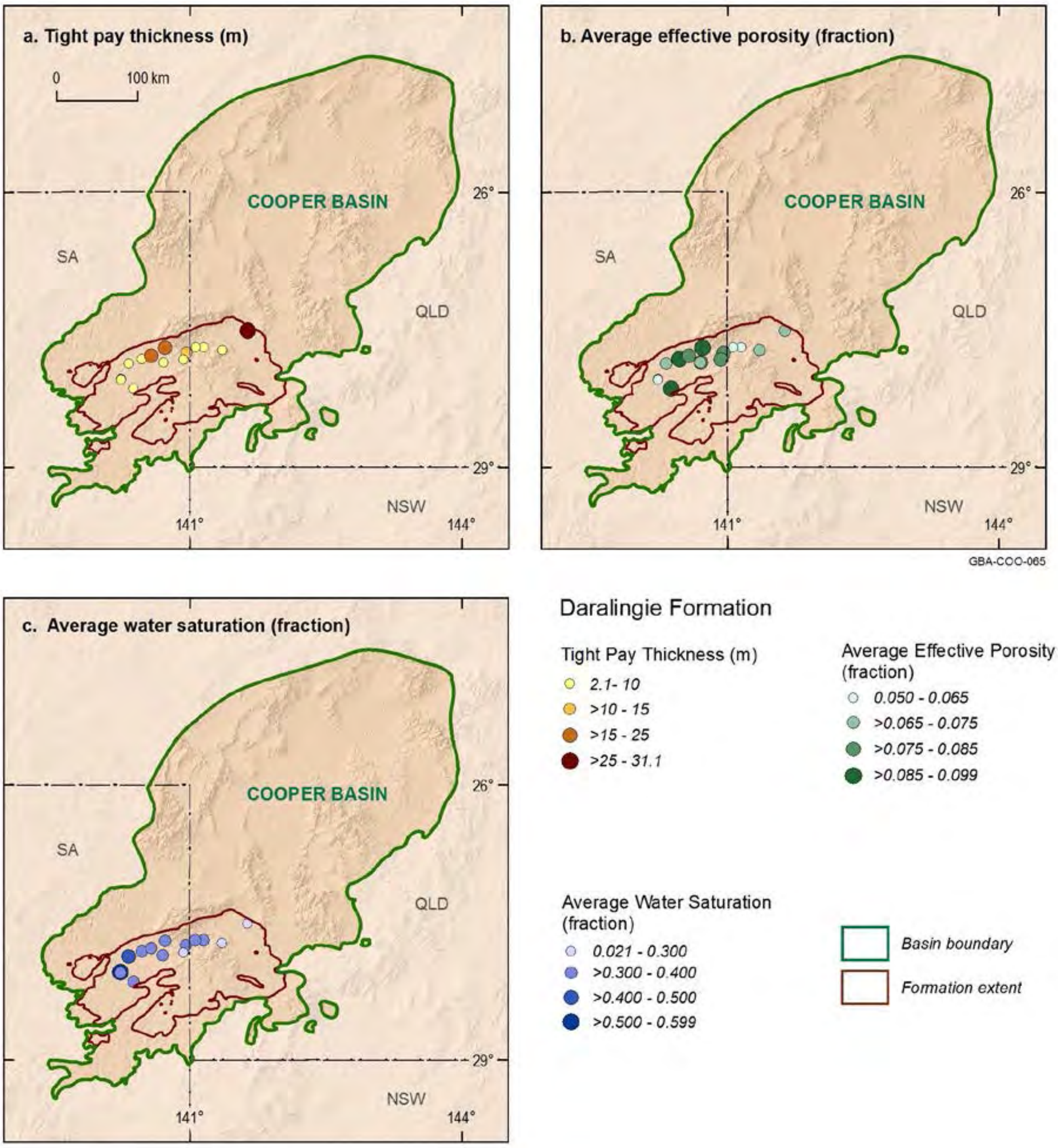

Figure 47 Log-derived (a) tight pay thickness, (b) average effective porosity and (c) average water saturation of the Daralingie Formation tight reservoirs in the Cooper Basin

Data: Department for Energy and Mining (SA) (2017, 2018a); Department of Natural Resources (2018a); Cooper Basin outline from Raymond et al. (2018)
Element: GBA-COO-065

4.1.6.6 Gas composition

Gas composition analysis on the desorbed gas samples from the Daralingie Formation in Encounter 1 and Holdfast 1 (Department for Energy and Mining (SA), 2017, 2018a) show that on average Daralingie Formation gas includes 74.89% methane, 2.36% ethane, 1.61% propane plus, and 21.14% of carbon dioxide (Table 49). An average CGR of 3.30 bbl/mmscf for the Daralingie Formation was determined from well test data (mainly the DSTs) compiled from publically available well completion reports.

Table 49 Average gas compositions of desorbed gas samples from the Daralingie Formation in the Cooper Basin

Well	Methane (mol%)	Ethane (mol%)	Propane plus (mol%)	Carbon dioxide (mol%)
Encounter 1	83.46	0.11	0.02	16.41
Holdfast 1	66.32	4.60	3.20	25.88
Average	74.89	2.36	1.61	21.14

Data: Encounter 1, Holdfast 1 (Department for Energy and Mining (SA), 2017, 2018a)

4.1.7 Toolachee Formation

Key features of the Toolachee Formation are summarised below in Table 50 and discussed in more detail in the following text.

Table 50 Key features of the Toolachee Formation

Unconventional Play type	Tight, shale and deep coal gas
Age	late Permian (Wuchiapingian to Changhsingian)
Extent	88,500 km^2
Top depth (m)	1090–3280 m
Gross formation thickness	0–430 m
Lithology	Sandstone, shale and minor coal
Depositional environment	Meandering fluvial, deltaic in part
Kerogen type	Type II/III to Type III; coal, DOM
TOC	0–96 wt%
Mean original HI	176 ± 70 mg HC/g TOC
Thermal maturity	Immature–over mature
Average permeability	0.593 mD (Air permeability from Gaschnitz 4)
Average effective porosity	0.078 (fraction) in tight pay
Average effective water saturation	0.327 (fraction) in tight pay
Pressure regime	Overpressured (Nappamerri Trough)
Exploration status	Under assessment with minor production

4.1.7.1 Age and stratigraphic relationships

The Toolachee Formation is late Permian in age (Figure 2) based on the updated ages of associated spore-pollen zones (Gray and McKellar, 2002; Nicoll et al., 2015; Price, 1997).

The Toolachee Formation is the uppermost unit in the Gidgealpa Group (Gatehouse, 1972; Morton and Gatehouse, 1985; Kapel, 1972). The Toolachee Formation unconformably overlies the Daralingie Formation and older rocks on ridges (Figure 2). The unit is overlain either conformably, but slightly diachronously, by the Arrabury Formation, or unconformably by sediments of the Eromanga Basin (Figure 2) (Alexander et al., 1998a; Owens et al., 2020).

4.1.7.2 Extent, depth and gross formation thickness

The Toolachee Formation is the most widespread of all Permian units in Queensland and extends across the entire south-western Cooper Basin (Gray and McKellar, 2002), covering an area of approximately 88,500 km^2 (Hall et al., 2015a). The Toolachee Formation may have been eroded off many of the ridge crests, including those of the Murteree and Dunoon ridges, as well as in the southern Tenappera Trough (Alexander et al., 1998a; Hall et al., 2015a).

The depth to the top of the Toolachee Formation ranges from 1090 m along the south and south-east edge of the formation to a maximum of 3280 m (Figure 48) (Hall et al., 2015a).

The Toolachee Formation is on average 61 m thick, with a maximum thickness of over 400 m in the Nappamerri Trough (Figure 48) (Hall et al., 2015a; Alexander et al., 1998a). In Queensland the Toolachee Formation is generally 25–50 m thick, but thickens to 100–130 m immediately north of the JNP Trend (Hall et al., 2015a).

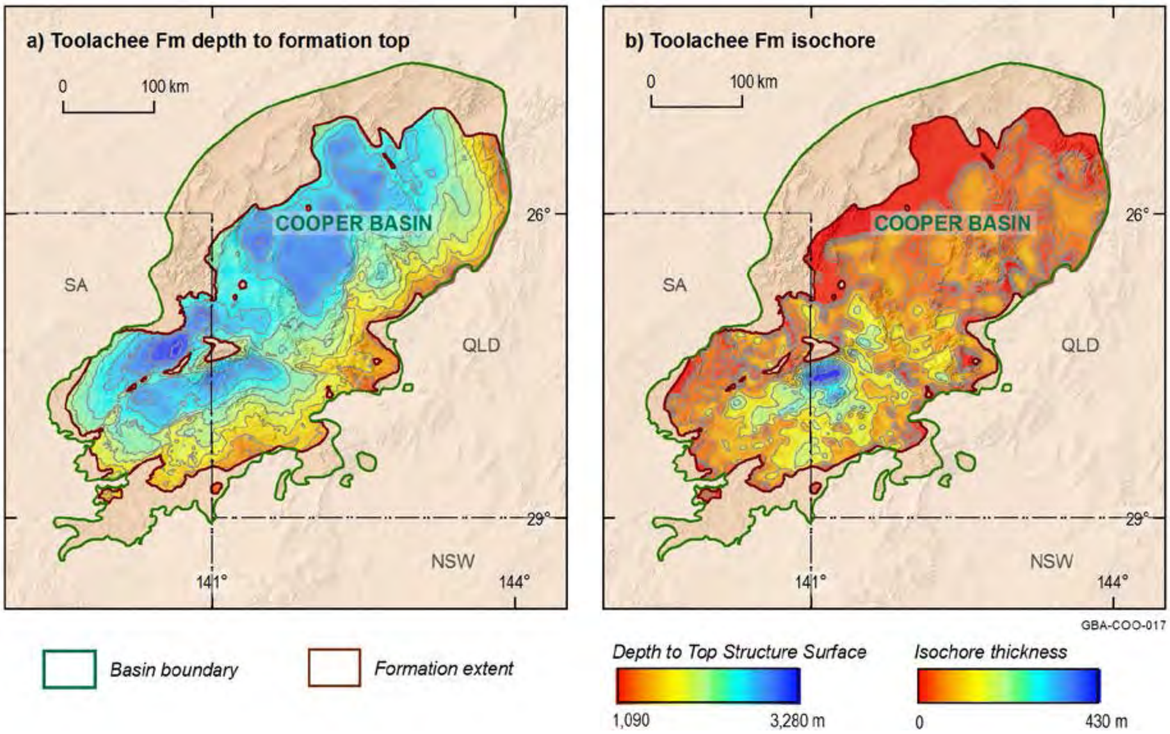

Figure 48 a) Toolachee Formation top depth (m), b) Toolachee Formation total vertical thickness (m)

Source: Hall et al. (2015a)
Data: Hall et al. (2016a); Cooper Basin outline from Raymond et al. (2018)
Element: GBA-COO-017

4.1.7.3 Lithology and palaeoenvironment

The Toolachee Formation comprises interbedded fine to coarse-grained quartzose sandstone, mudstone, carbonaceous shale with thin coal seams and conglomerates (Figure 49) (Alexander et al., 1998a; Gray and McKellar, 2002; Nakanishi and Lang, 2001).The lower part of the Toolachee Formation was deposited by meandering streams and in back swamps on floodplains. The upper part was deposited in flood basin lakes and during overbank flooding (Alexander et al., 1998a; Gray and McKellar, 2002).

The lower Toolachee Formation mainly consists of thick (up to 6 m) upward-fining packages, with minor upward-coarsening packages and coal seams, and the upper part of Toolachee Formation is dominated by mudstone and coal seams, with multiple thin upward-coarsening packages (Alexander et al., 1998a).

The lower Toolachee Formation was mainly formed by fluvial channels, ephemeral lakes and backswamps on the flood-basin, and the upper part of Toolachee Formation was formed by overbank flooding and perennial flood-basin lakes (Williams, 1984). Backswamp coals and lacustrine muds are sharply overlain by crevasse splay sandstones with rooted and bioturbated tops (Alexander et al., 1998a).

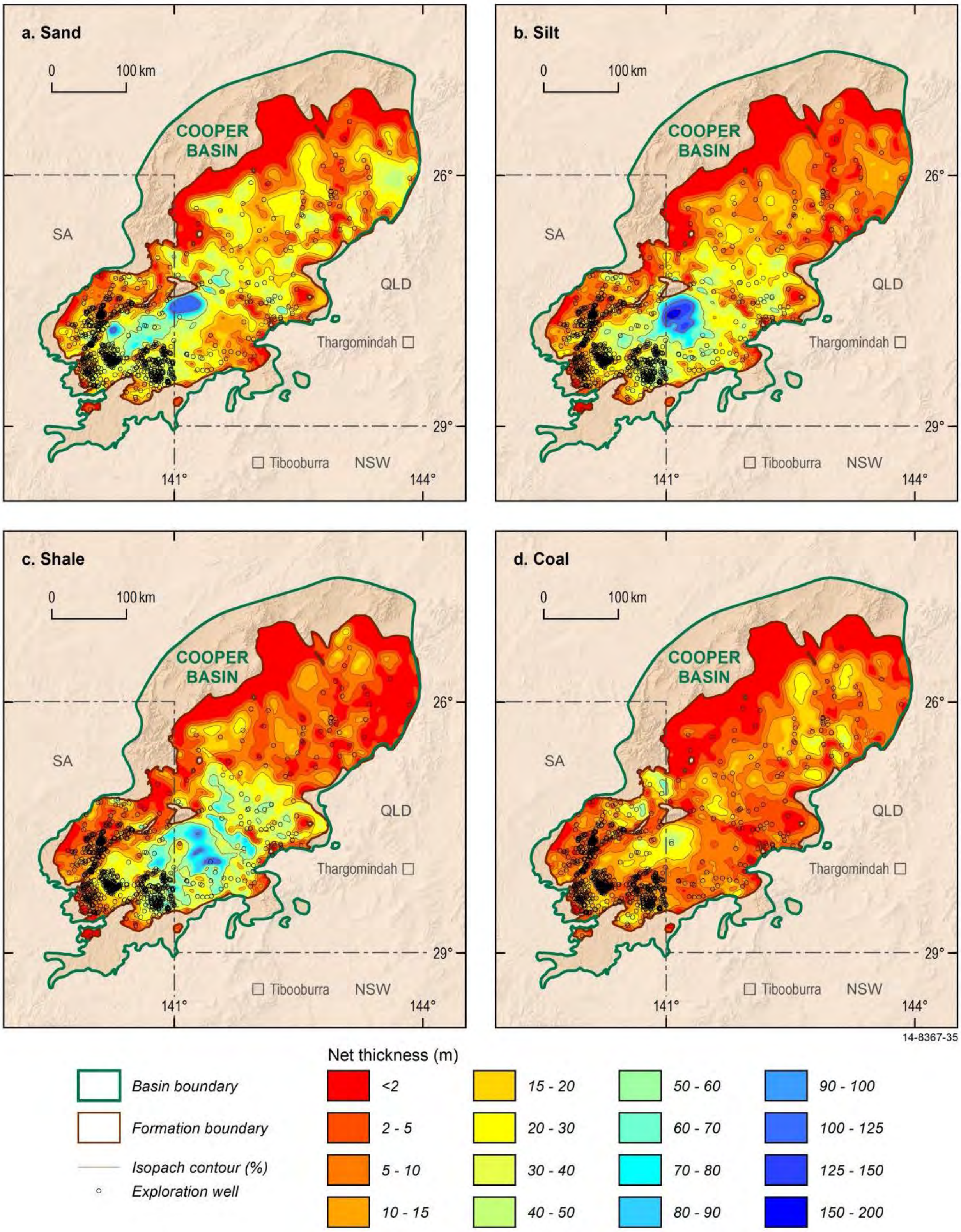

Figure 49 Toolachee Formation isolith maps by lithology, as total net thickness in metres for (a) sand, (b) silt, (c) shale and (d) coal

Shale incorporates shale, coaly shale and / or shaly coal. These are approximately equivalent to samples with a TOC range of 0.5–50 wt%.
Source: Hall et al. (2015a)
Data: Hall et al. (2016a); Cooper Basin outline from Raymond et al. (2018)
Element: GBA-COO-2-311

4.1.7.4 Source rock distribution, geochemistry and maturity

The source rocks of the Toolachee Formation include coal, carbonaceous shale and shale.

Maps of net coal and shale thickness show an abundance of potential petroleum source rock facies within the Toolachee Formation in the central and southern part of the basin (Figure 49) (Hall et al., 2015a). Although the source rock potential of the shale facies in the Windorah Trough and Ullenbury Depression is lower due to limited total formation thickness, there is still source rock potential from the coal facies in this region.

Cumulative net coal thickness (equivalent to clean coals with TOC > 50 wt%) is greatest in the northern depocentres in South Australia, reaching over 40 m in the northern Patchawarra Trough and over 25 m in the Arrabury Depression (Figure 49) (Sun and Camac, 2004; Hall et al., 2015a). Cumulative net coal thickness decreases to the south, but still reaches 20 m in the Nappamerri Trough and in parts of the Tenappera Trough (Sun and Camac, 2004; Hall et al., 2015a). Cumulative Toolachee Formation coal thickness is regionally much lower in the north-eastern basin, where the Permian section is thinner (Hall et al., 2015a; Draper, 2002).

The cumulative net thickness of the shale, coaly shale and shaly coal facies (approximately equivalent to samples with a TOC range of 0.5–50 wt%) is greatest in the deepest sections of the basin around the Nappamerri Trough, where it reaches over 180 m (Figure 49) (Hall et al., 2015a). Net shale thicknesses are much less in the north of the basin, with few areas exceeding a net thickness of 20 m.

The TOC of Toolachee Formation ranges from <1 to 96 wt% (Figure 50) (Hall et al., 2016b). The present day TOC map for the shale–shaly coal facies shows that good to excellent source rocks (TOC > 2 wt%) are present within the formation across its entire lateral extent (Figure 51).

Present day mean HI is approximately 143 ± 60 mg HC/g TOC, with the values ranging from 13 to 339 mg HC/g TOC, and mean original HI is estimated at HI_o of 176 ± 70 mg HC/g TOC. This indicates that source rock quality is highly variable, with a mixture of both oil and gas-prone Type II to Type III and gas-prone Type III kerogen (Figure 50) (Hall et al., 2016b). The coal-rich source rocks have a mean HI of 171 ± 9 mg HC/g TOC for coal; 182 ± 61 mg HC/g TOC for shaly coal and 163 ± 60 mg HC/g TOC for coaly shale. The shaly facies have a mean HI of 117 ± 56 mg HC/g TOC, reflecting predominantly gas-prone Type III kerogen.

The maturity of the mid Toolachee Formation is highest in the central Nappamerri Trough where it reaches the dry gas window (R_o > 2%; TR > 70%; Figure 52), reflecting greater burial depths and proximity to the high heat producing Big Lake Suite granodiorites (Hall et al., 2016c). In the Patchawarra Trough, maturity ranges from early oil window in the west to late oil in the east (R_o 1–1.2%; TR > 50–70%). Large areas of the Toolachee Formation reach the wet gas window across the Windorah Trough (R_o 1.2–2%; TR > 50–70%; Figure 52) (Hall et al., 2016c).

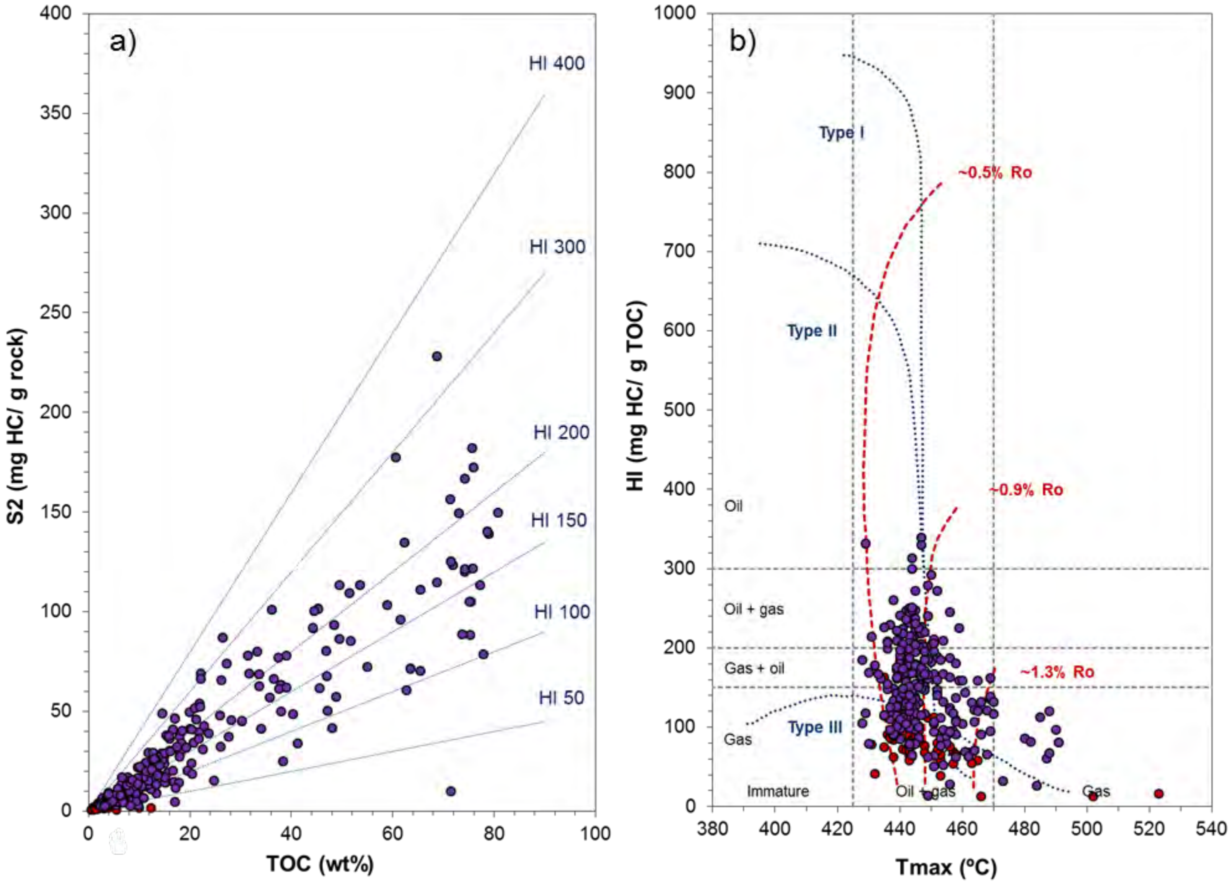

Figure 50 Rock-Eval pyrolysis data plots for the Toolachee Formation: a) TOC content vs S2 yield; and b) T_{max} vs HI

Purple dots: effective source rocks (TOC > 2 wt%; S1 + S2 > 3 mg HC/g rock); red dots: samples with either no original generation potential or are spent source rocks.
Source: Hall et al. (2016b)
Data: Hall et al. (2016a)
Element: GBA-COO-2-303

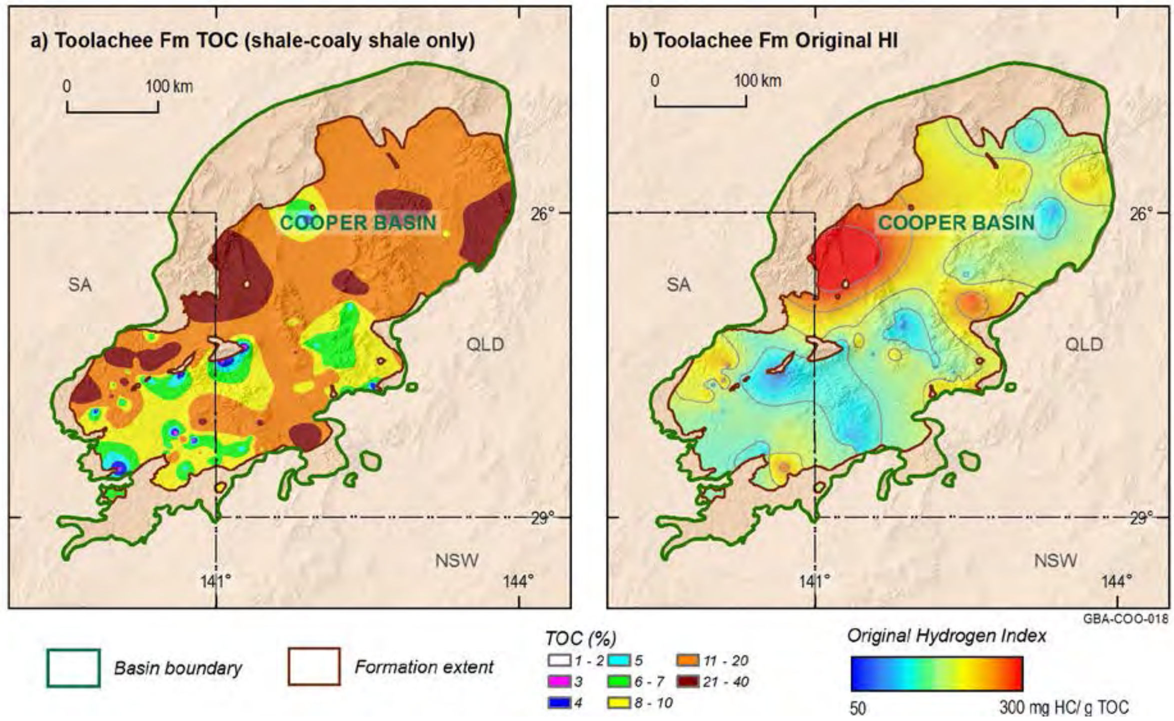

Figure 51 Toolachee Formation source rock geochemistry maps: (a) Present day average Total Organic Carbon (TOC) for shale-coaly shale facies (TOC < 50 wt%); and (b) mean Original Hydrogen Index (HI_o)

Source: Hall et al. (2016b)
Data: Hall et al. (2016a); Cooper Basin outline from Raymond et al. (2018)
Element: GBA-COO-018

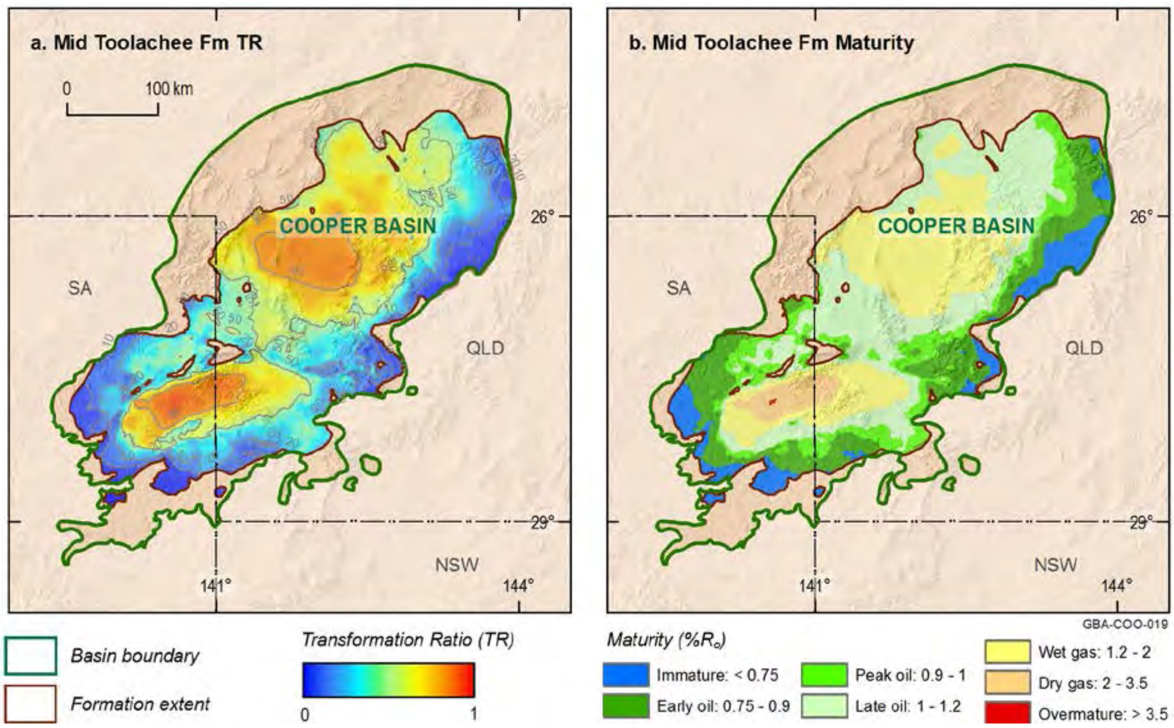

Figure 52 Toolachee Formation (a) transformation ratio and (b) maturity (%R_o)

Source: Hall et al. (2016b)
Data: Hall et al. (2016a); Cooper Basin outline from Raymond et al. (2018)
Element: GBA-COO-019

4.1.7.5 Tight reservoir characteristics

The Toolachee Formation hosts conventional reservoirs mostly within stacked, moderately thick (up to 6 m) higher porosity, point bar sands in the lower part of the formation (Gravestock et al., 1998a). In addition, the Toolachee Formation hosts tight gas reservoir intervals in finer grained sandstone and siltstone intervals. The net sandstone thickness of the Toolachee Formation is greater than 100 m in the central Nappamerri Trough, with an equivalent thickness of net siltstone (Sun and Camac, 2004; Hall et al., 2015a).

Log-derived tight pay thickness, average effective porosity and water saturation of the Toolachee Formation tight reservoirs were calculated from 32 wells (Department for Energy and Mining (SA), 2017, 2018a; Department of Natural Resources, 2018a). The average net pay thickness is 24.23 m, the average effective porosity is 7.9% and the average water saturation is 33.9% (Table 51; Figure 47).

Table 51 Log-derived tight pay thickness, average effective porosity and average water saturation statistics for the Toolachee Formation tight reservoirs in the Cooper Basin

Well	Tight Pay Thickness (m)	Average Effective Porosity (fraction)	Average Water Saturation (fraction)
Minimum	2.74	0.052	0.062
Maximum	80.09	0.126	0.610
Average	24.37	0.078	0.327
Median	24.23	0.079	0.339

The net tight pay interval was defined by the following criteria: volume fraction of shale less than 50%, effective porosity greater than 4% and water saturation less than 70%.
Data: Beach Energy wells Boston 1, Boston 2, Dashwood 1, Etty 1, Encounter 1, Geoffrey 1, Halifax 1, Hervey 1, Holdfast 1, Marble 1, Moonta 1ST1, Nepean 1, Rapid 1, Redland 1, Streaky 1, Santos wells Bindah 3, Bobs Well 2, Coonatie 13, Gaschnitz 1ST1, Gaschnitz 4, Kirralee 2, Langmuir 1, Moomba 175, Moomba 191, Moomba 192, Roswell 1, Van Der Waals 1, Washington 1, Whanto 4, Whanto South West 1 and Real Energy Queensland wells Queenscliff 1 and Tamarama 1 (Department for Energy and Mining (SA), 2017, 2018a; Department of Natural Resources, 2018a)

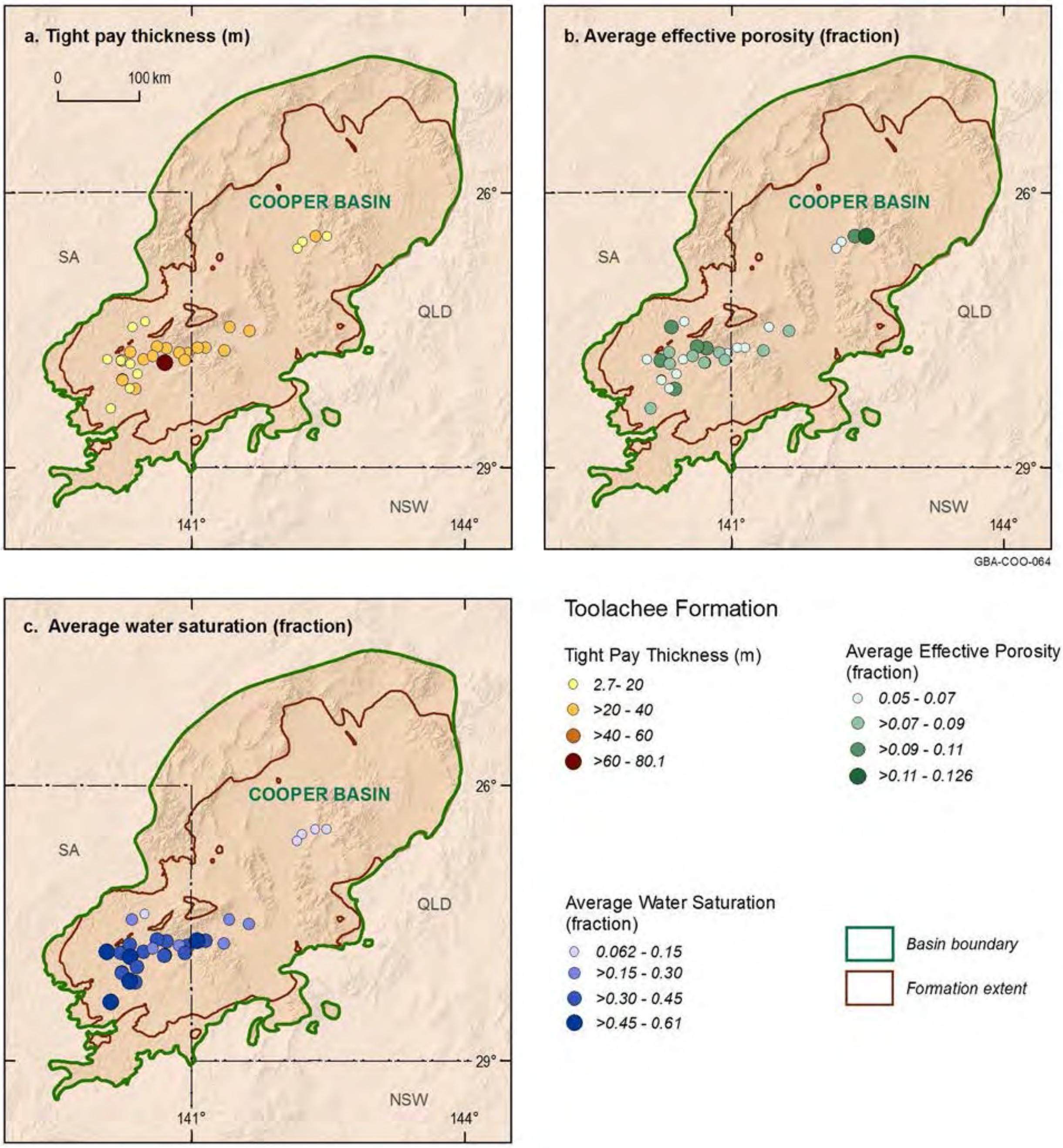

Figure 53 Log-derived tight pay thickness, average effective porosity and average water saturation of the Toolachee Formation tight reservoirs in the Cooper Basin

Data: Beach Energy wells Boston 1, Boston 2, Dashwood 1, Etty 1, Encounter 1, Geoffrey 1, Halifax 1, Hervey 1, Holdfast 1, Marble 1, Moonta 1ST1, Nepean 1, Rapid 1, Redland 1, Streaky 1, Santos wells Bindah 3, Bobs Well 2, Coonatie 13, Gaschnitz 1ST1, Gaschnitz 4, Kirralee 2, Langmuir 1, Moomba 175, Moomba 191, Moomba 192, Roswell 1, Van Der Waals 1, Washington 1, Whanto 4, Whanto South West 1 and Real Energy Queensland wells Queenscliff 1 and Tamarama (Department for Energy and Mining (SA), 2017, 2018a; Department of Natural Resources, 2018a); Cooper Basin outline from Raymond et al. (2018)
Element: GBA-COO-064

4.1.7.6 Deep coal reservoir characteristics

The distribution of Toolachee Formation coal is presented in Figure 49 (Hall et al., 2016). In the Weena Trough area, the average net thickness of the Toolachee Formation coal seams is 37.9 m in the wells Klebb 1, 2, 3 and 4 (Department for Energy and Mining (SA), 2018a) (Table 52).

Table 52 Thickness of composite coal seams (m) in the Toolachee Formation

	Klebb 1	Klebb 2	Klebb 3	Klebb 4	Average
Toolachee Formation coal	50.1	35.3	37.9	28.4	37.9

Data: wells Klebb 1, 2, 3 and 4, (Department for Energy and Mining (SA), 2018a)

The composition of Toolachee Formation deep coals was assessed in 2 wells. The average maceral composition was found to be 71.95 vol% inertinite (Type IV), 19.66 vol% vitrinite (Type III) and minor liptinite (Type I and/or II) and mineral components (Table 53). The main maceral types include 76.9% of inertinite (Type IV) and 15.80% of Vitrinite (Type III) in Vintage Crop 1. The average components of these coal seams from proximate analysis are listed in Table 54. The average content of volatile matter is 28.88 wt%, indicating the Toolachee Formation deep coals are mainly the medium-volatile bituminous coals (Mastalerz and Harper, 1998).

Table 53 Average maceral components of the Toolachee Formation coal seams in Marsden 1 and Vintage Crop 1

Well	Vitrinite (vol%)	Liptinite (vol%)	Inertinite (vol%)	Minerals (vol%)
Marsden 1	23.75	0.85	68.20	7.00
Vintage Crop 1	15.57	3.57	75.70	1.70
Average	19.66	2.21	71.95	4.35

Data: Marsden 1 and Vintage Crop 1 (Department for Energy and Mining (SA), 2017, 2018a)

Table 54 Average components of the Toolachee Formation coals based on proximate analyses for key wells in the Cooper Basin

Well	Moisture (wt%)	Ash (wt%)	Volatile matter (wt%)	Fixed carbon (wt%)
Marsden 1	4.25	7.60	27.05	61.10
Vintage Crop 1	2.85	11.43	30.70	55.03
Average	3.55	9.51	28.88	58.06

Data: Marsden 1 and Vintage Crop 1 (Department for Energy and Mining (SA), 2017, 2018a)

The laboratory test for geomechanical properties on the Toolachee Formation coal samples in Washington 1 show that the average as-received bulk density, quasi-static Young's modulus and Poisson's ratio are respectively 1.33 g/cc, 683700 psi and 0.40 (Table 55).

Table 55 Geomechanical test results of the Toolachee Formation coal samples in Washington 1

Sample ID	WSH1-1	WSH3-1	Average
Depth (m)	3319.51	3318.90	3319.21
As-Received Bulk Density (g/cm^3)	1.36	1.31	1.33
Effective Confining Pressure (psi)	4300	4300	4300
Effective Compressive Strength (psi)	17,340	19,760	18,550
Effective Residual Compressive Strength (psi)	13,245	12,455	12,850
Quasi-static Young's Modulus (psi)	693,200	674,200	683,700
Quasi-static Poisson's Ratio	0.40	0.41	0.40

Data: Washington 1 (Department for Energy and Mining (SA), 2017, 2018a)

As for shale gas, gas in deep coal is stored as adsorbed gas on the organic matter, free gas stored meso- and macro-porous inertinite-rich matrix and dissolved gas in the formation water.

Table 56 lists the as-received total gas content test results of desorbed gas from the Toolachee Formation coal samples in Marsden 1. The average as-received total gas content of Toolachee Formation coal seams is 10.17 scc/g. Table 57 gives the methane isotherm test results of the Toolachee Formation coal samples in Marsden 1.

Table 56 As-received total gas content test results of desorbed gas from the Toolachee Formation coal samples in Marsden 1

Top depth (m)	Bottom depth (m)	As-received total gas content (scc/g)	Dry, ash free total gas content (scc/g)
1911.15	1911	11.56	na
1913.15	1913	11.74	13.24
1916.15	1916	8.61	na
1917	1917	11.14	na
1919.15	1919	9.07	na
1920.15	1920	12.21	na
1923.15	1923	10.21	11.61
1926	1926	6.8	na
	Average	10.17	12.43

Data: Marsden 1 (Department for Energy and Mining (SA), 2017, 2018a)

Table 57 Methane isotherm test data of the Toolachee Formation coal samples in Marsden 1

Sample Parameters	Sample 1	Sample 1	Sample 2	Sample 2	Sample 2
Sample Top Depth (m)	1913.15	1913.15	1923.15	1923.15	1923.15
Sample Bottom Depth (m)	1913.45	1913.45	1923.45	1923.45	1923.45
Measurement Gas	methane	methane	methane	methane	methane
Measurement Temperature (°C)	50	80	50	80	120
Moisture Content (wt frac)	0.0676	0.0676	0.1584	0.1626	0.1335
Ash Content (wt frac)	0.0924	0.0923	0.0582	0.059	0.062
Organic Content (wt frac)	0.8401	0.8402	0.7833	0.7785	0.8045
Langmuir Storage Capacity, dry, ash-free (scc/g)	20.87	23.44	30.94	44.73	30.31
Langmuir Storage Capacity, in situ (scc/g)	17.53	19.69	24.24	34.82	24.38
Langmuir Pressure (kPa)	11573.60	17732.70	21282.40	40521.60	34110.60
Reservoir Pressure (kPa)	20684.30	20684.30	20684.30	20684.30	20684.30
Storage Capacity, dry, ash-free (scc/g)	13.38	12.62	15.25	15.12	11.44
Storage Capacity, in situ (scc/g)	11.24	10.6	11.95	11.77	9.2

Data: Marsden 1 (Department for Energy and Mining (SA), 2017, 2018a)

The well flow tests on the Permian coals (Table 58) in Washington 1 show that the initial flow was very liquid rich. About 100 stb of condensate was produced in the first 12 hours with the choke of 36/64 inch, and the fluid had a gas-to-oil ratio (GOR) of approximately 3000 scf/stb. With the choke size increased to be 40/64 inch, then 44/64 inch, the GOR was observed to be approximately 100,000 scf/stb. The salinities of two formation water samples were measured as 28,880 mg/L and 23,465 mg/L.

Table 58 Intervals perforated in the Permian coal seams in Washington 1

Formation	Interval perforated (mMD)
Toolachee PC20 Coal	3255 - 3258
Toolachee PC30 Coal	3276 - 3281
Toolachee PC35 Coal	3308.5 - 3317.5
Epsilon TC20 Coal	3353 - 3356
Patchawarra Coal	3442.5 - 3443.5
Patchawarra Coal	3451.5 - 3452.5
Patchawarra Coal	3470 - 3471
Patchawarra Coal	3490 - 3491

MD = measured depth along the borehole

Data: Washington 1 (Department for Energy and Mining (SA), 2017, 2018a)

4.1.7.7 Gas composition

The gas composition analysis on the desorbed gas samples from the Toolachee Formation in 3 wells (Department for Energy and Mining (SA), 2018a, 2017; Department of Natural Resources and Mines (Qld), 2017) show that on average Toolachee Formation gas includes 62.28% methane, 10.20% ethane, 3.29% propane plus, and 24.20% carbon dioxide (Table 59). An average CGR of 9.18 bbl/mmscf was determined for the Toolachee Formation from well test data (mainly the DSTs) compiled from publically available well completion reports.

Table 59 Average gas compositions of desorbed gas samples from the Toolachee Formation

Well	Methane (mol%)	Ethane (mol%)	Propane plus (mol%)	Carbon dioxide (mol%)
Marsden 1	71.65	13.14	3.74	11.47
Sasanof 1	57.29	9.69	2.85	30.17
Vintage Crop 1	57.89	7.78	3.29	30.96
Average	62.28	10.20	3.29	24.20

Data: Marsden 1, Sasanof 1 and Vintage Crop 1 (Department for Energy and Mining (SA), 2017, 2018a)

4.2 Regional stress and overpressure

4.2.1 Regional stress regime

Contemporary patterns of tectonic stress in the brittle crust act as a control over neotectonic deformation and seismicity, and acts as a primary control over both the formation and propagation of natural fractures and of hydraulically induced fractures (Bailey et al., 2017; Bell, 1996a, 2006; Fisher and Warpinski, 2012; Hillis et al., 2008; King et al., 2010; Lund Snee and Zoback, 2016; Olsen et al., 2007; Palano, 2014; Palmer, 2010; Pitcher and Davis, 2016; Rajabi et al., 2017b; Sandiford et al., 2004; Seeber and Armbruster, 2000; Sibson, 1992; Sibson et al., 2012; Sibson et al., 2011; Stein, 1999). The extraction of fluids from tight reservoirs, such as shales and low permeability sandstones, typically requires the creation of fracture pathways through hydraulic stimulation in order to enable adequate flows from the reservoir to the well (Bell, 1990; Bell and Babcock, 1986).

Tectonic stress regimes are defined by the relative orientations and magnitude of three orthogonal principal stresses, namely a maximum (σ_1), minimum, (σ_3), and intermediate (σ_2). One stress is generally vertical due to the mass of overburden (σ_v), constraining the two remaining stresses to the horizontal plane (Anderson, 1951; Bell, 1996b; Sibson, 1977; Zoback, 2007). These are referred to as the maximum (σ_H) and minimum (σ_h) horizontal stresses (Bell, 1996b) (Figure 54), and are usually expressed in terms of stress gradients at a given depth (e.g. MPa/km or psi/ft).

The relative magnitude of the three principal stresses dictates what type of failure will dominate a given stress regime (Figure 54), although pre-existing structures can exhibit hybrid failure modes (Heidbach and Höhne, 2008; Sibson, 1977). For further information regarding the definition of lithospheric stresses, see Bell (1990, 1996b, 1996a); Chan et al. (2014); Couzens-Schultz and Chan (2010); Plumb et al. (2000); Zoback (2007).

This section considers the potential impacts of the present day stress regime on hydraulic stimulation of tight, shale and deep coal gas plays in the Cooper Basin.

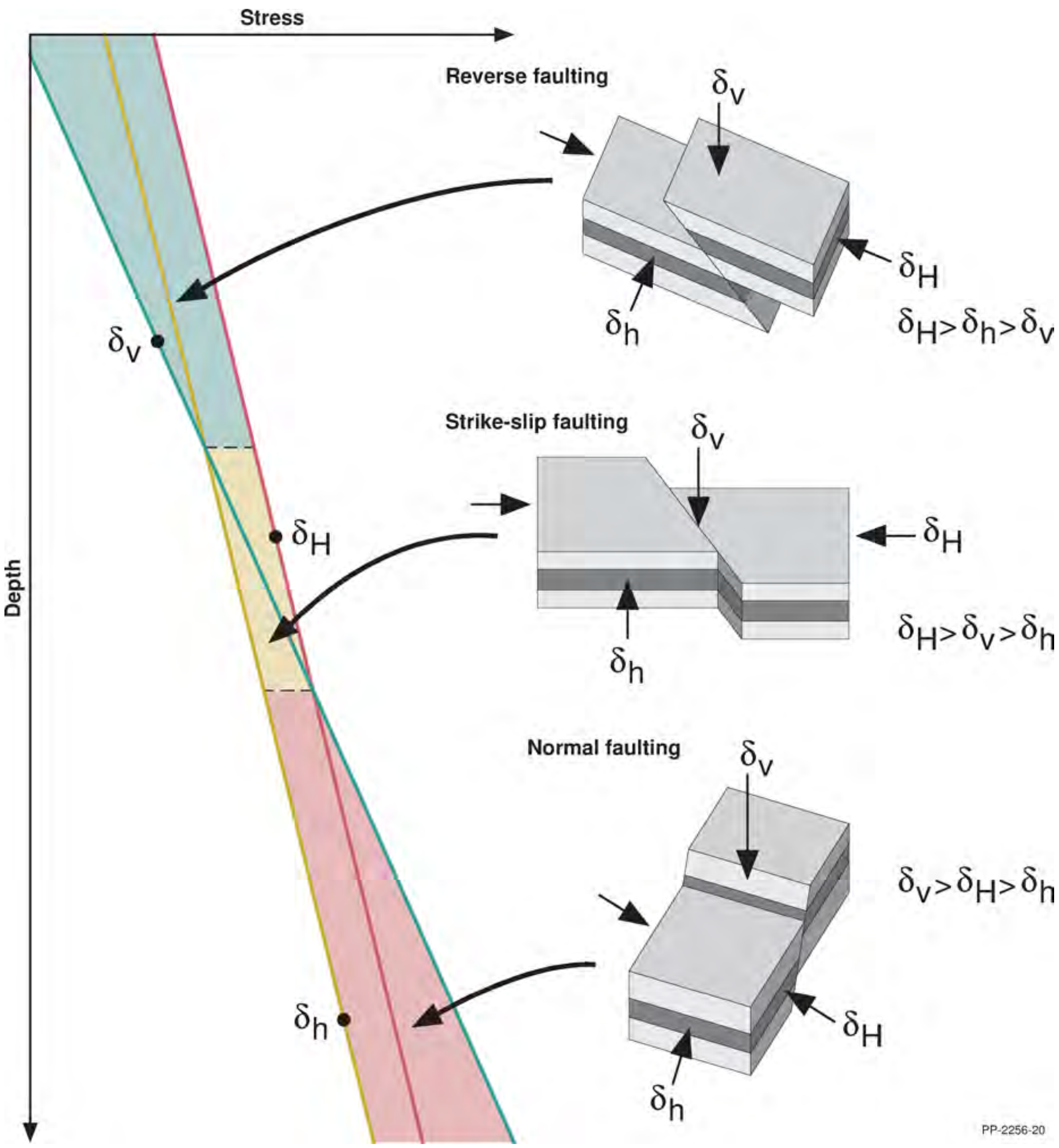

Figure 54 Tectonic stress regimes as defined by Anderson (1951), highlighting the relative magnitudes of the three principal stresses presented as gradients. Vertical stress is shown in green, maximum horizontal stress in red, and minimum horizontal stress in brown

Source: Brooke-Barnett et al. (2015)
Element: PP-2256-20

4.2.1.1 Present-day stress in the Cooper Basin

The Cooper Basin is interpreted as experiencing a strike-slip faulting stress regime with significant differences in magnitude recorded between σ_H and σ_v as well as σ_h (Gui et al., 2016; Reynolds et al., 2006).There are also notable variations observed with depth, lithology, and in the proximity of structures (Gui et al., 2016).

The presence of coal intervals of varying thickness within the major depocentres affects stress measurement in the Cooper Basin. Coals complicate the calculation of σ_v as they are an abnormally low density sediment, depressing σ_v gradients where thick coal beds are present. They are typically associated with poor hole conditions such as washouts (Reynolds et al., 2006). In well testing, coal intervals are unlikely to indicate stress conditions within siliciclastic sediments (Bowker et al., 2018; Gui et al., 2016; Reynolds et al., 2006).

There have been several studies characterising the regional stress of the Cooper Basin, beginning with continent-wide studies by Hillis et al. (1998) and Hillis and Reynolds (2000) as part of the Australian Stress Map project (Rajabi et al., 2017b). These studies characterised regional stresses on a continental scale and attempted to place diagnosed stress provinces within a failure regime. Further understanding of stresses within the Cooper Basin was added by Reynolds et al. (2004); Reynolds et al. (2006); Reynolds et al. (2005); Nelson et al. (2007); King et al. (2011); Conlay (2014); and Gui et al. (2016) who looked at both continent- and basin-scale stresses throughout the Cooper Basin (Table 60).

Significantly elevated magnitudes of vertical stress due to overburden (σ_v) are not observed in existing datasets (Table 60). This is in part due to the lack of significant dense carbonate or volcanic intervals throughout the basin.

Table 60 Previously reported stress magnitudes from the Cooper Basin. All values are given as MPa/km and where provided, the depths that gradient was calculated at is listed

<table>
<tr><th rowspan="2">Source</th><th rowspan="2">Depth (km)</th><th colspan="2">Vertical Stress (MPa/km)</th><th colspan="2">Maximum Horizontal Stress (MPa/km)</th><th colspan="2">Minimum Horizontal Stress (MPa/km)</th></tr>
<tr><th>Lower</th><th>Upper</th><th>Lower</th><th>Upper</th><th>Lower</th><th>Upper</th></tr>
<tr><td>King et al. (2011)</td><td>1</td><td>17.0</td><td>20.4</td><td colspan="2">26.9</td><td colspan="2">14.8</td></tr>
<tr><td>King et al. (2011)</td><td>3</td><td>18.0</td><td>21.7</td><td colspan="2">26.4</td><td colspan="2">20.0</td></tr>
<tr><td>Reynolds et al. (2006)</td><td>1</td><td>16.8</td><td>19.8</td><td>-</td><td>-</td><td>-</td><td>-</td></tr>
<tr><td>Reynolds et al. (2006)</td><td>3</td><td>19.9</td><td>22.6</td><td>-</td><td>-</td><td>-</td><td>-</td></tr>
<tr><td>Reynolds et al. (2006) (Bulyeroo 1)</td><td>-</td><td>-</td><td>-</td><td>37.9</td><td>38.6</td><td colspan="2">15.5</td></tr>
<tr><td>Reynolds et al. (2006) (Dullingari North-8)</td><td>-</td><td>-</td><td>-</td><td>38.8</td><td>40.8</td><td colspan="2">15.5</td></tr>
<tr><td>Reynolds et al. (2006) (minifrac data)</td><td>-</td><td>-</td><td>-</td><td>-</td><td>-</td><td>13.6</td><td>24.9</td></tr>
<tr><td>Nelson et al. (2007)</td><td>-</td><td>-</td><td>-</td><td colspan="2">41.9</td><td colspan="2">18.1</td></tr>
<tr><td>Nelson et al. (2007)</td><td>-</td><td>-</td><td>-</td><td colspan="2">41.9</td><td>12.4</td><td>27.2</td></tr>
<tr><td>Gui et al. (2016)</td><td>-</td><td>-</td><td>-</td><td>-</td><td>-</td><td colspan="2">16.8</td></tr>
<tr><td>Gui et al. (2016)</td><td></td><td>22.8</td><td>23.1</td><td>-</td><td>-</td><td>14.4</td><td>21.2</td></tr>
<tr><td>Conlay (2014)</td><td>3</td><td>21.2</td><td>22.6</td><td>25.0</td><td>45.0</td><td>16.0</td><td>22.0</td></tr>
</table>

Calculated stress magnitudes range from 16.8–19.8 MPa/km at 1 km depth to 19.89–22.61 MPa/km at 3 km depth (Nelson et al., 2007; Reynolds et al., 2006). These values are supported by (King et al., 2011), who identify a strike-slip faulting regime in the upper 3 km, and a strike-slip to reverse faulting regime at depths greater than 3 km (Tyiasning and Cooke, 2016). Broadly, the horizontal stresses are constrained so that σ_h magnitude ranges from 12.4–27.2 MPa/km and σ_H is approximately 42 MPa/km (Nelson et al., 2007).

Highly anisotropic horizontal stresses are observed in sand and some coal intervals within the Cooper Basin, in contrast to the low anisotropy observed in shale units. This is likely due to lithology based stress-partitioning, where sandstones act as a load-bearing unit and, hence, host high stress concentrations relative to shales (Nelson et al., 2007; Tyiasning and Cooke, 2016). This has significant implications for fracture propagation and containment, and is discussed in more detail in section 4.2.1.6.

4.2.1.2 Maximum horizontal stress azimuth

The Australian Stress Map project considers the Cooper-Eromanga Basin to be one of 30 Australian stress provinces, with a mean σ_H azimuth of 099°N (s.d. 14°) (Figure 55) based on 78 stress orientation records of sufficient quality (Rajabi et al., 2017b). This approximately east-west stress azimuth is similar to proximal areas of southern Australia and agrees with stress trajectory models of the Australian continent (Dyksterhuis et al., 2005; Müller and Dyksterhuis, 2005; Rajabi et al., 2017a; Reynolds et al., 2002).

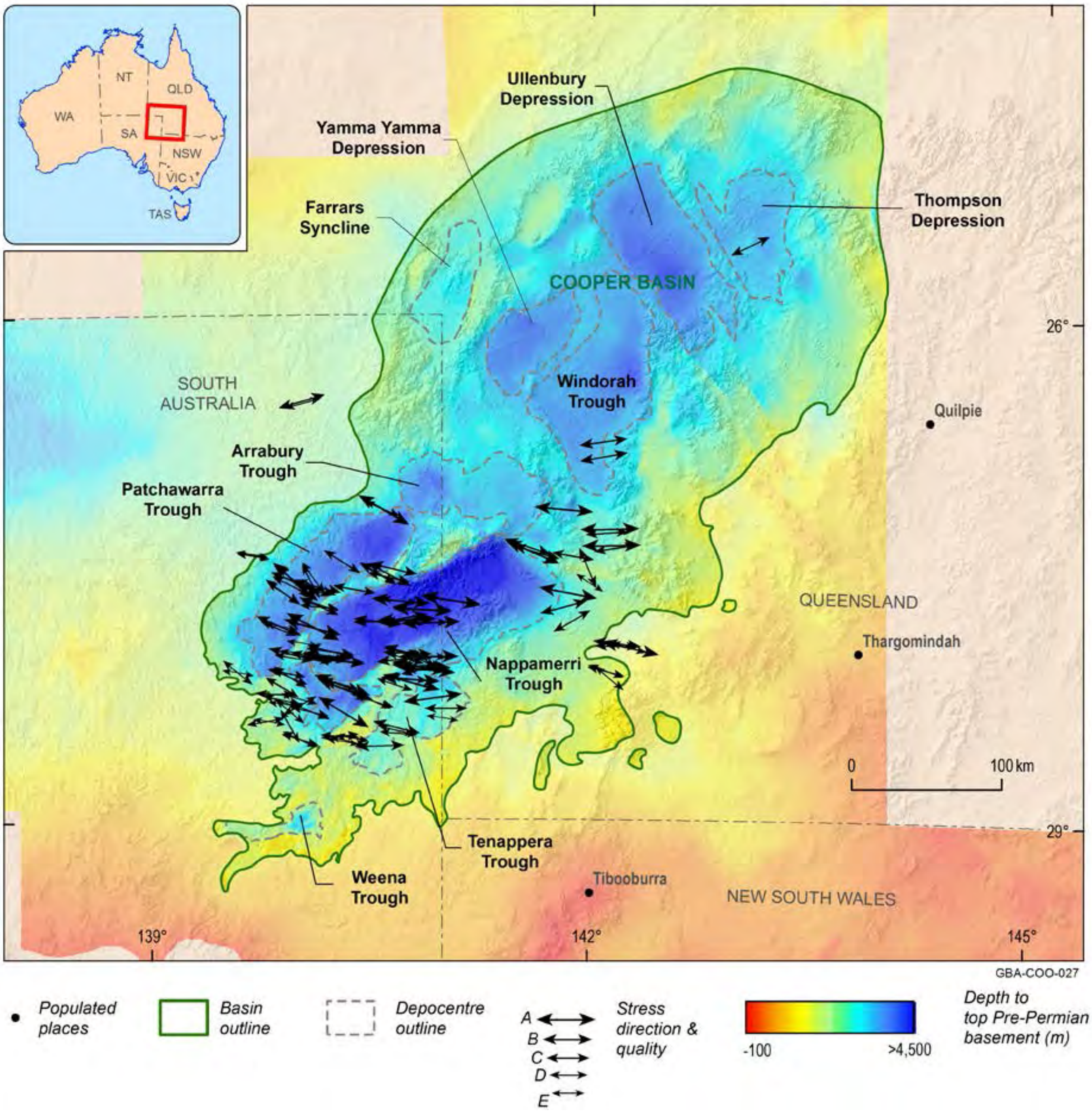

Figure 55 Maximum horizontal stress azimuths for the Cooper-Eromanga Stress Province, overlain on depth to top Pre-Permian basement

Source: Rajabi et al. (2017b)
Data: Heidbach et al. (2016); Cooper Basin outline from Raymond et al. (2018)
Element: GBA-COO-027

4.2.1.3 Patchawarra Trough stress magnitudes

Regional stress studies in the Cooper Basin region are primarily based on data from the Nappamerri Trough. Additional data from the Patchawarra Trough enables a broader regional interpretation (e.g. Nelson et al., 2007; Reynolds et al., 2006). A transitional strike-slip to reverse faulting stress regime is likely hosted in the Patchawarra Trough based on reported stress magnitudes (i.e. $\sigma_H > \sigma_h \sim \sigma_V$) (Gui et al., 2016; Kulikowski et al., 2016b; Nelson et al., 2007; Reynolds et al., 2006). The magnitude of σ_v in the Patchawarra Trough varies from 22.8 MPa/km to 23.1 MPa/km at 3 km depth (Gui et al., 2016), which is in the upper range of Cooper Basin stress magnitudes. Vertical stress magnitude throughout the rest of the basin varies from 19.89–23.10 MPa/km at 3 km depth (Reynolds et al., 2006).

A large range of values for σ_h magnitude in the Patchawarra Trough are calculated by Gui et al. (2016) from both leak-off test (LOT) and diagnostic fracture injection test data; these range from 15.1–20.5 MPa/km with a mean value of 16.8 MPa/km at 1 km depth for LOT data to 14.4–21.2 MPa/km at 3 km depth from Diagnostic Fracture Injection Testing (DFIT) data. Both of these σ_h ranges overlap with the calculated magnitudes of σ_v, suggesting that in some instances minimum horizontal stress may exceed vertical stress in the Patchawarra Trough and more broadly in the basin (Bailey et al., 2017; Zoback, 2007).

4.2.1.4 Patchawarra Trough coal stress magnitudes

Deep Permian coals within the Patchawarra Formation are an emerging and significant play within the Cooper Basin and they retain significant volumes of hydrocarbons (Camac et al., 2018; Dunlop et al., 2017; Hall et al., 2019; Bowker et al., 2018). Recent experience from hydraulic stimulation trials in development wells demonstrate that the deep Permian coals are over-saturated with both free and adsorbed gas and do not require dewatering prior to production, though they require comparatively large fracture stimulations to produce at economic rates (Camac et al., 2018; Dunlop et al., 2017). Recent work from Santos posits that high treatment pressures are likely associated with high fracture complexity due to local perturbations in the present-day stress field around discontinuities such as faults (Bowker et al., 2018; Camac et al., 2018; Camac et al., 2006).

One-dimensional Mechanical Earth Models constructed over the Tirrawarra-Gooranie oil and gas field (Figure 3) demonstrate a highly variable stress state within the subsurface, with coals hosting significantly decreased horizontal stresses as a result of their mechanical properties (Figure 56), when compared to underlying sandstone intervals (Bowker et al., 2018; Cooke et al., 2006; Thiercelin and Plumb, 1994; Underwood et al., 2003). These stress contrasts result in variation of stress regimes between each rock type, with normal and strike-slip faulting regimes interpreted respectively (Bowker et al., 2018). This is discussed in more detail in section 4.2.1.6.

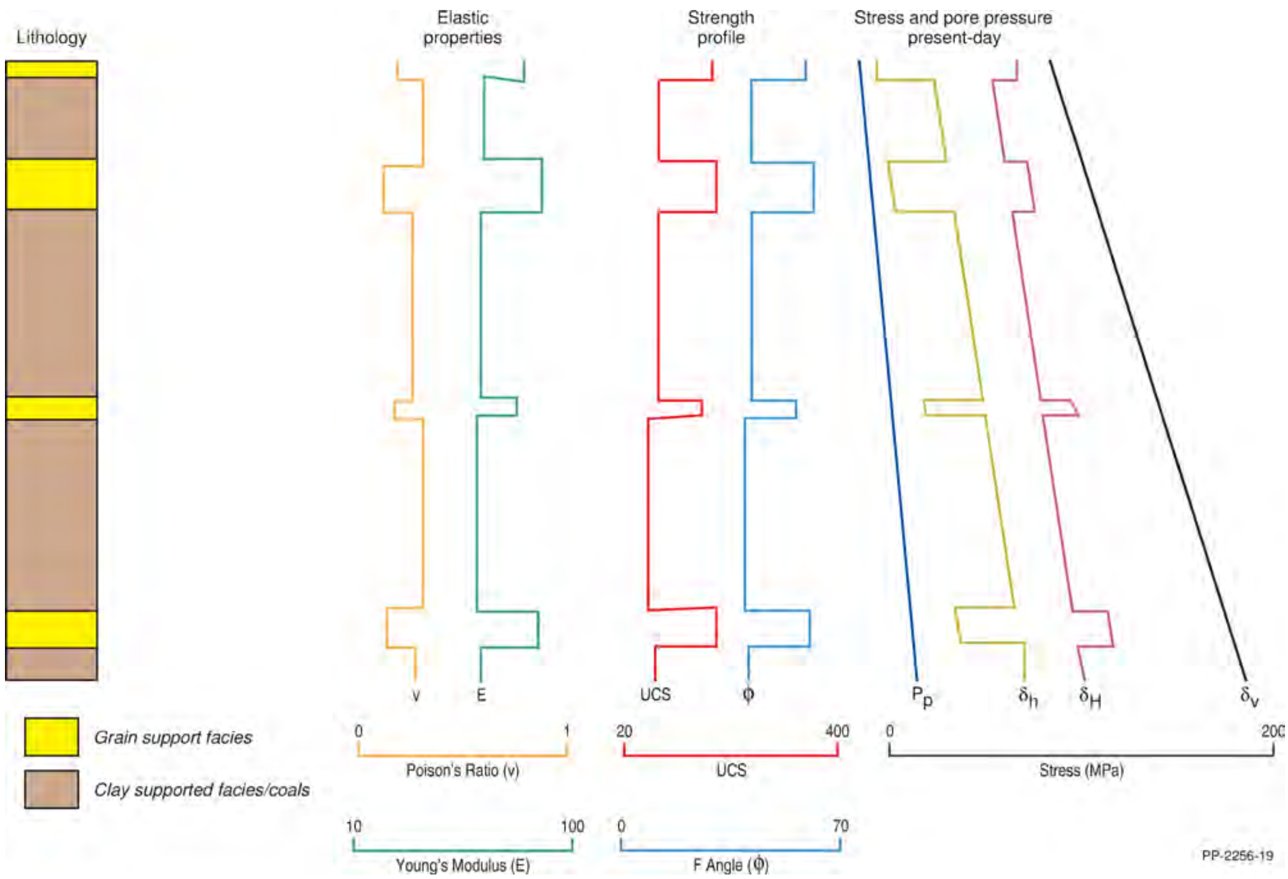

Figure 56 Schematic mechanical earth model showing lithology, mechanical stratigraphy, and calculated stress profiles

Source: Plumb et al. (2000)
Element: PP-2256-19

4.2.1.5 Nappamerri Trough stress magnitudes

All three of the stress regimes indicated in Figure 54 possibly exist within the subsurface of the Nappamerri Trough, although the most likely configuration is a transitional strike-slip to reverse faulting stress regime (i.e. $\sigma_H > \sigma_h \sim \sigma_V$) (Conlay, 2014) (Figure 54). Vertical stress is consistent throughout both the greater basin area, where it varies from 19.89–22.61 MPa/km at 3 km depth (Reynolds et al., 2006) and throughout the Nappamerri Trough, where it varies from 21.26–22.58 MPa/km at 3 km depth (Conlay, 2014). Reynolds et al. (2006) determined a minimum gradient for σ_h as 15.5 MPa/km, however, some results are as high as σ_v, implying that σ_h may exceed σ_v in some areas of the basin. In the Nappamerri Trough similar results are observed. At 3 km depth σ_h estimates vary from 16.13 MPa/km to 22.37 MPa/km, again reaching magnitudes approximately equivalent to σ_v magnitude (Conlay, 2014).

Maximum horizontal stress estimates based upon direct measurements vary from a lower bound of 21.9–30.7 MPa/km (strike-slip regime where $\sigma_V > \sigma_h$) to an upper bound of 38.5 MPa/km–

50.0 MPa/km (reverse faulting regime where $\sigma_V < \sigma_h$) at 3 km depth (Conlay, 2014). This compares with a basin-wide estimate of between 27 MPa/km and 51 MPa/km (Reynolds et al., 2006).

Geomechanical models suggest that the Permian strata within the central Nappamerri Trough are presently subject to a variable stress regime. Beach Energy interprets a dominant strike-slip faulting stress regime that transitions to reverse faulting throughout much of the Permian section (Figure 57) (Beach Energy, 2012). This is noticeably different to the overlying Triassic strata, where reverse faulting stress regimes dominate the Nappamerri Group sediments (Figure 57) (Beach Energy, 2012). While vertical stress gradients remain consistent throughout the column, horizontal stresses are calculated to vary significantly based on lithological changes (Beach Energy, 2012). Shales and coal intervals in the Toolachee Formation, shales in the Daralingie Formation, and the Roseneath and Murteree shales exhibit distinctly reduced horizontal stresses, edging the stress regime in these formations towards isotropy (Beach Energy, 2012). In such intervals, like the base of the Murteree Shale or throughout the Roseneath Shale, stress regimes are interpreted to transition from high-stress reverse faulting, towards strike-slip to normal faulting conditions due to depressed horizontal stress magnitudes. The sandstones and siltstones of the Cooper Basin host high horizontal stresses, and as a result these sediments generally host reverse-faulting dominated stress regimes (Figure 57).

Compressional stress regimes are observed to dominate throughout the succession, however, it is notable that shale and coal intervals are inferred to host extensional regimes or transitional regimes that are significantly different to the dominant faulting regime (Beach Energy, 2012).

4.2.1.6 Implications for fracture propagation

Mechanical properties control the amount of stress which can be supported by a given lithology. Differences in mechanical properties of rock units, a concept known as mechanical stratigraphy, constitutes a significant control over the formation and propagation of fractures in the sub-surface (Laubach et al., 2009). Natural barriers to fracture propagation are formed where there are contrasts between these mechanical units, (Zoback, 2007). Typically a significant change in stresses from unit to unit will result in the termination of fracture propagation.

Fundamentally, low Poisson's Ratio rocks with a high Young's Modulus support anisotropic horizontal stresses (i.e. lower magnitudes in the minimum horizontal stress direction and elevated magnitudes in the maximum horizontal stress direction), whereas rocks with a high Poisson's Ratio and low Young's Modulus are incapable of supporting those anisotropies and so tend towards more isotropic stresses (i.e. higher magnitudes in the minimum horizontal stress direction and lower magnitudes in the maximum horizontal stress direction) (Plumb et al., 2000). Grain-supported facies such as sandstones or carbonates typically exhibit anisotropic horizontal stresses; other facies such as mudstones and shale tend to approach isotropic stress conditions (Plumb et al., 2000; Zoback, 2007). Induced fractures can be naturally constrained using an understanding of mechanical stratigraphy.

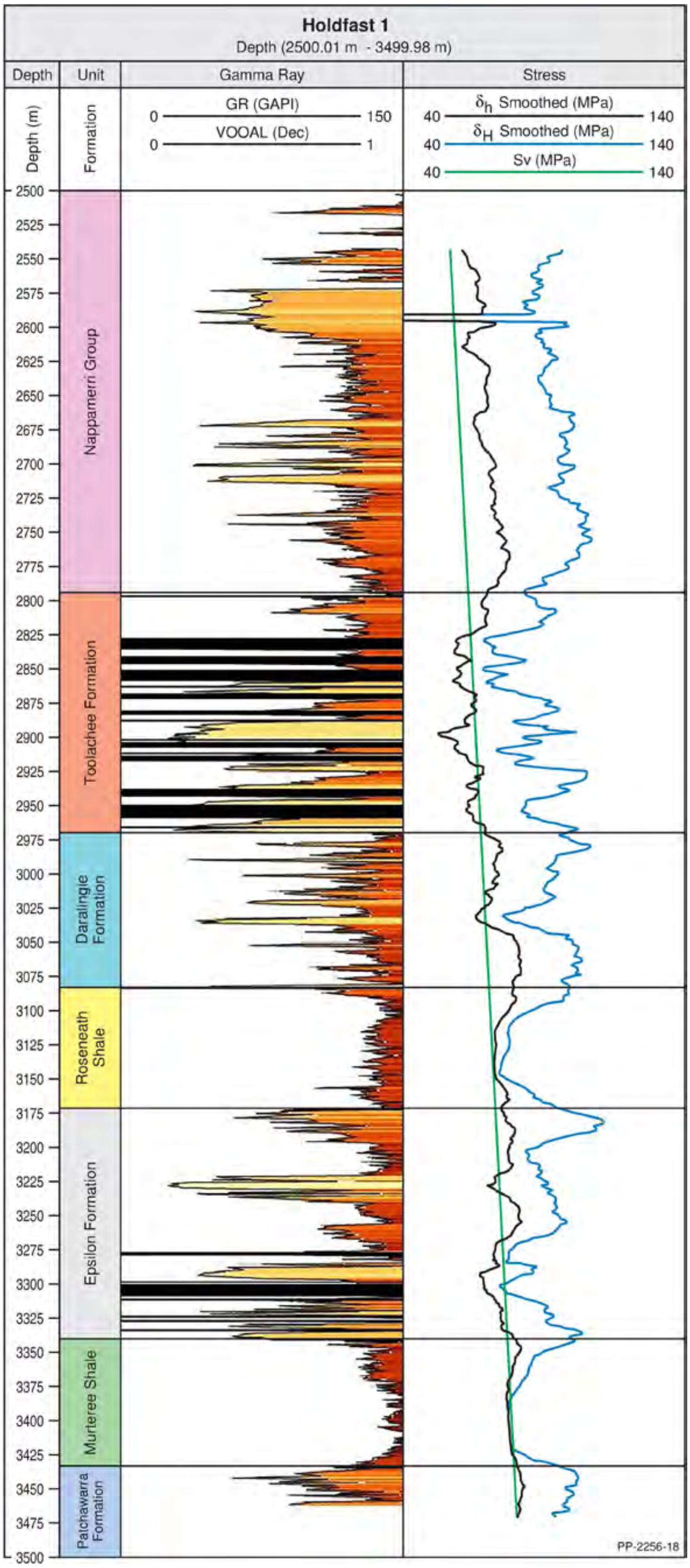

Figure 57 Stress components calculated from one dimensional mechanical earth model constructed for the Beach Energy shale gas exploration well Holdfast 1. Vertical stress is in green, minimum horizontal stress is in black, and maximum horizontal stress is in blue

Source: Modified from Beach Energy (2012); Rajabi et al. (2017b)
Element: GBA-COO-2-306

Significant variation of the stress regime with depth in the Cooper Basin is likely to act as an impediment to fracture propagation. Fracture growth in Permian strata is likely to be controlled by stress contrasts between mechanically distinct units. For example, Figure 57 shows a one-dimensional mechanical earth model from the Nappamerri Trough well Holdfast 1. The shale gas targets of the Murteree and Roseneath shales host near-isotropic, transitional stress regimes as a result of distinctly reduced horizontal stresses due to a high Poisson's ratio and low Young's modulus. Tiltmeter data from previous hydraulic stimulation programs performed by Beach Energy within the well Holdfast 1 demonstrate that induced fractures in these formations are most likely to have formed and propagated vertically (i.e. $\sigma_h<\sigma_V$) (Beach Energy, 2012). However, significant increases in horizontal stress magnitudes above and below the formations (due to the low Poisson's ratios and high Young's modulus of these sandstones and siltstones) mean that the shale units are bracketed by mechanical units that host reverse-faulting stress regimes, where horizontal fractures are preferred (i.e. $\sigma_h>\sigma_V$). Hence, any vertical fractures propagating within these formations are likely to be contained not only by the stress increase, but also the change in preferred fracture propagation direction (Anderson, 1951; Baumgärtner and Zoback, 1989; Hossain et al., 2000; Hubbert and Willis, 1957; Sibson, 1990; Zoback, 2007).

Highly variable stress magnitudes due to lithological changes imply significant mechanical contrasts between gas saturated Permian sediments and the overlying Triassic Nappamerri Group. The Nappamerri Group forms a natural barrier to induced fracture propagation between the target Permian intervals and the overlying Jurassic strata of the Eromanga Basin. Figure 57 illustrates that in Holdfast 1, horizontal stresses increase in magnitude by approximately 25% from (2825–2775 m depth), clearly changing from a strike-slip faulting stress regime in the late Permian Toolachee Formation to a reverse-faulting stress regime in the Triassic Nappamerri Group. Given these stress discrepancies, as well as the generally low permeability of the Nappamerri Group sediments, it is unlikely that induced fractures would propagate beyond the top of the Toolachee Formation nor transmit gas (Beach Energy, 2012).

Modelling undertaken by Iqbal et al. (2018) for the Roseneath and Murteree shales, as intersected in the Beach Energy wells Holdfast 1 and Encounter 1 in the Nappamerri Trough, suggests that within these formations there are significant variations in rock properties that may constitute intraformational fracture barriers. Taking into account calculated rock brittleness, thickness, σ_h magnitude, and breakdown pressure (the pressure required to break the rock), Iqbal et al. (2018) divided the studied formations into mechanical zones, which were then assessed as hosting properties that were favourable for fracturing, constituted a partially brittle layer, or could be considered as a fracture barrier. They conclude that the Roseneath Shale likely contains more intervals with favourable fracturing potential, and that fractures will likely propagate within this formation (as a result of being more brittle, hosting lower stress magnitudes, and requiring lower treating pressures). The Murteree Shale also contains numerous zones favourable to fracturing.

Iqbal et al. (2018) suggest that while their identified potential fracture barriers could be considered negative as they may result in unwanted reservoir compartmentalisation, they are a prime factor in vertical containment of fracture growth. Poor confinement of fracture growth has been demonstrated to have a negative impact on production, particularly where communication is established with a water-bearing interval (Fjar et al., 2008).

The influences of mechanical differences between lithologies is highlighted by the previously mentioned coals of the Tirrawarra-Gooranie oil and gas field (Figure 3) (Bowker et al., 2018; Cooke et al., 2006; Thiercelin and Plumb, 1994; Underwood et al., 2003). Coals tend to have very high Poisson's ratios and very low Young's moduli compared to coarse grained clastic rocks, (Levine, 1996) (Figure 56). Consequently, coal intervals are generally unable to support significant anisotropic horizontal stresses. This is observed in one-dimensional mechanical earth models from wells intersecting the deep Permian coals in the Tirrawarra-Gooranie field; while σ_h and σ_v magnitudes are essentially unchanged between the coals and the underlying sandstone horizons, there is a significant difference in the magnitude of σ_H within the two lithologies. Within the coals, horizontal stresses are nearly isotropic whereas in the sandstones a strong anisotropy is present, with an order of magnitude difference between the horizontal differential stress (that is, the difference between the two horizontal stresses) observed in each rock type (Bowker et al., 2018) (Figure 58). Interpreted stress regimes vary between normal and strike-slip faulting regimes, respectively, as a result of these stress contrasts. This has implications for fracture initiation, propagation, and containment during hydraulic stimulation, as significant stress variations are likely to exist between such mechanically different sediments (Bowker et al., 2018).

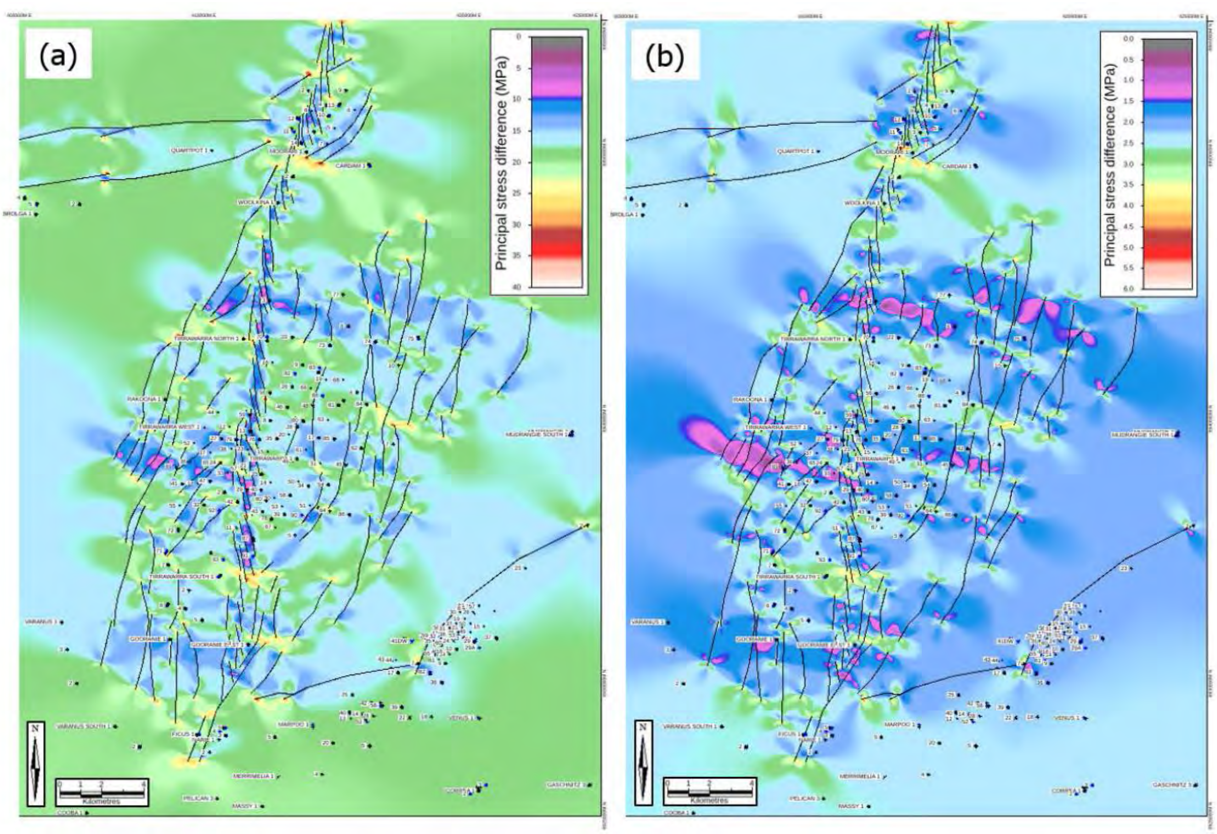

Figure 58 Modelled stress variations in the Tirrawarra-Gooranie oil and gas field, within: (a) sandstone, and; (b) coal intervals

Scale bars differ in range from 0-40 MPa in (a) and 0-6 MPa in (b). Black lines represent modelled faults and black circles represent petroleum wells. Black lines represent modelled faults and black circles represent petroleum wells.
Source: Bowker et al. (2018). This figure is covered by a Third Party Creative Commons Attribution licence
Element: GBA-COO-2-305

Numerical stress modelling within the coals demonstrates the importance of understanding even small perturbations of the stress field; while stress magnitude variations were observed to have little effect on hydraulic stimulations, areas modelled to have stress rotations of greater than approximately 4° from the mean σ_H orientation of approximately 105°N demonstrate significantly reduced productivity coupled with elevated bottom hole treating pressures. This is interpreted as due to increased tortuosity of the induced fractures (Bowker et al., 2018).

4.2.2 Overpressure

The term overpressure describes an in situ pore fluid pressure that exceeds the equivalent hydrostatic pressure value (Tingate et al., 2001). The pore pressure gradient is said to be normal if it approaches the hydrostatic gradient; hydrostatic pressure gradients range from 9.8 MPa km^{-1} (0.433 psi/ft) for fresh water to 11.3 MPa km^{-1} (0.5 psi/ft) for denser, completely salt saturated water.

Produced formation water from the Cooper Basin typically has salt concentrations of approximately 4000 mg/L, though concentrations as high as 15,000-20,000 mg/L have been reported (see hydrogeology appendix for further information (Evans et al., 2020)). Based on these salinity values, a reasonable estimate of hydrostatic pore pressure within the Cooper Basin is 9.8–10.1 MPa/km (0.433–0.446 psi/ft). In order to exceed this hydrostatic gradient, a mechanism other than the buoyancy force of a continuous column of static fluid is required (Osborne and Swarbrick, 1997). The most common mechanisms through which this is achieved are: a) disequilibrium compaction, b) generation of hydrocarbons, c) fluid expansion, and, d) tectonic loading (Bowers, 1995; Grauls and Baleix, 1994; Tingay et al., 2003; Tingay et al., 2007, 2009; Wangen, 2001).

Knowledge of overpressure and accurate pore pressure prediction is essential to petroleum exploration and production in order to ensure safe drilling, proper well design, and is an essential input for reservoir planning and reserve estimation (Tingate et al., 2001; Tingay et al., 2009). Overpressure can influence seal integrity, fracture reactivation, reservoir quality, and the effective magnitude of in situ stresses (van Ruth et al., 2004; Zoback, 2007).

A regional understanding of overpressures within the Cooper Basin has only recently been attempted (e.g. Gui et al., 2016; Kulikowski et al., 2016a), as previous studies focussed on pore pressure prediction and defining the mechanism of overpressure generation (Kulikowski et al., 2016a; Meixner et al., 2000; Reynolds et al., 2006; van Ruth and Hillis, 2000; van Ruth et al., 2003). Recent studies have characterised the fundamental distribution of overpressures within the South Australian Cooper Basin (e.g. Conlay, 2014; Gui et al., 2016; Kulikowski et al., 2016a; Department of State Development (SA), 2018).Overpressures are regularly reported within deeper sediments and pressure gradients of up to 18.3 MPa/km (0.809 psi/ft) have been recorded in the deeper sediments of the Nappamerri Trough (EIA, 2015; van Ruth and Hillis, 2000; van Ruth et al., 2003).

Kulikowski et al. (2016a) demonstrates that overpressures in the Cooper Basin are present along both structural lows and highs, with considerable overpressure in the Nappamerri Trough and within the Patchawarra Trough. Moderate overpressures are observed in the Tenappera Trough, primarily in the vicinity of large structures, and along the GMI Ridge where they are particularly prominent from the Gidgealpa and Merrimelia fields data (Figure 3) (Kulikowski et al., 2016a). The authors note that overpressures are first observed from approximately 2100 m depth, with significant overpressures from approximately 2400 m. Overpressures in the Patchawarra Trough and on the GMI Ridge are reported to begin deeper; significant overpressures in the Patchawarra

Trough are reported from approximately 2800–3000 m and slight overpressures are observed on the GMI Ridge from approximately 2650 m (Gui et al., 2016).

4.2.2.1 Basin-wide overpressure distribution

Overpressures in the Cooper Basin are generally accepted to be constrained to the sediments of the Gidgealpa Group, with the Toolachee Formation being the shallowest occurrence of significant overpressure (Gui et al., 2016; Kulikowski et al., 2016a; van Ruth and Hillis, 2000). However, shallower sediments within the Eromanga Basin are identified as hosting formation pressures in excess of hydrostatic (Figure 59), though these are usually lower in magnitude.

Kulikowski et al. (2016a) analysed a database of over 8,000 direct pressure measurements from the South Australian Cooper Basin, and clearly demonstrated areas of significant overpressure within the Gidgealpa Group. A majority of the sample points (50.4%) plot along a hydrostatic gradient for fluids of 0.95–1.025 g/cc, corresponding to approximately 9.7–10.1 MPa/km. Data points that plot on higher gradients than this are considered to be overpressured and comprise 35.3% of the total reported data points. Of these, almost half are considered to be highly overpressured and plot on gradients >11.5 MPa/km. The remaining 14.3% of data plots below the hydrostatic gradient and are considered to be underpressured. The authors infer that this is a result of pressure depletion from earlier and adjacent wells in laterally continuous reservoirs (Kulikowski et al., 2016a).

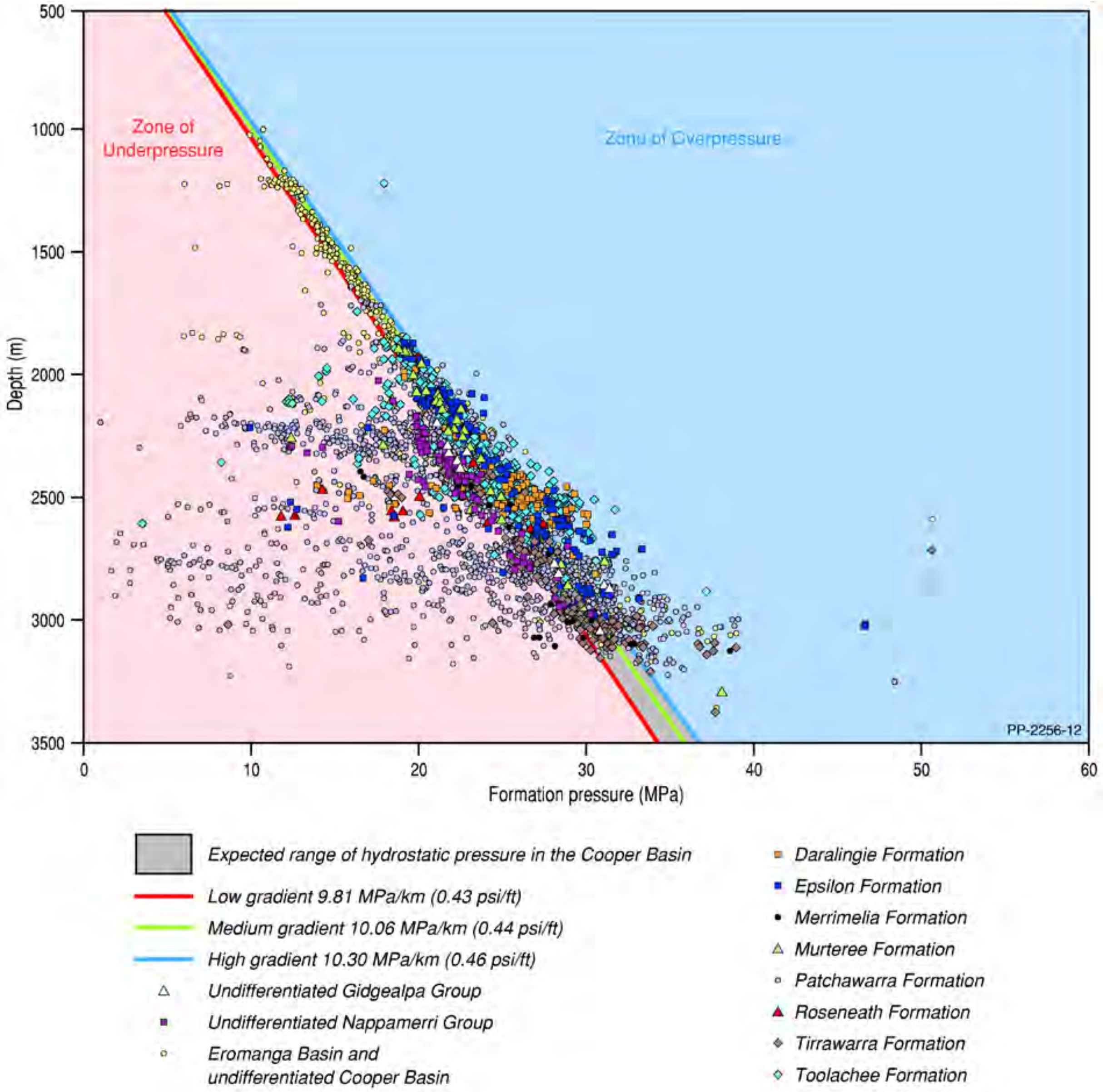

Figure 59 Measured formation pressures from the Cooper Basin in South Australia, by formation. Hydrostatic gradients at densities of 1.000 g/cc (green), 1.025 g/cc (purple), and 1.050 g/cc (blue) are displayed to highlight overpressures

Source: Kulikowski et al. (2016a)
Element: GBA-COO-2-187

Pressure gradient mapping for the REM section (Figure 60) was carried out using well testing and drill mud weight data from South Australia Geological Survey (SARIG) and Geoscience Australia databases (Hall et al., 2015). Table 61 lists the formation pressures of shale in the Nappamerri, Patchawarra and Tenappera troughs. The overpressured zones of the REM succession are mainly distributed in the deep trough areas, particularly in the Nappamerri Trough.

Table 61 Formation pressure (psi) statistics for the Murteree and Roseneath shales by region and their equivalents converted to MPa

Formation	Region	Pressure – Min (psi)	Pressure – Min (MPa)	Pressure – Max (psi)	Pressure – Max (MPa)	Pressure – Median (psi)	Pressure – Median (MPa)	Pressure – Ave (psi)	Pressure – Ave (MPa)
Murteree Shale	Cooper Basin	1482.91	10.22	8664.64	59.74	3704.65	25.54	3995.15	27.55
	Nappamerri Trough	3260.43	22.48	8664.64	59.74	5313.49	36.64	5532.49	38.15
	Patchawarra Trough	3153.26	21.74	5677.98	39.15	4096.5	28.25	4254.75	29.34
	Tenappera Trough	2512.13	17.32	3894.79	26.85	3161.21	21.80	3179.02	21.92
Roseneath Shale	Cooper Basin	1600.69	11.04	7915.12	54.57	3455.89	23.83	3820.49	26.34
	Nappamerri Trough	3149.11	21.71	7915.12	54.57	5052.59	34.84	5223.09	36.01
	Patchawarra Trough	3046.75	21.01	3836.33	26.45	3538.6	24.40	3534.59	24.37
	Tenappera Trough	2371.74	16.35	3625.14	25.00	2971.85	20.49	2989.6	20.61

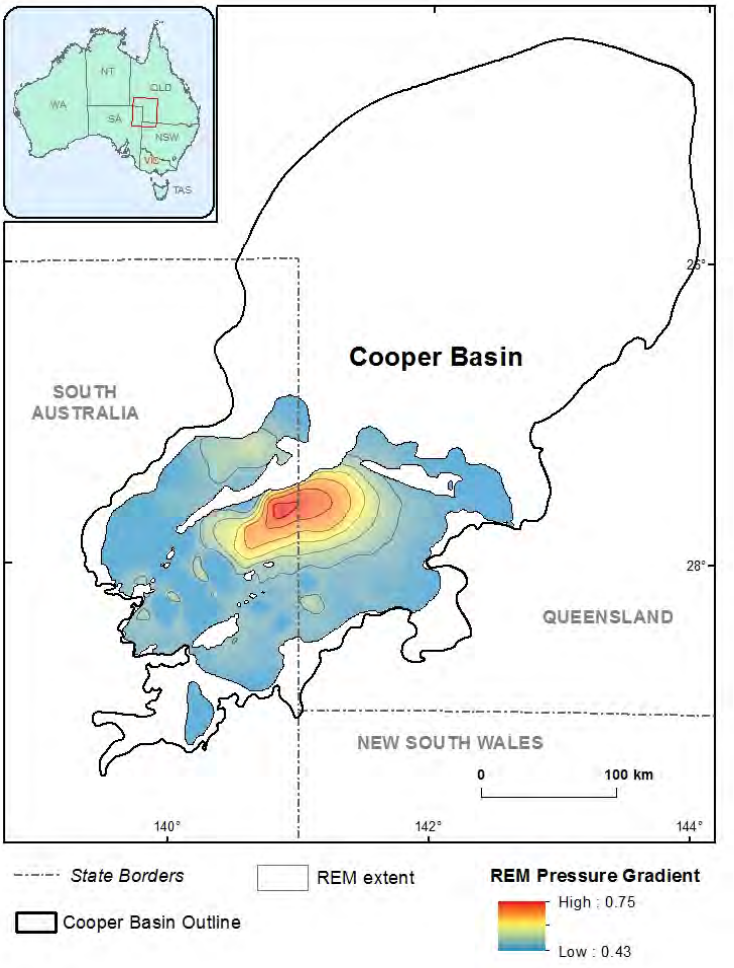

Figure 60 Pressure gradient (psi/ft) of Roseneath Shale, Epsilon Formation and Murteree Shale (REM) play in the Cooper Basin ranging from 0.432 psi/ft (9.8 KPa/km) to 0.75 Psi (17 KPa/km)

Element: GBA-COO-2-307

4.2.2.2 Overpressures in the Patchawarra Trough

Formation pressure in the Patchawarra Trough varies significantly, with minor overpressures of up to 10.4 MPa/km (0.46 psi/ft) observed in the Cretaceous lacustrine Murta Formation, as well as the Jurassic sands of the Birkhead Formation and Hutton Sandstone within the overlying Eromanga Basin (Figure 2). The Cooper Basin sediments host more notable overpressures, particularly within the Carboniferous to Permian units where formation pressures of up to 13.1 MPa/km (0.58 psi/ft) are observed (Figure 61).

Eromanga Basin overpressures are observed from approximately 1400 m depth, with slight overpressures in the Cooper Basin beginning at approximately 2500 m depth and significant overpressures from approximately 2800-3200 m depth (Figure 61). Gui et al. (2016) noted that in the Patchawarra Trough, the starting depth for overpressured Cooper Basin sediments relates to the top of the Toolachee Formation, regardless of well location, suggesting a formation rather than depth based control over overpressure.

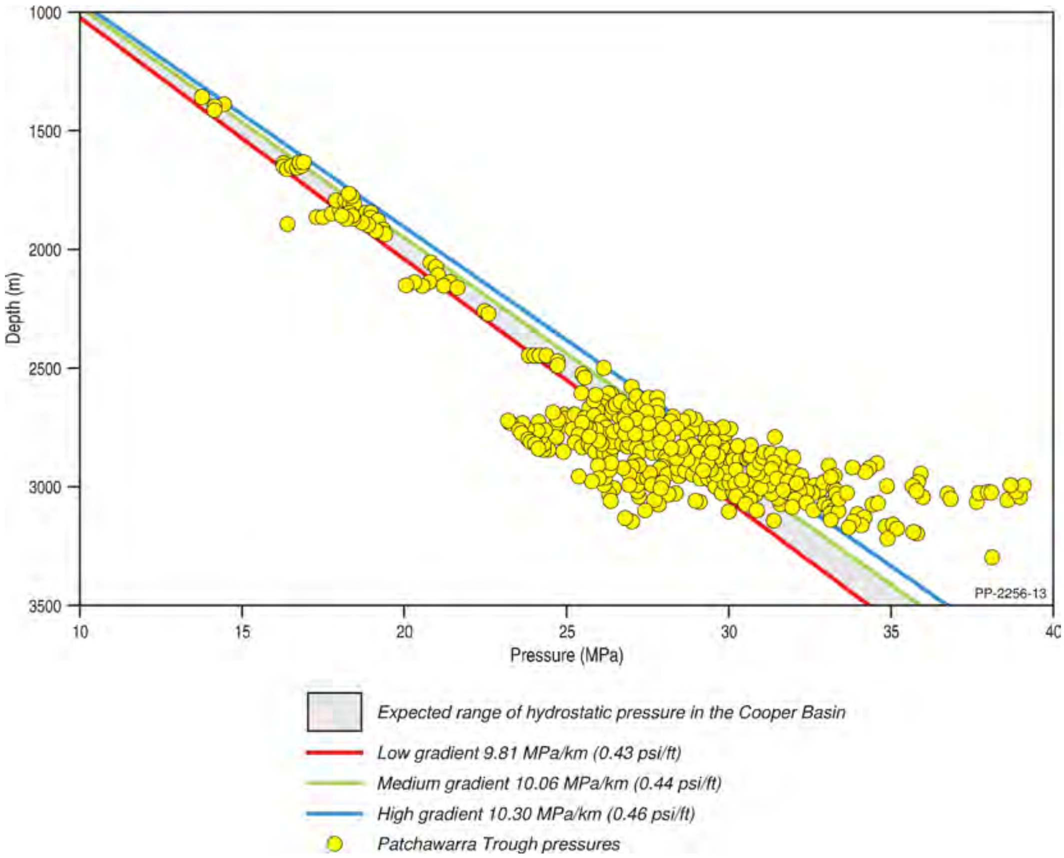

Figure 61 Measured formation pressures from the Patchawarra Trough in the Cooper Basin in South Australia. Hydrostatic gradients at densities of 1.000 g/cc (red), 1.025 g/cc (green) and 1.050 g/cc (purple) are displayed to highlight overpressures. Values of less than 8 MPa/km have been assumed to be either failed tests or due to pressure depletion and are excluded

Source: Kulikowski et al. (2016a)
Element: PP-2256-13

4.2.2.3 Overpressures in the Nappamerri Trough

Overpressures in the Nappamerri Trough can be identified from as shallow as approximately 1500 m depth within the overlying Eromanga Basin sediments, where formation pressures of up to 10.8 MPa/km (0.48 psi/ft) have been identified within sandstone intervals of the Early Cretaceous Murta Formation (Figure 62). Within the Cooper Basin proper, minor overpressures up to 10.7 MPa/km (0.47 psi/ft) can be observed from approximately 2150 to approximately 2350 m depth within the Toolachee, Daralingie, Epsilon, and Patchawarra formations. Significant overpressures are observed at depths greater than approximately 2350 m (Figure 62). In these deeper parts of the basin, formation pressure gradients as high as 15.4 MPa/km (0.68 psi/ft) are commonly observed within the Toolachee, Epsilon, and Patchawarra formations as well as the Tirrawarra Sandstone, and infrequently observed within the Daralingie Formation and the Roseneath and Murteree shales. Extreme overpressures of up to 18.0 MPa/km (0.79 psi/ft) are observed at depths greater than 3000 m (Figure 62).

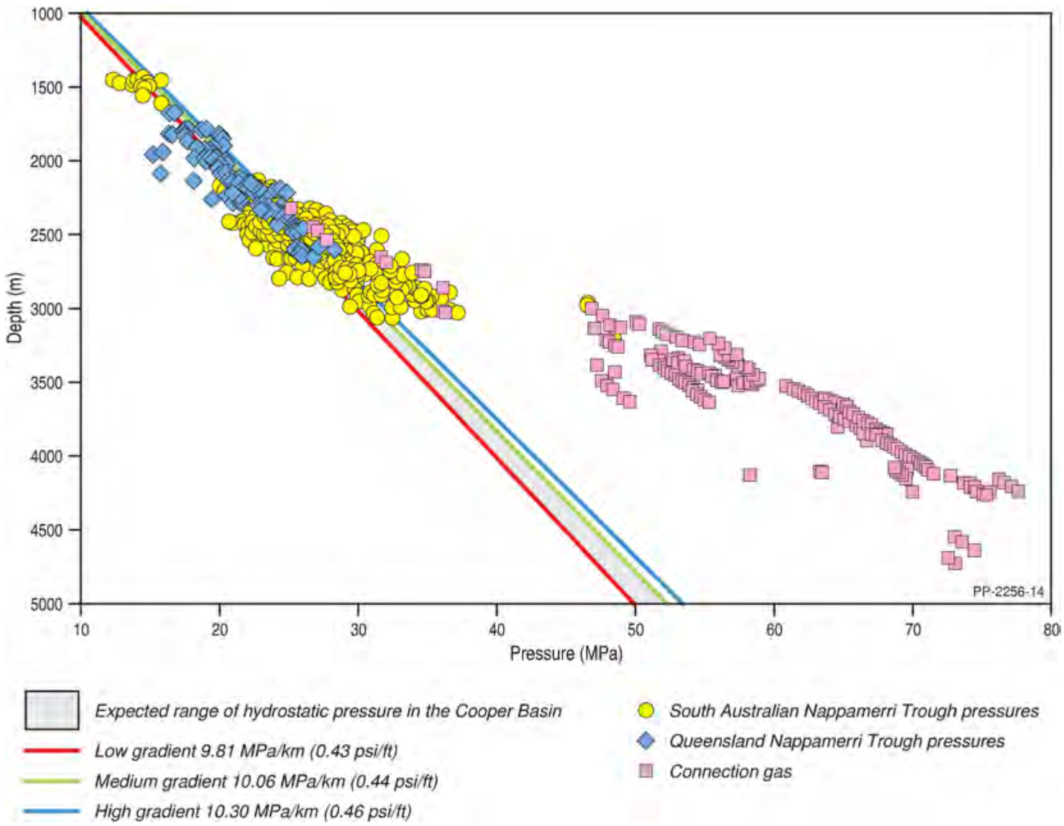

Figure 62 Measured formation pressures from the Nappamerri Trough in the Cooper Basin in South Australia.

This dataset includes the QLD and SA Nappamerri Trough Drill Stem test (DST) results, as well as connection gas pressures of several deeper Nappamerri Trough wells (Bulyeroo 1, Burley 1, Burley 2, Kirby 3, Habanero 1, Habanero 2, Habenero 3, Encounter 1, Jolokia 1, and Savina 1). Hydrostatic gradients at densities of 1.000 g/cc (red), 1.025 g/cc (green) and 1.050 g/cc (purple) are displayed to highlight overpressures. Values of less than 8 MPa/km have been assumed to be either failed tests or due to pressure depletion and are excluded
Source: Kulikowski et al. (2016a)
Element: PP-2256-14

4.2.2.4 Overpressures in the Gidgealpa, Merrimelia, Innamincka, Warra and Packsaddle ridges

Slight overpressures are observed within overlying Eromanga Basin sediments from approximately 1400 m depth, with pressures only marginally exceeding hydrostatic (Figure 63). Slight overpressure occurs in the Cooper Basin succession from approximately 1900 m depth, with significant overpressures observed from approximately 2100 m depth (Figure 63). Formation pressure gradients up to 11.4 MPa/km are observed in the Callamurra Member, Toolachee Formation, Patchawarra Formation, Tirrawarra Sandstone and Merrimelia Formation.

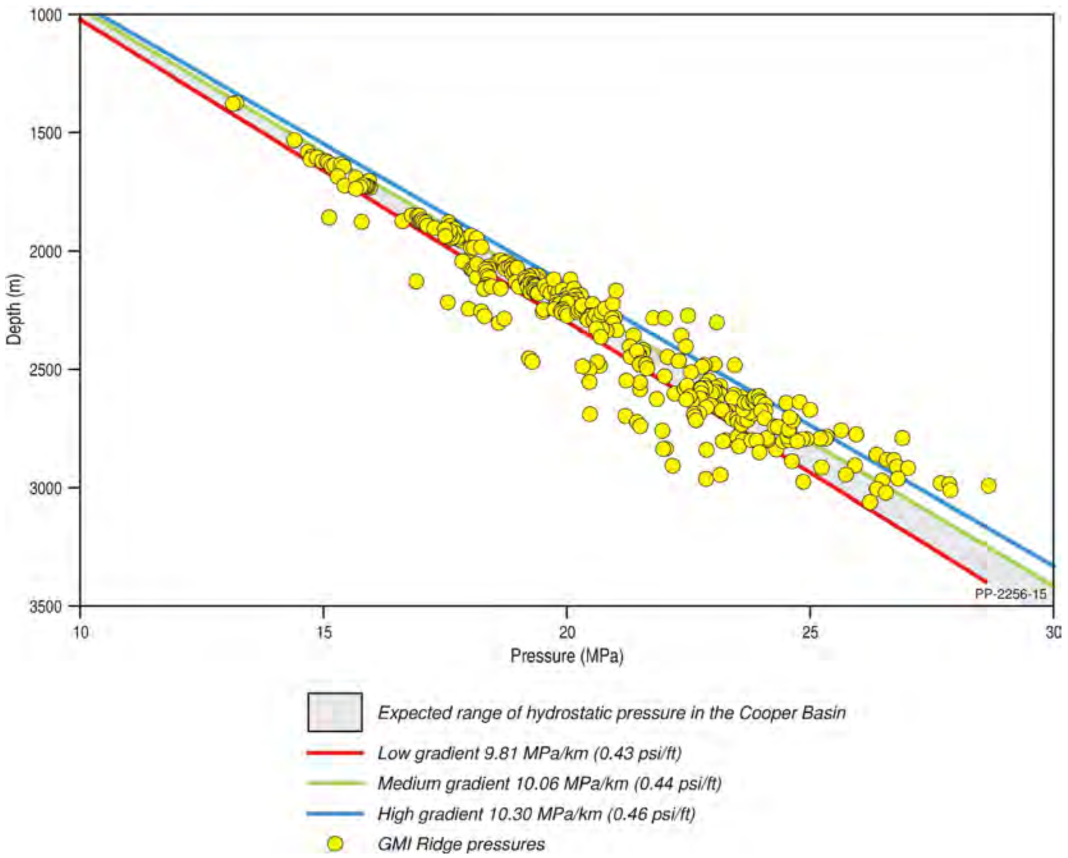

Figure 63 Measured formation pressures from the GMI Ridge in the Cooper Basin in South Australia.

Hydrostatic gradients at densities of 1.000 g/cc (red), 1.025 g/cc (green) and 1.050 g/cc (purple) are displayed to highlight overpressures. Values of less than 8 MPa/km have been assumed to be either failed tests or due to pressure depletion and are excluded
Source: Kulikowski et al. (2016a)
Element: PP-2256-15

4.2.2.5 Overpressures in the Tenappera Trough

The pressure data in the Tenappera Trough implies the presence of overpressured intervals, though the magnitude of that overpressure is not as significant as is observed within the Nappamerri and Patchawarra troughs (Figure 64). The shallowest occurrence of overpressure is observed at approximately 1900 m depth within the Epsilon Formation, at only slightly above hydrostatic pressure at 10.5 MPa/km. Overpressure is observed both higher and lower in the stratigraphy, in the Toolachee, Roseneath, Murteree and Patchawarra formations, however, more significant overpressures are primarily observed within the Epsilon and Patchawarra formations at depths greater than approximately 2100 m (Figure 64). These pressures vary in magnitude from 10.1–11.1 MPa/km.

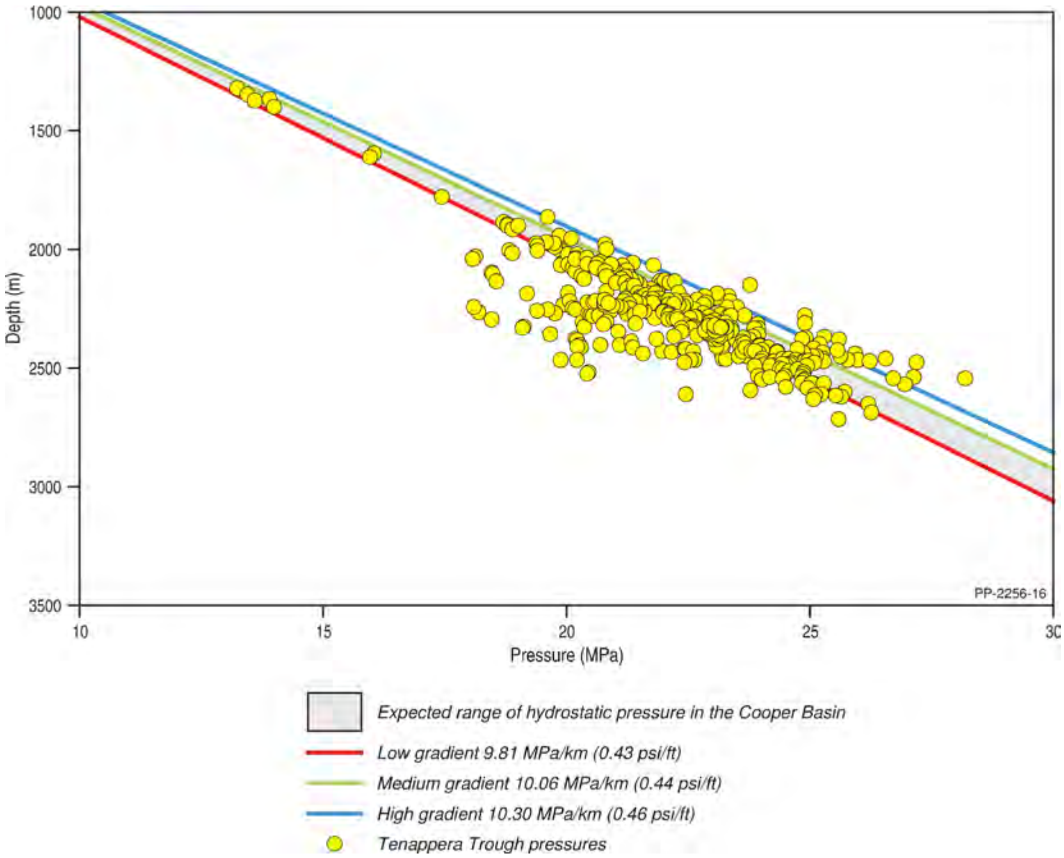

Figure 64 Measured formation pressures from the Tenappera Trough in the Cooper Basin in South Australia.

Hydrostatic gradients at densities of 1.000 g/cc (red), 1.025 g/cc (green) and 1.050 g/cc (purple) are displayed to highlight overpressures. Values of less than 8 MPa/km have been assumed to be either failed tests or due to pressure depletion and are excluded

Source: Kulikowski et al. (2016a)

Element: PP-2256-16

4.2.2.6 Overpressures in the Windorah Trough

Data availability in the Windorah Trough is limited relative to data in the Nappamerri and Patchawarra troughs, with only approximately 20 wells drilled to date. Of these, many lack measurements of formation pressure. Nevertheless, available data does suggest that the deeper sediments of the Windorah Trough are likely to host overpressured zones in a manner similar to the rest of the Cooper Basin (Figure 65). Overpressures observed within the overlying Adori and Namur sandstones and Poolowanna Formation of the Eromanga Basin, from approximately 1850 m depth, are predominantly minor (~10.5-11.5 MPa/km), with one point from a DST within the Adori Sandstone provides a formation pressure of 14.3 MPa/km (Delhi Australian Petroleum Limited et al., 1987).

There is an observed increase in pore pressures at greater than approximately 2500 m depth in the Cooper Basin, though recorded formation pressures suggest modest increases above hydrostatic pressure (Figure 65). Pressures ranging from 10.2–11.7 MPa/km are reported within the Tinchoo, Arrabury, Toolachee and Patchawarra formations. Analysis of drilling mudweight data from three wells (Queenscliff 1, Ramses 2, and Tamarama 1) demonstrate significantly increased mud weights from approximately 2500 m depth. The well Ramses 2 demonstrates increased mud pressures throughout much of the Eromanga Basin sediments, likely to balance the previously mentioned overpressures (Figure 65).

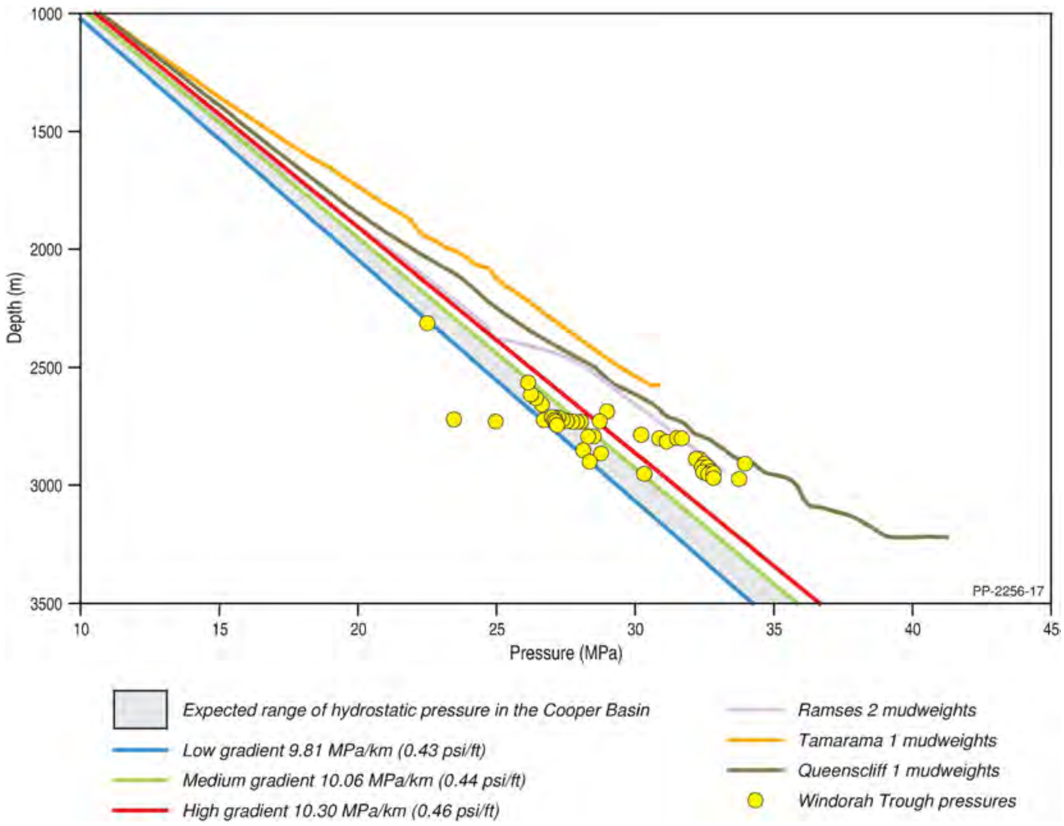

Figure 65 Measured formation pressures from the Windorah Trough of the Cooper Basin in Queensland.

Hydrostatic gradients at densities of 1.000 g/cc (red), 1.025 g/cc (green) and 1.050 g/cc (purple) are displayed to highlight overpressures. Values of less than 8 MPa/km have been assumed to be either failed tests or due to pressure depletion and are excluded. Due to low data availability, drilling mudweights from three wells are included as proxies for formation pressure (dotted lines).
Source: Kulikowski et al. (2016a)
Element: PP-2256-17

4.3 Prospectivity confidence mapping

Prospectivity mapping, sometimes referred to as ‘chance of success’, ‘play fairway’ or ‘common risk segment’ mapping (Royal Dutch Shell, 2017; Salter et al., 2014), was used to determine the likely prospective area of the Cooper Basin shale gas, tight gas and deep coal gas plays. Results inform where plays are most likely to be located with respect to overlying assets.

The plays types and formation assessed are listed below and are shown on Figure 66:

- Shale gas plays: Patchawarra Formation, Murteree and Roseneath shales
- Deep coal gas plays (wet and dry): Patchawarra, Epsilon and Toolachee formations
- Tight gas plays: combined Gidgealpa Group basin-centred gas play including the Toolachee, Daralingie, Epsilon and Patchawarra formations and the Tirrawarra Sandstone.

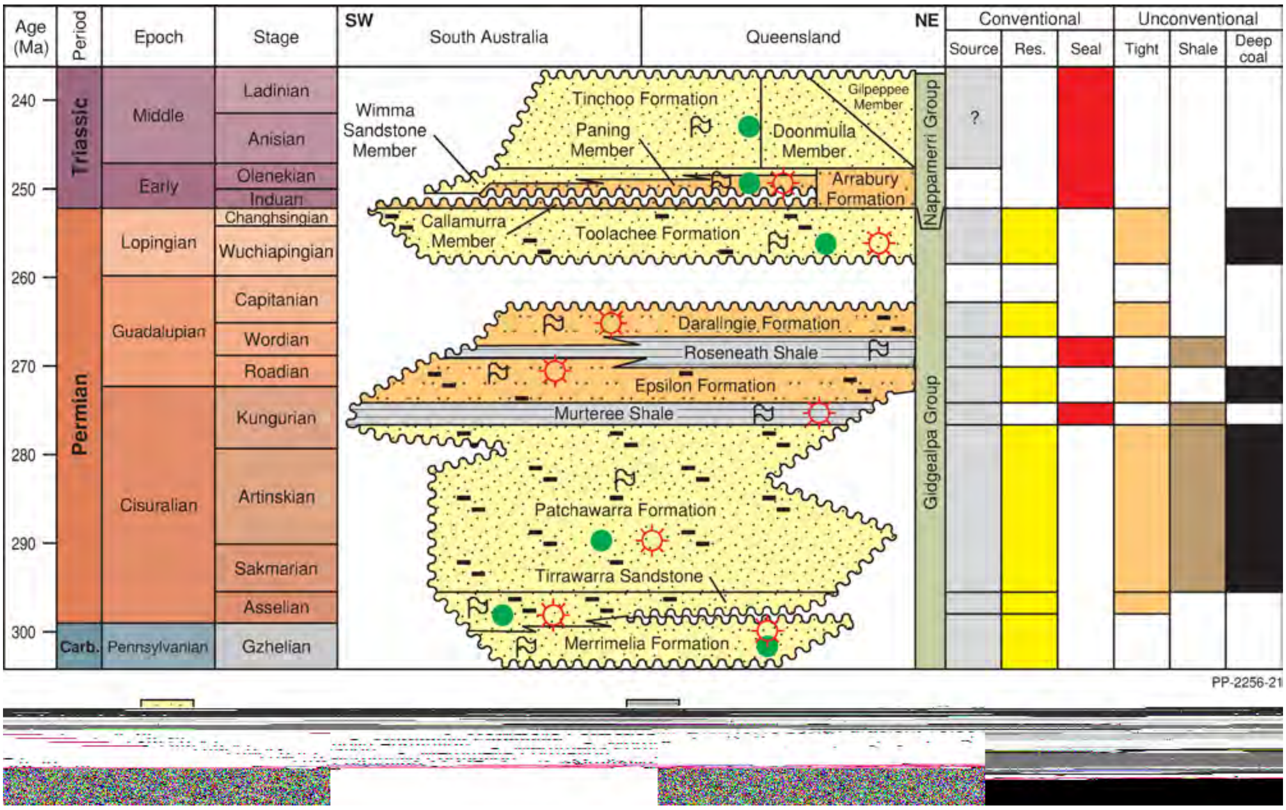

Figure 66 Schematic diagram showing unconventional petroleum systems elements in the Cooper Basin assessed in this report

Source: Stratigraphy after Hall et al. (2015a); hydrocarbon plays after Hall et al. (2015b)
Element: PP-2256-21

4.3.1 Workflow

Criteria to assess the relative prospectivity for shale, deep coal and tight gas plays were selected from the geological properties evaluated in Sections 4.1 and 4.2, such as formation thicknesses and extents, source rock properties, reservoir characteristics and pressure regimes. Separate criteria were developed for the different play types.

Published literature, where available, guided criteria selection. The shale gas play criteria were readily available and based primarily on previous work undertaken by US federal agencies e.g. EIA (2013); and Charpentier and Cook (2011). Criteria for other play types were developed in consultation with State government agencies, universities and industry, using also the published literature referenced in the criteria tables (Table 62, Table 65 and Table 68).

Input maps were based on classified parameters that represented the criteria. Each input parameter was assigned a ranking between zero and one (Zero 0, Low 0.25, Med 0.5, High 1). If a critical parameter was absent at a particular location, this would results in a zero relative prospectivity for that play at that location. No weightings were applied.

Non-mappable criteria were not integrated into the prospectivity mapping but were used to better understand the geological characteristics of the formations (Table 63, Table 64, Table 66, and Table 67).

The classified input parameter maps were multiplied together to create a map highlighting the relative prospectivity for each play type by formation across the basin.

In addition, a combined relative prospectivity maps for each play type was created by taking the maximum prospectivity value of the formation-specific maps for that play type.

The workflow was set up as a batch task file using Petrosys software (Petrosys Pty Ltd, Version 17.7sp6). A workflow was developed for each play type using the equation below to develop the final relative prospectivity confidence maps that are displayed in the results sections for each play type.

$$Prospectivity\ (C) = c_1 \times c_2 \times c_3 \times \ldots \times c_n$$

This workflow is also illustrated in Figure 67.

As the tight gas of the Gidgealpa Group was assessed as one play, the workflow differed slightly to that of shale and deep coal gas. This is discussed further in Section 4.3.4–Tight gas plays.

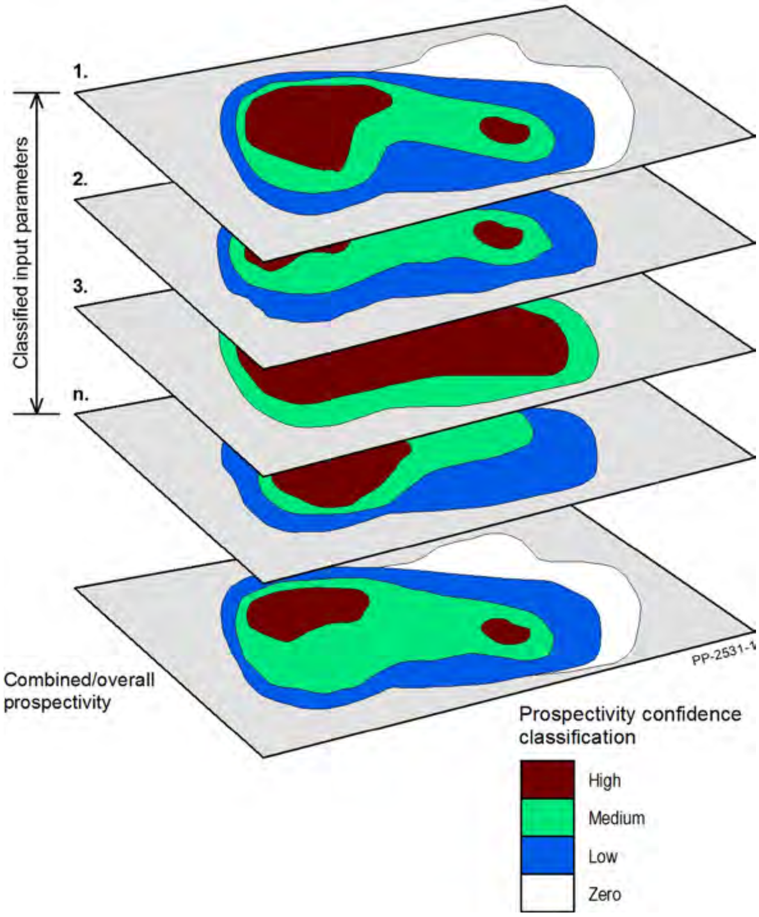

Figure 67 Schematic workflow for combining classified input parameter maps to obtain the relative prospectivity of a formation or play

Element: GBA-COO-2-176

4.3.2 Shale gas plays

The Murteree and Roseneath shales and the Patchawarra Formation were chosen for assessment of shale gas prospectivity. The geological properties used to map shale gas prospeectivity were:

- the net source thickness, represented by the cumulative thickness of organically rich shale with a TOC > 2 wt%;
- source rock quality, represented by Hydrogen Index;
- source rock maturity, and;
- pressure gradient.

The criteria associated with these properties are described in Table 62. The areas of highest relative prospectivity for shale gas are defined where the net source rock thickness exceeds 30 m thickness, TOC is greater than 2% and the formation is overpressured.

4.3.2.1 Shale gas mappable criteria

Table 62 Summary of shale gas play specific input parameters and classifying criteria used to develop combined relative prospectivity confidence maps. Associated data sources, assumptions, limitations and references are also provided

Parameter (P)	Classified input parameter thresholds				Comments	Data source	Description/Assumptions	Limitations	Reference for threshold criteria
	Zero (0)	Low (0.25)	Medium (0.5)	High (1)					
Net thickness of organically rich shale (TOC > 2 wt%)	<15 m	na	≥15–<30 m	≥30 m	Minimum requirement by Charpentier and Cook (2011)	Shale thickness from Hall et al. (2015a)	Used 3D model from Hall et al. (2015a). Derived from gross shale thickness multiplied by net organic rich ratio. True vertical thickness used	Variable density and irregular distribution of well tops and velocity data may affect the quality of structural modelling results	Charpentier and Cook (2011); Boyer (2018)
Pressure regime (Roseneath and Murteree shales)		<0.433 psi/ft (<9.79 MPa/km)	≥0.433–<0.55 psi/ft (≥9.79–<12.44 MPa/km)	≥0.55 psi/ft (≥12.44 MPa/km)	Desirable requirement by Charpentier and Cook (2011)	Pressures in well completion reports	Pressure-depth thresholds used to identify top of overpressured zone basin-wide. See Section 4.2.2 on overpressure for further information	Pressure map for REM[ii] available only. Well coverage is concentrated in producing fields; all formations are not sampled equally or consistently	EIA (2013); Hall et al. (2015b); Boyer (2018)
Pressure regime (Patchawarra Formation)		na	<2800 m	≥2800 m	Single threshold used to estimate pressure regime therefore less confidence than Roseneath and Murteree shales. Desirable requirement by Charpentier and Cook (2011)	Depth surface maps from Hall et al. (2015a); Measured formation pressures in well completion reports from Kulikowski et al. (2016a)	Basin specific pressure-depth thresholds for middle of formations determined from data. See Section 4.2.2 on overpressure for further information	Gridded pressure maps not available. Non-REM formations use a depth-based proxy for likelihood of overpressure occurring. Dataset highlights pressure depletion and poorly reported tests. After Kulikowski et al. (2016a)	Defined by Geoscience Australia analyst based on well data from Kulikowski et al. (2016a)
Total organic carbon (TOC)	<1 wt%	na	≥1–<2 wt%	≥2 wt%	Minimum requirement by Charpentier and Cook (2011)	Hall et al. (2019)	Present day average TOC	Errors of up to 10% can occur between 'LECO' and 'Rock-Eval' methods (coals are the most difficult to measure accurately using the Rock-Eval method) (Hall et al., 2015a)	Hall et al. (2015b)
Thermal maturity	<0.75%Ro (oil) or >3.5%Ro (gas)	na	≥0.75–<1.2%Ro (oil)	≥1.2–≤3.5%Ro (wet/dry gas)	Modified from minimum requirement by Charpentier and Cook (2011)	Hall et al. (2019)	Vitrinite reflectance map for middle of formation	Variation of maturity throughout formation thickness not considered. Additional variability present in kinetic parameters and uncertainties in temperature history, palaeo-temperature data etc. See Hall et al. (2016b)	Hall et al. (2015b); Hall et al. (2019)
HI_o (original Hydrogen Index)	<50 mg HC/g TOC	≥50–<150 mg HC/g TOC	≥150 –<250 mg HC/g TOC	≥250 mg HC/g TOC	Minimum requirement by Charpentier and Cook (2011)	Hall et al. (2016b)	Derived from present day HI. For rocks with TOC <3 wt% the HI can be suppressed, resulting in underestimation of true hydrocarbon potential. HI_o also represents kerogen type	Data density varies depending on formation and location in the basin. Therefore, the maps may not be representative of the entire basin. HI_o is a highly variable parameter, and as it is derived from HI, confidence in these maps is reduced	Modified from Charpentier and Cook (2011); Hill (2019)

HIo = original hydrogen index; MPa/km = Megapascals per kilometre; na = not applicable; Roseneath Shale, Epsilon Formation and Murteree Shale; %Ro = thermal maturity; psi/ft = pounds per square inch per foot; TOC = total oraganic carbon; wt% = weight (as a percentage)

This table has been optimised for printing on A3 paper (297 mm x 420 mm).

4.3.2.2 Shale gas mapping results by formation

Classified individual parameter maps for each formation (Patchawarra Formation, Murteree Shale, Roseneath Shale) are shown in Figure 68, Figure 70, and Figure 72. Formation specific relative prospectivity confidence maps are displayed in Figure 69, Figure 71 and Figure 73.

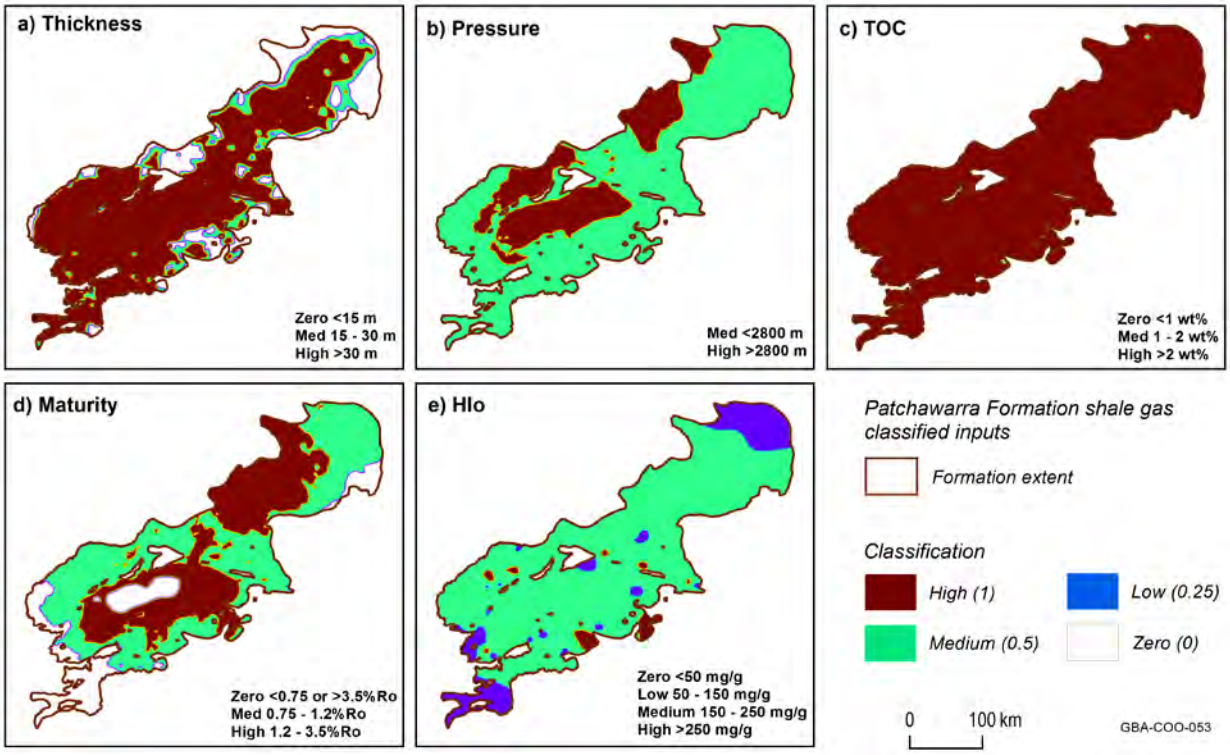

Figure 68 Classified mappable prospectivity confidence input parameters for the Patchawarra Formation shale gas play

Data: Geological and Bioregional Assessment Program (2019b); Cooper Basin outline from Raymond et al. (2018)
Element: GBA-COO-053

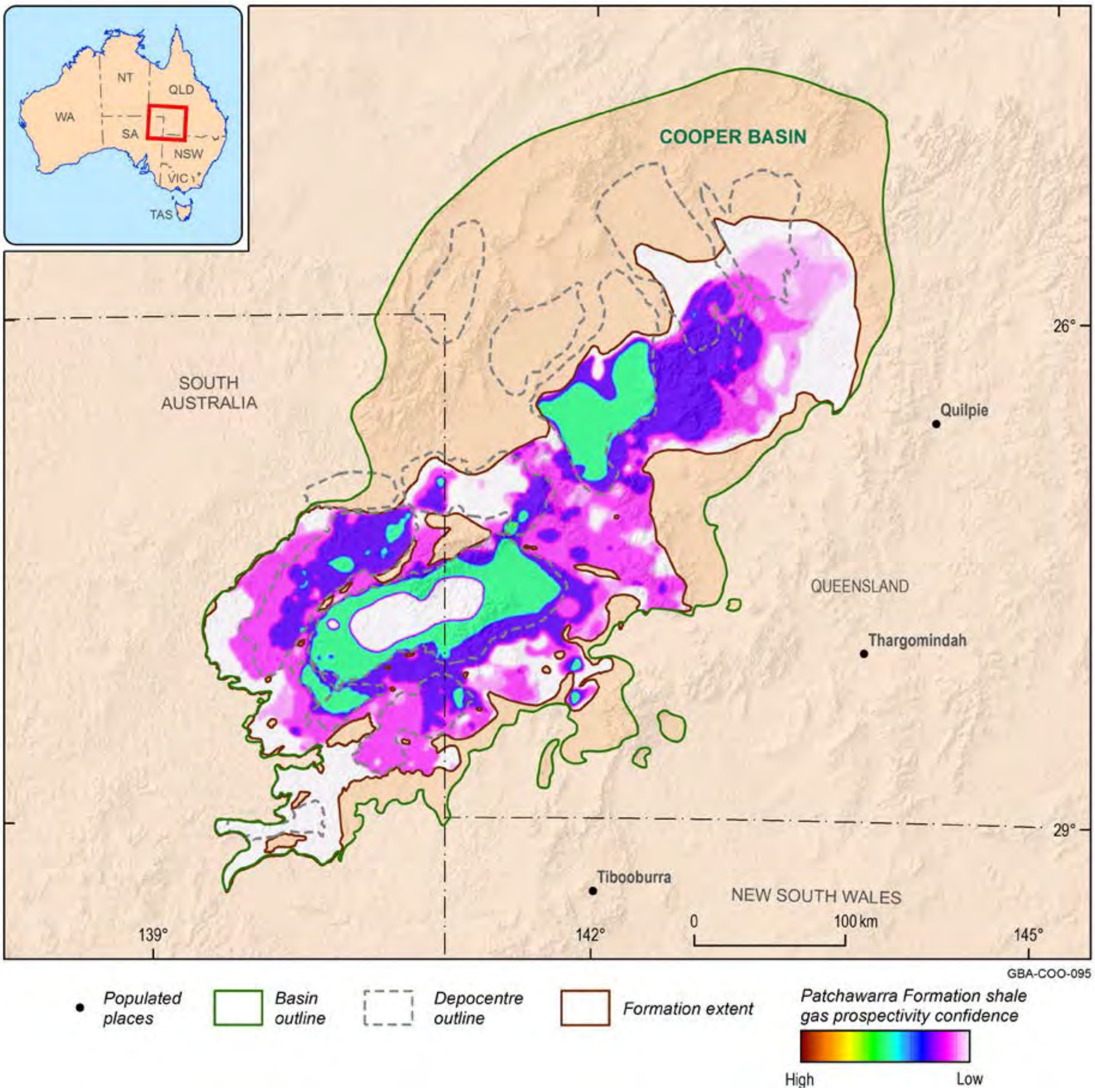

Figure 69 Formation specific relative prospectivity confidence map for the Patchawarra Formation shale gas play. The distribution of available data used for generating the maps is shown in Figure 93 and Figure 94

Data: Geological and Bioregional Assessment Program (2019b); Cooper Basin outline from Raymond et al. (2018)
Element: GBA-COO-095

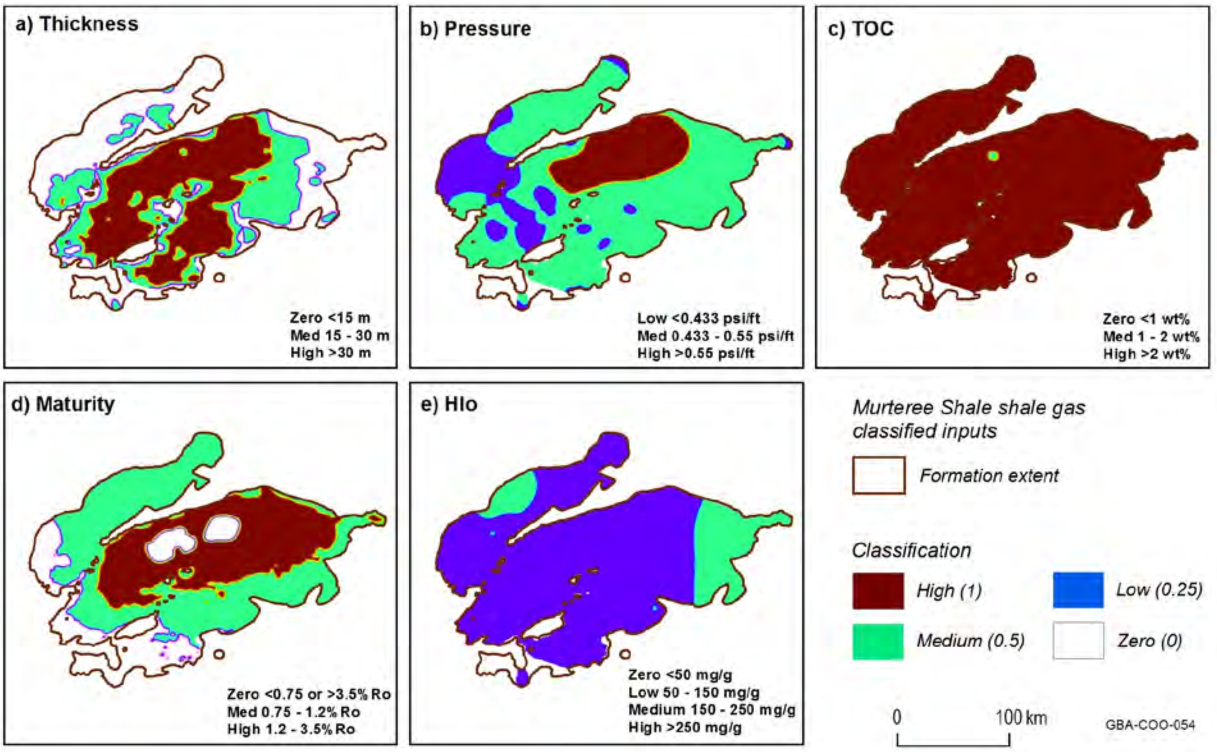

Figure 70 Classified mappable prospectivity confidence input parameters for the Murteree Shale shale gas play

Data: Geological and Bioregional Assessment Program (2019b); Cooper Basin outline from Raymond et al. (2018)
Element: GBA-COO-054

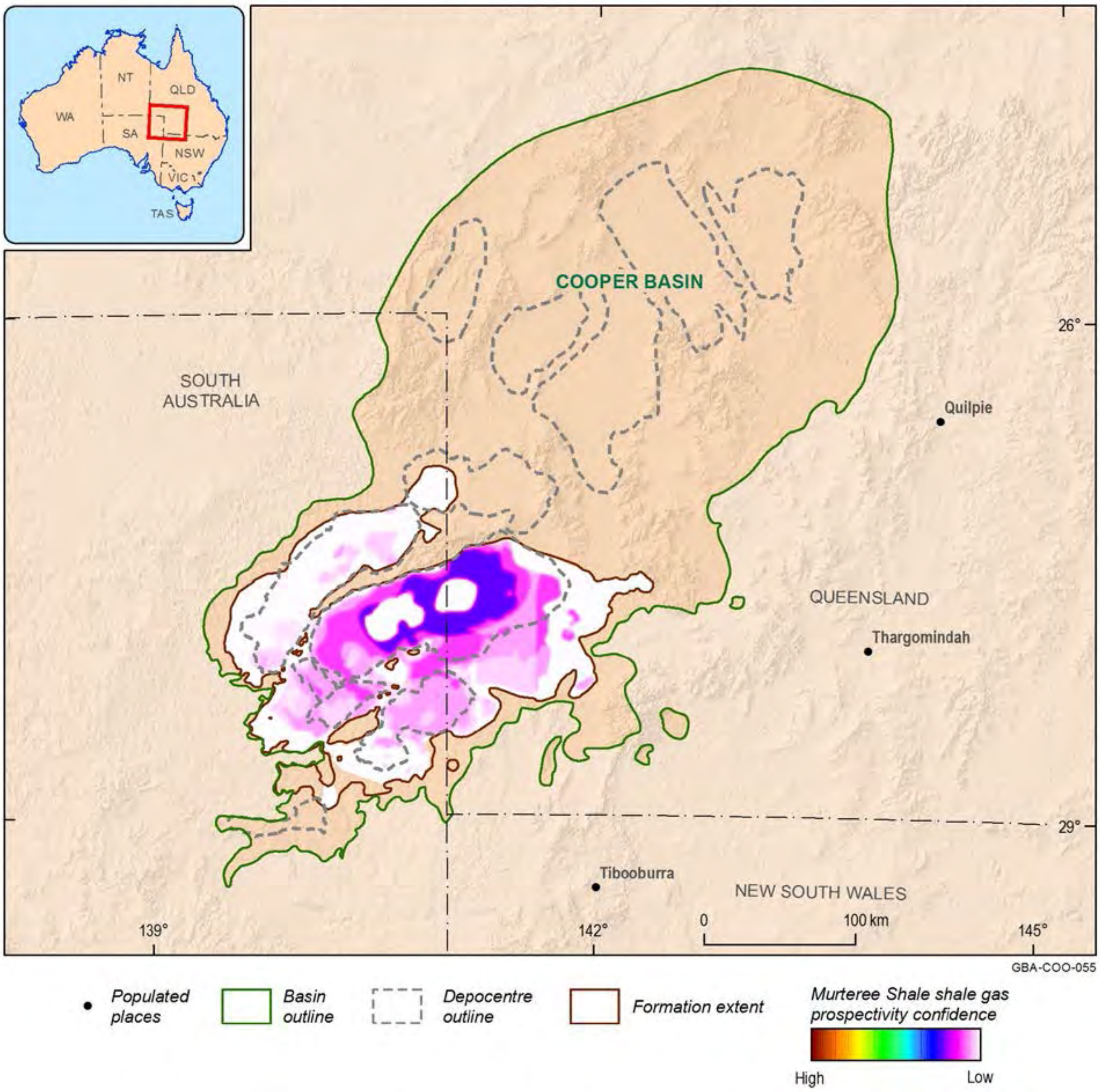

Figure 71 Formation specific relative prospectivity confidence map for the Murteree Shale shale gas play. The distribution of available data used for generating the maps is shown in Figure 93 and Figure 94

Data: Geological and Bioregional Assessment Program (2019b); Cooper Basin outline from Raymond et al. (2018)
Element: GBA-COO-055

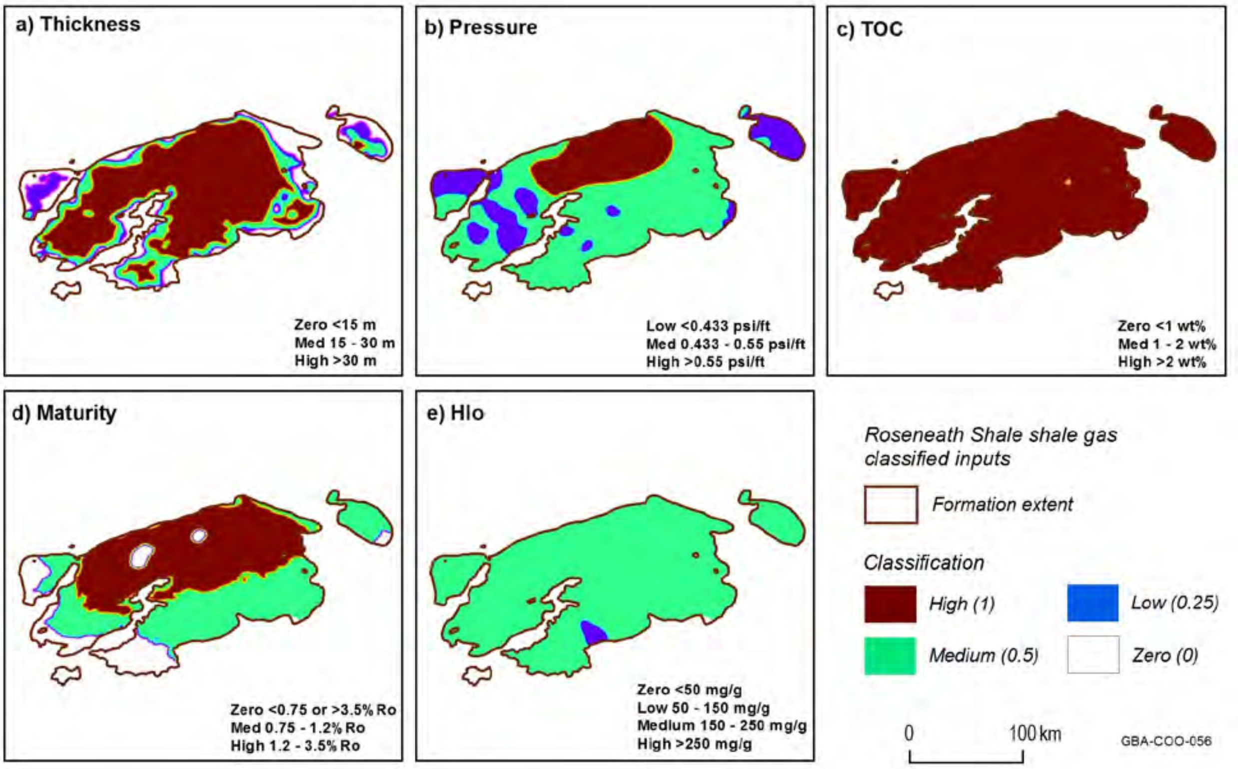

Figure 72 Classified mappable prospectivity confidence input parameters for the Roseneath Shale shale gas play

Data: Geological and Bioregional Assessment Program (2019b); Cooper Basin outline from Raymond et al. (2018)
Element: GBA-COO-056

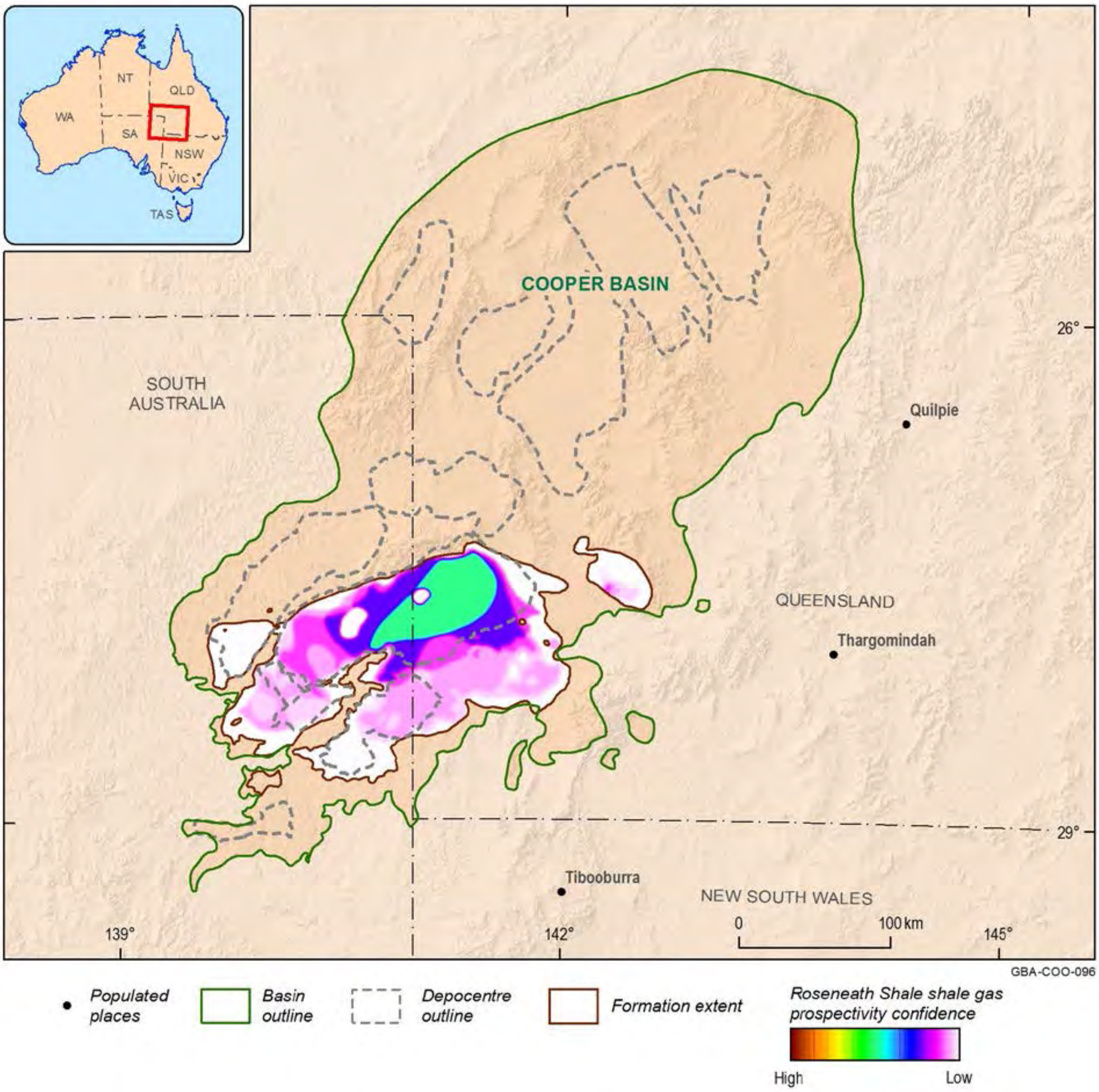

Figure 73 Formation specific relative prospectivity confidence map for the Roseneath Shale shale gas play. The distribution of available data used for generating the maps is shown in Figure 93 and Figure 94

Data: Geological and Bioregional Assessment Program (2019b); Cooper Basin outline from Raymond et al. (2018)
Element: GBA-COO-096

4.3.2.3 Overall shale gas prospectivity confidence results

Formation specific relative prospectivity confidence results were combined to develop play-based relative prospectivity confidence map to better understand each play type (Figure 74).

Results show no areas of high relative prospectivity were identified for the shale gas plays. The Nappamerri, southern Windorah, Wooloo and Allunga troughs were identified as medium relative prospectivity for shale gas.

Overpressure, thermal maturity, reservoir thickness and source rock quality (hydrogen index) are the primary influencing input parameters to the shale gas prospectivity (Figure 68, Figure 70, and Figure 75).

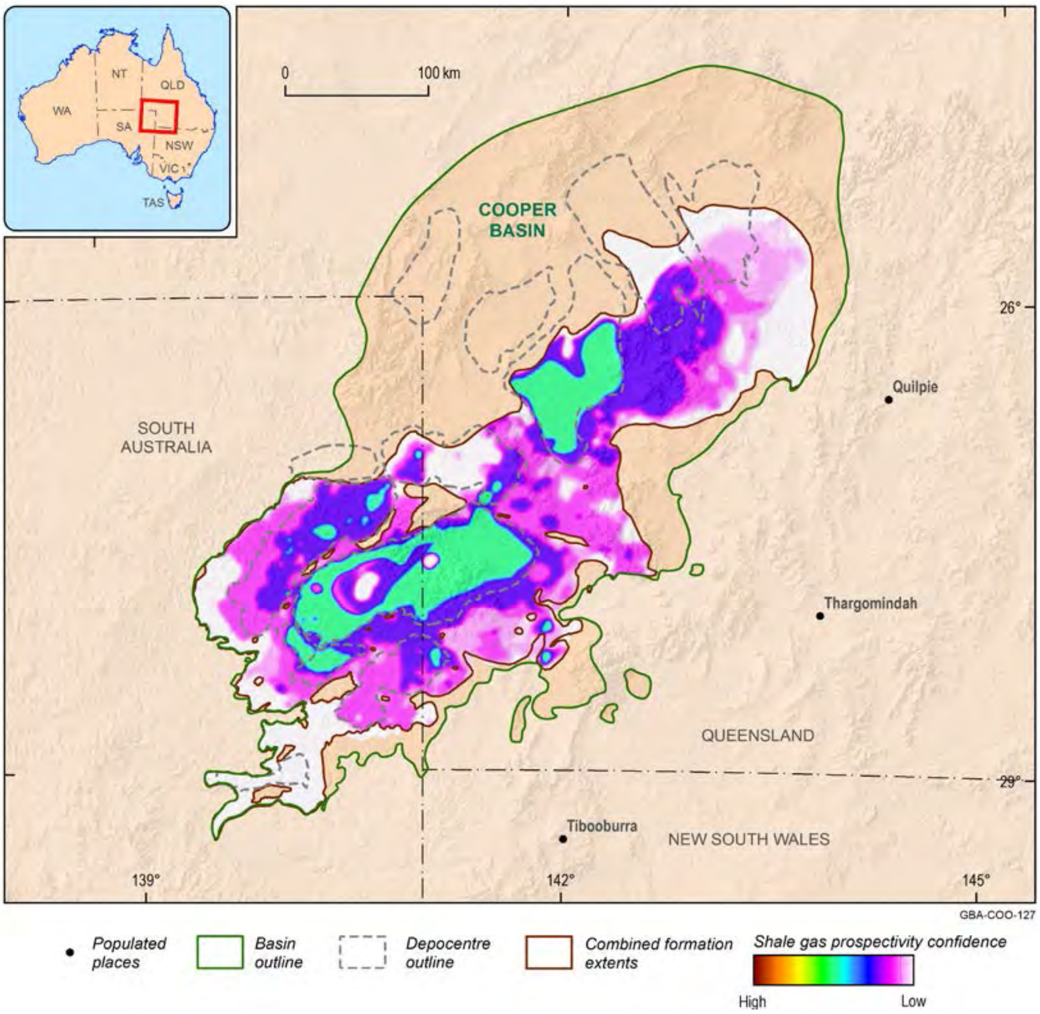

Figure 74 Relative prospectivity confidence map for combined shale gas plays. The distribution of available data used for generating the maps is shown in Figure 93 and Figure 94

Data: Geological and Bioregional Assessment Program (2019b); Cooper Basin outline from Raymond et al. (2018)
Element: GBA-COO-127

4.3.2.4 Other characteristics to consider when assessing shale gas plays

Non-mappable criteria used to characterise the prospectivity of the reservoir are displayed in Table 63 and Table 64. Based on available data, the brittleness, permeability and total gas content of the shale gas plays were moderately favourable to highly favourable.

Table 63 Summary of non-mappable shale gas play specific parameters that should be considered when assessing this play type (not included in map results). Assumptions, limitations and references are listed

Non-mappable play characteristics	Desirable characteristics	Description/Assumptions	Limitations	Reference for threshold criteria
Brittleness (brittleness index)	≥0.48 (brittle)	Averaged shale rock brittleness calculated based on XRD test results	The wells are located in the Nappamerri, Tenappera and Allunga troughs in South Australia. These may not be representative of the entire basin due to lateral variations in lithofacies. Data available varies between formations	Ariketi et al. (2017); Perez Altamar and Marfurt (2014); Wang and Gale (2009)
Permeability	≥0.0001 mD	Average laboratory measured property	Data density varies depending on formation and location in the basin.	Faraj (2018); King (2010)
Total gas content	>0.5 scc/g	Lab measured. Represents effective water saturation and effective porosity.	Data density varies depending on formation and location in the basin.	Defined by Geoscience Australia analyst based on well data
Evidence of gas	Positive field test (or gas show)	Extracted from relevant mud log, DST's, log analysis, drilling summary or relevant section	The wells are located in the Nappamerri, Tenappera and Allunga troughs in South Australia. These may not be representative of the entire basin due to lateral variations in lithofacies.	Defined by Geoscience Australia analyst based on well data
Gas type	Thermogenic (not biogenic)	All gas is thermogenic as not assessing CSG.	na[iii]	Charpentier and Cook (2011)

mD = millidarcy; scc/g = standard cubic centimetre per gram; XRD = X-ray diffraction

Source: Refer to previous sections for data sources

Table 64 Non-mappable assessment data rated against shale gas play desirable characteristics (Table 63)

	Brittleness index	Permeability	Total gas content	Evidence of gas	Gas type
Patchawarra Formation	High (0.695)	Medium (3.08E-05 mD)	High	Present	Thermogenic
Murteree Shale	Medium (0.374)	High (6.69E-03 mD)	High	Present	Thermogenic
Roseneath Shale	Medium (0.343)	High (3.30E-03 mD)	High	Present	Thermogenic

mD = millidarcy

Data: Permeability and brittleness index values from Table 9, Table 25 and Table 38 respectively

4.3.3 Deep coal gas plays

Deep coal gas is a relatively new and underutilised resource in the Cooper Basin. Although commercial viability is yet to be proven, the deep coal gas play was investigated by Santos Limited in 2007 with their proof-of-concept for the 5 million acre (20,000 km^2) Cooper Basin deep coal gas play (Dunlop et al., 2017).

Deep coal gas plays are present in the Toolachee, Epsilon and Patchawarra formations. These are thermogenic coals that contain no mobile water and retain gas and gas liquids (Camac et al., 2018). Electron microscopy of the Patchawarra Formation coals has shown that they contain sufficient mesoporosity for coal gas production, despite occurring below the coal seam gas (CSG) production floor (generally considered 2000 m).

Dunlop et al. (2017) provides a comprehensive comparison between CSG and deep coal gas in the Cooper Basin. Since 2012, more than 50 wells have been tested for production variability in the South Australian part of the Cooper Basin. Some of these deep coal gas targets have been additional targets in conventional gas development wells to increase gas production (Camac et al., 2018).

The Toolachee, Epsilon and Patchawarra formations were chosen for assessment of deep coal gas prospectivity. The geological properties used to map deep coal prospeectivity were:

- the net coal thickness, represented by the cumulative thickness of clean coal within the formation (TOC > 50 wt%), and;
- source rock maturity.

The criteria associated with these properties are described in Table 65. These Cooper Basin specific criteria for deep coal gas were developed based on advice from Santos.

4.3.3.1 Deep coal gas mappable criteria

Table 65 Summary of deep coal gas play specific input parameters and classifying criteria used to develop relative prospectivity confidence maps. Associated data sources, assumptions and limitations and references are also provided

Parameter (P)	Classified input parameter thresholds				Comments	Data source	Description/Assumptions	Limitations	Reference for threshold criteria
	Zero (0)	Low (0.25)	Medium (0.5)	High (1.0)					
Net coal thickness	<10 m	na	≥10–<25 m	≥25 m	Minimum requirement	Net coal thickness from Hall et al. (2015a)	True vertical thickness in. 3D model from Hall et al. (2015a)	Variable density and irregular distribution of well tops and velocity data may affect the quality of structural modelling results	Camac et al. (2018); Department for Energy and Mining (SA) (2018c)
Thermal maturity (wet gas)	<0.75%Ro or ≥1.4%Ro	na	≥0.75–<0.9%Ror	≥0.9–<1.4%Ro	Modified from minimum requirement by Charpentier and Cook (2011). Based on generation of gas, transformation ratios (i.e. not gas expelled or migrated)	Hall et al. (2019)	Vitrinite reflectance map for middle of formation, Transformation ratios from Hall et al. (2016c) used to determine thresholds as follows: low (0-10%), medium (10-50%); high (50-90%)	Variation of maturity throughout formation thickness not considered. Additional variability present in kinetic parameters and uncertainties in temperature history, palaeo-temperature data etc. See Hall et al. (2016c)	Mastalerz and Harper (1998); Hall et al. (2016c); Camac (2018); Hissey (2018)
Thermal maturity (dry gas)	<1.4%Ro or ≥3.5%Ro	<2.5%Ro-≥3.5%Ro	≥2–<2.5%Ro	≥1.4–<2%Ro	Modified from minimum requirement by Charpentier and Cook (2011). Based on generation of gas, transformationn ratios (i.e. not gas expelled or migrated)	Hall et al. (2019)	Vitrinite reflectance map for middle of formation, Transformation ratios from Hall et al. (2016c) used to determine thresholds as follows: low (0-10%), medium (10-50%); high (50-90%)	Variation of maturity throughout formation thickness not considered. Additional variability present in kinetic parameters and uncertainties in temperature history, palaeo-temperature data etc. See Hall et al. (2016c)	Mastalerz and Harper (1998); Hall et al. (2016c); Hissey (2018); Camac (2018)

na = not applicable; %Ro = thermal maturity
Cooper Basin specific criteria for deep coal gas was developed based on advice from Santos. See reference column for further details.
This table has been optimised for printing on A3 paper (297 mm x 420 mm).

4.3.3.2 Deep coal wet gas mapping results by formation

Classified individual parameter maps for specific formations (Patchawarra, Epsilon and Toolachee formations) are shown in Figure 75, Figure 76 and Figure 77. Formation specific relative prospectivity confidence maps are displayed Figure 78, Figure 79 and Figure 80.

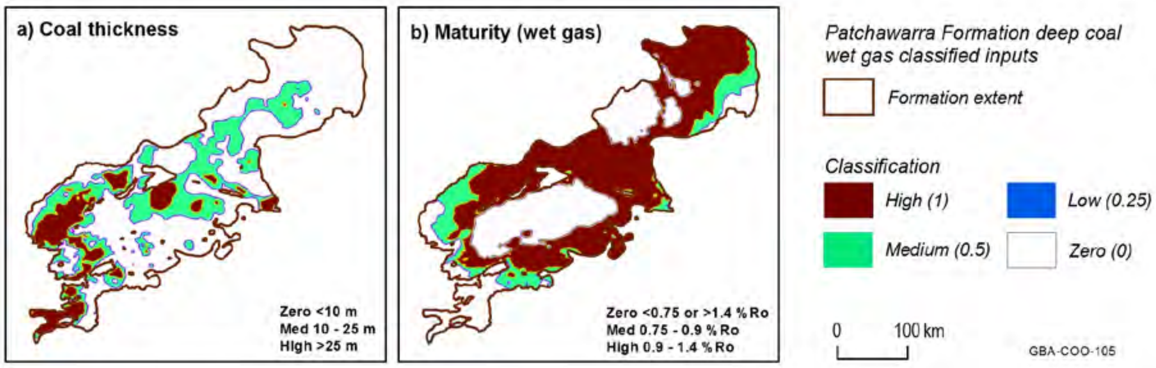

Figure 75 Classified mappable prospectivity confidence input parameters for the Patchawarra Formation deep coal wet gas play

Data: Geological and Bioregional Assessment Program (2019b); Cooper Basin outline from Raymond et al. (2018)
Element: GBA-COO-105

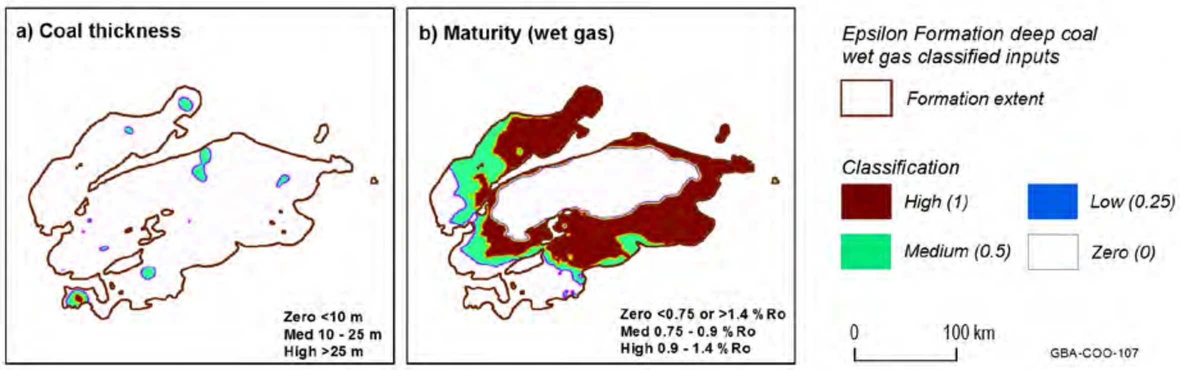

Figure 76 Classified mappable prospectivity confidence input parameters for the Epsilon Formation deep coal wet gas play

Data: Geological and Bioregional Assessment Program (2019b); Cooper Basin outline from Raymond et al. (2018)
Element: GBA-COO-107

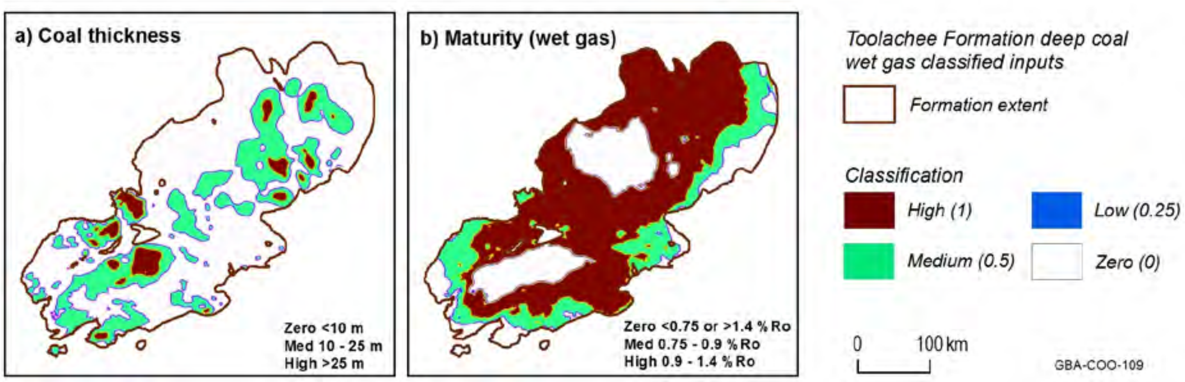

Figure 77 Classified mappable prospectivity confidence input parameters for the Toolachee Formation deep coal wet gas play

Data: Geological and Bioregional Assessment Program (2019b); Cooper Basin outline from Raymond et al. (2018)
Element: GBA-COO-109

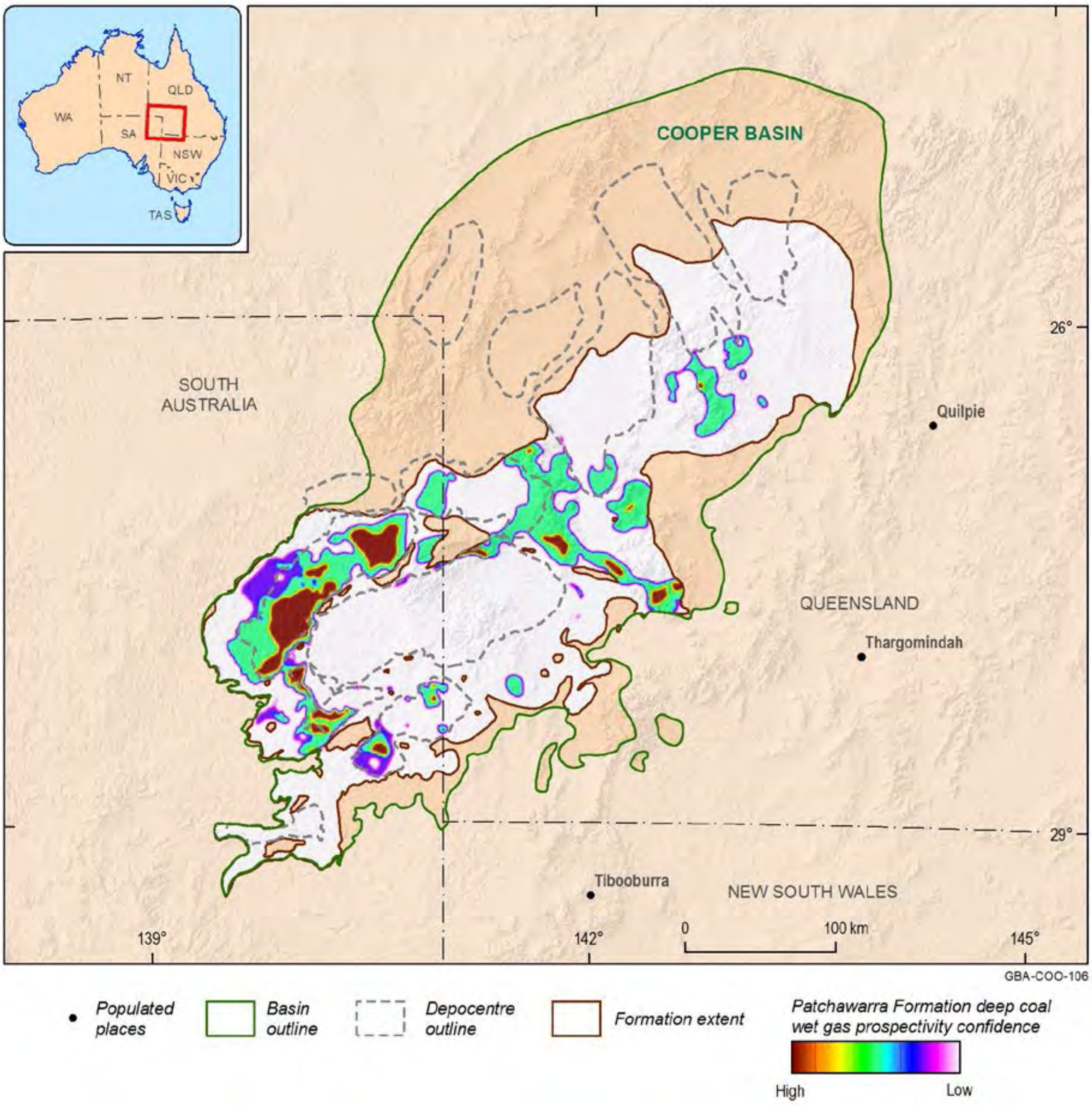

Figure 78 Formation specific relative prospectivity confidence map for the Patchawarra Formation deep coal wet gas play. The distribution of available data used for generating the maps is shown in Figure 93 and Figure 94

Data: Geological and Bioregional Assessment Program (2019b); Cooper Basin outline from Raymond et al. (2018)
Element: GBA-COO-106

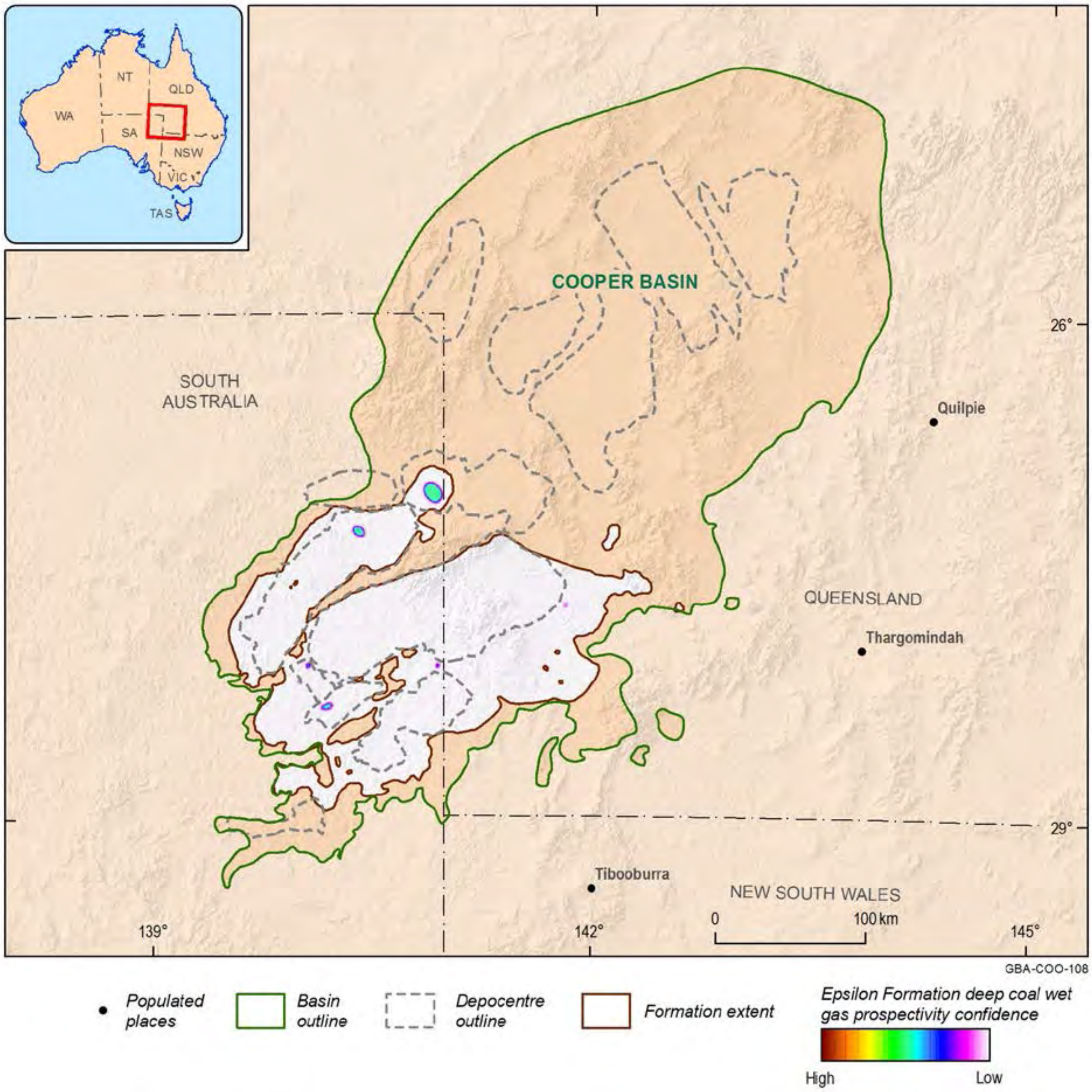

Figure 79 Formation specific relative prospectivity confidence map for the Epsilon Formation deep coal wet gas play. The distribution of available data used for generating the maps is shown in Figure 93 and Figure 94

Data: Geological and Bioregional Assessment Program (2019b); Cooper Basin outline from Raymond et al. (2018)
Element: GBA-COO-108

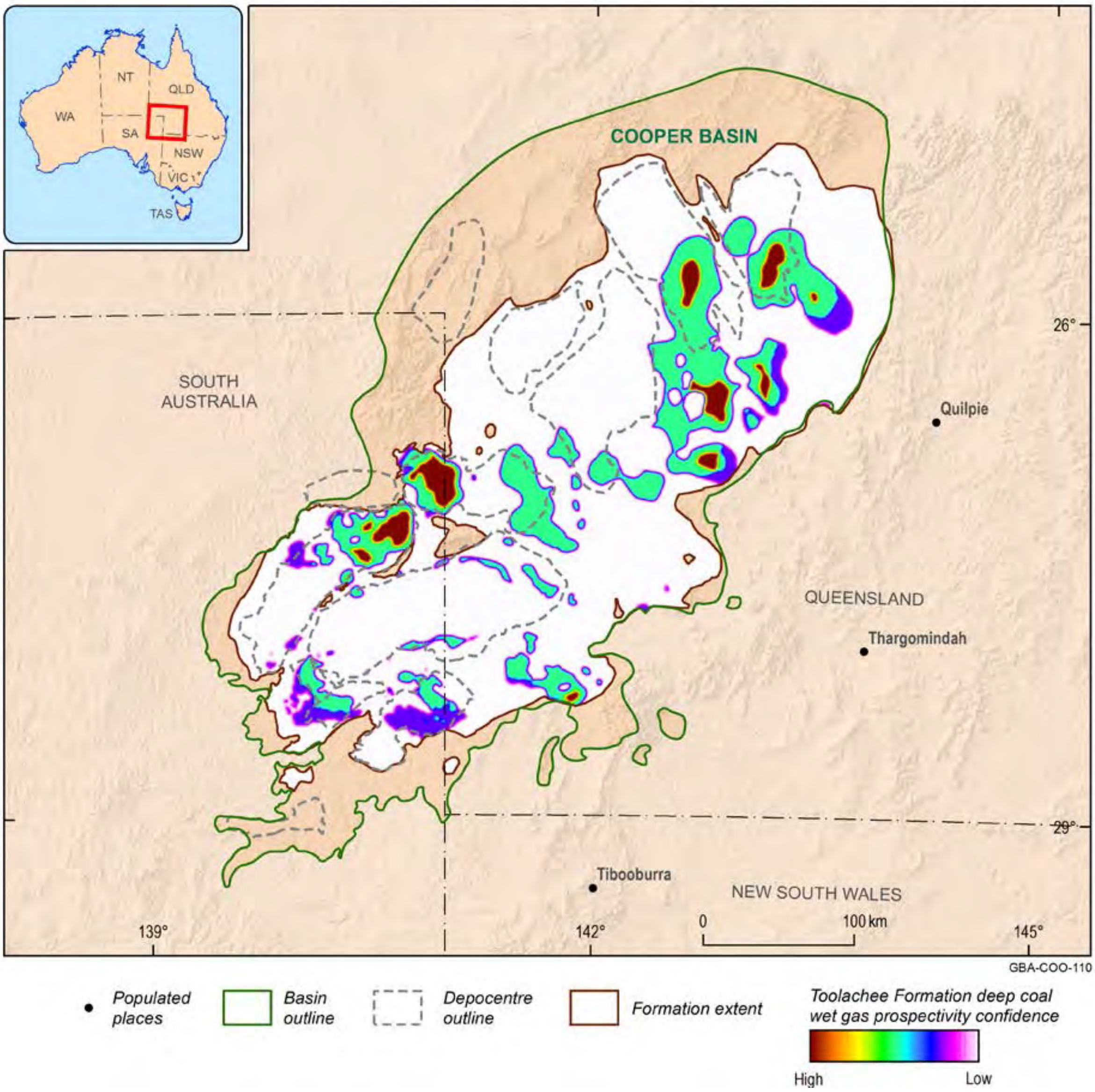

Figure 80 Formation specific relative prospectivity confidence map for the Toolachee Formation deep coal wet gas play. The distribution of available data used for generating the maps is shown in Figure 93 and Figure 94

Data: Geological and Bioregional Assessment Program (2019b); Cooper Basin outline from Raymond et al. (2018)
Element: GBA-COO-110

4.3.3.3 Deep coal dry gas mapping results by formation

Classified individual parameter maps for specific formations (Patchawarra, Epsilon and Toolachee formations) are shown in Figure 81, Figure 82 and Figure 83. Formation specific relative prospectivity confidence maps are displayed in Figure 84, Figure 85 and Figure 86.

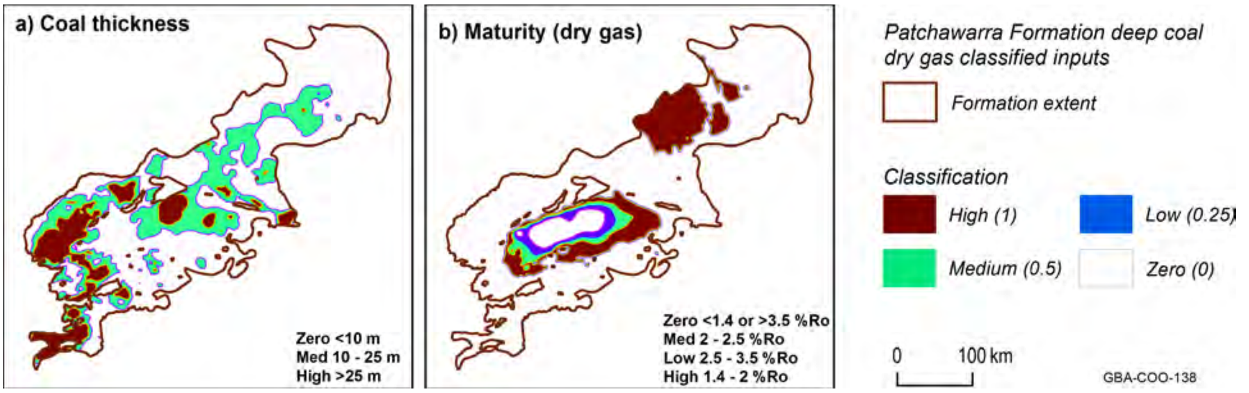

Figure 81 Classified mappable prospectivity confidence input parameters for the Patchawarra Formation deep coal dry gas play

Data: Geological and Bioregional Assessment Program (2019b); Cooper Basin outline from Raymond et al. (2018)
Element: GBA-COO-138

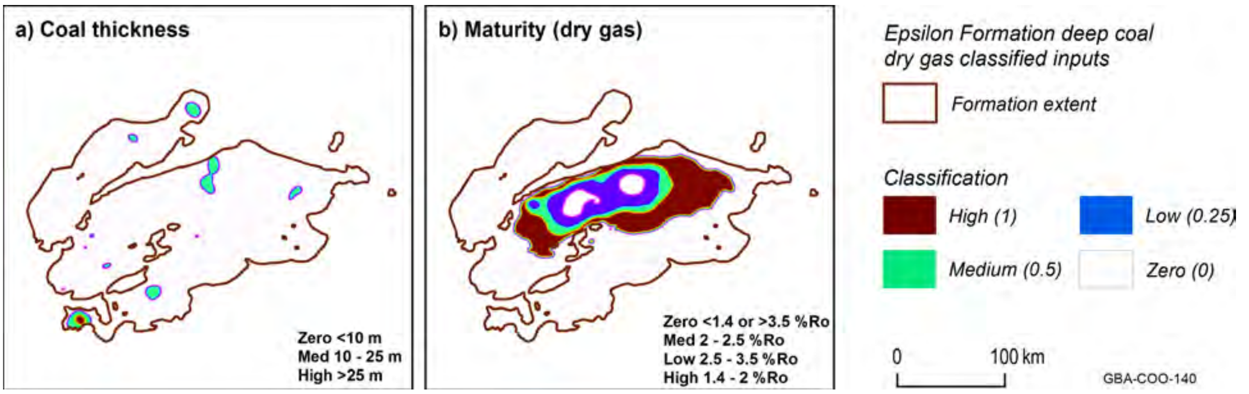

Figure 82 Classified mappable prospectivity confidence input parameters for the Epsilon Formation deep coal dry gas play

Data: Geological and Bioregional Assessment Program (2019b); Cooper Basin outline from Raymond et al. (2018)
Element: GBA-COO-140

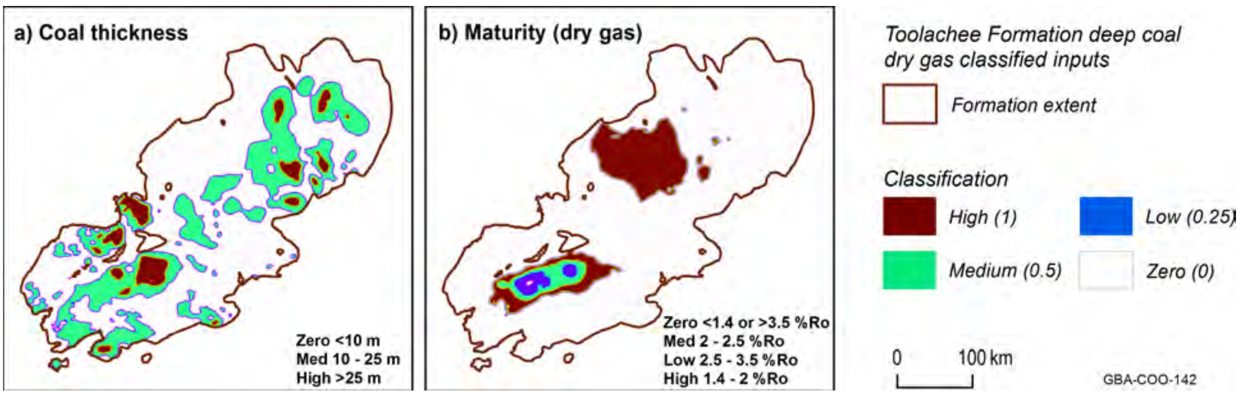

Figure 83 Classified mappable prospectivity confidence input parameters for the Toolachee Formation deep coal dry gas play

Data: Geological and Bioregional Assessment Program (2019b); Cooper Basin outline from Raymond et al. (2018)
Element: GBA-COO-142

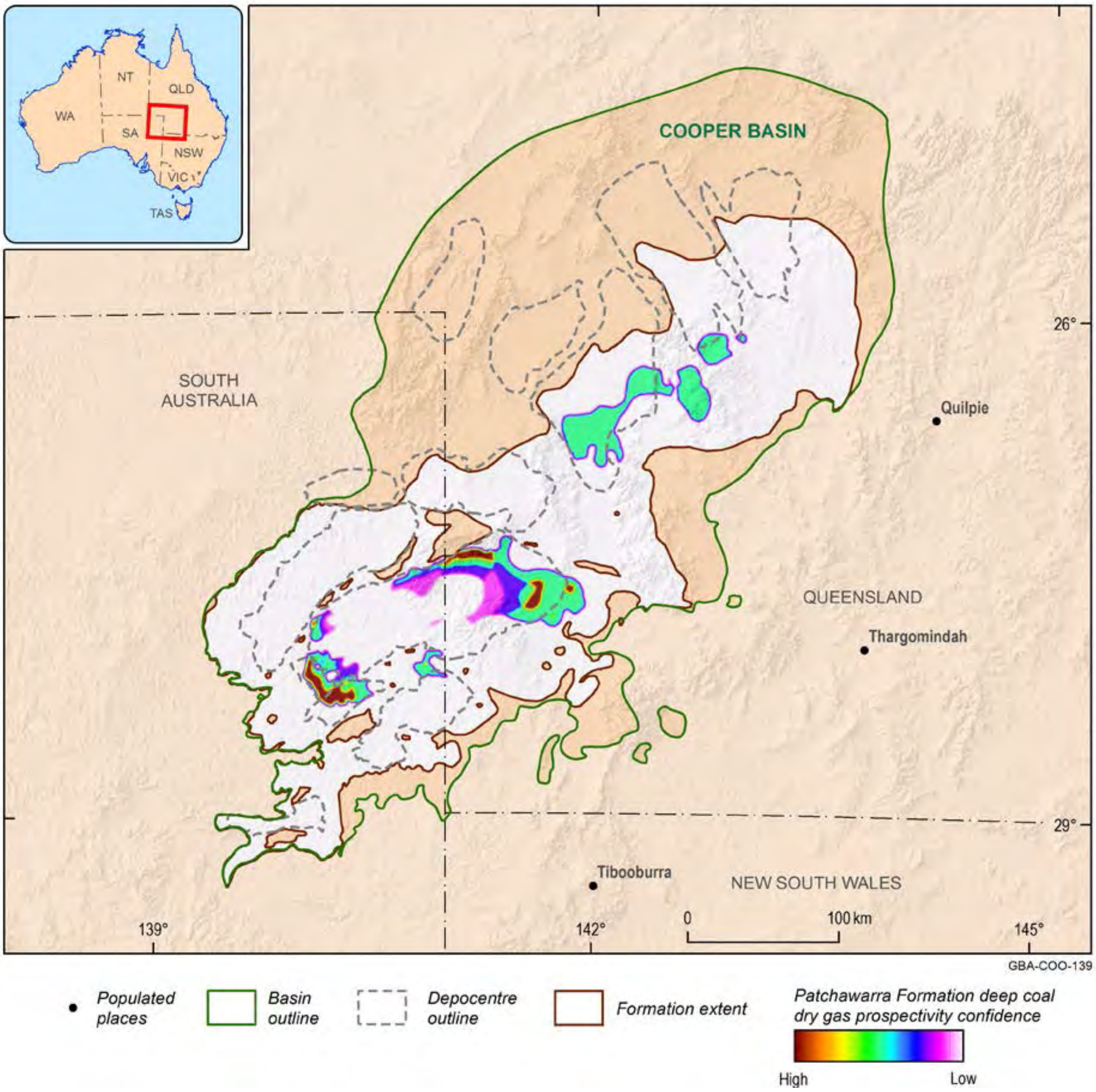

Figure 84 Formation specific relative prospectivity confidence map for the Patchawarra Formation deep coal dry gas play. The distribution of available data used for generating the maps is shown in Figure 93 and Figure 94

Data: Geological and Bioregional Assessment Program (2019b); Cooper Basin outline from Raymond et al. (2018)
Element: GBA-COO-139

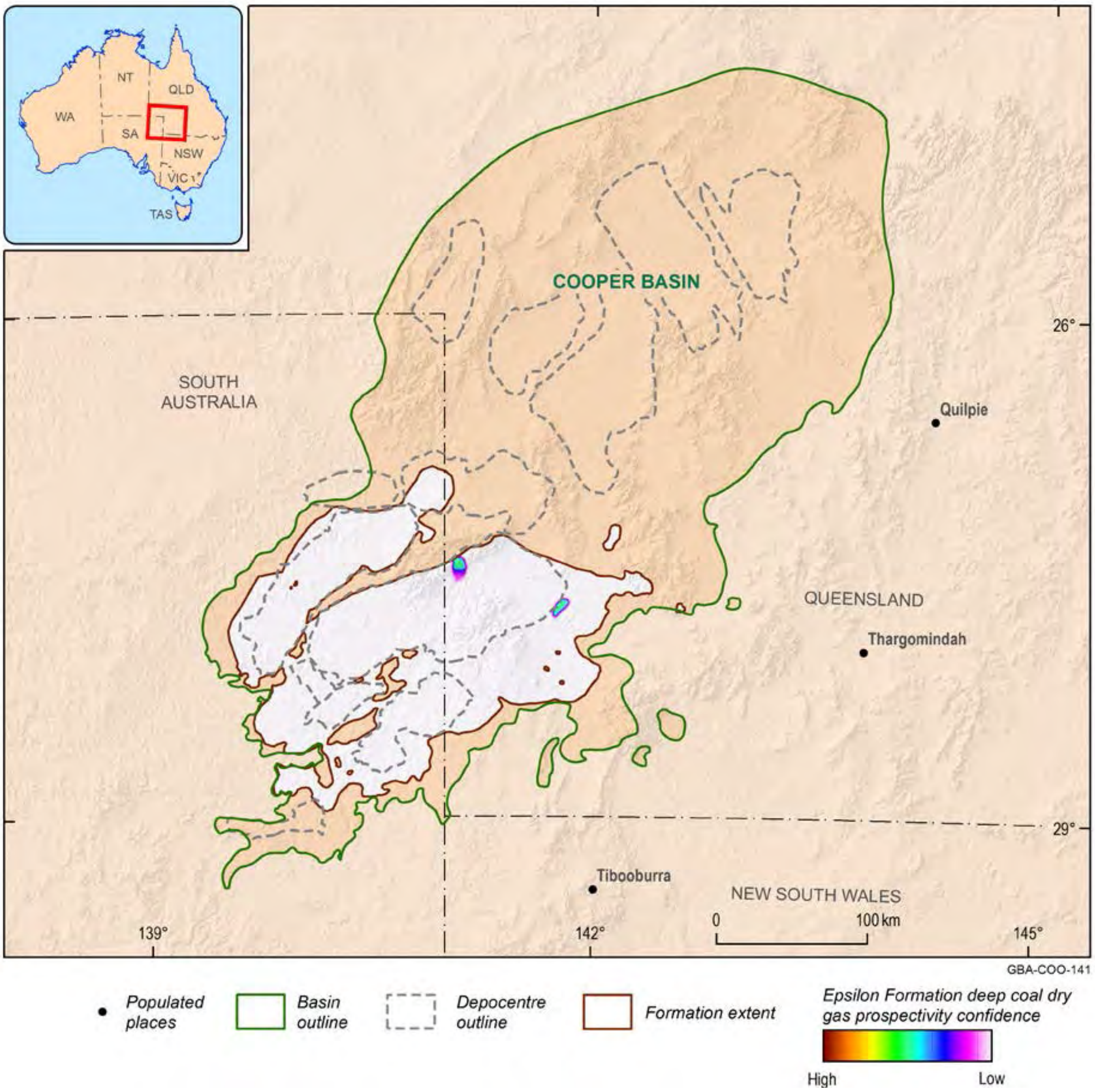

Figure 85 Formation specific relative prospectivity confidence map for the Epsilon Formation deep coal dry gas play. The distribution of available data used for generating the maps is shown in Figure 93 and Figure 94

Data: Geological and Bioregional Assessment Program (2019b); Cooper Basin outline from Raymond et al. (2018)
Element: GBA-COO-141

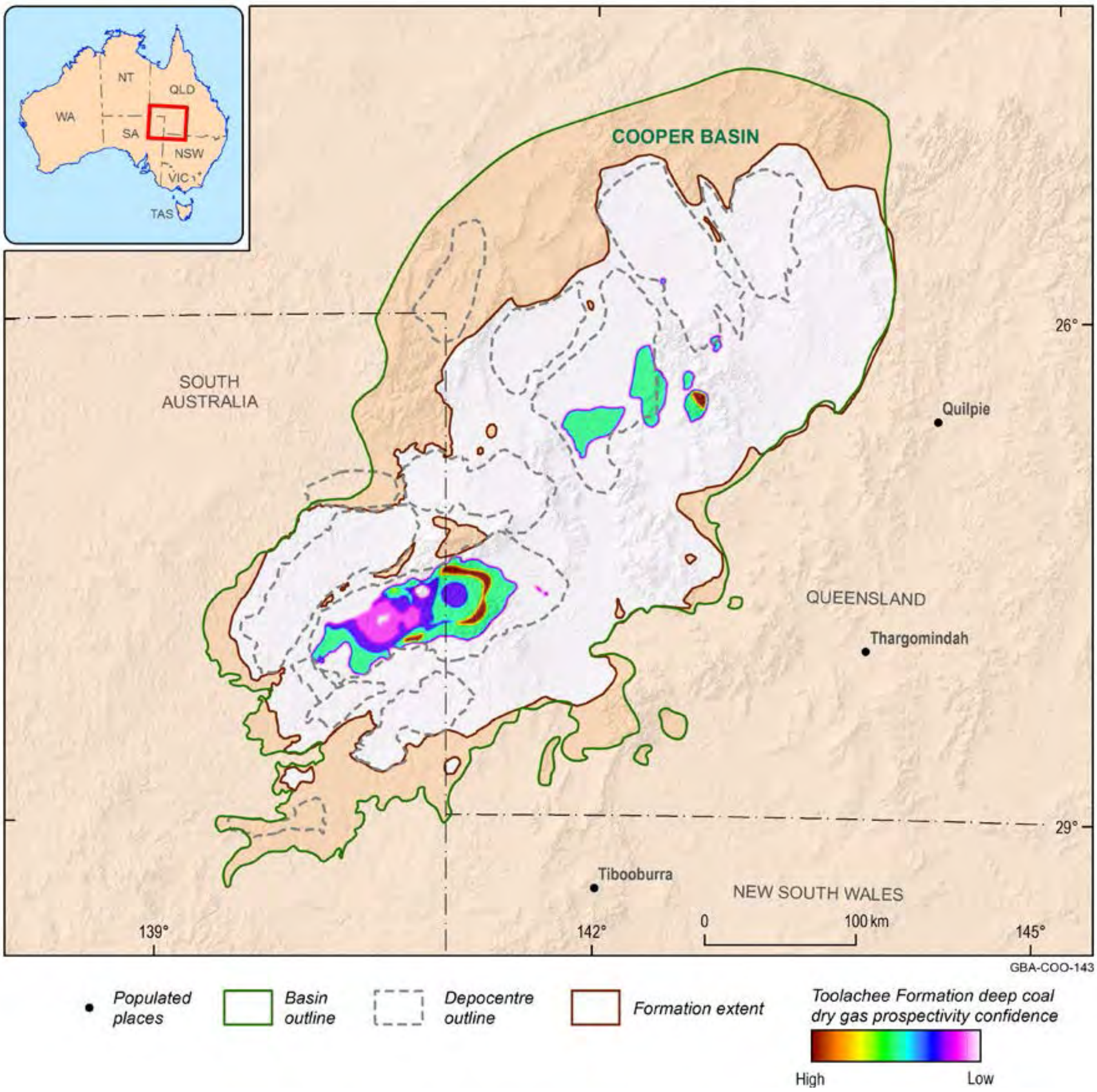

Figure 86 Formation specific relative prospectivity confidence map for the Toolachee Formation deep coal dry gas play. The distribution of available data used for generating the maps is shown in Figure 93 and Figure 94

Data: Geological and Bioregional Assessment Program (2019b); Cooper Basin outline from Raymond et al. (2018)
Element: GBA-COO-143

4.3.3.4 Overall deep coal gas prospectivity confidence results

Prospectivity confidence results were combined to develop a prospectivity confidence map for deep coal wet and dry gas plays.

Results for the overall deep coal wet gas play show the highest relative prospectivity confidence in areas of the Patchawarra, Allunga, Wooloo troughs and the southern Thomson and Ullenbury depressions, with high to moderate confidence in all those areas already mentioned, as well as the eastern Arrabury and Tenappera troughs (Figure 87).

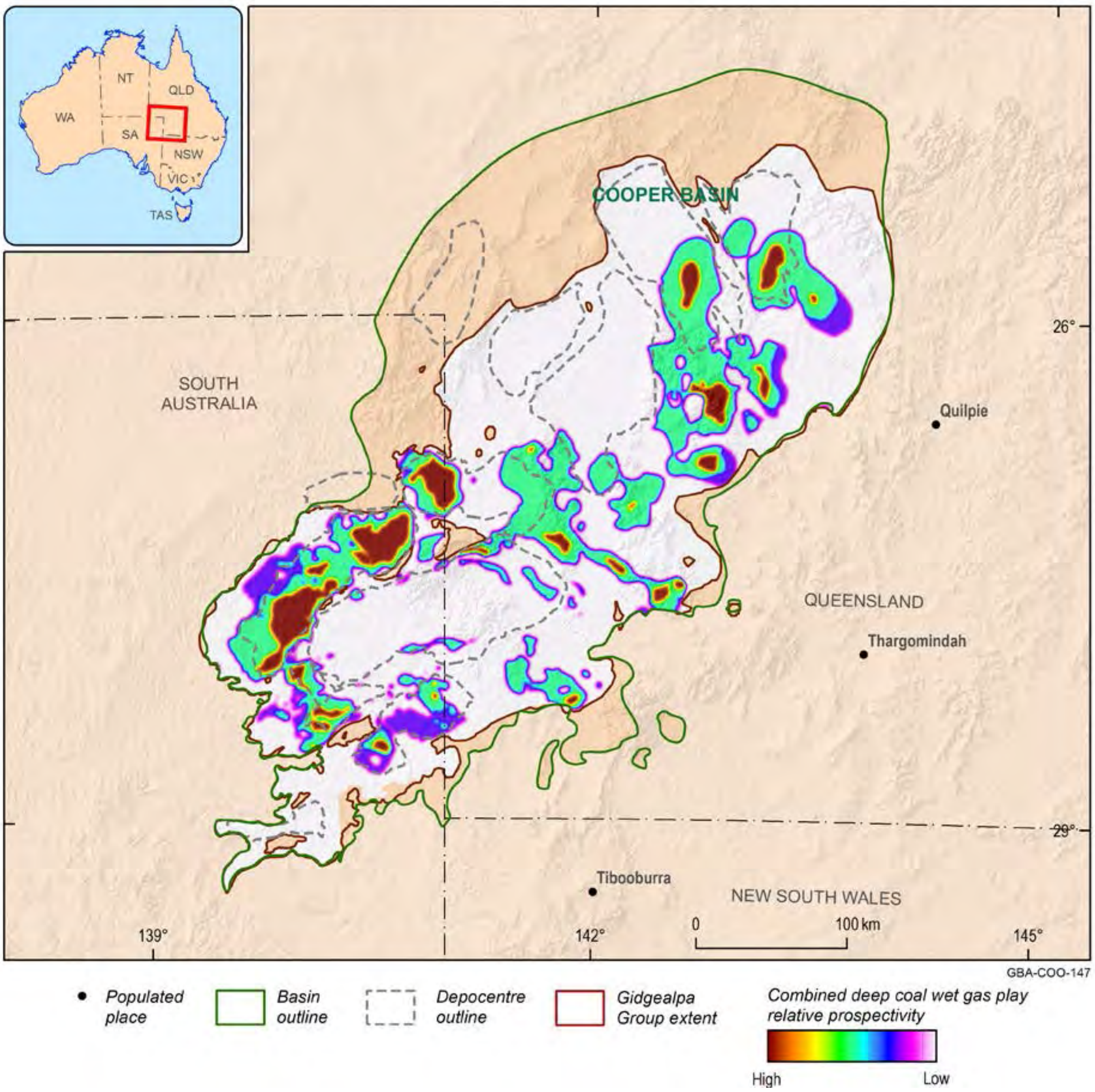

Figure 87 Relative prospectivity confidence for combined deep coal wet gas plays. The distribution of available data used for generating the maps is shown in Figure 93 and Figure 94

Data: Geological and Bioregional Assessment Program (2019b); Cooper Basin outline from Raymond et al. (2018)
Element: GBA-COO-147

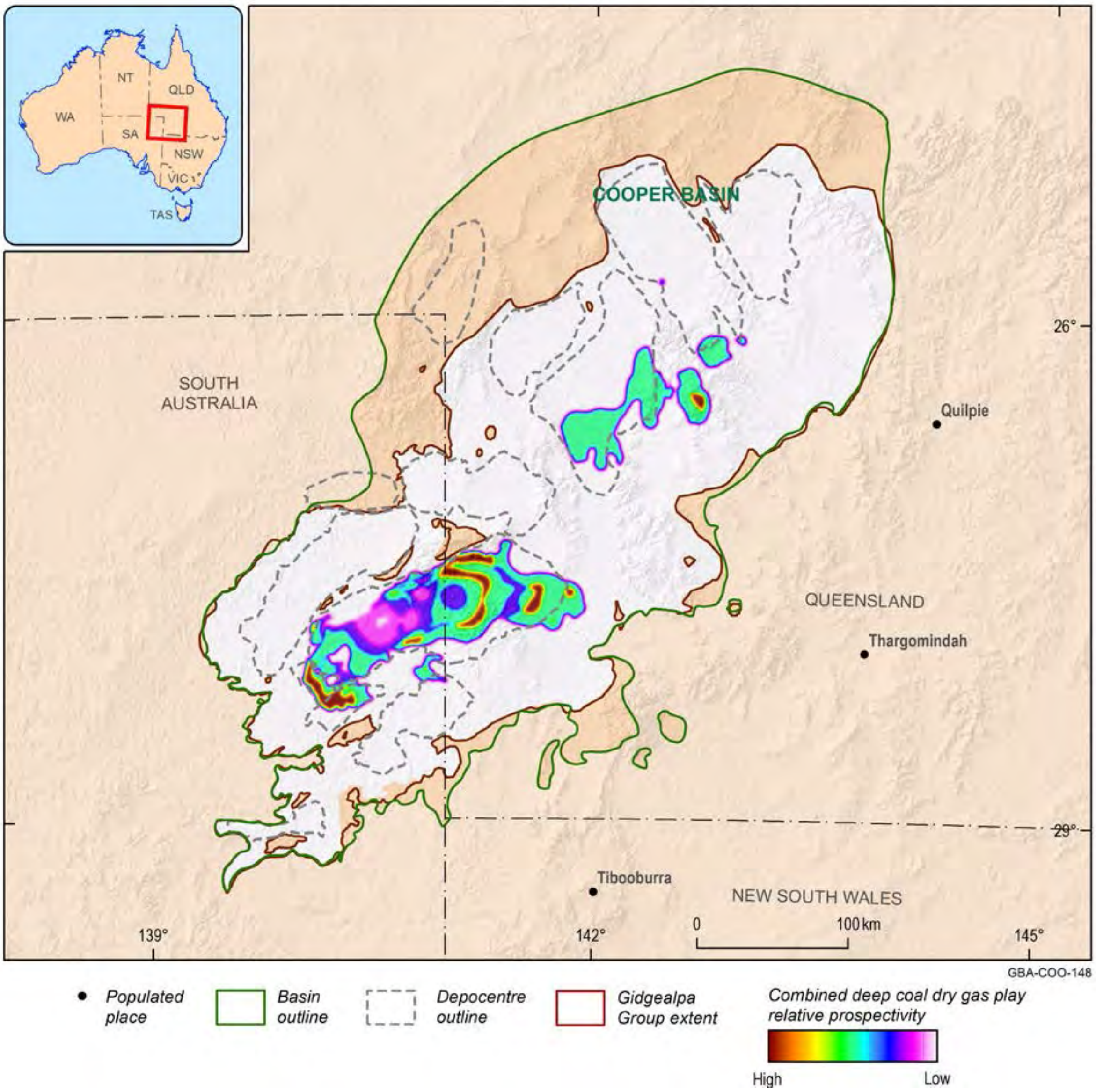

Figure 88 Relative prospectivity confidence for combined deep coal gas dry plays. The distribution of available data used for generating the maps is shown in Figure 93 and Figure 94

Data: Hall et al. (2016a); Geological and Bioregional Assessment Program (2019b); Cooper Basin outline from Raymond et al. (2018)
Element: GBA-COO-148

The highest relative prospectivity confidence for the deep coal dry gas play is focussed in the Nappamerri Trough. High to moderate confidence is also located in the southern Windorah Trough (Figure 88).

The amalgamated wet and dry gas prospectivity confidence map for deep coal gas is shown in Figure 89.

Based on the deep coal gas assessment criteria (Table 65), source rock maturity and coal thickness inputs have the strongest influence on the prospectivity confidence results.

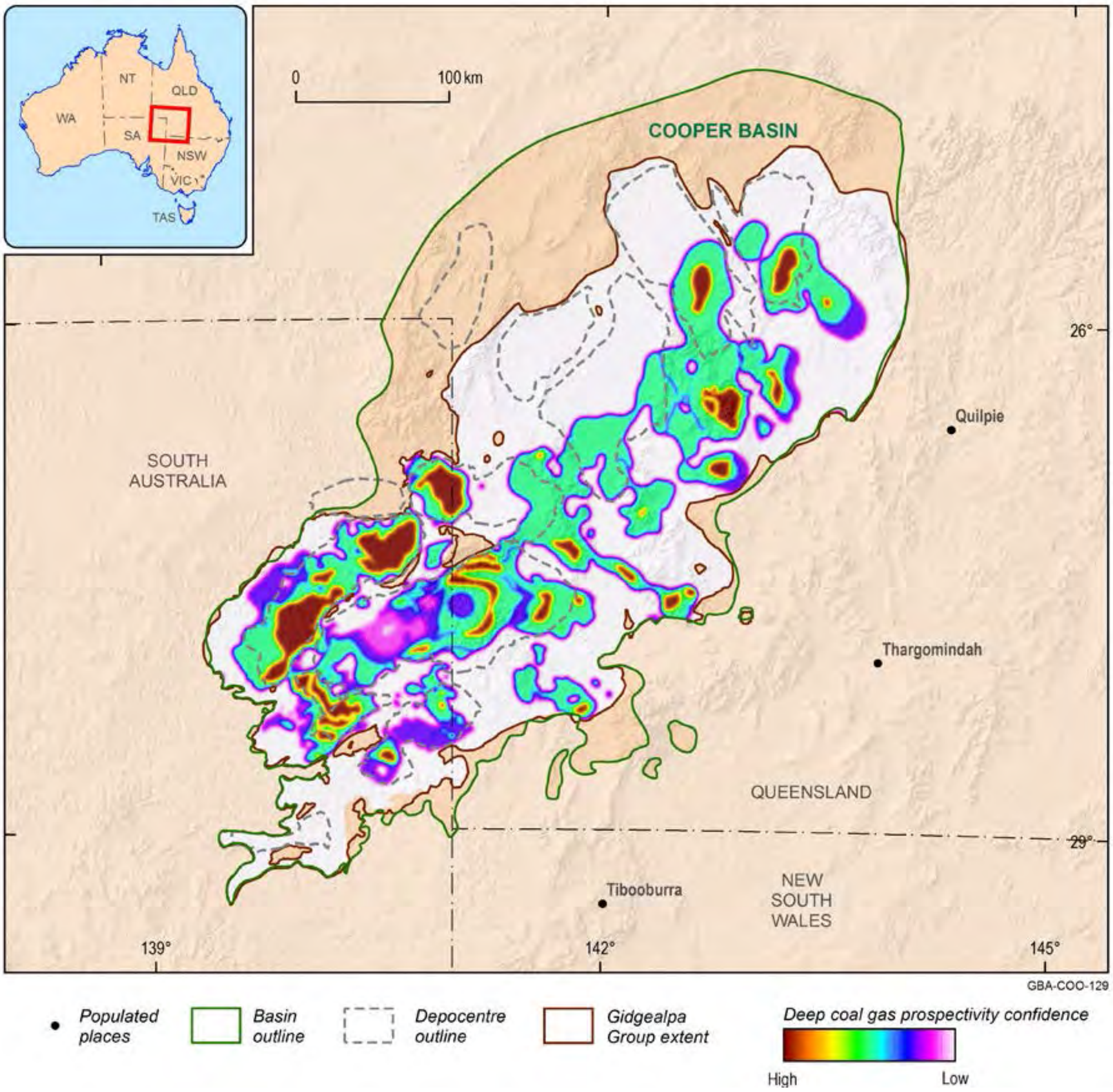

Figure 89 Relative prospectivity confidence for all deep coal gas plays (wet and dry gas). The distribution of available data used for generating the maps is shown in Figure 93 and Figure 94

Data: Geological and Bioregional Assessment Program (2019b); Cooper Basin outline from Raymond et al. (2018)
Element: GBA-COO-129

4.3.3.5 Other characteristics to consider when assessing deep coal gas plays (non-mappable)

Non-mappable criteria that are used to better characterise the prospectivity of the reservoir are displayed in Table 66 and Table 67. The presence of liptinite and inertinite was deemed as favourable.

Table 66 Summary of non-mappable deep coal gas play specific parameters that should be considered when assessing this play type (not included in map results). Assumptions, limitations and references are listed

Non-mappable play characteristics	Desirable characteristics	Description/Assumptions	Limitations	Reference for threshold criteria
Macerals/organic matter type	Liptinite = Type I and/or II Vitrinite = Type III Inertinite = Type IV	Optical versus chemical classification schemes	Generally a relatively poor 1:1 correlation between maceral composition and chemical composition (Powell et al., 1991)	Powell et al. (1991)

Source: Refer to previous sections for data sources

Table 67 Non-mappable assessment data rated against deep coal gas play criteria (Table 66)

	Suitable macerals/organic matter type
Patchawarra Formation	Present
Epsilon Formation	Present
Toolachee Formation	Present

4.3.4 Tight gas plays

All the Gidgealpa Group formations, with the exception of the Roseneath, Murteree shales and the Merrimelia Formation, have the necessary elements for valid tight gas plays (Goldstein et al., 2012). As the thickness of the Toolachee, Daralingie, Epsilon, Patchawarra and Tirrawarra formations is usually combined to make one exploration target, these formations have been included as a combined Gidgealpa Group tight gas play prospectivity map. Here, the net sand thickness beneath the top of the major overpressure zone (2800 m depth) was identified as the primary area of interest.

This prospectivity assessment evaluates the composite gas resource associated with basin-centred gas. Discrete tight gas accumulations have been excluded from the subsequent prospectivity assessment, as these are typically developed in conjunction with adjacent conventional fields.

4.3.4.1 Tight gas criteria

Table 68 Summary of tight play specific input parameters and classifying criteria used to develop combined relative prospectivity confidence maps. Associated data sources, assumptions and limitations and references are also provided

Parameter (P)	Classified input parameter thresholds				Comments	Data source	Description/Assumptions	Limitations	Reference for threshold criteria
	Zero (0)	Low (0.25)	Medium (0.5)	High (1)					
Reservoir thickness (sand) within major overpressure zone (>2800 m)	<10 m	≥10–<50 m	≥50–<100 m	≥100 m	Minimum requirement by Charpentier and Cook (2011)	Formation extent, depth, net sand + silt thickness from Hall et al. (2015a).	Used 3D model from Hall et al. (2015a) & structural surfaces provided by Department of Energy and Mining (SA) for the Tirrawarra Sandstone (Geological and Bioregional Assessment Program, 2019b). In the absence of a net sand thickness map for the Tirrawarra Sandstone, an arbitrary 50% net to gross was used	Variable sample density and irregular distribution of well tops and velocity data may affect the quality of structural modelling results	No published critera; results calibrated against location of wells targeting tight gas plays

This table has been optimised for printing on A3 paper (297 mm x 420 mm).

4.3.4.2 Tight mapping results for combined Gidgealpa Group formations

In order to obtain a prospectivity confidence map for the Gidgealpa Group tight gas play, the following, modified workflow was adopted:

1. All structure surfaces clipped to the minimum depth of the top of the hard overpressure zone of 2800 m.
2. Clipped structure surfaces were used to calculate maps of gross formation thickness below the depth threshold (2800 m).
3. Total sand thickness by formation below depth cut off was calculated using the gross formation thickness below 2800 m, multiplied by the percentage sand content of the formation. In the case of the Tirrawarra Sandstone, a sand content of 50% was assumed.
4. Total cumulative Gidgealpa Group net sand thickness below 2800 m (Figure 90) was derived by summing the net thickness of each formation (i.e. Toolachee, Daralingie, Epsilon, Patchawarra formations and Tirrawarra Sandstone) together.

Source rock geochemistry maps for TOC and HI_o, for individual formations, indicate an abundance of effective source rocks over the majority of the basin (See Hall et al. (2016b) and Section 4.1. Consequently these parameters have not been used to create the relative prospectivity confidence maps. Furthermore, migration distances for unconventional hydrocarbons is poorly defined which inhibits mapping of these parameters.

Overall relative prospectivity confidence map for tight gas plays are displayed in Figure 91.

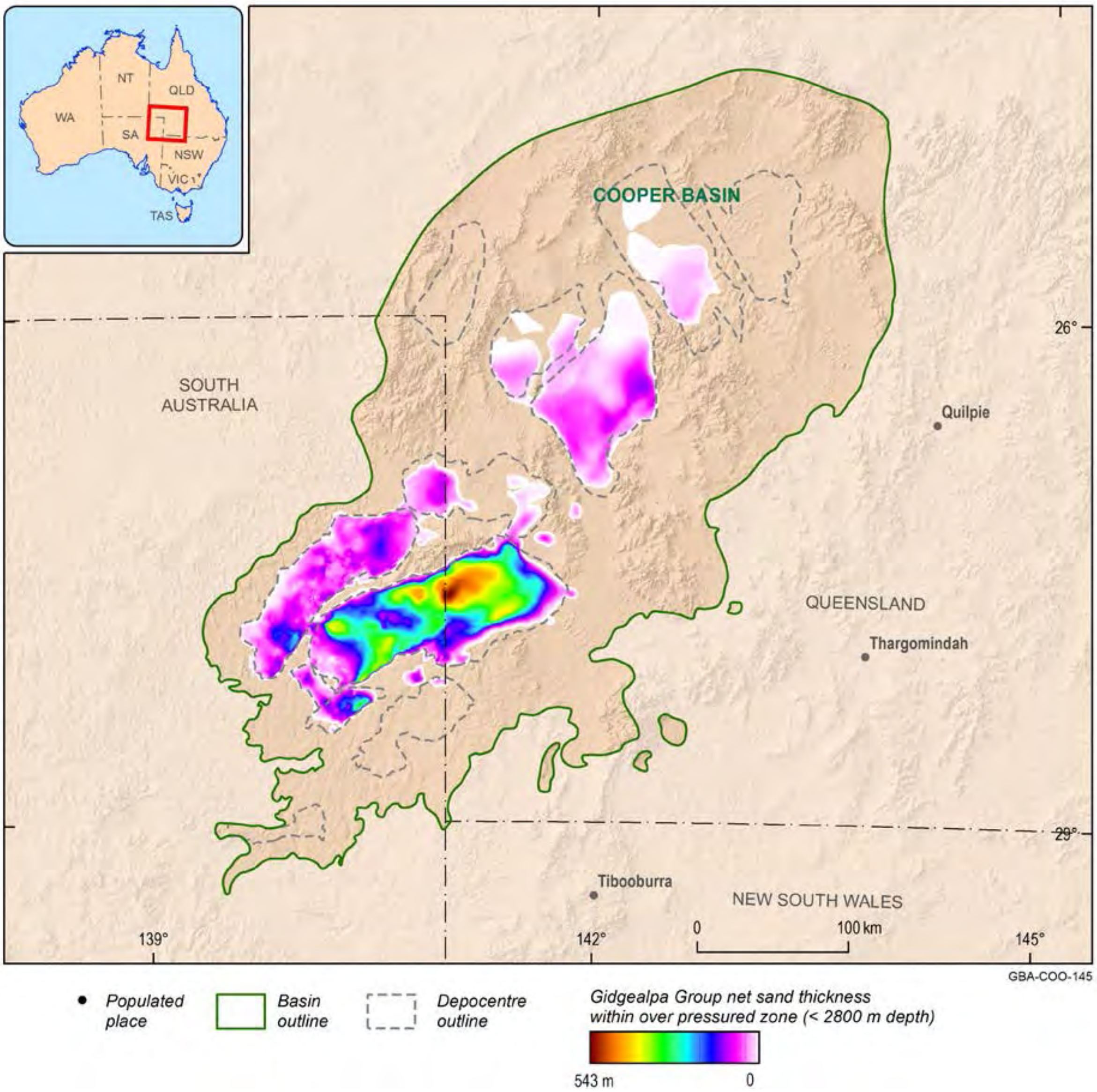

Figure 90 Patchawarra, Epsilon, Daralingie and Toolachee formations (Gidgealpa Group) cumulative net sand thickness within the abnormally overpressured zone, estimated to be below a depth of 2800 m

Data: Geological and Bioregional Assessment Program (2019b); Cooper Basin outline from Raymond et al. (2018)
Element: GBA-COO-145

4.3.4.3 Overall tight gas prospectivity confidence results

Results for the tight gas Gidgealpa Group play show the highest prospectivity in the Nappamerri and Allunga troughs (Figure 91). Moderate-high prospectivity confidence is present in the Patchawarra, Wooloo and Windorah troughs. Based on tight gas assessment criteria (Table 68), and assuming that effective source rocks are present across the basin, the prospectivity confidence mapping results are influenced by sandstone reservoir thickness and the presence of overpressure.

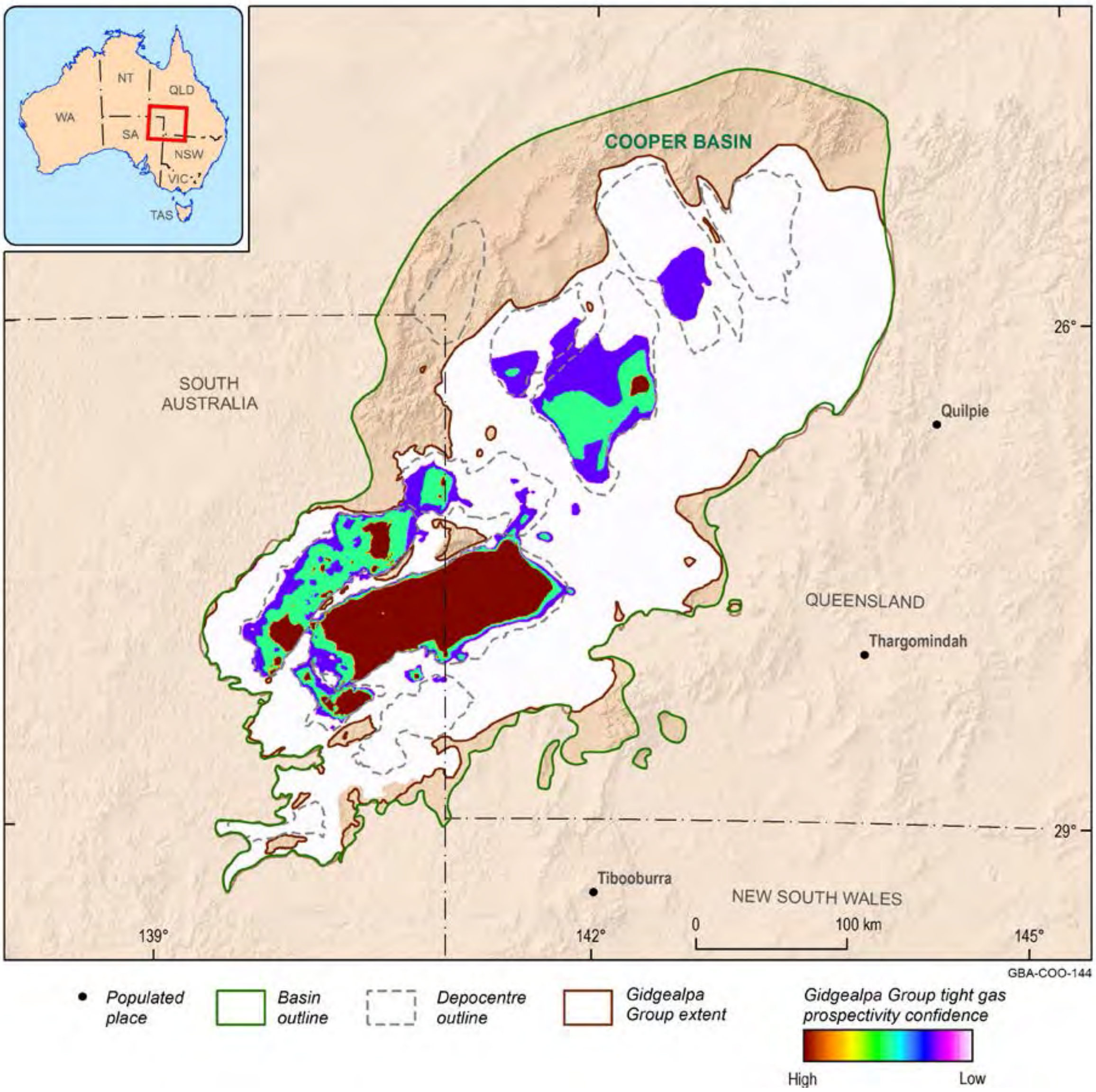

Figure 91 Relative prospectivity confidence map for tight gas plays of the Gidgealpa Group

Data: Geological and Bioregional Assessment Program (2019b); Cooper Basin outline from Raymond et al. (2018)
Element: GBA-COO-144

4.3.4.4 Other characteristics to consider when assessing tight gas plays (non-mappable)

Non-mappable criteria that are used to better characterise the prospectivity of the reservoir are displayed in Table 69 and Table 70. Based on available data, the non-mappable characteristics of the tight gas plays were varied from less favourable to highly favourable.

Table 69 Summary of non-mappable tight gas play specific parameters that should be considered when assessing this play type (not included in map results). Assumptions, limitations and references are listed

Non-mappable play characteristics	Desirable characteristics	Description/ Assumptions	Limitations	Reference for cut-off criteria
Effective porosity (Φ)	≥ 8%	Lab measured	Single average value (non-mappable). Sample distribution may not be representative of the entire basin. Data available varies between formations	Beach Energy (2011); Santos-Beach-Origin (2012)
Effective water saturation	≤ 70%	Lab measured	As above	Beach Energy (2011); Santos-Beach-Origin (2012)
Gas type	Thermogenic	All basin-centred tight gas assumed to be thermogenic	Single binary value (non-mappable). As above	Minimum requirement Charpentier and Cook (2011)

Source: Refer to previous sections for data sources

Table 70 Non-mappable assessment data rated against tight gas play desirable characteristics (Table 69)

	Effective porosity	Effective water saturation	Gas type	Effective source rock
Tirrawarra Formation	Medium (7.6%)	Low (46.2%)	Thermogenic	Present
Patchawarra Formation	Medium (7.2%)	Low (33.1%)	Thermogenic	Present
Epsilon Formation	Medium (6.7%)	Low (33.0%)	Thermogenic	Present
Daralingie Formation	Medium (7.4%)	Low (34.0%)	Thermogenic	Present
Toolachee Formation	Medium (7.8%)	Low (32.7%)	Thermogenic	Present

Source: Reservoir porosity and effective water saturation from Table 8, Table 10, Table 11, Table 35, Table 48 and Table 51

4.3.5 Area of interest for hazard analysis

In order to inform hazard and development scenario analysis, and assess the impact that the exploration and development of shale, tight and deep coal gas resources might have on water and the environment, an area of interest for each play type was developed (Figure 92). This represents the maximum possible area within which each play type may be present, and no development scenarios for this play need to be considered outside this region. The area of interest for each play type was derived from the relative prospectivity maps using a cut-off value of 0.2. This value was chosen as it best represented the envelop around key wells targeting each play type. Significant overlap is present between the three play types.

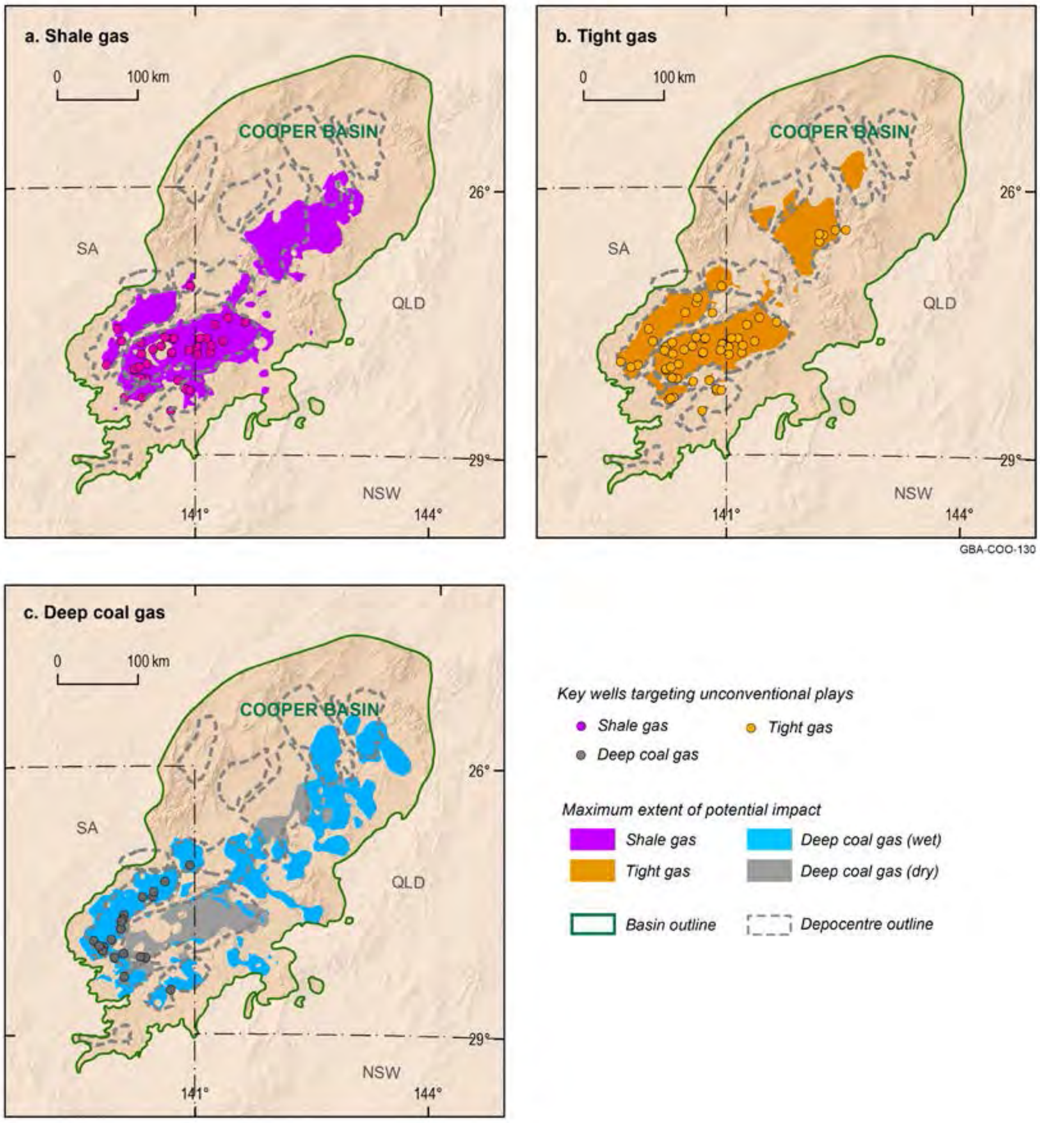

Figure 92 Potential area of impact for hazard assessment for (a) shale gas, (b) tight gas, and (c) deep coal gas resources

Key wells used in shale, tight and deep coal gas characterisation only are shown.
Data: Geological and Bioregional Assessment Program (2019b); Cooper Basin outline from Raymond et al. (2018)
Element: GBA-COO-130

5 Conclusions

5.1 Key findings

This appendix reviews the regional petroleum prospectivity, exploration history, and the characterisation and analysis of shale, tight and deep coal gas plays hosted in the Cooper Basin. It presents the geological factors likely to assist in identifying whether a viable petroleum play is likely to be present.

Key findings are listed below:

- Areas of high relative prospectivity for tight gas are identified within the Nappamerri, Patchawarra and Windorah troughs, consistent with recent exploration activity.
- Areas of high relative prospectivity for deep coal gas are identified in the Patchawarra Trough, consistent with the location of recent exploration activity for liquids rich deep coal plays.
- Prospectivity confidence maps identify areas of relative high prospectivity for deep coal gas in underexplored regions in Queensland, including the Windorah Trough and the southern Ullenbury Depression.
- No areas of high relative prospectivity were identified for the shale gas plays. The Nappamerri and Windorah troughs were identified as medium relative prospectivity for shale gas.
- Pressure and thermal maturity input parameters have the greatest influence on the shale and tight gas prospectivity, while thickness of the formations and thermal maturity are the principal drivers for deep coal gas prospectivity.
- Overpressure, thermal maturity and reservoir thickness are the primary influencing input parameters to the shale gas prospectivity, while thickness of the formations and thermal maturity are the principle drivers for deep coal gas prospectivity. The presence of overpressure and effective source rocks and reservoir thickness are the primary influencing factors for tight gas plays.
- Overall, reservoir characteristics including brittleness, total gas content, porosity and permeability are high or moderately favourable for all play types assessed. Effective water saturation is less favourable.

The extents of shale, tight and deep coal gas plays defined by the prospectivity mapping inform where the plays are most likely to be located with respect to overlying asset, which in turn aids assessment of potential connectivity to overlying surface water–groundwater systems and associated assets.

5.2 Gaps, limitations and opportunities

A number of limitations and assumptions were identified as part of the shale gas, tight gas and deep coal gas prospectivity assessment. Those associated with the prospectivity confidence assessment criteria are outlined in Section 4.3.1. Data and knowledge gaps and subsequent potential opportunities for further work were also identified. These are outlined below:

- Although comparisons between the individual and combined prospectivity confidence maps can be made, each play was assessed using different threshold criteria customised for that play therefore comparisons between plays are not recommended. There is also variability in data quality and quantity, and the criteria used between formations.
- The prospectivity analysis was undertaken based on the regional-scale geological conceptualisation detailed in the Geology technical appendix (Owens et al., 2020). The data input maps are regional-scale datasets. Although they are unsuitable for prospect scale evaluations, they identify areas where more detailed work can be undertaken. In addition, lithological characteristics vary vertically and horizontally (King, 2010). Due to these local variations, not all of the areas identified as a having a high relative prospectivity confidence will result in gas discoveries.
- Shale gas exploration in the United States over a number of years has ensured a set of well-established criteria for assessing these plays. There is less information available in the public domain for tight and deep coal gas. As additional information becomes available, there is an opportunity to rerun the results with revised criteria.
- The reliability of the prospectivity confidence maps are limited by the quality and distribution of publically available data (Figure 93 and Figure 94). Assumptions and limitations specifically relating to the mapping inputs are available in Section 4.3.1. Mappable parameter inputs, which were derived from existing publications on formation characteristics (see Section 4.1), have not taken into account wells drilled subsequent to the release of these studies. Due to the lack of data for the non-mappable characteristics, e.g. permeability, porosity, water saturation, total gas content etc., these were not used to derive the prospectivity confidence maps. Additional collation and assessment of this data would provide additional input maps to further rank the relative prospectivity of each play type. Gridded pressure maps were obtained from existing studies and were only available for the Roseneath and Murteree shales and the Epsilon Formation. Consequently proxy maps were used for the other formations. A comprehensive review of pressure data is needed to enable pressure to be gridded for the remaining formations.

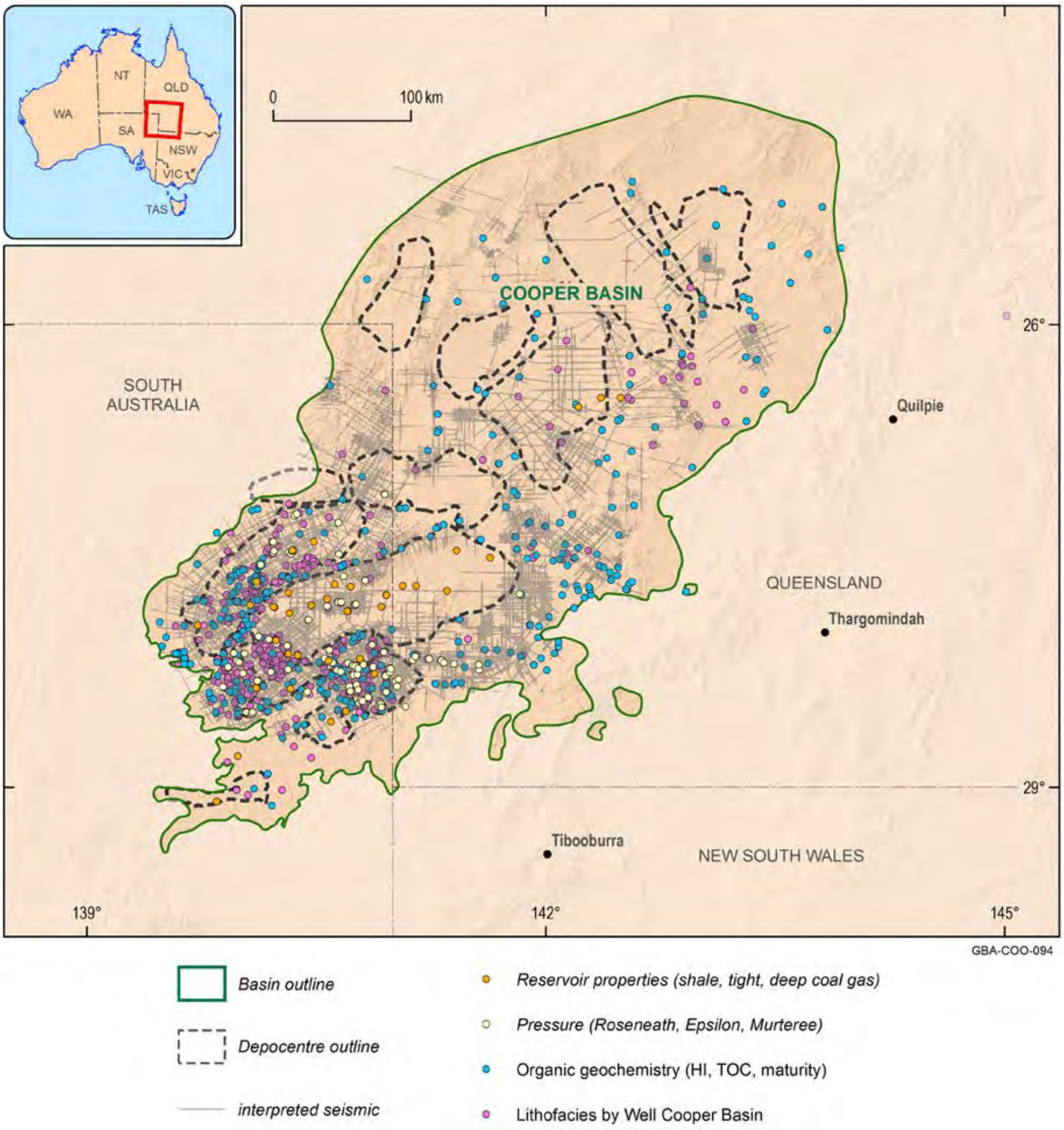

Figure 93 Distribution of available data for the Cooper Basin used in the prospectivity confidence mapping for shale, deep coal and tight gas

Data: Geological and Bioregional Assessment Program (2019a); Cooper Basin outline from Raymond et al. (2018)
Element: GBA-COO-094

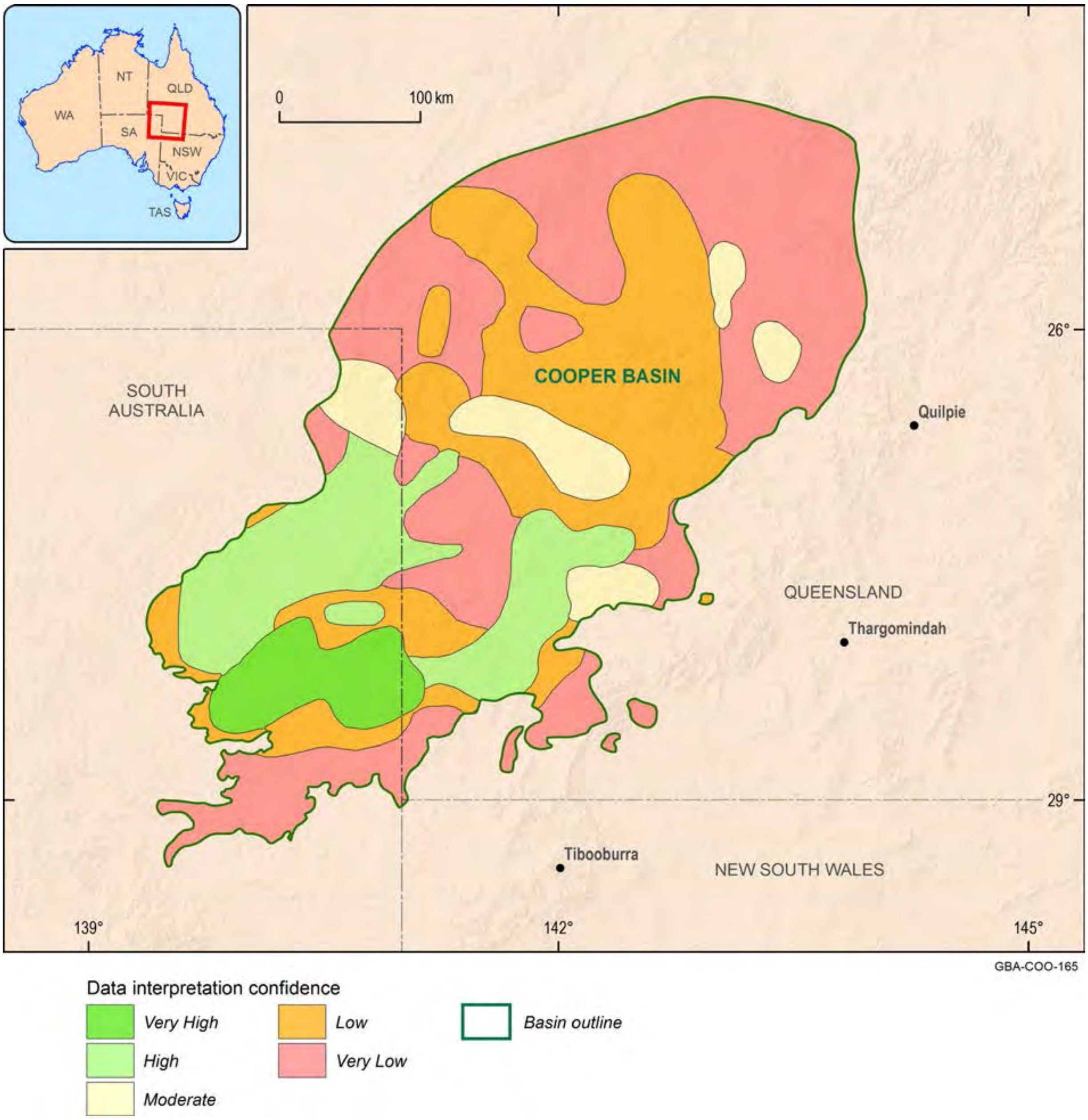

Figure 94 Confidence map based on the data distribution of interpreted seismic and well data for the Cooper Basin prospectivity assessment for shale, deep coal and tight gas

Data: Geological and Bioregional Assessment Program (2019a); Cooper Basin outline from Raymond et al. (2018)
Element: GBA-COO-165

- The maps could be updated with further data from conventional and unconventional wells in the Cooper Basin as they become publically available.
- Although the Tirrawarra Sandstone was identified as a key tight gas target, the absence of associated lithofacies, thermal maturity and thickness maps mean prospectivity confidence maps could not be created. Additional seismic interpretation to define the true extent of the Tirrawarra Sandstone is needed.
- A high proportion of the shale, tight and deep coal gas targets require hydraulic stimulation. There is potential to investigate natural fracture plays as an additional play type.
- Irregular data coverage of seismic and wells across the Cooper Basin (Figure 93 and Figure 94) has resulted in greater uncertainty in areas where limited data points make verifying

interpretation difficult. The data distribution should be taken into account when assessing the relative prospectivity confidence maps as there is more certainty in the southern Cooper Basin compared to the northern part of the basin.

- Petrophysical data available for use to define the reservoir characteristics varied depending on the wells. These data may not be representative for the whole basin due to lateral variability in lithofacies across the basin. Incorporating additional well data would reduce this uncertainty. Reservoir permeability and fracture/fault data are critical for reservoir stimulation and future production of unconventional resources. The currently available well data are not sufficient to characterise the 3D distributions of permeability/fracture/faults. Integrations of additional well and seismic data would help better characterise the reservoir for fracture simulation.
- While relatively dense present-day stress orientation data is available from the Australian Stress Map Project (Rajabi et al., 2017b), information on stress magnitudes is available primarily as a regional dataset at a basin-wide scale, with little detail at finer scales. Consequently, stress regimes cannot be incorporated into the prospectivity confidence mapping for this study. Present-day stresses form a primary control over fracture initiation and propagation (see Section 4.2.1), and so ideally should be included in the prospectivity confidence mapping in the form of regional stress thresholds that define favourable and unfavourable conditions for hydraulic stimulation operations. The creation and correlations of one-dimensional mechanical earth models for each play type and formation of interest are beyond the scope of this study.

The results presented here summarise only the geological factors required for a viable petroleum play to be present. They do not assess the economic viability of play development. Therefore to inform future development scenarios and associated hazards and impacts, it is essential to consider development of each play in an economic context.

The prospectivity maps presented in this report inform where the plays are most likely to be located with respect to overlying assets, however they do not provide any economic context and hence are insufficient to effectively inform future development scenarios alone. To place this work in an economic context, the following additional work is required:

- Resource assessments to estimate the total volume of gas-in-place for priority play types, based on the geological understanding of the plays outlined in this report.
- Estimation of the proportion of gas-in-place that is technically recoverable.
- Economic analysis to understand what would be economic to produce, based on market conditions.

References

AER (Australian Energy Regulator) (2017) State of the energy market, May 2017. Viewed 16 January 2018, https://www.aer.gov.au/publications/state-of-the-energy-market-reports/state-of-the-energy-market-may-2017>.

Alexander EM, Gravestock DI, Cubitt C and Chaney A (1998a) Chapter 6: Lithostratigraphy and environments of deposition. In: Gravestock DI, Hibburt JE and Drexel JF (eds), The Petroleum Geology of South Australia. Volume 4: Cooper Basin. SA Department of Primary Industries and Resources, Adelaide, Australia, 69–116.

Alexander R, Larcher AV, Kagi RI and Price PL (1998b) The use of plant-derived biomarkers for correlation of oils with source rocks in the Cooper–Eromanga basin system, Australia. APEA Journal 28(1), 310–324.

Anderson EM (1951) The dynamics of faulting and dike formation with application to Britain. Oliver and Boyd, Edinburgh.

Ariketi R, Bhui UK, Chandra S and Biswal S (2017) Brittleness modeling of Cambay shale formation for shale gas exploration: a study from Ankleshwar area, Cambay Basin, India. Journal of Petroleum Exploration Production Technology 7, 911-923.

Arouri KR, McKirdy DM, Schwark L, Leythaeuser D and Boult PJ (2004) Accumulation and mixing of hydrocarbons in oil fields along the Murteree Ridge, Eromanga Basin. Organic geochemistry 35, 1597–1618.

ASX (Australian Securities Exchange) (2014) Chapter 5 - Additional reporting on mining and oil and gas production and exploration activities. Viewed 22 October 2018, http://www.asx.com.au/documents/rules/Chapter05.pdf.

Australian Government (2018) Bioregional Assessment Program. Viewed 21 March 2019, https://www.bioregionalassessments.gov.au/bioregional-assessment-program.

AWT International (2013) Shale gas prospectivity potential. Viewed 16 January 2018, http://acola.org.au/wp/PDF/SAF06Consultants/AWTShale%20Gas%20Prospectivity%20Potential%20Jan2013.pdf.

Bailey A, Tenthorey E and Ayling B (2017) Characterising the present-day stress regime of the Georgina Basin. Australian Journal of Earth Sciences 64(1), 121-136.

Baumgärtner J and Zoback M (1989) Interpretation of hydraulic fracturing pressure-time records using interactive analysis methods. International Journal of Rock Mechanics and Mining Sciences & Geomechanics Abstracts 26, 461-469.

Beach Energy (2011a) Holdfast-1 well completion report, PEL 2018, South Australia. Unpublished.

Beach Energy (2011b) Encounter-1 well completion report, PEL 2018, South Australia. Unpublished.

Beach Energy (2012) Environmental impact report: fracture stimulation of Deep Shale Gas and Tight Gas targets in the Nappamerri Trough (Cooper Basin), South Australia.

Beach Energy (2014) FY14 Full year review results roadshow. Viewed 22 October 2018, www.asx.com.au/asxpdf/20140828/pdf/42rtkq464xqggw.pdf.

Beach Energy (2015a) ASX/Media Release - Monthly drilling report November 2015 Viewed 11 July 2018, http://www.beachenergy.com.au/irm/PDF/4564_0/MonthlyDrillingReportNovember2015

Beach Energy (2015b) ASX/Media Release - Upgrade of Nappamerri Trough natural gas contingent resources Viewed 11 June 2018, http://www.beachenergy.com.au/IRM/Company/ShowPage.aspx/PDFs/3985-10000000/NTNGContingentResources.

Beach Energy (2015c) ASX/Media Release - Monthly drilling report July 2015. Viewed 22 October 2018, https://www.asx.com.au/asxpdf/20150805/pdf/4309tzh5l22s98.pdf.

Beach Energy (2016) ASX/Media Release - 1P, 2P and 3P reserves 2C contingent resources as at 30 June 2016. Viewed 10 August 2018, http://www.beachenergy.com.au/irm/PDF/6210_0/ReservesandContingentResourcesasat30June201.

Beach Energy (2018) ASX/Media Release - Monthly drilling report January 2018. Viewed 22 October 2018, http://www.beachenergy.com.au/irm/PDF/6949_0/MonthlyDrillingReportJanuary2018.

Bell J and Babcock E (1986) The stress regime of the Western Canadian Basin and implications for hydrocarbon production. Bulletin of Canadian Petroleum Geology 34(3), 364-378.

Bell J (1990) Investigating stress regimes in sedimentary basins using information from oil industry wireline logs and drilling records. Geological Society, London, Special Publications 48(1), 305-325.

Bell J (1996a) Petro Geoscience 2. In situ stresses in sedimentary rocks (part 2): applications of stress measurements. Geoscience Canada 23(3), 135-153.

Bell J (1996b) Petro Geoscience 1. In situ stresses in sedimentary rocks (part 1): measurement techniques. Geoscience Canada 23(2), 85-100.

Bell J (2006) In-situ stress and coal bed methane potential in Western Canada. Bulletin of Canadian Petroleum Geology 54(3), 197-220.

Boreham CJ and Hill AJ (1998) Source rock distribution and hydrocarbon geochemistry. In: Gravestock DI, Hibburt JE and Drexel JF (eds), The Petroleum Geology of South Australia, Volume 4: Cooper Basin. SA Department of Primary Industries and Resources, Adelaide, Australia, 129–142.

Boreham CJ and Summons RE (1999) New insights into the active petroleum systems in the Cooper and Eromanga basins, Australia. The APPEA Journal 39, 263–296.

Boucher RK (2001) Cooper Basin ridges - Are they structural? MESA Journal 21, 30-32.

Bowers GL (1995) Pore pressure estimation from velocity data: Accounting for overpressure mechanisms besides undercompaction. SPE Drilling & Completion 10(02), 89-95.

Bowker C, Camac B and Fraser S (2018) Predicting Structural Permeability in the Deep Coal Play, Tirrawarra-Gooranie fields, Cooper Basin. ASEG Extended Abstracts 2018(1), 1-9.

Boyer C, (7 August 2018). [Personal communication: Deep coal gas, shale gas criteria: Feedback by C Boyer, Advisor for Unconventional Reservoirs, Schlumberger (D2018-140704)].

Bradshaw MT (1993) Australian petroleum systems. PESA Journal 21, 43–53.

Bradshaw MT, Edwards DS, Bradshaw J, Foster C, Loutit T, McConachie B, Moore A, Murray AP and Nobels RA (1997) Australian and Eastern Indonesian petroleum systems. In: Howes JVC and Noble RA (eds), Proceedings of the conference on petroleum systems of SE Asia and Australasia. Indonesian Petroleum Association, Jakarta.

Bradshaw MT, Borissova I, Edwards DS, Gibson GM, Hashimoto T, Nelson GJ, Rollet N and Totterdell JM (2012) Out of Gondwana. In: Blewitt R (ed), Shaping a nation: a geology of Australia. Geoscience Australia and ANU E Press, Canberra.

Brooke-Barnett S, Flottmann T, Paul PK, Busetti S, Hennings P, Reid R and Rosenbaum G (2015) Influence of basement structures on in situ stresses over the Surat Basin, southeast Queensland. Journal of Geophysical Research: Solid Earth 120(7), 4946-4965.

Business Queensland - Queensland Government (2018) Queensland's unconventional petroleum potential - shale oil and gas, tight gas and coal seam gas. Viewed 26 February 2018, https://www.dnrm.qld.gov.au/__data/assets/pdf_file/0018/291330/unconventional-petroleum-potential-2017.pdf.

Camac B, (7 May 2018). [Personal communication: Cooper Deep Coal gas criteria: Feedback discussion with B Camac, Exploration Geoscientist, Santos Pty Ltd (D2018-138787)].

Camac BA, Hunt SP and Boult PJ (2006) Local rotations in borehole breakouts—observed and modeled stress field rotations and their implications for the petroleum industry. International Journal of Geomechanics 6(6), 399-410.

Camac BA, Benson JM, Chan V and Goedecke A (2018) Cooper Basin deep coal – the new unconventional paradigm: deepest producing coals in Australia. In: ASEG Extended Abstracts, 1-7

Carr LK, Korsch RJ, Palu TJ and Reese B (2016) Onshore basin inventory: the McArthur, South Nicholson, Georgina, Wiso, Amadeus, Warburton, Cooper and Galilee basins, central Australia. Geoscience Australia Record 2016/04, 164. Doi: http://dx.doi.org/10.11636/Record.2016.004.

Chan A, Hauser M, Couzens-Schultz B and Gray G (2014) The role of shear failure on stress characterization. Rock mechanics and rock engineering 47(5), 1641-1646.

Charpentier RR and Cook TA (2011) USGS methodology for assessing continuous petroleum resources. U.S. Geological Survey Open-File Report 2011–1167, 75.

Coates DF and Parsons RC (1966) Experimental criteria for classification of rock substances. International Journal of Rock Mechanics and Mining Science & Geomechanics 3(3), 181-189. Doi: 10.1016/0148-9062(66)90022-2.

Conlay S (2014) Pore Pressure and Geomechanical Assessment of Nappamerri Trough Wells with Emphasis on the Exploration and Development of Unconventional Petroleum Resources., University of Adelaide, Adelaide. Viewed 1 November 2018, https://asp.adelaide.edu.au/about/theses/conleysj/.

Cook AG, Bryan SE and Draper JJ (2013a) Chapter 7: Post-orogenic Mesozoic basins and magmatism. In: Jell PA (ed), Geology of Queensland. Geological Survey of Queensland, Brisbane, Australia, 62.

Cook P, Beck V, Brereton D, Clark R, Fisher B, Kentish S, Toomey J and Williams J (2013b) Engineering energy: unconventional gas production - a study of shale gas in Australia, final report. Australian Council of Learned Academies (ACOLA), Melbourne, Victoria, https://acola.org.au/wp/PDF/SAF06FINAL/Final%20Report%20Engineering%20Energy%20June%202013.pdf.

Cooke ML, Simo J, Underwood CA and Rijken P (2006) Mechanical stratigraphic controls on fracture patterns within carbonates and implications for groundwater flow. Sedimentary Geology 184(3-4), 225-239.

Cooper G, Xiang R, Agnew N, Fabian M and Tupper N (2015) A systematic approach to unconventional play analysis: the oil and gas potential of the Kockatea Shale and Carynginia Formation, North Perth Basin, Western Australia. APPEA Journal 55(1), 192-214.

Core Energy Group (2016) Cooper-Eromanga Basin Outlook | 2035. Adelaide. Viewed 8 May 2018, http://petroleum.statedevelopment.sa.gov.au/__data/assets/pdf_file/0005/283919/Core_Energy_-_Cooper-Eromanga_Basin_Outlook_-_Final_-_Oct2016v1.pdf.

Couzens-Schultz BA and Chan AW (2010) Stress determination in active thrust belts: An alternative leak-off pressure interpretation. Journal of Structural Geology 32(8), 1061-1069.

Deighton I and Hill AJ (1998) Thermal and burial history. In: Gravestock DI, Hibburt JE and Drexel JF (eds), The petroleum geology of South Australia, Volume 4: Cooper Basin. SA Department of Primary Industries and Resources, Adelaide, Australia, 143–156.

Deighton I, Draper JJ, Hill AJ and Boreham CJ (2003) A hydrocarbon generation model for the Cooper and Eromanga basins. The APPEA Journal 43(1), 433-451.

Delhi Australian Petroleum Limited, Santos Limited, Vamgas, Aquitaine, Alliance, Peko and Consolidated (1987) Marengo-1 well completion report. Unpublished.

Delhi Australian Petroleum Ltd (1968) Tinga Tingana-1, well completion report – Basic and interpretative data. Unpublished.

Department for Energy and Mining (SA) (2017) Petroleum wells. Viewed 8 May 2018, https://map.sarig.sa.gov.au/. GBA data repository GUID: 57B6AA29-1375-4C0E-8D31-6AB2B6FD529E.

Department for Energy and Mining (SA) (2018a) Cooper Basin gas well information for unconventional reservoir plays. Viewed 8 May 2018, http://petroleum.statedevelopment.sa.gov.au/prospectivity/resource_plays/cooper_basin_gas_well_information_for_unconventional_reservoir_plays.

Department for Energy and Mining (SA) (2018b) Cooper Basin. Viewed 8 May 2018, http://petroleum.statedevelopment.sa.gov.au/prospectivity/cooper_basin.

Department for Energy and Mining (SA) (2018c) Resource Plays - Cooper Basin Proven & Potential plays. Viewed 12 December 2018, http://petroleum.statedevelopment.sa.gov.au/prospectivity/resource_plays.

Department of Natural Resources, Mines and Energy (Qld) (2018a) QDEX Reports. Viewed 25 October 2018, https://www.business.qld.gov.au/industries/mining-energy-water/resources/online-services/qdex-reports. GBA data repository GUID: 57B6AA29-1375-4C0E-8D31-6AB2B6FD529E.

Department of Natural Resources, Mines and Energy (Qld) (2018b) Petroleum in Queensland's outback: The Cooper and Eromanga basins. Viewed 15 May 2018, http://apps.dnrm.qld.gov.au/mobileapp/Factsheets/petroleum_in_queenslands_outback_the_cooper%20and_eromanga_basins.pdf.

Department of Natural Resources and Mines (Qld) (2017) Petroleum well locations – Queensland. http://qldspatial.information.qld.gov.au/catalogue/custom/detail.page?fid=%7bCBBE665F-60A8-4116-87C8-AEBF0D21B97C%7d. GBA data repository GUID: F2E516E4-5FC6-44FC-A70A-C45A1288AE83.

Department of State Development (SA) (2018) Petroleum Exploration and Production System (PEPS) — South Australia Viewed 14 May 2018, http://www.petroleum.statedevelopment.sa.gov.au/data_and_publications/peps-sa.

Draper JJ (ed) (2002) Geology of the Cooper and Eromanga Basins, Queensland. Queensland Department of Natural Resources and Mines, Brisbane.

Drillsearch (2015) ASX/Media Release - 2015 reserves and contingent resource statement Viewed 13 August 2018, http://www.asx.com.au/asxpdf/20150826/pdf/430t3gtkqdgjjt.pdf.

Dunlop EC, Warner DS, Warner PER and Coleshill LR (2017) Ultra-deep Permian coal gas reserviors of the Cooper Basin: insights from new studies. The APPEA Journal 57, 218-262.

Dyksterhuis S, Müller R and Albert R (2005) Paleostress field evolution of the Australian continent since the Eocene. Journal of Geophysical Research: Solid Earth 110(B5).

EIA (2011) World Shale Gas Resources: An Initial Assessment of 14 Regions Outside the United States. United States Energy Information Administration, Washington, D.C.

EIA (2013) Technically recoverable shale oil and shale gas resources: An assessment of 137 shale formations in 41 countries outside the United States. United States Energy Information Administration. Viewed 23 January 2018, https://www.eia.gov/analysis/studies/worldshalegas/pdf/overview.pdf.

EIA (2015) Technically recoverable shale oil and shale gas resources: Australia. United States Energy Information Administration. Viewed 13 January 2018, https://www.eia.gov/analysis/studies/worldshalegas/pdf/Australia_2013.pdf.

Elliott LG (2015a) Water washing: a major hydrocarbon alteration process. Part 2 – processes, controls and hydrocarbon type prediction. In: AAPG/SEG International Conference & Exhibition 2015. Viewed 29 August 2018, http://www.searchanddiscovery.com/pdfz/documents/2015/41750elliott/ndx_elliott.pdf.html.

Elliott LG (2015b) Using biodegradation to date hydrocarbon entry into reservoirs: examples from the Cooper/Eromanga Basin, Australia. In: AAPG/SEG International Conference & Exhibition 2015. Viewed 29 August 2018, http://www.searchanddiscovery.com/pdfz/documents/2015/41749eliott/ndx_elliott.pdf.html.

Evans TJ, Martinez J, Lai ÉCS, Raiber M, Radke BM, Sundaram B, Ransley TR, Dehelean A, Skeers N, Woods M, Evenden C and Dunn B (2020) Hydrogeology of the Cooper GBA region. Technical appendix for the Geological and Bioregional Assessment: Stage 2. Department of the Environment and Energy, Bureau of Meteorology, CSIRO and Geoscience Australia, Australia.

Fairburn WA (1992) Geometry of reservoir trends in the Epsilon Formation sands, southern Cooper Basin, South Australia. APEA Journal 32, 339–358.

Fall A, Eichhubl P, Cumella SP, Bodnar RJ, Laubach SE and Becker SP (2002) Testing the basin-centered gas accumulation model using fluid inclusion observations: Southern Piceance Basin, Colorado. AAPG Bulletin 96(12), 2297–2318.

Faraj B (2018) Shale gas critical fundamentals, techniques and tools for exploration and production. PESA ACT training course, 8-9 May 2018. Canberra.

Fisher MK and Warpinski NR (2012) Hydraulic-fracture-height growth: Real data. SPE Production & Operations 27(01), 8-19.

Fjar E, Holt RM, Raaen A, Risnes R and Horsrud P (2008) Petroleum related rock mechanics. Elsevier Science.

Gatehouse CG (1972) Formations of the Gidgealpa Group in the Cooper Basin. Australasian Oil and Gas Review 18(2), 10-15.

Geological and Bioregional Assessment Program (2019a) Interpreted seismic and well data confidence map. https://repo.bioregionalassessments.gov.au/metadata/928BDFB4-B3E1-45B2-8DEA-428F4103581A. GBA data repository GUID: 928BDFB4-B3E1-45B2-8DEA-428F4103581A.

Geological and Bioregional Assessment Program (2019b) Prospectivity confidence inputs and results Final. [spatial]. Viewed 04 June 2019, https://repo.bioregionalassessments.gov.au/metadata/A891A605-680B-4CEE-B82D-139E45A17388. GBA data repository GUID: A891A605-680B-4CEE-B82D-139E45A17388.

Geoscience Australia (2015a) Oil and gas platforms. Viewed 16 January 2018, https://ecat.ga.gov.au/geonetwork/srv/eng/search#!0a4a79dc-978a-0e89-e054-00144fdd4fa6.

Geoscience Australia (2015b) Oil and gas infrastructure. [Map Server]. Viewed 23 July 2017, http://services.ga.gov.au/site_9/rest/services/Oil_Gas_Infrastructure/MapServer. GBA data repository GUID: 0BC08E3D-71BC-4EA3-ACC0-00FDE2BE2E8C.

Geoscience Australia (2017) GEODATA TOPO 250K Series 3 Topographic Data. Viewed 1 October 2018, http://pid.geoscience.gov.au/dataset/ga/64058. GBA data repository GUID: BCA7C9F6-6639-45C4-ABC8-5027EFA14B40.

Geoscience Australia (2018) Australian Energy Resources Assessment (AERA) interim report. Geoscience Australia. Viewed 16 Janurary 2018, https://aera.ga.gov.au/.

Goldstein B, Menpes S, Hill A, Wickham A, Alexander E, Jarosz M, Pepicelli D, Malavazos M, Staritski K, Taliangis P, Coda J, Hill D and Webb M (2012) Roadmap for unconventional gas projects in South Australia. Department for Manufacturing, Innovation, Trade, Resources and Energy.

Goldstein B (2016) Energy Resource Investment Insights. In: South Australian Resource Exploration & Investment Conference. Viewed 10 August 2018, http://www.petroleum.statedevelopment.sa.gov.au/__data/assets/pdf_file/0006/274875/SAREIC_20_April_2016_-_Energy_Resource_Insights_for_Investment.pdf.

Gradstein FM, Ogg JG, Schmitz M and Ogg G (eds) (2012) The Geologic Time Scale 2012. Elsevier.

Grauls D and Baleix J (1994) Role of overpressures and in situ stresses in fault-controlled hydrocarbon migration: A case study. Marine and Petroleum Geology 11(6), 734-742.

Gravestock DI and Jensen-Schmidt B (1998) Structural setting. In: Gravestock DI, Hibburt JE and Drexel JF (eds), The petroleum geology of South Australia, Volume 4: Cooper Basin. SA Department of Primary Industries and Resources, Adelaide, Australia, 47–68.

Gravestock DI, Alexander EM, Morton JG and Sun X (1998a) Chapter 10: Reservoirs and Seals. In: Gravestock DI, Hibburt JE and Drexel JF (eds), The Petroleum Geology of South Australia, Volume 4: Cooper Basin. SA Department of Primary Industries and Resources, Adelaide, Australia, 157–180.

Gravestock DI, Jensen-Schmidt B, Sansome A, Frears RA and Morton JG (1998b) Field summaries. In: Gravestock DI, Hibburt JE and Drexel JF (eds), The petroleum geology of South Australia, Volume 4: Cooper Basin. SA Department of Primary Industries and Resources, Adelaide, Australia, 189–196.

Gray A and Draper JJ (2002) Petroleum Geology. In: Draper JJ (ed), Geology of the Cooper and Eromanga basins, Queensland. Queensland Department of Natural Resources and Mines, Queensland. Minerals and Energy Review Series, 63–74.

Gray ARG, McKillop M and McKellar JL (2002) Eromanga Basin stratigraphy. In: Draper JJ (ed), Geology of the Cooper and Eromanga Basins, Queensland. Queensland Minerals and Energy Review Series. Queensland Department of Natural Resources and Mines, Queensland, 30–56.

Gray ARG and McKellar JL (2002) Cooper Basin stratigraphy. In: Draper JJ (ed), Geology of the Cooper and Eromanga Basins, Queensland. Queensland Natural Resources and Mines, Brisbane, 9–26.

Greenstreet C (2015) From play to production: the Cooper unconventional story—20 years in the making. The APPEA Journal 55(2), 407-407.

Gui F, Rahman K, Lockhart D, Cunha D and Meadows D (2016) High Stress Contrast between Different Lithologies and its Implications for Drilling and Stimulation in the Northern Cooper Basin. In: SPE Asia Pacific Oil & Gas Conference and Exhibition. Society of Petroleum Engineers. Viewed 8 November 2018, https://www.onepetro.org/conference-paper/SPE-182178-MS.

Hall LS, Hill AJ, Troup A, Korsch RJ, Radke B, Nicoll RS, Palu TJ, Wang L and Stacey A (2015a) Cooper Basin architecture and lithofacies: Regional hydrocarbon prospectivity of the Cooper Basin, Part 1. Geoscience Australia Record 2015/31. Doi: http://dx.doi.org/10.11636/Record.2015.031.

Hall LS, Hill AJ, Wang L, Kuske T, Edwards DS, Troup A and Boreham CJ (2015b) Unconventional gas prospectivity of the Cooper Basin. The APPEA Journal 55(2), 428-428. Doi: https://doi.org/10.1071/AJ14063.

Hall LS, Lawson C, Edwards DS, Boreham CJ, Palu TJ, Hill AJ and Troup A (2016a) Cooper Basin Source Rock Atlas GIS. Viewed 14 April 2018, http://pid.geoscience.gov.au/dataset/ga/90687. GBA data repository GUID: BC07EB2B-27D7-46FE-B79E-0C9A1F8B40A3.

Hall LS, Boreham CJ, Edwards DS, Palu TJ, Buckler T, Hill AJ and Troup A (2016b) Cooper Basin Source Rock Geochemistry: Regional Hydrocarbon Prospectivity of the Cooper Basin, Part 2. Geoscience Australia Record 2016/06. Doi: http://dx.doi.org/10.11636/Record.2016.006.

Hall LS, Palu TJ, Murray AP, Boreham CJ, Edwards DS, Hill AJ and Troup A (2016c) Petroleum Systems Modelling of Cooper Basin: Regional Hydrocarbon Prospectivity of the Cooper Basin, Part 3. Geoscience Australia Record 2016/29. Doi: http://dx.doi.org/10.11636/Record.2016.029

Hall LS, Buchanan S, Totterdell JM, Lai ÉCS, Langford RP, Sundaram B, Ransley TR, Glenn KC, Heugh A, Inskeep C, Zhu R, Skeers N and Stewart G (2018) Rapid regional prioritisation for tight and shale gas potential of eastern and northern Australian basins. Geoscience Australia, https://www.bioregionalassessments.gov.au/assessments/geological-and-bioregional-assessment-program/rapid-regional-prioritisation/rapid-regional-prioritisation-report.

Hall LS, Palu TJ, Murray AP, Boreham CJ, Edwards DS, Hill A and Troup A (2019) Hydrocarbon prospectivity of the Cooper Basin, Australia. AAPG Bulletin 103, 31-63. Doi: https://doi.org/10.1306/05111817249

Heidbach O and Höhne J (2008) CASMI—a visualization tool for the World Stress Map database. Computers & Geosciences 34(7), 783-791.

Heidbach O, Rajabi M, Reiter K, Ziegler M and WSM Team (2016) World Stress Map database release 2016. http://dataservices.gfz-potsdam.de/wsm/showshort.php?id=escidoc:1680890. GBA data repository GUID: 01CA975D-695B-4BFB-8E56-69C4B8208876.

Hill A, (15 February 2019). [Revised HIo cut-off (150 mg HC/g TOC) for shale gas criteria, SA Government (D2019-20741)].

Hillis R and Reynolds S (2000) The Australian stress map. Journal of the Geological Society 157(5), 915-921.

Hillis RR, Meyer JJ and Reynolds SD (1998) The Australian stress map. Exploration Geophysics 29(4), 420-427.

Hillis RR, Morton JG, Warner D and Penney RK (2001) Deep basin gas: a new exploration paradigm in the Nappamerri Trough, Cooper Basin, South Australia. The APPEA Journal 2001, 185-200.

Hillis RR, Sandiford M, Reynolds SD and Quigley MC (2008) Present-day stresses, seismicity and Neogene-to-Recent tectonics of Australia's 'passive' margins: intraplate deformation controlled by plate boundary forces. Geological Society, London, Special Publications 306(1), 71-90.

Hissey E, (16 October 2018). [Personal communication: Cooper Deep Coal gas criteria: Feedback discussion with E Hissey, Exploration geoscientist, Santos Pty Ltd (D2018-140696)].

Hossain M, Rahman M and Rahman S (2000) Hydraulic fracture initiation and propagation: roles of wellbore trajectory, perforation and stress regimes. Journal of Petroleum Science and Engineering 27(3-4), 129-149.

Hubbert MK and Willis DG (1957) Mechanics of hydraulic fracturing. Petroleum Transactions 210, 153-168.

Hutchinson MF, Stein JL, Stein JA, Anderson H and Tickle PK (2008) GEODATA 9 second DEM and D8: Digital Elevation Model Version 3 and Flow Direction Grid. Viewed 21 September 2018, https://ecat.ga.gov.au/geonetwork/srv/eng/catalog.search?node=srv#/metadata/a05f7892-d78f-7506-e044-00144fdd4fa6. GBA data repository GUID: A9745284-35AC-4AB5-8976-C2F5F1E1B85A.

Icon Energy (2015) Fraccing Halifax No. 1 in Cooper Basin. Viewed 10 December 2018, http://www.qupex.org.au/wp-content/uploads/2015/07/icon_energy_drilling_for_shale_in_the_cooper_baisin_qupex_presentation.pdf.

Iqbal O, Ahmad M and Kadir Aa (2018) Effective evaluation of shale gas reservoirs by means of an integrated approach to petrophysics and geomechanics for the optimization of hydraulic fracturing: A case study of the Permian Roseneath and Murteree Shale Gas reservoirs, Cooper Basin, Australia. Journal of Natural Gas Science and Engineering 58, 34-58.

Jadoon QK, Roberts E, Blenkinsop T and Wust R (2016) Unconventional shale gas reservoir characterization and modelling of the Permian Roseneath and Murturee shales in the Cooper Basin, Australia. Doctorate of Philisophy. James Cook University. Viewed 8 November 2018, https://researchonline.jcu.edu.au/46477/1/46477-jadoon-thesis-2016.pdf.

Jarvie DM, Hill R, J. and Ruble TE (2007) Unconventional shale-gas systems: The Mississipian Barnett Shale of north-central Texas as one model for thermogen ic shale-gas assessment. AAPG Bulletin 91(475-499).

Kapel AJ (1966) The Cooper's Creek Basin. The APEA Journal 6(2), 71-75.

Kapel AJ (1972) The geology of the Patchawarra area, Cooper Basin. The APEA Journal 12(1), 53-57. Doi: https://doi.org/10.1071/AJ71009.

King GE (2010) Thirty Years of Gas Shale Fracturing: What Have We Learned? In: SPE Annual Technical Conference and Exhibition. Society of Petroleum Engineers, 49. Viewed 1 August 2018, https://www.onepetro.org/conference-paper/SPE-133456-MS.

King R, Khair HA, Bailey A, Backé G, Holford S and Hand M (2011) Integration of in-situ stress analysis and three-dimensional seismic mapping to understand fracture networks in Australian basins. Proceedings of the 4th Australian Geothermal Energy Conference.

King RC, Neubauer M, Hillis RR and Reynolds SD (2010) Variation of vertical stress in the Carnarvon Basin, NW Shelf, Australia. Tectonophysics 482(1-4), 73-81.

Korsch RJ and Totterdell JM (2009a) Subsidence history and basin phases of the Bowen, Gunnedah and Surat Basins, eastern Australia. Australian Journal of Earth Sciences 56(3), 335-353. Doi: 10.1080/08120090802698687.

Korsch RJ and Totterdell JM (2009b) Evolution of the Bowen, Gunnedah and Surat Basins, eastern Australia. Australian Journal of Earth Sciences 56(3), 271-272. Doi: 10.1080/08120090802695733.

Korsch RJ, Totterdell JM, Fomin T and Nicoll MG (2009) Contractional structures and deformational events in the Bowen, Gunnedah and Surat Basins, eastern Australia. Australian Journal of Earth Sciences 56(3), 477-499. Doi: 10.1080/08120090802698745.

Kulikowski D, Cooke D and Amrouch K (2016a) Constraining the distribution and relationship between overpressure, natural fracture density and temperature in the Cooper Basin, Australia. The APPEA Journal 56(1), 11-28.

Kulikowski D, Amrouch K and Cooke D (2016b) Geomechanical modelling of fault reactivation in the Cooper Basin, Australia. Australian Journal of Earth Sciences 63(3), 295-314.

Kulikowski D, Amrouch K, Cooke D and Gray ME (2017) Basement structural architecture and hydrocarbon conduit potential of polygonal faults in the Cooper-Eromanga Basin, Australia. Geophysical Prospecting. Doi: 10.1111/1365-2478.12531.

Kulikowski D and Amrouch K (2018) 3D seismic analysis investigating the relationship between stratigraphic architecture and structural activity in the intra-cratonic Cooper and Eromanga basins, Australia. Marine and Petroleum Geology 91, 381-400. Doi: https://doi.org/10.1016/j.marpetgeo.2018.01.019.

Lang SC, Grech P, Root R, Hill A and Harrison D (2001) The application of sequence stratigraphy to exploration and reservoir development in the Cooper-Eromanga-Bowen-Surat Basin system. The APPEA Journal 41(1), 223-250. Doi: https://doi.org/10.1071/AJ00011.

Lang SC, Ceglar N, Forder S, Spencer G and Kassan J (2002) High resolution sequence stratigraphy, reservoir analogues, and 3D seismic interpretation - Application to exploration and reservoir development in the Baryulah complex, Cooper Basin, southwest Queensland. The APPEA Journal 42(1), 511-522. Doi: https://doi.org/10.1071/AJ01028.

Laubach SE, Olson JE and Gross MR (2009) Mechanical and fracture stratigraphy. AAPG Bulletin 93(11), 1413-1426.

Law BE and Curtis JB (2002) Introduction to unconventional petroleum systems. AAPG Bulletin 86, 1851-1852.

Levine JR (1996) Model study of the influence of matrix shrinkage on absolute permeability of coal bed reservoirs. Geological Society, London, Special Publications 109(1), 197-212.

Lund Snee JE and Zoback MD (2016) State of stress in Texas: Implications for induced seismicity. Geophysical Research Letters 43(19).

Mastalerz M and Harper D (1998) Coal in Indiana—A geologic overview. Indiana Geological Survey Special Report 60.

McKellar JL (2013) The Cooper Basin. In: Jell PA (ed), Geology of Queensland. Geological Survey of Queensland, Brisbane, 204-212.

McKirdy DM, Yu X, Leythaeuser D, Schward L and Arouri KR (2001) A pilot study of secondary migration and reservoir filling in the Cooper/Eromanga Basin, South Australia. 20th International Meeting on Organic Geochemistry. Nancy, France.

Meixner TJ, Gunn PJ, Boucher RK, Yeates TN, Richardson LM and Frears RA (2000) The nature of the basement to the Cooper Basin region, South Australia. Exploration Geophysics 31(2), 24-32.

Menpes S and Hill T (2012) Emerging continuous gas plays in the Cooper Basin, South Australia. The APPEA Journal 52(2), 671-671. Doi: https://doi.org/10.1071/AJ11085.

Menpes S, Hill A and Pepicelli D (2013) Characteristics of the Gidgealpa Group composite resource play in the Cooper Basin, South Australia. Unconventional Resources Technology Conference (URTEC).

Michaelsen BH and McKirdy DM (2001) Migration and mixing of oils in the Cooper and Eromanga basins, central Australia. In: Eastern Australian basins Symposium; a refocused energy perspective for the future. Petroleum Exploration Society of Australia, Special Publication, 289–300. Viewed 11 August 2018, http://archives.datapages.com/data/petroleum-exploration-society-of-australia/conferences/001/001001/pdfs/289.htm.

Morton JG and Gatehouse CG (1985) A revision of the Toolachee and Daralingie Formations, Cooper Basin, South Australia. Quarterly Geological Notes 94, 8-15.

Morton JG (2016) Weena Trough stratigraphic review study: summary report. Energy Resources Division, Department of State Development, South Australia.

Moussavi-Harami R (1996a) Burial history of the Cooper, Eromanga and Lake Eyre Basins in northeast South Australia. Open file Envelope 9024, unpublished, South Australia Department of Mines and Energy.

Moussavi-Harami R (1996b) Burial history. In: Alexander EM and Hibburt JE (eds), Petroleum Geology of South Australia. South Australia Department of Mines and Energy, 125-140.

Müller R and Dyksterhuis S (2005) Current and palaeo-stress models for central Australian basins: in Proceedings of the Central Australian Basins Symposium. Alice Springs, August, 1-9.

Nakanishi T and Lang SC (2001) The search for stratigraphic traps goes on - visualisation of fluival-lacustrine successions in the Moorari 3D survey, Cooper-Eromanga Basin. The APPEA Journal 41, 115-137.

Nelson EJ, Chipperfield ST, Hillis RR, Gilbert J, McGowen J and Mildren SD (2007) The relationship between closure pressures from fluid injection tests and the minimum principal stress in strong rocks. International Journal of Rock Mechanics and Mining Sciences 44(5), 787-801.

Nicoll RS, McKellar J, Esterle J, Crowley JL, Laurie J, Wood. G, Areeba Ayaz S and Bodorkos S (2015) CA–IDTIMS dating of tuffs, calibration of palynostratigraphy and stratigraphy of the Bowen and Galilee basins. In: Bowen Basin symposium, 2015. Viewed 16 November 2018, https://www.researchgate.net/publication/283298530.

O'Neil BJ (1998) Chapter 2: History of Petroleum Exploration and Development. In: Gravestock DI, Hibburt JE and Drexel JF (eds), The Petroleum Geology of South Australia, Volume 4: Cooper Basin. SA Department of Primary Industries and Resources, Adelaide, Australia, 7–36.

Olsen TN, Bratton TR, Tanner KV and Koepsell R (2007) Application of indirect fracturing for efficient stimulation of coalbed methane. In: Rocky Mountain Oil & Gas Technology

Symposium. Society of Petroleum Engineers. Viewed 16 November 2018, https://doi.org/10.2118/107985-MS.

Osborne MJ and Swarbrick RE (1997) Mechanisms for generating overpressure in sedimentary basins: A reevaluation. AAPG Bulletin 81(6), 1023-1041.

Owens R, Hall L, Smith M, Orr M, Lech M, Evans T, Skeers N, Woods M and Inskeep C (2020) Geology of the Cooper GBA region. Technical appendix for the Geological and Bioregional Assessment: Stage 2. Department of the Environment and Energy, Bureau of Meteorology, CSIRO and Geoscience Australia, Australia.

Palano M (2014) On the present-day crustal stress, strain-rate fields and mantle anisotropy pattern of Italy. Geophysical Journal International 200(2), 969-985.

Palmer I (2010) Coalbed methane completions: a world view. International Journal of Coal Geology 82(3-4), 184-195.

Passey QR, Creaney S, Kulla JB, Moretti FJ and Stroud JD (1990) A practical model for organic richness from porosity and resistivity logs. AAPG Bulletin 74(12), 1777-1794.

Passey QR, Bohacs KM, Esch WL, Klimentidis R and Sinha S (2010) From oil-prone source rock to gas-producing shale reservoir: geologic and petrophysical characterization of unconventional shale-gas reservoirs: SPE paper 131350. In: International Oil and Gas Conference and Exhibition. Viewed 16 November 2018, https://www.onepetro.org/conference-paper/SPE-131350-MS.

Perez Altamar R and Marfurt K (2014) Mineralogy-based brittleness prediction from surface seismic data: Application to the Barnett Shale. Interpretation 2(4), T255-T271.

Petrosys Pty Ltd (2019) Oil and gas field outlines and pipeline routes from the GPinfo petroleum database [spatial]. Viewed 05 August 2019, http://www.gpinfo.com.au/. GBA data repository GUID: A7CD2D93-7BDD-40CB-B8D4-D77BB9837A06.

Pitcher T and Davis TL (2016) Geomechanical analysis of in-situ stress and its influence on hydraulic fracturing at the Wattenberg Field, Colorado. First Break 34(3), 45-50.

Plumb R, Edwards S, Pidcock G, Lee D and Stacey B (2000) The mechanical earth model concept and its application to high-risk well construction projects. In: IADC/SPE Drilling Conference. Society of Petroleum Engineers. Viewed 1 August 2018, https://www.onepetro.org/conference-paper/SPE-59128-MS.

Powell TG, Boreham CJ, McKirdy DM, Michaelsen BH and Summons RE (1989) Petroleum geochemistry of the Murta Member, Mooga Formation, and associated oils, Eromanga Basin. The APEA Journal 29, 114–129.

Powell TG, Boreham CJ, Smyth M, Russell N and Cook AC (1991) Petroleum source rock assessment in non-marine sequences: pyrolysis and petrographic analysis of Australian coals and carbonaceous shales. Organic geochemistry 17(3), 375-394.

Price PL (1997) Permian to Jurassic palynostratigraphic nomenclature of the Bowen and Surat Basins. In: Green PM (ed), The Surat and Bowen Basins, south-east Queensland. Queensland Minerals and Energy Review Series, 137-178.

PRMS (2007) Petroleum Resources Management System (PRMS). Society of Petroleum Engineers, American Association of Petroleum Geologists, World Petroleum Council, and Society of Petroleum Evaluation Engineers. Viewed 10 August 2018, http://www.spe.org/industry/docs/Petroleum_Resources_Management_System_2007.pdf .

Radke BM (2009) Hydrocarbon & Geothermal Prospectivity of Sedimentary Basins in Central Australia: Warburton, Cooper, Pedirka, Galilee, Simpson & Eromanga Basins. Geoscience Australia Record 2009/25, 161.

Rajabi M, Heidbach O, Tingay M and Reiter K (2017a) Prediction of the present-day stress field in the Australian continental crust using 3D geomechanical–numerical models. Australian Journal of Earth Sciences 64(4), 435-454.

Rajabi M, Tingay M, Heidbach O, Hillis R and Reynolds S (2017b) The present-day stress field of Australia. Earth-Science Reviews 168, 165-189.

Ransley TR, Radke B and Kellett JR (2012) Cenozoic Geology. In: Ransley TR and Smerdon BD (eds), Hydrostratigraphy, hydrogeology and system conceptualisation of the Great Artesian Basin. A technical report to the Australian Government from the CSIRO Great Artesian basin Water Resource Assessment. CSIRO Water for a Healthy Country Flagship, Australia.

Raymond OL, Totterdell JM, Stewart AJ and Woods MA (2018) Australian geological provinces, 2018.01 edition. Viewed 06 July 2018, https://ecat.ga.gov.au/geonetwork/srv/eng/catalog.search?node=srv#/metadata/af11c9e2-12ac-43a2-a085-edf24cd51c94. GBA data repository GUID: 686747D2-44B0-4ECD-A880-58C8FC7F4110.

Real Energy (2014) ASX/Media Release - Real Energy updates gas resource estimates. Viewed 10 August 2018, http://www.asx.com.au/asxpdf/20141215/pdf/42vgvlxz43rrl1.pdf.

Real Energy (2018) ATP 927P Viewed 23 October 2018, http://www.realenergy.com.au/current-projects/view-projects/atp-927p.html.

Reynolds S, Mildren S, Hillis R and Meyer J (2004) The in situ stress field of the Cooper Basin and its implications for hot dry rock geothermal energy development. In: PESA Eastern Australasian Basins Symposium II 431-440. Viewed 1 August 2018, https://pdfs.semanticscholar.org/a320/e289b629820b7f3d569672182018b5526a85.pdf.

Reynolds SD, Coblentz DD and Hillis RR (2002) Tectonic forces controlling the regional intraplate stress field in continental Australia: Results from new finite element modeling. Journal of Geophysical Research: Solid Earth 107(B7), 15. Doi: https://doi.org/10.1029/2001JB000408

Reynolds SD, Mildren SD, Hillis RR, Meyer JJ and Flottmann T (2005) Maximum horizontal stress orientations in the Cooper Basin, Australia: implications for plate-scale tectonics and local stress sources. Geophysical Journal International 160(1), 331-343.

Reynolds SD, Mildren SD, Hillis RR and Meyer JJ (2006) Constraining stress magnitudes using petroleum exploration data in the Cooper–Eromanga Basins, Australia. Tectonophysics 415(1-4), 123-140.

Rickman R, Mullen M, Petre E, Grieser B and Kundert D (2008) A practical use of shale petrophysics for stimulation design optimization: All shale plays are not clones of the Barnett shale. In:

SPE Annual Technical Conference and Exhibition, 21-24. Viewed 8 November 2018, https://www.onepetro.org/conference-paper/SPE-115258-MS.

RISC (2013) ASX reserves and reousrces reporting for oil and gas companies. Public seminar, July 2013. Viewed 23 October 2018, http://www.asx.com.au/documents/asx-compliance/asx-oil-and-gas-risc-presentation-july-2013_2.pdf.

Sandiford M, Wallace M and Coblentz D (2004) Origin of the in situ stress field in south-eastern Australia. Basin Research 16(3), 325-338.

Santos-Beach-Origin (2012) Moomba-191 well completion report. Unpublished.

Santos–Delhi–Origin (2010) Bobs Well-2 well completion report. Unpublished.

Santos (2012) Cooper Basin Unconventional Gas Opportunities & Commercialisation: November 2012. Viewed 12 December 2018, https://www.santos.com/media-centre/announcements/cooper-basin-unconventional-gas-opportunities-and-commercialisation/.

Santos (2013) Moomba 191 and beyond. Viewed 22 August 2018, https://www.santos.com/media/2132/130828_moomba_191_and_beyond.pdf.

Santos (2015) Second Quarter Activities Report - For period ending 30 June 2015. Viewed 22 August 2018, https://www.santos.com/media/2584/2015_second_quarter_activities_report.pdf.

Santos (2018a) Historical highlights. Viewed 22 August 2018, https://www.santos.com/who-we-are/history/historical-highlights/.

Santos (2018b) Ballera. Viewed 22 August 2018, https://www.santos.com/what-we-do/activities/queensland/eromanga-basin/ballera/.

Santos (2018c) Moomba. Viewed 22 August 2018, https://www.santos.com/what-we-do/activities/south-australia/cooper-basin/moomba/.

Santos (2018d) Cooper Basin. Viewed 22 August 2018, https://www.santos.com/what-we-do/assets/cooper-basin/.

Schenk CJ and Pollastro RM (2002) Natural gas production in the United States. Viewed 13 April 2018, http://pubs.usgs.gov/fs/fs-0113-01/.

Schmoker JW, Crovelli RA and Balay RH (1995) Potential additions to technically recoverable resources for each continuous-type unconventional play of the U.S. Geological Survey: National assessment of United States oil and gas resources; Graphical and tabular presentations. US Geological Survey open-file report 95-75E.

Schmoker JW (2002) Resource assessment perspectives for unconventional gas systems. AAPG Bulletin 86(11), 1993-1999.

Seeber L and Armbruster JG (2000) Earthquakes as beacons of stress change. Nature 407(6800), 69.

Senex Energy Ltd (2013) ASX Announcement: Major contingent gas resource upgrade to 5.5 Tcf. Viewed 22 August 2018, https://www.senexenergy.com.au/wp-content/uploads/2016/01/Major-contingent-gas-resource-upgrade-to-5.5-Tcf.

Sibson R (1977) Fault rocks and fault mechanisms. Journal of the Geological Society 133(3), 191-213.

Sibson R (1992) Implications of fault-valve behaviour for rupture nucleation and recurrence. Tectonophysics 211(1-4), 283-293.

Sibson R, Ghisetti F and Ristau J (2011) Stress control of an evolving strike-slip fault system during the 2010–2011 Canterbury, New Zealand, earthquake sequence. Seismological Research Letters 82(6), 824-832.

Sibson R, Ghisetti F and Crookbain R (2012) Andersonian wrench faulting in a regional stress field during the 2010–2011 Canterbury, New Zealand, earthquake sequence. Geological Society, London, Special Publications 367(1), 7-18.

Sibson RH (1990) Conditions for fault-valve behaviour. Geological Society, London, Special Publications 54(1), 15-28.

Smith ML, Pavey C, Ford J, Sparrow A and Radke BM (2016) Conceptual modelling for the Cooper subregion. Product 2.3 for the Cooper subregion from the Lake Eyre Basin Bioregional Assessment. Department of the Environment and Energy, Bureau of Meteorology, CSIRO and Geoscience Australia, Australia, http://data.bioregionalassessments.gov.au/product/LEB/COO/2.3.

Stein RS (1999) The role of stress transfer in earthquake occurrence. Nature 402(6762), 605.

Strike Energy (2015) ASX Announcement - DUG Australia conference presentation - July 2015.

Strong PC, Wood GR, Lang SC, Jollands A, Karalaus E and Kassan J (2002) High resolution palaeogeographic mapping of the fluvial-lacustrine Patchawarra formation in the Cooper Basin, South Australia. The APPEA Journal 42(1), 65-81. Doi: https://doi.org/10.1071/AJ01005.

Summons RE, Zumberge JE, Boreham CJ, Bradshaw MT and Edwards DS (2002) Oils of Eastern Australia: petroleum geochemistry and correlation. Geoscience Australia, Canberra, http://www.ga.gov.au/metadata-gateway/metadata/record/gcat_68754.

Sun X and Camac BA (2004) Cooper Basin Electrofacies Mapping. SA Department of State Development, Resources and Energy. Viewed 10 July 2018, https://sarig.pir.sa.gov.au/Map.

Thiercelin M and Plumb R (1994) A core-based prediction of lithologic stress contrasts in east Texas formations. In: SPE Formation Evaluation, 251-258. Viewed 8 November 2018, https://doi.org/10.2118/21847-PA.

Tingate P, Khaksar A, Van Ruth P, Dewhurst D, Raven M, Young H, Hillis R and Dodds K (2001) Geological controls on overpressure in the Northern Carnarvon Basin. The APPEA Journal 41(1), 573-594.

Tingay MR, Hillis RR, Morley CK, Swarbrick RE and Okpere EC (2003) Pore pressure/stress coupling in Brunei Darussalam—implications for shale injection. Geological Society, London, Special Publications 216(1), 369-379.

Tingay MR, Hillis RR, Swarbrick RE, Morley CK and Damit AR (2007) ‘Vertically transferred’ overpressures in Brunei: Evidence for a new mechanism for the formation of high-magnitude overpressure. Geology 35(11), 1023-1026.

Tingay MR, Hillis RR, Swarbrick RE, Morley CK and Damit AR (2009) Origin of overpressure and pore-pressure prediction in the Baram province, Brunei. AAPG Bulletin 93(1), 51-74.

Trembath C, Elliot L and Pitkin M (2012) The Nappamerri Trough, Cooper Basin unconventional plays: proving a hypothesis. Extended abstract. In: APPEA conference. Viewed 10 May 2018, http://www.publish.csiro.au/AJ/AJ11076.

Tupper NP and Burcjhardt DM (1990) Use of methylphenanthrene index to characterise expulsion of Cooper and Eromanga basin oils. The APPEA Journal 39(1), 373–385.

Tyiasning S and Cooke D (2016) Anisotropy signatures in the Cooper Basin of Australia: Stress versus fractures. Interpretation 4(2), SE51-SE61.

U.S. Geological Survey (2016) National and global petroleum assessment: Assessment of continuous oil and gas resources of the Cooper Basin Australia, 2016. Viewed 28 March 2019, https://pubs.usgs.gov/fs/2016/3050/fs20163050.pdf

Underwood CA, Cooke ML, Simo JA and Muldoon MA (2003) Stratigraphic controls on vertical fracture patterns in Silurian dolomite, northeastern Wisconsin. AAPG Bulletin 87(1), 121-142.

Upstream Petroleum Resources Working Group (2015) Coal seam, shale and tight gas in Australia: resources assessment and operation overview 2015. Geoscience Australia. Viewed 18 August 2018, https://scer.govspace.gov.au/workstreams/upstream-petroleum-and-offshore-minerals/unconventional-gas-reserves/.

van Ruth P and Hillis R (2000) Estimating pore pressure in the Cooper Basin, South Australia: sonic log method in an uplifted basin. Exploration Geophysics 31(2), 441-447.

van Ruth P, Hillis R, Tingate P and Swarbrick R (2003) The origin of overpressure in 'old' sedimentary basins: an example from the Cooper Basin, Australia. Geofluids 3(2), 125-131.

van Ruth P, Hillis R and Tingate P (2004) The origin of overpressure in the Carnarvon Basin, Western Australia: Implications for pore pressure prediction. Petroleum Geoscience 10(3), 247-257.

Wang FP and Gale JFW (2009) Screening criteria for shale-gas systems. Gulf Coast Association of Geological Societies Transactions 59, 779-793.

Wangen M (2001) Communication between overpressured compartments. Geofluids 1(4), 273-287.

Williams BP (1984) Reservoir geometry and alluvial architecture of the Toolachee Formation, Moomba Field, south Cooper Basin. 7th Australian Geological Convention. Geological Society of Australia, Sydney.

Zoback M (2007) Reservoir geomechanics: earth stress and rock mechanics applied to exploration, production and wellbore stability. Cambridge Press.

Glossary

The register of terms and definitions used in the Geological and Bioregional Assessment Program is available online at https://w3id.org/gba/glossary (note that terms and definitions are respectively listed under the 'Name' and 'Description' columns in this register). This register is a list of terms, which are the preferred descriptors for concepts. Other properties are included for each term, including licence information, source of definition and date of approval. Semantic relationships (such as hierarchical relationships) are formalised for some terms, as well as linkages to other terms in related vocabularies. Many of the definitions for these terms have been sourced from external glossaries – several from international sources; spelling variations have been preserved to maintain authenticity of the source.

accumulation: in petroleum geosciences, an 'accumulation' is referred to as an individual body of moveable petroleum

activity: for the purposes of Impact Modes and Effects Analysis (IMEA), a planned event associated with unconventional gas resource development. For example, activities during the exploration life-cycle stage include drilling and coring, ground-based geophysics and surface core testing. Activities are grouped into ten major activities, which can occur at different life-cycle stages.

aeolian: relating to or arising from the action of wind

anticline: an arch-shaped fold in rock in which rock layers are upwardly convex. The oldest rock layers form the core of the fold, and outward from the core progressively younger rocks occur.

aquifer: rock or sediment in a formation, group of formations, or part of a formation that is saturated and sufficiently permeable to transmit quantities of water to bores and springs

aquitard: a saturated geological unit that is less permeable than an aquifer, and incapable of transmitting useful quantities of water. Aquitards commonly form a confining layer over an artesian aquifer.

asset: an entity that has value to the community and, for the purposes of geological and bioregional assessments, is associated with a GBA region. An asset is a store of value and may be managed and/or used to maintain and/or produce further value. An asset may have many values associated with it that can be measured from a range of perspectives; for example, the values of a wetland can be measured from ecological, sociocultural and economic perspectives.

barrel: a standard unit of measurement for all production and sales of oil. It has a volume of 42 US gallons [0.16 m^3].

basement: the oldest rocks in an area; commonly igneous or metamorphic rocks of Precambrian or Paleozoic age that underlie other sedimentary formations. Basement generally does not contain significant oil or gas, unless it is fractured and in a position to receive these materials from sedimentary strata.

bed: in geosciences, the term 'bed' refers to a layer of sediment or sedimentary rock, or stratum. A bed is the smallest stratigraphic unit, generally a centimetre or more in thickness. To be labeled a bed, the stratum must be distinguishable from adjacent beds.

bore: a narrow, artificially constructed hole or cavity used to intercept, collect or store water from an aquifer, or to passively observe or collect groundwater information. Also known as a borehole or piezometer.

burial history: the depth of a sedimentary layer versus time, usually corrected for compaction

charge: in petroleum geoscience, a 'charge' refers to the volume of expelled petroleum available for entrapment

clastic: sedimentary rock that consists of fragments or clasts of pre-existing rock, such as sandstone or shale

cleat: the vertical cleavage of coal seams. The main set of joints along which coal breaks when mined.

coal: a rock containing greater than 50 wt.% organic matter

coal seam gas: coal seam gas (CSG) is a form of natural gas (generally 95% to 97% pure methane, CH_4) extracted from coal seams, typically at depths of 300 to 1000 m. Also called coal seam methane (CSM) or coalbed methane (CBM).

compression: lateral force or stress (e.g. tectonic) that tends to decrease the volume of, or shorten, a substance

conceptual model: an abstraction or simplification of reality that describes the most important components and processes of natural and/or anthropogenic systems, and their response to interactions with extrinsic activities or stressors. They provide a transparent and general representation of how complex systems work, and identify gaps or differences in understanding. They are often used as the basis for further modelling, form an important backdrop for assessment and evaluation, and typically have a key role in communication. Conceptual models may take many forms, including descriptive, influence diagrams and pictorial representations.

conglomerate: a sedimentary rock dominated by rounded pebbles, cobbles, or boulders

context: the circumstances that form the setting for an event, statement or idea

conventional gas: conventional gas is obtained from reservoirs that largely consist of porous sandstone formations capped by impermeable rock, with the gas trapped by buoyancy. The gas can often move to the surface through the gas wells without the need to pump.

Cooper Basin: the Cooper Basin geological province is an Upper Carboniferous – Middle Triassic geological sedimentary basin that is up to 2500 m thick and occurs at depths between 1000 and 4400 m. It is overlain completely by the Eromanga and Lake Eyre basins. Most of the Cooper Basin is in south-west Queensland and north-east SA, and includes a small area of NSW at Cameron Corner. It occupies a total area of approximately 130,000 km^2, including 95,740 km^2 in Queensland, 34,310 km^2 in SA and 8 km^2 in NSW.

craton: the old, geologically stable interior of a continent. Commonly composed of Precambrian rocks at the surface or covered only thinly by younger sedimentary rocks.

crust: the outer part of the Earth, from the surface to the Mohorovicic discontinuity (Moho) dataset: a collection of data in files, in databases or delivered by services that comprise a related set of information. Datasets may be spatial (e.g. a shape file or geodatabase or a Web Feature Service) or aspatial (e.g. an Access database, a list of people or a model configuration file).

deep coal gas: gas in coal beds at depths usually below 2000 m are often described as 'deep coal gas'. Due to the loss of cleat connectivity and fracture permeability with depth, hydraulic fracturing is used to release the free gas held within the organic porosity and fracture system of the coal seam. As dewatering is not needed, this makes deep coal gas exploration and development similar to shale gas reservoirs.

deformation: folding, faulting, shearing, compression or extension of rocks due to the Earth's forces

delta: a low, nearly flat area near the mouth of a river, commonly forming a fan-shaped plain that can extend beyond the coast into deep water. Deltas form in lakes and oceans when sediment supplied by a stream or river overwhelms that removed by tides, waves, and currents

depocentre: an area or site of maximum deposition; the thickest part of any specified stratigraphic unit in a depositional basin

deposition: sedimentation of any material, as in the mechanical settling of sediment from suspension in water, precipitation of mineral matter by evaporation from solution, and accumulation of organic material

depositional environment: the area in which, and physical conditions under which, sediments are deposited. This includes sediment source; depositional processes such as deposition by wind, water or ice; and location and climate, such as desert, swamp or river.

development: a phase in which newly discovered oil or gas fields are put into production by drilling and completing production wells

discovered: the term applied to a petroleum accumulation/reservoir whose existence has been determined by its actual penetration by a well, which has also clearly demonstrated the existence of moveable petroleum by flow to the surface or at least some recovery of a sample of petroleum. Log and/or core data may suffice for proof of existence of moveable petroleum if an analogous reservoir is available for comparison.

dome: a type of anticline where rocks are folded into the shaped of an inverted bowl. Strata in a dome dip outward and downward in all directions from a central area.

effect: for the purposes of Impact Modes and Effects Analysis (IMEA), a change to water or the environment, such as changes to the quantity and/or quality of surface water or groundwater, or to the availability of suitable habitat. An effect is a specific type of an impact (any change resulting from prior events).

Eromanga Basin: an extensive geologic sedimentary basin formed from the Early Jurassic to the Late Cretaceous that can be over 2500 m thick. It overlies several older geological provinces including the Cooper Basin, and is in part overlain by the younger Cenozoic province, the Lake Eyre Basin. The Eromanga Basin is found across much of Queensland, northern SA, southern NT, as well as north-western NSW. The Eromanga Basin encompasses a significant portion of the Great Artesian Basin.

erosion: the wearing away of soil and rock by weathering, mass wasting, and the action of streams, glaciers, waves, wind, and underground water

exploration: the search for new hydrocarbon resources by improving geological and prospectivity understanding of an area and/or play through data acquisition, data analysis and interpretation. Exploration may include desktop studies, field mapping, seismic or other geophysical surveys, and drilling.

extraction: the removal of water for use from waterways or aquifers (including storages) by pumping or gravity channels. In the oil and gas industry, extraction refers to the removal of oil and gas from its reservoir rock.

facies: the characteristics of a rock unit that reflect the conditions of its depositional environment

fault: a fracture or zone of fractures in the Earth’s crust along which rocks on one side were displaced relative to those on the other side

field: in petroleum geoscience, a 'field' refers to an accumulation, pool, or group of pools of hydrocarbons or other mineral resources in the subsurface. A hydrocarbon field consists of a reservoir with trapped hydrocarbons covered by an impermeable sealing rock, or trapped by hydrostatic pressure.

floodplain: a flat area of unconsolidated sediment near a stream channel that is submerged during or after high flows

fluvial: sediments or other geologic features formed by streams

fold: a curve or bend of a formerly planar structure, such as rock strata or bedding planes, that generally results from deformation

formation: rock layers that have common physical characteristics (lithology) deposited during a specific period of geological time

fracture: a crack or surface of breakage within rock not related to foliation or cleavage in metamorphic rock along which there has been no movement. A fracture along which there has been displacement is a fault. When walls of a fracture have moved only normal to each other, the fracture is called a joint. Fractures can enhance permeability of rocks greatly by connecting pores together, and for that reason, fractures are induced mechanically in some reservoirs in order to boost hydrocarbon flow. Fractures may also be referred to as natural fractures to distinguish them from fractures induced as part of a reservoir stimulation or drilling operation. In some shale reservoirs, natural fractures improve production by enhancing effective permeability. In other cases, natural fractures can complicate reservoir stimulation.

free gas: the gaseous phase present in a reservoir or other contained area. Gas may be found either dissolved in reservoir fluids or as free gas that tends to form a gas cap beneath the top seal on the reservoir trap. Both free gas and dissolved gas play important roles in the reservoir-drive mechanism.

geological formation: stratigraphic unit with distinct rock types, which is able to mapped at surface or in the subsurface, and which formed at a specific period of geological time

granite: an intrusive igneous rock with high silica (SiO_2) content typical of continental regions

groundwater: water occurring naturally below ground level (whether stored in or flowing through aquifers or within low-permeability aquitards), or water occurring at a place below ground that has been pumped, diverted or released to that place for storage there. This does not include water held in underground tanks, pipes or other works.

hydraulic fracturing: also known as 'fracking', 'fraccing' or 'fracture simulation'. This is a process by which geological formations bearing hydrocarbons (oil and gas) are 'stimulated' to increase the flow of hydrocarbons and other fluids towards the well. In most cases, hydraulic fracturing is undertaken where the permeability of the formation is initially insufficient to support sustained flow of gas. The process involves the injection of fluids, proppant and additives under high pressure into a geological formation to create a conductive fracture. The fracture extends from the well into the production interval, creating a pathway through which oil or gas is transported to the well.

hydrocarbons: various organic compounds composed of hydrogen and carbon atoms that can exist as solids, liquids or gases. Sometimes this term is used loosely to refer to petroleum.

hydrogeology: the study of groundwater, including flow in aquifers, groundwater resource evaluation, and the chemistry of interactions between water and rock

impact: the difference between what could happen as a result of activities and processes associated with extractive industries, such as shale, tight and deep coal gas development, and what would happen without them. Impacts may be changes that occur to the natural environment, community or economy. Impacts can be a direct or indirect result of activities, or a cumulative result of multiple activities or processes.

isopach: a contour that connects points of equal thickness. Commonly, the isopachs, or contours that make up an isopach map, display the stratigraphic thickness of a rock unit as opposed to the true vertical thickness. Isopachs are true stratigraphic thicknesses (i.e. perpendicular to bedding surfaces).

Lake Eyre Basin: a geologic province containing Cenozoic terrestrial sedimentary rocks within the Lake Eyre surface water catchment. It covers parts of northern and eastern SA, south-eastern NT, western Queensland and north-western NSW. In the Cooper GBA region, the basin sedimentary package is less than 300 m thick.

likelihood: probability that something might happen lithology: the description of rocks, especially in hand specimen and in outcrop, on the basis of characteristics such as color, mineralogic composition and grain size

mantle: the region of the Earth composed mainly of solid silicate rock that extends from the base of the crust (Moho) to the core–mantle boundary at a depth of approximately 2900 km

material: pertinent or relevant

migration: the process whereby fluids and gases move through rocks. In petroleum geoscience, 'migration' refers to when petroleum moves from source rocks toward reservoirs or seep sites. Primary migration consists of movement of petroleum to exit the source rock. Secondary migration occurs when oil and gas move along a carrier bed from the source to the reservoir or seep. Tertiary migration is where oil and gas move from one trap to another or to a seep.

Moho: the Mohorivicic discontinuity (seismic reflector) at the base of the crust

natural gas : the portion of petroleum that exists either in the gaseous phase or is in solution in crude oil in natural underground reservoirs, and which is gaseous at atmospheric conditions of pressure and temperature. Natural gas may include amounts of non-hydrocarbons.

oil: a mixture of liquid hydrocarbons and other compounds of different molecular weights. Gas is often found in association with oil. Also see Petroleum.

oil-prone: organic matter that generates significant quantities of oil at optimal maturity

operator: the company or individual responsible for managing an exploration, development or production operation

organic matter: biogenic, carbonaceous materials. Organic matter preserved in rocks includes kerogen, bitumen, oil and gas. Different types of organic matter can have different oil-generative potential.

orogeny: the process of mountain building; the process whereby structures within fold-belt mountainous areas formed

outcrop: a body of rock exposed at the surface of the Earth

palaeoenvironment: an ancient depositional environment

permeability: the measure of the ability of a rock, soil or sediment to yield or transmit a fluid. The magnitude of permeability depends largely on the porosity and the interconnectivity of pores and spaces in the ground.

petroleum: a naturally occurring mixture consisting predominantly of hydrocarbons in the gaseous, liquid or solid phase petroleum system: the genetic relationship between a pod of source rock that is actively producing hydrocarbon, and the resulting oil and gas accumulations. It includes all the essential elements and processes needed for oil and gas accumulations to exist. These include the source, reservoir, seal, and overburden rocks, the trap formation, and the hydrocarbon generation, migration and accumulation processes. All essential elements and processes must occur in the appropriate time and space in order for petroleum to accumulate.

play: a conceptual model for a style of hydrocarbon accumulation used during exploration to develop prospects in a basin, region or trend and used by development personnel to continue exploiting a given trend. A play (or group of interrelated plays) generally occurs in a single petroleum system.

porosity: the proportion of the volume of rock consisting of pores, usually expressed as a percentage of the total rock or soil mass

producing: a well or rock formation from which oil, gas or water is produced

production: in petroleum resource assessments, 'production' refers to the cumulative quantity of oil and natural gas that has been recovered already (by a specified date). This is primarily output from operations that has already been produced.

production well: a well used to remove oil or gas from a reservoir

prospectivity assessment: the assessment of an area to determine the likelihood of discovering a given resource (e.g. oil, gas, groundwater) by analysing the spatial patterns of foundation datasets. The key objective is to identify areas of increased likelihood of discovering previously unrecognised potential. Sometimes referred to as ‘chance of success’ or ‘common risk segment’ analysis.

reservoir: a subsurface body of rock having sufficient porosity and permeability to store and transmit fluids and gases. Sedimentary rocks are the most common reservoir rocks because they have more porosity than most igneous and metamorphic rocks and form under temperature conditions at which hydrocarbons can be preserved. A reservoir is a critical component of a complete petroleum system.

reservoir rock: any porous and permeable rock that contains liquids or gases (e.g. petroleum, water, CO_2), such as porous sandstone, vuggy carbonate and fractured shale

reverse fault: a fault in which the hanging wall appears to have moved upward relative to the footwall. Common in compressional regimes.

ridge: a narrow, linear geological feature that forms a continuous elevated crest for some distance (e.g. a chain of hills or mountains or a watershed)

risk: the effect of uncertainty on objectives (ASNZ ISO 3100). This involves assessing the potential consequences and likelihood of impacts to environmental and human values that may stem from an action, under the uncertainty caused by variability and incomplete knowledge of the system of interest.

sandstone: a sedimentary rock composed of sand-sized particles (measuring 0.05–2.0 mm in diameter), typically quartz

seal: a relatively impermeable rock, commonly shale, anhydrite or salt, that forms a barrier or cap above and around reservoir rock such that fluids cannot migrate beyond the reservoir. A seal is a critical component of a complete petroleum system.

sediment: various materials deposited by water, wind or glacial ice, or by precipitation from water by chemical or biological action (e.g. clay, sand, carbonate)

sedimentary rock: a rock formed by lithification of sediment transported or precipitated at the Earth's surface and accumulated in layers. These rocks can contain fragments of older rock transported and deposited by water, air or ice, chemical rocks formed by precipitation from solution, and remains of plants and animals.

sedimentation: the process of deposition and accumulation of sediment (unconsolidated materials) in layers

seismic survey: a method for imaging the subsurface using controlled seismic energy sources and receivers at the surface. Measures the reflection and refraction of seismic energy as it travels through rock.

shale: a fine-grained sedimentary rock formed by lithification of mud that is fissile or fractures easily along bedding planes and is dominated by clay-sized particles

shale gas: generally extracted from a clay-rich sedimentary rock, which has naturally low permeability. The gas it contains is either adsorbed or in a free state in the pores of the rock.

shear: a frictional force that tends to cause contiguous parts of a body to slide relative to each other in a direction parallel to their plane of contact

siltstone: a sedimentary rock composed of silt-sized particles (0.004 to 0.063 mm in diameter)

source rock: a rock rich in organic matter which, if heated sufficiently, will generate oil or gas. Typical source rocks, usually shales or limestones, contain about 1% organic matter and at least 0.5% total organic carbon (TOC), although a rich source rock might have as much as 10% organic matter. Rocks of marine origin tend to be oil-prone, whereas terrestrial source rocks (such as coal) tend to be gas-prone. Preservation of organic matter without degradation is critical to creating a good source rock, and necessary for a complete petroleum system. Under the right conditions, source rocks may also be reservoir rocks, as in the case of shale gas reservoirs.

spring: a naturally occurring discharge of groundwater flowing out of the ground, often forming a small stream or pool of water. Typically, it represents the point at which the watertable intersects ground level.

stratigraphy: the study of the history, composition, relative ages and distribution of stratified rock strata, and its interpretation to reveal Earth's history. However, it has gained broader usage to refer to the sequential order and description of rocks in a region.

strike-slip fault: a type of fault whose surface is typically vertical or nearly so. The motion along a strike-slip fault is parallel to the strike of the fault surface, and the fault blocks move sideways past each other. A strike-slip fault in which the block across the fault moves to the right is described as a dextral strike-slip fault. If it moves left, the relative motion is described as sinistral.

structure: a geological feature produced by deformation of the Earth's crust, such as a fold or a fault; a feature within a rock, such as a fracture or bedding surface; or, more generally, the spatial arrangement of rocks

subsidence: the sudden sinking or gradual downward settling of the Earth's surface with little or no horizontal motion. The movement is not restricted in rate, magnitude, or area involved.

surface water: water that flows over land and in watercourses or artificial channels and can be captured, stored and supplemented from dams and reservoirs

syncline: a concave-upward fold in rock that contains stratigraphically younger strata toward the center

tectonics: the structural behaviour of the Earth's crust

terrane: an area of crust with a distinct assemblage of rocks (as opposed to terrain, which implies topography, such as rolling hills or rugged mountains)

thrust fault: a low-angle reverse fault, with inclination of fault plane generally less than 45 °

tight gas: tight gas is trapped in reservoirs characterised by very low porosity and permeability. The rock pores that contain the gas are minuscule, and the interconnections between them are so limited that the gas can only migrate through it with great difficulty.

total organic carbon: the quantity of organic matter (kerogen and bitumen) is expressed in terms of the total organic carbon (TOC) content in mass per cent. The TOC value is the most basic measurement for determining the ability of sedimentary rocks to generate and expel hydrocarbons.

trap: a geologic feature that permits an accumulation of liquid or gas (e.g. natural gas, water, oil, injected CO_2) and prevents its escape. Traps may be structural (e.g. domes, anticlines), stratigraphic (pinchouts, permeability changes) or combinations of both.

unconformity: a surface of erosion between rock bodies that represents a significant hiatus or gap in the stratigraphic succession. Some kinds of unconformities are (a) angular unconformity – an unconformity in which the bedding planes above and below the unconformity are at an angle to each other; and (b) disconformity – an unconformity in which the bedding planes above and below the stratigraphic break are essentially parallel.

unconventional gas: unconventional gas is generally produced from complex geological systems that prevent or significantly limit the migration of gas and require innovative technological solutions for extraction. There are numerous types of unconventional gas such as coal seam gas, deep coal gas, shale gas and tight gas.

water-dependent asset: an asset potentially impacted, either positively or negatively, by changes in the groundwater and/or surface water regime due to unconventional gas resource development

watertable: the upper surface of a body of groundwater occurring in an unconfined aquifer. At the watertable, pore water pressure equals atmospheric pressure.

weathering: the breakdown of rocks and other materials at the Earth's surface caused by mechanical action and reactions with air, water and organisms. Weathering of seep oils or improperly sealed oil samples by exposure to air results in evaporative loss of light hydrocarbons.

well: typically a narrow diameter hole drilled into the earth for the purposes of exploring, evaluating, injecting or recovering various natural resources, such as hydrocarbons (oil and gas), water or carbon dioxide. Wells are sometimes known as a 'wellbore'.

www.bioregionalassessments.gov.au

Australian Government

Department of Agriculture, Water and the Environment

Bureau of Meteorology

Geoscience Australia

CSIRO